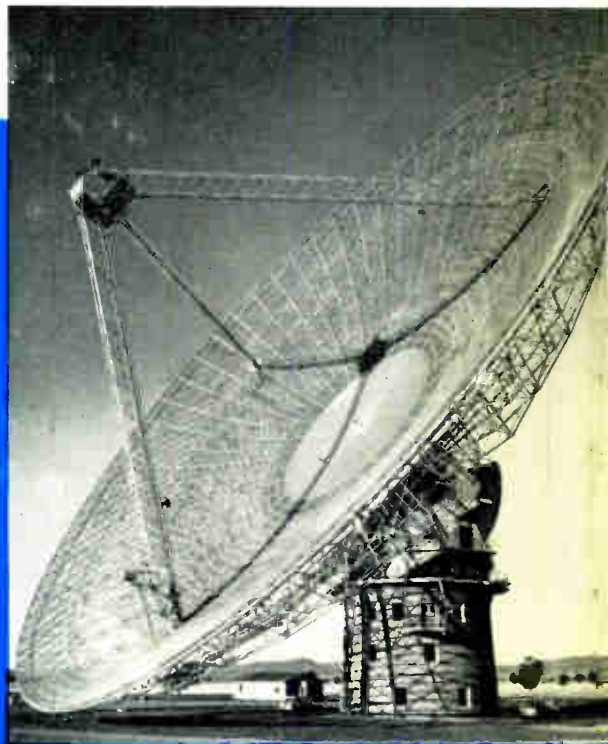


Advances in **RADIO RESEARCH**

VOLUME 2

Edited by
J. A. SAXTON



ACADEMIC PRESS
LONDON AND NEW YORK

MICROWAVE ENGINEERING

A. F. HARVEY, D.Phil., B.Sc.(Eng.), M.I.E.E.

Royal Radar Establishment, Malvern, England

1963, xlii+1,313 pages, 520 illustrations, 80 tables, 10,000 references, 250s.

For engineers, physicists, teachers . . .

This unique work is specifically designed to provide a centralized source of information on the principles, techniques, and applications of microwaves. It is essential to engineers practising in the fields of antennas, components, electron devices, and systems. The detailed consideration of physical principles and phenomena is of value to physicists who are engaged in microwave research or who use microwaves as research tools. In addition, the modern complete coverage provides the general background necessary to evaluate the applicability of microwave technology to various professional and educational areas of interest.

Definitive coverage . . .

The contents of the book form three interwoven subject areas. The first deals mainly with passive components and circuits and considers guiding structures in both uniform and periodic form, circuit elements and components, methods of measurement, optical-type instruments, antennas, and manufacturing techniques. The second group of chapters considers the electrical behaviour of microwave systems as modified by the incorporation of active materials or media. Examination is made of the general properties of materials showing dispersive and quantum effects, including gyromagnetic media. Descriptions are given of detection, amplification, generation, and switching by electron tubes, solid-state devices, and gaseous plasmas. The concluding chapters deal with the many important applications of microwaves.

Throughout the book, particular features and illustrations have been selected to emphasize novel principles and current practice. Nomenclature follows current international usage. The text is supplemented by extensive bibliographies covering the world literature.



ACADEMIC PRESS
LONDON AND NEW YORK

Berkeley Square House, Berkeley Square, London, W.1

111 Fifth Avenue, New York, New York 10003

ADVANCES IN RADIO RESEARCH

Edited by

J. A. SAXTON

*Scientific Attaché, British Embassy, Washington D.C.
formerly Deputy Director, Radio Research Station
Slough, England*

Volume 2

1964



ACADEMIC PRESS · LONDON · NEW YORK

ACADEMIC PRESS INC. (LONDON) LTD
BERKELEY SQUARE HOUSE
BERKELEY SQUARE
LONDON, W.1

U.S. Edition published by

ACADEMIC PRESS INC.
111 FIFTH AVENUE
NEW YORK 3, NEW YORK

Copyright © 1964 By Academic Press Inc. (London) Ltd

ALL RIGHTS RESERVED

NO PART OF THIS BOOK MAY BE REPRODUCED IN ANY FORM BY
PHOTOSTAT, MICROFILM, OR ANY OTHER MEANS, WITHOUT WRITTEN
PERMISSION FROM THE PUBLISHERS

Library of Congress Catalog Card Number: 64-19688

Printed in Great Britain by The Whitefriars Press Ltd.
London and Tonbridge

CONTRIBUTORS TO VOLUME 2

JOHN W. FINDLAY, *National Radio Astronomy Observatory, Green Bank,
West Virginia, U.S.A.*

F. HORNER, *D.S.I.R. Radio Research Station, Slough, England.*

C. M. MINNIS, *IQSY Secretariat, London, England.*

PREFACE

The first volume of this series is concerned mainly with matters relating to the propagation of radio waves over the ground and through the troposphere. In this second volume the emphasis shifts on the one hand to a consideration of topics in which the ionosphere is involved, and on the other to a description of techniques used in radio astronomy which, however, may have wider applications.

Until the advent of communication satellites the main means of long-distance radio communication was through the use of waves in the high frequency band which are reflected by the ionosphere. Although the years immediately ahead will undoubtedly see great developments in the application of satellite communication techniques, it seems likely that extensive use will continue to be made of short wave communication by way of the ionosphere. In order that such communication shall be carried out effectively and with the most efficient use of the available radio frequencies it is necessary to have a continuous guide to the ionospheric characteristics relevant to the communication problem. One chapter in this volume presents a discussion of ionospheric indices, a knowledge of which is essential to the prediction of frequencies most suitable for long distance transmission at different times of the day, for different seasons and epochs in the cycle of solar activity.

In planning a communication system it is not sufficient only to know what is a suitable frequency for propagation over a given transmission path, it is also vital to know what background level of radio noise must be overcome at the point of reception. Apart from man-made noise from electrical equipment (and, in some circumstances, cosmic noise) most important sources of such noise over a considerable part of the radio frequency spectrum are the electrical disturbances in the atmosphere caused by lightning; and the study of these disturbances goes back to the pioneer investigations of Marconi and Popov. Another chapter in the present volume contains an account of knowledge of this radio noise due to "atmospherics". The nature of lightning strokes and the characteristics of the resulting radio emissions are discussed: consideration is also given to the influence of the ionosphere on the propagation of the noise radiation and to the practical implications for radio communications.

The remaining chapter of Volume 2 is concerned with aeriels and receivers developed for use in radio astronomy. This is a field in which much progress has been made since the end of the Second World War, and a description is given of large reflectors, interferometers and aerial systems involving aperture synthesis, together with a discussion of modern developments in the design of low-noise receivers. The techniques now available to the radio astronomer are of interest in other fields. For example, both space communication systems and tropospheric scatter links frequently require the use of large

aerials (steerable in space communications, though not necessarily so for tropospheric scatter applications) and sensitive receivers; and the material presented here should thus have a wide appeal.

The editor is again indebted to the contributing authors for the helpful manner in which they have facilitated the preparation of this volume.

J. A. SAXTON

Washington
February, 1964

CONTENTS

CONTRIBUTORS TO VOLUME 2	v
PREFACE	vii

IONOSPHERIC INDICES

C. M. Minnis

I. INTRODUCTION	1
II. IONOSPHERIC INDICES BASED ON <i>E</i> LAYER DATA	4
III. IONOSPHERIC INDICES BASED ON THE F_2 LAYER	17
IV. SOLAR ACTIVITY INDICES AND IONOSPHERIC PREDICTIONS	25
V. OTHER IONOSPHERIC INDICES	30
APPENDIX I	32
ACKNOWLEDGMENT	35
REFERENCES	35

ANTENNAS AND RECEIVERS FOR RADIO ASTRONOMY

John W. Findlay

INTRODUCTION	37
I. RECEIVERS FOR RADIO ASTRONOMY	38
II. PARABOLIC REFLECTOR ANTENNAS	72
III. OTHER TYPES OF RADIO ASTRONOMY ANTENNAS	93
REFERENCES, SECTION I	112
REFERENCES, SECTION II	115
REFERENCES, SECTION III	116
REFERENCES, GENERAL	119

RADIO NOISE FROM THUNDERSTORMS

F. Horner

I. TERRESTRIAL NOISE: ORIGINS AND IMPORTANCE	122
II. SOURCES OF NOISE AND NATURE OF LIGHTNING DISCHARGES	124
III. FIELD CHANGES AND ATMOSPHERICS NEAR THE SOURCE	130
IV. SPECTRUM NEAR THE SOURCE	133

V.	AMPLITUDE VARIABILITY OF ATMOSPHERICS	142
VI.	NUMBERS AND DISTRIBUTIONS OF LIGHTNING DISCHARGES	143
VII.	PROPAGATION OF ATMOSPHERICS	147
VIII.	CHARACTERISTICS AND MEASUREMENT OF ATMOSPHERIC NOISE	154
IX.	DIRECT MEASUREMENT OF INTERFERENCE	174
X.	WORLD DISTRIBUTION OF NOISE INTENSITY	175
XI.	NOISE INTERFERENCE TO RADIO SERVICES	181
XII.	LOCATING SOURCES OF ATMOSPHERICS	183
XIII.	WHISTLING ATMOSPHERICS	189
XIV.	CONCLUSION	194
	REFERENCES	194
AUTHOR INDEX		205
SUBJECT INDEX		211

IONOSPHERIC INDICES

C. M. MINNIS

IQSY Secretariat, London, England

I.	Introduction	1
A.	The Concept of an Index Number	1
B.	Primary Indices of Solar Activity	2
C.	Secondary Indices of Solar Activity	3
D.	Applications of Indices	4
II.	Ionospheric Indices based on <i>E</i> Layer Data	4
A.	Fundamental Ideas	4
B.	The Critical Frequency and the Character Figure	5
C.	The Monthly Character Figure in Practice	7
D.	A Daily <i>E</i> Layer Character Figure	11
E.	Relations between Daily Indices	14
F.	The Critical Frequency Ratio	16
III.	Ionospheric Indices Based on the <i>F</i> ₂ Layer	17
A.	Fundamental Ideas	17
B.	<i>F</i> ₂ Layer Indices depending on a Primary Index	18
C.	Indices based on Ionospheric Data from Several Stations	20
D.	Applications of <i>F</i> ₂ Layer Indices	23
E.	Indices Depending on Ionospheric Data Alone	23
IV.	Solar Activity Indices and Ionospheric Predictions	25
A.	Ionospheric Prediction Services	25
B.	Classification of Ionospheric Variations	26
C.	Classification of Ionospheric Predictions	27
D.	The Choice of an Index for Ionospheric Predictions	27
E.	The Choice of an Index for Short-term Predictions	28
F.	Relative Merits of Indices for Short-term Predictions	29
V.	Other Ionospheric Indices	30
A.	Particle Streams	30
B.	<i>D</i> Layer Absorption	31
	Appendix I	32
	References	35

I. INTRODUCTION

A. THE CONCEPT OF AN INDEX NUMBER

The concept of numerical indices, or index numbers, is much less familiar in the physical sciences than in the study of economics where, for example, indices of commodity prices, industrial production and the cost of living are typical of a large variety of numerical indicators of trends. The distinguishing feature of such indices is that the variations in them represent changes in the magnitude of something which can fairly easily be visualized in a qualitative way, but which cannot easily be measured by any simple or direct method. Another important characteristic of an index number is that its absolute

magnitude generally is of considerably less importance than the way in which it varies, usually with time.

In practice, the calculation of, for example, an index of commodity prices is normally based on the prices of only a representative sample of different commodities. Some or all of these prices may be subject to large seasonal variations and, assuming that the long-term change in prices is of primary importance, it may be necessary first to remove the seasonal component of the variation in order to produce an acceptable final index number. For some applications of such an index, it may also be necessary to make adjustments which take into account not only the relative amounts of the various commodities which are consumed, but also the inevitable large differences in the prices of common and scarce commodities.

The method of making these allowances and adjustments, the removal of seasonal variations, and the choice of the commodities to be used in compiling the index, all call for some degree of personal judgment. In consequence, differences in opinion can easily arise as to whether the final index satisfactorily represents what it is intended to represent, and whether it is the best index to use in a particular application. In the study of ionospheric indices, very similar problems arise and it is common to find differences of opinion concerning the construction of indices and the way in which these indices ought to be used.

B. PRIMARY INDICES OF SOLAR ACTIVITY

The principal subject of discussion in this review will be those indices which purport to represent "solar activity". This term is interpreted in many different ways by astronomers, geophysicists, radio engineers and others, and it must be stated at once that there is no single index of solar activity which is capable of satisfying all the different requirements for such an index.

For many years, measurements have been made of the component of the radiant solar energy that lies in the visible and infra-red portions of the spectrum. Most of this radiation penetrates to the lowest levels of the earth's atmosphere and it appears that the changes with time in the energy flux amount to less than 1 or 2 per cent of the total.

On the other hand, it is well known that many of the visible features of the sun vary considerably with time. The numbers of sunspots, calcium plages, and prominences that can be observed at any time vary fairly regularly with a principal period of about 11 years. Similar cyclic changes occur in the shape of the solar corona and in the intensity of the coronal emission lines. During the past 15 years or so, measurements of the flux of solar radio noise have been made over a wide range of frequencies. These measurements also show that there is a long-term variation, with a period of about 11 years, in the mean values of the flux and also in the number and character of the different radio noise "events" which occur.

Solar observations such as those referred to above confirm the existence of periodic changes in the sun, and they provide the basic data from which a number of widely different indices of solar activity have been produced.

It is important to note that these observations all depend either on the direct measurement of solar radiation, or on the frequency of occurrence of some visible feature of the sun's surface or of its atmosphere; the observations are influenced very little, if at all, by the earth's atmosphere through which the radiation must have passed before being recorded. For these reasons it is convenient to refer to the indices based on measurements of this kind as "primary indices" of solar activity

C. SECONDARY INDICES OF SOLAR ACTIVITY

The changes in solar activity that are disclosed by the primary indices mentioned in the previous section would be of little importance in everyday life if it were not for the fact that corresponding variations have been found to occur in some geomagnetic parameters and in the number density of free electrons in the terrestrial ionosphere at heights above 50 km. It is now known that this link between solar and terrestrial phenomena owes its existence to the irradiation of the earth's upper atmosphere by solar radiations of various kinds which lie outside the visible region of the spectrum and which are totally absorbed in the atmosphere before reaching ground level. Quite apart from their scientific interest, the geomagnetic and ionospheric variations to which reference has been made have important practical implications, mainly in the fields of radio communication, navigation and geographical surveying.

If the particular components of the variations in geomagnetic and ionospheric parameters that are caused by changes in solar activity could be isolated from those due to annual and seasonal effects, then it is clear that these components would provide a basis for constructing numerical indices which would represent the variations with time of solar activity. Several indices of this kind have been produced and, since they are not based directly on measurements of solar characteristics, it is convenient to refer to them as "secondary indices".

It is generally accepted that the large solar cyclic changes which are found in such secondary indices are due to variations with time in the flux of the ultra-violet and X-radiation that is emitted by the sun, but which is almost totally absorbed in its passage through the earth's atmosphere. The absorption of this radiation and the resulting production of free electrons is ultimately responsible for the existence of the terrestrial ionosphere. The electric currents which, in turn, flow in the ionosphere give rise to many geomagnetic phenomena which can be measured and which have been studied for many years.

In the light of what has been said it will be clear that, from the practical point of view, the radiations that are absorbed in the earth's atmosphere are of great importance and it would be very valuable to have continuous measurements of their absolute intensities, or at least of the variations in the intensity of each type of radiation during the solar cycle. In recent years, direct measurements of this kind have been made intermittently by means of instruments carried to great heights in rockets, and later in artificial earth

satellites. It will, however, be many years before a sufficiently long, continuous and detailed series of measurements of this kind becomes available which will be capable of satisfying all the needs of geophysicists and radio communication engineers. In the meantime, for most purposes it will be necessary to use either primary indices based on measurements of other radiations from the sun, or those secondary indices that are believed to reflect as accurately as possible the changes in the various radiations that give rise to the important ionospheric and geomagnetic phenomena on which ground-based observations can be made.

D. APPLICATIONS OF INDICES

An outline report on some of the more important primary and secondary indices of solar activity was presented at the XIIIth General Assembly of URSI by Minnis (1960b). The applications of such indices in the field of radio communications have been kept under consideration for some years and are referred to particularly in the reports of the IXth and Xth Plenary Assemblies of CCIR (CCIR 1959; in press).

II. IONOSPHERIC INDICES BASED ON *E* LAYER DATA

A. FUNDAMENTAL IDEAS

It has been suggested in Section I, C that the variations in the electron density of the ionosphere could be used as a starting point for the calculation of indices of solar activity. This possibility is based on two assumptions: that the electron density depends in a known way on the intensity of the incident solar radiation, and that the appropriate corrections can be made for those variations in electron density that are due to causes other than variations in the intensity of the incident solar radiation.

In general, the electron density in the ionosphere depends not only on the intensity of the incident radiation, but also on the time of day, the season of the year and the latitude and longitude of the station at which the measurements are made. Obviously then, the basic experimental data must be modified in various ways in order to obtain an index which refers to some agreed standard set of terrestrial conditions. The way in which this reduction of the basic data can be achieved will be illustrated by referring to the *E* layer of the ionosphere which was the first to be used in the calculation of an index based on measurements of electron density.

To a first approximation, the *E* layer behaves in the way predicted by Chapman (1931) for a model atmosphere which is assumed to have a constant scale height and to be irradiated by monochromatic ionizing radiation from the sun. As a result of photoionization of the atmosphere, the maximum rate of production of electrons per unit volume (q_{\max}) is given by

$$q_{\max} = \frac{\beta S_0}{eH} \cos X \quad (1)$$

where S_0 = intensity of the radiation before it enters the atmosphere;
 β = number of electrons produced per unit quantity of radiation;
 H = scale height of the atmosphere;
 X = zenith angle of the sun;
 e = base of natural logarithms.

At any height, the relation between the electron number density (N) and the rate of production (q) is given by the continuity equation

$$\frac{dN}{dt} = q - \alpha N^2 \tag{2}$$

in which α is the electron-ion recombination coefficient. At times of day near local noon, $\frac{dN}{dt}$ is small and we can write

$$q = \alpha N^2 \tag{3}$$

In the E layer, the height at which N reaches its maximum value occurs near the height at which q is maximum. In consequence, equations (1) and (3) can be combined to give

$$\frac{\beta S_0}{eH} \cos X = \alpha N_{\max}^2 \tag{4}$$

or, if $\beta/\alpha H$ is assumed to remain constant,

$$S_0 = N_{\max}^2 \sec X \tag{5}$$

B. THE CRITICAL FREQUENCY AND THE CHARACTER FIGURE

If the electron density of an ionospheric layer attains a maximum value at some particular height, the layer will reflect radio waves only up to a corresponding maximum frequency (f_c) known as the critical frequency. This frequency can be measured by well-known radio sounding techniques and, during the last two decades, regularly measured hourly values of f_c have become available in tabulated form for many locations. The critical frequency corresponding to the ordinary magnetoionic component of the reflected wave is simply related to N_{\max} :

$$N_{\max} = k f_c^2 \tag{6}$$

where k is constant, and hence, by combining equations (4) and (6), we can write:

$$\frac{\beta S_0}{\alpha H} \cdot \frac{1}{k^2 e} = f_c^4 \sec X (= Ch_E) \tag{7}$$

The quantity on the right-hand side of equation (7) is usually referred to as the "character figure" (Ch_E) of the layer and, provided that $\beta/\alpha H$ remains constant, its magnitude would be expected to be proportional to S_0 , the intensity of the incident ionizing radiation. It will be convenient to refer to the character figure of the E layer, as defined in equation (7), as Ch_E .

The obvious implication of equation (7) is that, for a constant level of solar activity as defined by S_0 ,

$$f_c \propto \cos^{\frac{1}{2}} X \quad (8)$$

We shall suppose that, during a period of 12 months, solar activity remains at a constant level and that the noon values of the critical frequency (f_{noon}) can be represented by

$$f_{\text{noon}} = f_0 \cos^{\frac{1}{2}} X_{\text{noon}} \quad (9)$$

in which f_0 is a constant which represents the critical frequency extrapolated to the condition where $X = 0$. The character figure which results from using the noon critical frequency for any month is, therefore, given by

$$Ch_E = f_{\text{noon}}^4 \sec X_{\text{noon}} = f_0^4 \quad (10)$$

Thus, the character figure is equivalent to the fourth power of the critical frequency at a location where the sun is overhead at noon, that is, where $X = 0$. Although the actual annual variation of the noon critical frequency at many stations is closely represented by equation (9), it is often found that the daily variation during a particular month is more nearly proportional to $\cos^{\frac{1}{2}} X$ and the critical frequency at time t is then given by

$$f_t = f_r \cos^{\frac{1}{2}} X_t \quad (11)$$

where f_r is a constant which again represents the critical frequency when $X = 0$. Both f_0 (equation (9)) and f_r (equation (11)) represent the critical frequency extrapolated to the condition $X = 0$; the essential difference between them is that the two extrapolations are based on different data: the annual variation in f_c for f_0 , and the diurnal variation for f_r .

It seems logical, at first sight, to suggest that f_r could be determined using the expression

$$f_r = f_t \sec^{\frac{1}{2}} X_t \quad (12)$$

and then substituted as an alternative to f_0 in equation (10). Further consideration shows that f_0 and f_r behave differently and cannot be interchanged.

It follows from equation (11) that, at noon,

$$f_{\text{noon}} = f_r \cos^{\frac{1}{2}} X_{\text{noon}} \quad (13)$$

The combination of equations (9) and (13) gives

$$\frac{f_0}{f_r} = \cos^{\frac{1}{2}} X_{\text{noon}} \quad (14)$$

and it is immediately obvious that the variations in the ratio f_0/f_r must vary annually in a manner depending on the annual variation of X_{noon} and hence on the latitude of the observatory. At a station such as Slough, X_{noon} varies from 28° in June to 75° in December and f_0/f_r varies during the year by ± 5

per cent. Experience shows that f_0 ought to be used rather than f_r in calculating E layer character figures, and that a large seasonal variation would appear in the character figure if f_r were used instead, especially at middle latitude stations.

C. THE MONTHLY CHARACTER FIGURE IN PRACTICE

The first use of Ch_E , as defined by equation (10), was made by Appleton and Naismith (1939), who showed that the annual mean value of Ch_E at three stations varied over a range of more than 2/1 during the years 1931–38 (Fig. 1). These variations were found to be in phase with those of the sunspot

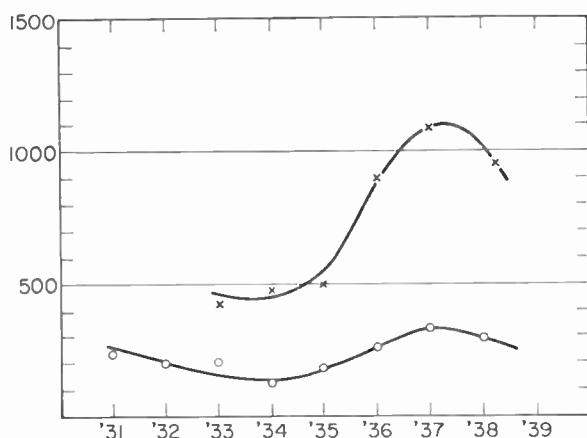


FIG. 1. The character figures for the E layer (lower curve) and F_1 layer (upper curve). (After Appleton and Naismith, 1939.)

cycle and hence the link between the number of free electrons in the E layer and the variations in the flux of the ionizing radiation from the sun was established.

The same authors also calculated character figures for the F_1 layer for the same period and reached a similar conclusion. No further reference will be made to F_1 layer indices in this review because the variation of electron density with height in this layer seldom has a well-defined maximum such as is found in the normal E and F_2 layers. In consequence, it is frequently impossible to make measurements of the F_1 layer critical frequency that can be considered sufficiently precise to justify their use in calculating an index of solar activity.

Occasional direct measurements for short periods have been made, by means of instruments in rockets and satellites, of the intensity of the particular ultra-violet and X-radiations that are assumed to be responsible for the existence of the E layer. Nevertheless, such data are not yet sufficiently numerous to permit a direct check to be made on the reliability of the E layer character figure as an indirect measure of solar activity. On the other hand, it is possible to make comparisons between the values of Ch_E and of

the other primary and secondary indices and to make deductions concerning the significance of Ch_E .

Denisse and Kundu (1957) compared values of Ch_E , which were based on noon data from Freiburg (Latitude 48°N), with the flux of solar radio-noise radiation (ϕ) measured at Ottawa on a wavelength of 10.7 cm by Medd and Covington (1958). Monthly mean values were used for both quantities and it was found that their variations with time were very similar. Figure 2 shows the variation in solar noise (ϕ), an E layer index (I_E) which is related to Ch_E , and the index I_{F_2} which is described in Section III. The observed similarity in behaviour can reasonably be expected because the radio noise radiation at this wavelength is emitted from approximately the same level in the sun's atmosphere as that from which the ionizing ultra-violet and X-radiations are believed to be emitted.

A closer examination of the relation between ϕ and Ch_E at Slough (Latitude 51°N) was made by Minnis and Bazzard (1958) who showed that the parameters which define the linear relation between the two indices do not remain constant, but that they vary slightly from month to month during the course of the year. It is most unlikely that this cyclic variation can have its origin in ϕ and it must be concluded that the Ch_E values for Slough contain a small annual variation. Minnis and Bazzard (1960b) later found that somewhat similar annual variations were present in Ch_E values calculated using data from eight stations in the northern and southern hemispheres. The mean amplitude of the variation for the eight stations was about 10 per cent near the maximum of the solar cycle, but it was too small to be detected at the minimum. Since the variation was a semi-annual one, and since it had the same phase in both the northern and southern hemispheres, it was not possible to attribute it simply to residual seasonal variations in the values of Ch_E . It now seems probable that these variations may be due to geomagnetic influences which cause the actual behaviour of the E layer to depart from what could be expected in a layer formed strictly in accordance with the model used by Chapman.

In the course of an examination of the way in which the form of the daily variation of f_0E varied from one station to another, Beynon and Brown (1956, 1959a) and also Appleton *et al.* (1955) found that the behaviour of the E layer critical frequency was, in certain respects, dependent on the location of the observing station relative to circulating geomagnetic current systems which have been described by Chapman (1940) and which are the cause of the Sq variations in the geomagnetic field. This work led Eyfrig (1960) to investigate the characteristics of the E layer at a large number of stations and to conclude that the apparently anomalous behaviour of the layer, such as that reported by Minnis and Bazzard, was characteristic of middle-latitude stations.

In particular, Eyfrig found that at Lwiro and Nha-trang, stations which are both near the geomagnetic equator, the annual variation in f_0E extrapolated to $X = 0$ was too small to be detected. It has been pointed out by Minnis (1964) that the extrapolated f_0E values used by Eyfrig represent f_r in equation (11) and not f_0 in equation (9), and that the differences in the

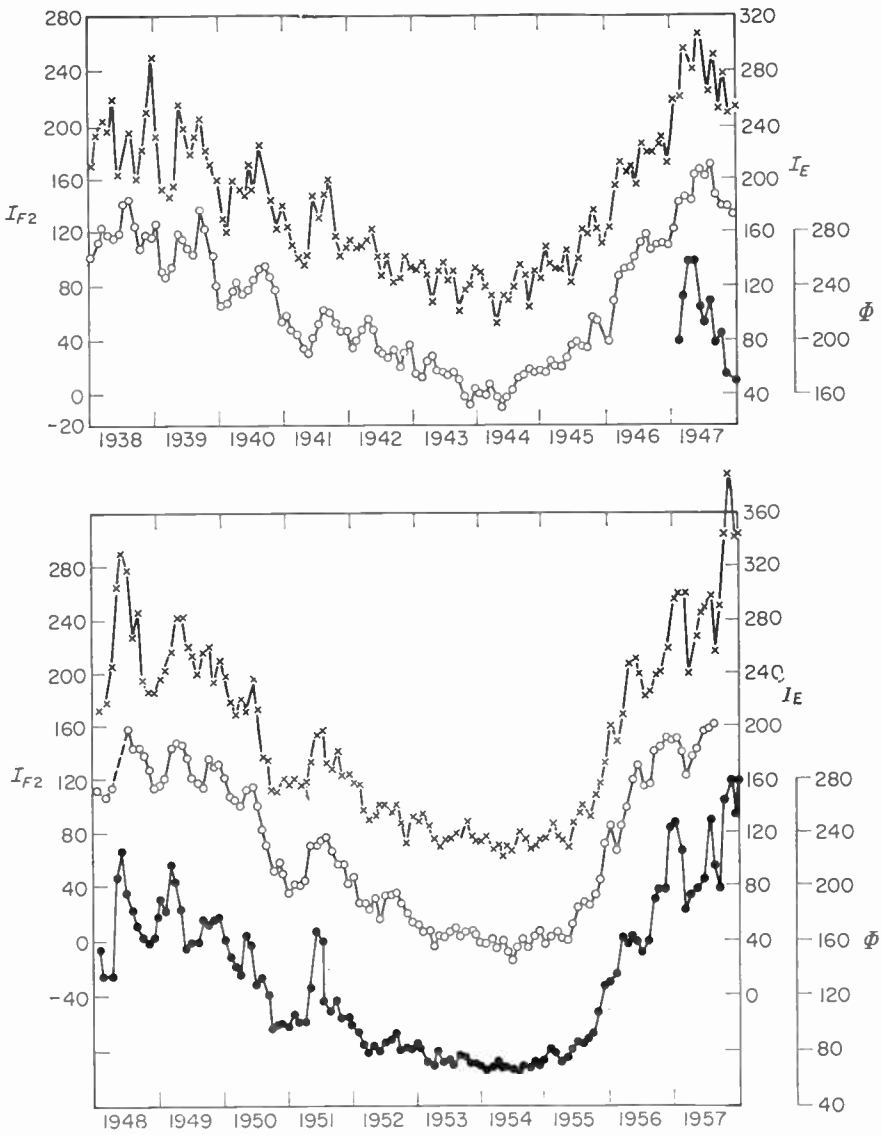


FIG. 2. Indices of solar activity based on:

- xxx E layer ionization (I_E)
- ooo F_2 layer ionization (I_{F2})
- Solar radio noise at 10.7 cm (ϕ)

(After Minnis and Bazzard, 1959a.)

amplitudes of the annual variations at the middle-latitude and equatorial stations are consistent with those expected from equation (14). It seems possible, therefore, that the difference in latitude may account for at least part of the apparently anomalous behaviour in the E layer at the middle-latitude stations studied by Eyfrig. If this suggestion is correct, the anomalies due to geomagnetic effects may be less than at first suspected.

Nevertheless, Eyfrig's data seem to show that if an E layer index is required in which the annual component is negligible, data from stations such as Lwiro and Nha-trang would probably provide the best starting point. Minnis and Bazzard (1958) investigated the correlation between monthly mean values of Ch_E at Slough and of ϕ and found that the mean correlation coefficient for the individual months was 0.950 as compared with 0.90 when the data for all months were considered together. The difference was due to the fact that the parameters which define the $Ch_E - \phi$ relation at Slough vary during the course of the year, as mentioned at the beginning of this section. Eyfrig (1962) has repeated this test, but has used values of Ch_E determined from E layer data from Lwiro. He found that the mean correlation coefficient for the individual months was 0.984 as compared with 0.980 for the year as a whole. This result seems to suggest that the semi-annual cycle which characterized the data from the eight stations studied by Minnis and Bazzard is not present in the Lwiro data.

On the evidence given by Eyfrig (1962) it appears that stations situated preferably near the equator and in certain longitude zones ought to be used for calculating E layer character figures. No such figures for the stations in question have so far been published, but monthly mean values of an E layer index based on data from Slough have been tabulated by Minnis and Bazzard (1959a) for the period January 1938 to September 1958. These authors were already aware of the semi-annual cycle which they described in more detail later (1960b), and their index, which is referred to as I_E is, in fact, the character figure (Ch_E) multiplied by a correction factor which reduces the semi-annual variation to negligible proportions.

It is interesting to note that if I_E is accepted as proportional to the intensity of the solar ionizing radiation, then the intensity must have risen by a factor of 3.6 during the interval between June 1954 when the sun was very quiet and October 1957 when solar activity, as measured by the sunspot number, attained the highest level recorded during at least the last 200 years. Minnis and Bazzard have fitted a second order equation to the monthly mean values of I_E and ϕ

$$I_E = 1.55\phi - 1.0 \cdot 10^{-3}\phi^2 + 14 \quad (15)$$

where ϕ is expressed in units of $10^{-22} Wm^{-2} (c/s)^{-1}$. The non-linearity reflects the fact that ϕ changes by a proportionally greater amount than I_E during the solar cycle. The increase in ϕ during the interval just referred to was 4.2 times as compared with 3.6 times for I_E .

The work of Eyfrig and of Minnis and Bazzard shows that f_0 rather than f_r is the correct E layer parameter to use when an E layer index of solar activity is required. There is, unfortunately, an additional complication; it

has been found that, for a given level of solar activity, the value of f_0 increases as the equator is approached and evidence for this has been described by Allen (1948), Harnischmacher (1950, 1955) and Shimazaki (1959). Eyfrig (1960) has reviewed the change of f_0 with latitude using a larger volume of data than was available to the earlier workers, and he suggests that it is no longer correct to assume that a simple relation of the type suggested by Harnischmacher is capable of accurately representing the observed latitude changes. More recent data published by Eyfrig (1962) suggest that the variation of f_0 with latitude depends on whether the winter or the summer hemisphere is considered. For the present, therefore, it will be necessary to exercise caution when comparing the absolute values of Ch_E for stations in different parts of the world, even after corrections have been made to allow for residual annual cyclic variations in Ch_E .

D. A DAILY E LAYER CHARACTER FIGURE

It is often difficult to measure the critical frequency of the E layer from the cusp on an ionogram to better than the nearest 0.05 Mc/s. The uncertainty may be even greater than this when the layer is stratified as in the ionogram reproduced in Fig. 3, and when, in consequence, it is difficult to identify the particular cusp which represents the normal E layer. Since the critical frequency is raised to the fourth power in the computation of the character figure, errors of 10 per cent can easily occur in the values of Ch_E based on single measurements of the critical frequency. When the monthly mean value of f_0E for a given hour is calculated, these errors tend to be averaged out and the resulting value for Ch_E is probably not seriously in error as a result of the uncertainties just mentioned.

During the International Geophysical Year (IGY), and afterwards as a result of the proposals for the compilation of an IGY Calendar (CSAGI 1962), the demand arose for daily solar and terrestrial indices of several types which would be suitable for use in the subsequent analysis and study of the IGY observational data. The problem of calculating daily E layer character figures for the IGY period was investigated by Minnis and Bazzard (1959b). Since the uncertainty in identifying the appropriate cusp and reading the single noon value of f_0E for each day would often have resulted in fairly large errors, the first step was to make a daily plot of $\log f_0E$ against $\log \cos X$; the critical frequencies plotted were read from the Slough ionograms for as many as possible of the 9 h 0800 to 1600 UT (Fig. 4). Inspection of these plots immediately brought to light any errors which had been made in the identification of the normal E layer cusp, since the plots for the hours in question were usually obviously inconsistent with those for adjacent hours on the same day. On numerous occasions, as reported by Bazzard (1961a), high values of f_0E could be associated with solar flares which were known to have occurred. On many days it was possible to read f_0E to the nearest 0.01 or 0.02 Mc/s and the points on the log-log plots usually lay fairly close to a line defined by $\log f_0E = (\log \cos X)/3 + \text{constant}$.

For a given day, the visual best-fit line through these points was assumed to represent a constant radiation intensity which was regarded as the average

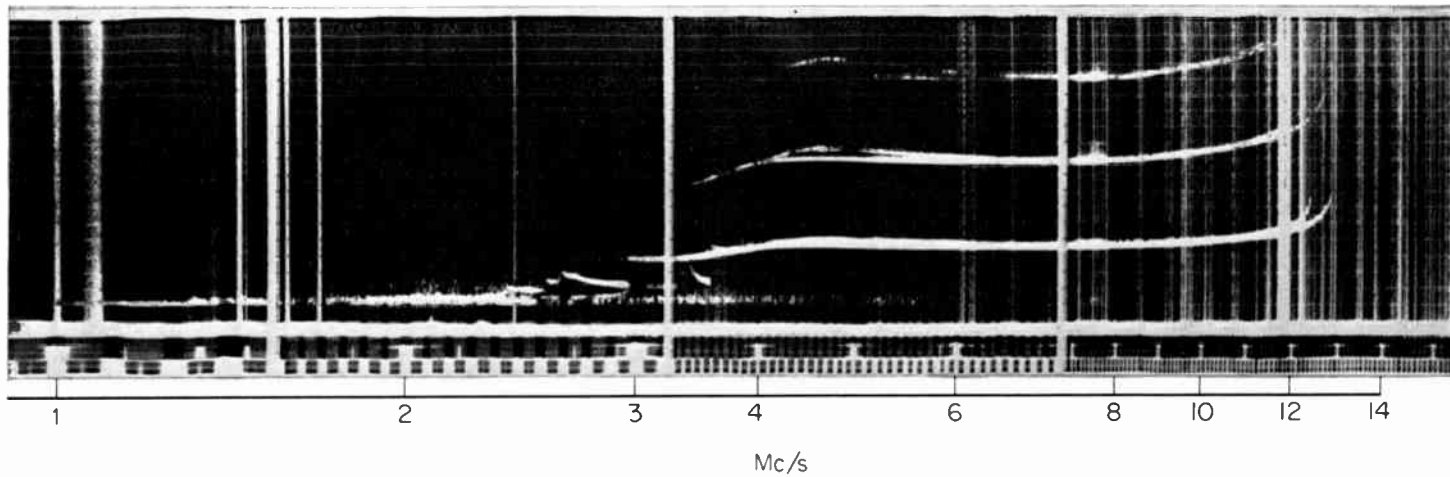


FIG. 3. Ionogram showing complex structure in the *E* region.

for that day. Given these assumptions, the noon value of f_0E as defined by this line, rather than by the actual measured value at noon, was then adopted as the appropriate value to use in calculating the value of Ch_E for the day. The difference between the actual frequency read from the ionogram for a given hour and that given by the best-fit line for the same day and hour was found to have a standard deviation of 0.07 Mc/s.

Since the plotted points for any given day did not all lie precisely on a straight line, the drawing of the visual best-fit line was subject to some

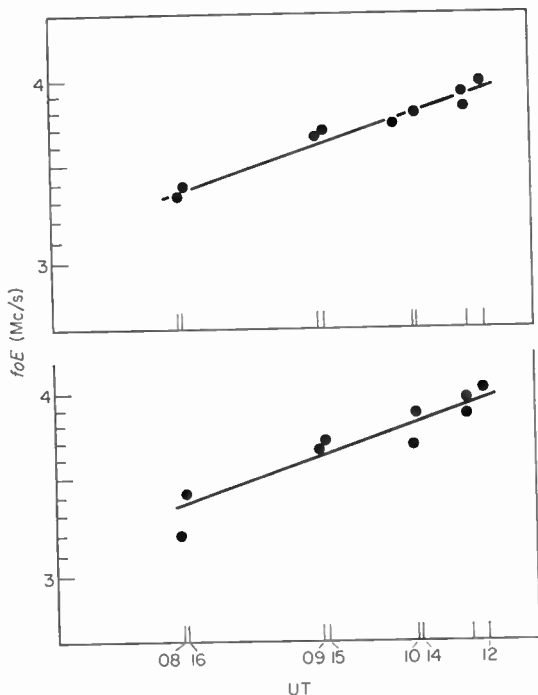


FIG. 4. Plots of $\log f_0E$ against $\log \cos X$. (Slough: 23, 24 April 1958.)

uncertainty which must have led to erratic errors in the value of f_0E at noon as defined by this line. A rough statistical test was made to determine the magnitude of these errors and the standard deviation of the error was estimated to be 0.02 Mc/s. At the peak of the solar cycle, the resulting error in the character figure was approximately 2 per cent, or about one-third of the error which would have been expected if only the noon ionogram had been used to determine f_0E on each day.

The tables of daily values (J_E) of the character figure published by Minnis and Bazzard (1959a) cover the period 1 January 1957 to 31 December 1958. The daily values for this period are plotted in Fig. 5, together with those for sunspot number (R) and solar radio noise flux (ϕ). Values for the period 1

January to 31 December 1959 have been given by Bazzard (1961b). The daily values for both these periods have been collected together by Minnis (1960a). The values for 1 January to 31 December 1960 have also been tabulated by Minnis (1961).

Although the daily values of J_E include a reading error estimated above at 2 per cent, it must be remembered that the critical frequency at a given station may be partially controlled by local influences and that, in consequence, the critical frequency used to calculate the character figure may not be controlled completely by the intensity of the ionizing radiation. Rawer (1959) has found that the correlation between the values of f_0E measured at different stations falls off rapidly with distance but, since this result is based on single hourly measurements, its implications do not necessarily apply to the daily index of Minnis and Bazzard who, in effect, used an interpolated critical frequency which depended on seven measurements made at intervals of 1 h rather than on a single observation.

E. RELATIONS BETWEEN DAILY INDICES

It is obviously impossible to check the absolute accuracy of the values of J_E since no comparable series of direct measurements of the solar ionizing radiation flux is available. Bazzard (1960) has, however, made comparisons between J_E and the daily values of ϕ , the solar noise flux at 10.7 cm. These comparisons show that there is generally a close similarity in the day-to-day variations of both these indices. On some occasions, however, outbursts of radio noise occur which are not accompanied by corresponding increases in J_E . It seems clear that, although there is a general similarity in the variations of ϕ and both the monthly mean and the daily E layer character figures, significant differences in behaviour are frequently found to occur. Such differences imply that ϕ cannot be adopted as a substitute for an ionospheric index in all circumstances.

Bazzard (1961b) has also made a number of statistical tests on the daily values of J_E for the 2½-yr period from 1 July 1957 to 31 December 1959. The tests were based on the daily values of δJ_E , which was defined as the difference between the value of J_E for a given day and its mean value for the 27-day period corresponding to a complete synodic rotation of the sun. As might be expected, the lengths of unbroken sequences of positive and negative values of J_E were found to vary from 1 to 14 days, but the numbers of the sequences having a duration of 5 days or more was found to be greater than the number expected by chance by a statistically significant amount. The existence of an unexpectedly large number of the longer sequences points to some external controlling cause which is, presumably, the solar radiation incident on the E layer.

Bazzard obtained independent confirmation of this conclusion by comparing the algebraic signs of δJ_E with those of δJ_G , the departures of the coronal green line index from its mean value. The coincidences in the signs of the two parameters did not occur randomly, but tended to run in sequences of up to 13 days in length. This fact leaves no doubt that there is a strong association between the value of J_E and the degree of solar activity as

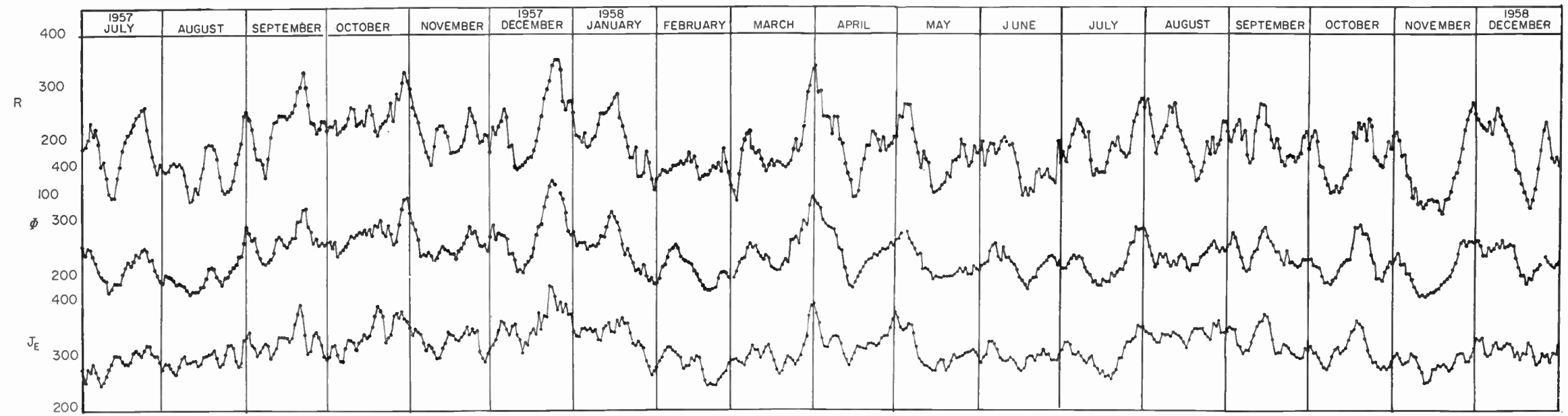


FIG. 5. Day-to-day variations in the daily E layer index (J_E), solar radio noise at 10.7 cm (ϕ) and sunspot number (R).

indicated by the intensity of the coronal green line. Bazzard also examined the auto-correlation function of J_E and found strong evidence for a 27-day period in J_E corresponding to the synodic rotation period of the sun (Fig. 6).

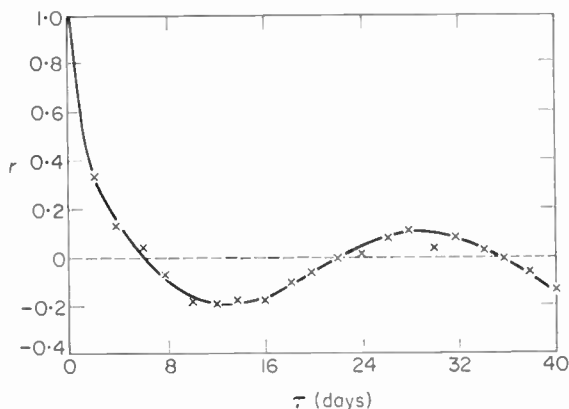


FIG. 6. The autocorrelation function of J_E . (After Bazzard, 1961b.)

This result also confirms that J_E is controlled by active areas on the sun and that some of these areas remain active for at least 27 days.

In view of the evidence presented by Bazzard, it must be concluded that a daily E layer index, calculated by the method indicated by Minnis and Bazzard, can be regarded as a useful indication of the day-to-day changes in the intensity of the E layer ionizing radiation. The index must, however, include errors arising from the day-to-day fluctuations in the layer that arise as a result of local influences but, as already stated, these are probably much less than those referred to by Rawer (1959). When sporadic- E ionization is strong there is always some uncertainty in reading the values of f_0E from the ionograms, but the published tables of J_E indicate those days when errors due to any cause probably exceed 3 per cent.

It is unfortunate that daily E layer indices, determined using the method of Minnis and Bazzard, have not been calculated for stations other than Slough. The comparison of several such indices would provide more information than is now available on the degree to which indices of this kind are influenced by local irregularities in the E layer and by errors of measurement.

It is worth noting that Beynon and Brown (1959b) have investigated the day-to-day changes in f_0E at Slough, Washington and Canberra for a 7-month period in 1951. The measured noon values of f_0E were used without interpolation and the standard deviation of the differences between the pairs of values would, therefore, be expected to be roughly 0.07 Mc/s, the figure quoted in Section II, D. Since there are considerable longitude differences between the three stations, the level of solar activity at local noon could differ appreciably from station to station. In spite of these facts, it is quite evident, from the evidence presented by Beynon and Brown, that the day-to-

day changes in f_0E at all three stations are closely related to each other. The changes show a prominent 27-day cycle which corresponds to a marked asymmetry in the activity of the sun as indicated by visual observations.

F. THE CRITICAL FREQUENCY RATIO

The indices that have been considered in the preceding sections are based on the E layer character figure and hence they depend ultimately on the absolute value of the critical frequency for the month in question. In the calculation of the character figure (Section II, B), the large seasonal variations in the critical frequency are removed by introducing a multiplying factor whose magnitude depends on the known solar zenith angle for the month. This procedure is obviously open to criticism since it is based on the assumption that the E layer has the characteristics of a Chapman layer.

Attempts to avoid this criticism have been made by Allen (1948) who defined an index (A_E) which is the ratio of the mean critical frequency ($f(m, R)$), at a given time of day and for a month in which the sunspot number is R , to the frequency ($f(m, 0)$) for the same month when the sunspot number is zero. Starting from equation (7), we can write

$$\left(\frac{f(m, R)}{f(m, 0)}\right)^4 = \frac{(S_0 \beta/\alpha H)_{mR}}{(S_0 \beta/\alpha H)_{m0}} \quad (16)$$

where the subscripts $mR, m0$ denote the values characteristic of month m at sunspot numbers R and zero. It follows that

$$A_E = \left\{ \frac{(S_0)_{mR}}{(S_0)_{m0}} \cdot \frac{(\beta/\alpha H)_{mR}}{(\beta/\alpha H)_{m0}} \right\}^{\frac{1}{4}} \quad (17)$$

Hence the index A_E^4 is proportional to S only if $\beta/\alpha H$ remains constant at all phases of the solar cycle and during all months. Evidence presented by Minnis and Bazzard (1959a, 1960b) shows that this assumption is not justified since the character figure contains a semi-annual cyclic variation, the amplitude of which varies with the solar cycle; this fact suggests the presence of both seasonal and solar cycle changes in $\beta/\alpha H$.

A second problem which arises in the use of the critical frequency ratio as an index is that there is an inherent difficulty which is associated with determination of $f(m, 0)$. Since R never remains at zero during a period of time sufficiently long to allow $f(m, 0)$ to be determined experimentally, it is necessary to find the 12 monthly values of $f(m, 0)$ by extrapolation to $R = 0$. This process is necessarily subject to some uncertainty, and the method used by Allen appears to result in values of $f(m, 0)$ in northern summer that are too high in relation to the winter values; in consequence, the northern summer values of A_E tabulated by Allen tend to be systematically lower than the winter values.

Thus, the critical frequency ratio (A_E) does not eliminate the semi-annual cycle which appears in the E layer character figure and it contains, moreover, an additional annual variation whose origin lies in the need to extrapolate each of the monthly values of $f(m, R)$ down to $f(m, 0)$.

III. IONOSPHERIC INDICES BASED ON THE F_2 LAYER

A. FUNDAMENTAL IDEAS

If the monthly median noon critical frequency (f_0F_2) of the F_2 layer at a particular station is plotted against time, the resulting curve will have two obvious characteristics: the annual cyclic variation and a relatively slow variation which has a period of 10 or 11 years (Fig. 7). The annual cycle

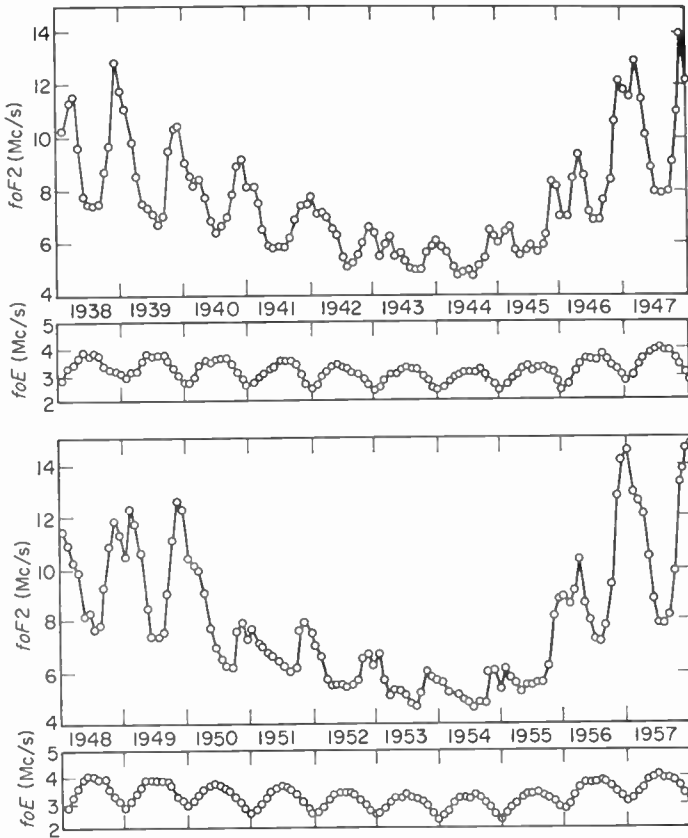


FIG. 7. The monthly mean noon critical frequencies of the E and F_2 layers at Slough. (After Minnis and Bazzard, 1959a.)

is the indirect result of the seasonal variation in the declination of the sun, while the longer cycle is due to the changes in the intensity of the ionizing radiation that is emitted by the sun and which varies with the solar cycle. Variations in f_0F_2 can be expressed formally by the equation:

$$f_0F_2 = \psi(S, m) \tag{18}$$

where ψ represents some function of the month (m) and the intensity (S) of

the solar radiation. If the form of the function ψ were known, it would be possible to transform equation (18) into the form where S is expressed as a function of f_0F_2 :

$$S = \xi(f_0F_2, m) \quad (19)$$

in which S now represents an index of solar activity based on a measured value of f_0F_2 .

Since the relation between f_0E and S is known under certain conditions, such a transformation can be achieved for the E layer, as explained earlier in Section II, B, and it leads to:

$$S = K(f_0E)^4 \sec X \quad (20)$$

Unfortunately, no such transformation is possible for the F_2 layer since the Chapman-layer model, which is valid for the E layer in the circumstances considered earlier, is quite inapplicable to conditions in the F_2 layer. The search for a model which would satisfactorily account for the behaviour of the F_2 layer has so far proved unsuccessful, but this has not prevented the investigation of empirical methods for calculating various F_2 layer indices; these methods do not depend on the availability of analytical expressions based on theory.

It is well known that, for a given station, the monthly mean values of f_0F_2 at a given time of day and for the same month change from year to year as solar activity changes and, if each month is considered separately, equation (18) becomes

$$f_0F_2 = \psi_m(S) \quad (21)$$

As explained earlier, the direct information which is available on the changes in the magnitude of S is insufficient to allow the function ψ to be determined experimentally. If, however, we assume that primary solar indices such as the sunspot number, the calcium index or solar radio noise flux can be expressed as simple functions of S , then equation (21) becomes

$$f_0F_2 = \mu_m(Y) \quad (22)$$

where Y represents the primary index. It is possible to determine the function μ for each month of the year by simple statistical methods and, provided that the relation between f_0F_2 and Y is a linear one, each of the twelve functions can be represented by two parameters which define one of the regression lines relating f_0F_2 and Y for the month in question. Once these twelve regression lines have been constructed, it is obviously possible to use them to convert the measured values of f_0F_2 for any month into the corresponding or equivalent values of Y which, in turn, can be regarded as indices of solar activity based on measurements of f_0F_2 , but converted to the equivalent values of Y or, alternatively, calibrated in terms of Y .

B. F_2 LAYER INDICES DEPENDING ON A PRIMARY INDEX

Goodall (1939a, b) was the first to apply the principle outlined in Section III, A to the production of an F_2 layer index. He used the monthly mean

values of f_0F_2 at 13h local time at Washington for the 6-year period 1933–1938, and he chose as his primary index the calcium character figures for the central zone of the sun’s disc (Fig. 8). Goodall’s main objective was not to produce a set of indices to be used in further applications, but to find a means of defining several constant levels of solar activity as represented by the calcium index. For each of a number of such constant levels, he used

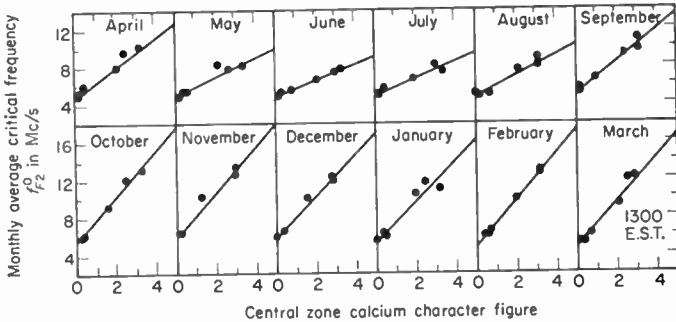


FIG. 8. The correlation between f_0F_2 (Washington 1300 E.S.T.) and central zone calcium character figure. (After Goodall, 1939b.)

the regression lines for 13h, and for other times of day, to derive the diurnal variations of f_0F_2 for each month and the annual variation for fixed times of day.

Each of the index values produced by Goodall depended on a single monthly mean value of f_0F_2 : that for 13h local time at Washington. The values were, therefore, subject to some uncertainty arising from errors of measurement of f_0F_2 and also, in some months, to errors arising from values of f_0F_2 that were unusually high or low depending on the frequency of occurrence of ionospheric storms. The risk of errors due to these causes was reduced by Burkard (1947), who used Goodall’s method to determine an equivalent monthly calcium character figure independently for each of the 24 hours of the day; he then calculated the average of these twenty-four values for each month of the period 1940–1944. By doing so, the effect of accidental errors of measurement was certainly reduced, but it seems possible that the effects of ionospheric storms may have been increased since the greatest changes in f_0F_2 during storm days often occur at night at middle latitude stations such as Kochel (South Germany), the station from which Burkard obtained his observational data.

Phillips (1947) also used the principle originated by Goodall, but adopted the sunspot number instead of the calcium character figure as the primary index. The ionospheric parameter used by Phillips was the mean value of f_0F_2 at Washington for the 5 hours centred on noon. This choice was made after it had been shown that the midday values of f_0F_2 varied with solar activity over a greater range than the values for other times of day. Since the primary index is the sunspot number, the index necessarily uses the same

units as the sunspot number, even though it is based on an ionospheric measurement and this has led to the occasional use of the term "ionospheric sunspot number". Phillips shows plots of the Zürich and the ionospheric sunspot numbers for the years 1934–1947 and it is clear that the erratic fluctuations in the latter are the smaller of the two.

C. INDICES BASED ON IONOSPHERIC DATA FROM SEVERAL STATIONS

Both Burkard and Phillips constructed indices which depended on data from a single observatory and which were, in consequence, sensitive to any changes in the F_2 layer that were due to causes other than variations in the intensity of the incident radiation. The most important of these causes is the arrival in the earth's atmosphere of bursts of corpuscular radiation which lead to disturbances in the ionosphere and which are often accompanied by important changes in f_0F_2 . During the daytime, these disturbances are generally characterized by increases in f_0F_2 at low latitude stations and decreases at middle latitudes. The differences in the sign of the change in f_0F_2 at stations in different locations suggest that it may be possible to combine the data from several stations in order to produce an index which is insensitive to the effects of ionosphere disturbances. This possibility was investigated by Minnis (1955), who used the monthly median noon values of f_0F_2 for Slough, Huancayo and Watheroo, and adopted the monthly mean sunspot number as the primary index. The final index (I_{F_2}) was the mean of the three component indices (R'), each of which was determined using a monthly median measured value of f_0F_2 at noon and the appropriate f_0F_2 - R regression line. Two such lines are shown in Fig. 9 and the index is plotted in Fig. 2.

To test the sensitivity of I_{F_2} to the effects of ionospheric disturbances, Minnis made two superposed epoch tests in which the I_{F_2} values for the months coinciding with the positive and negative peaks respectively in the international magnetic character figure (C) were superposed. The mean pulse amplitudes for C and I_{F_2} were then measured and it was found that the maximum change in I_{F_2} to be expected during a magnetic disturbance was three units measured in terms of the sunspot number scale used by the index I_{F_2} .

Since the index I_{F_2} makes use of sunspot numbers as the primary index, it must necessarily be expressed in terms of the sunspot number scale, just as Goodall's and Burkard's indices use the scale of the calcium index. Once the f_0F_2 - R regression lines have been constructed, it is possible to calculate I_{F_2} for future months without reference to the sunspot numbers for these months. The reason for this is that the same lines can be used indefinitely for future calculations provided that the sunspot and ionospheric data that were used in calculating them covered a number of years which was great enough to provide good approximations to the intercepts and slopes of the regression lines. It is often asked why, in these circumstances, it is necessary to introduce the sunspot number at all, and why it is not possible to derive an index from the f_0F_2 values alone. The answer to this question is that the sunspot number is used in such a way that it provides an absolute scale for

the measurement of solar activity; this scale allows fixed levels of solar activity to be defined in any month of the year. Although this explanation is a plausible one, it is probably easier to accept when it is expressed mathematically as in Appendix I.

The index originally defined by Minnis (1955) was based on ionospheric measurements from only three observatories which were selected in such a way that the combination of the component indices based on the three

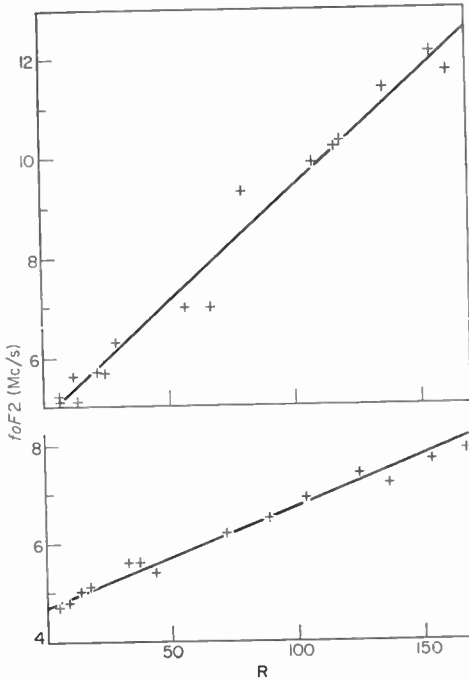


FIG. 9. Regression lines relating 3 month weighted mean sunspot number with noon f_0F_2 at Slough. March (upper line), July (lower line).

values of f_0F_2 for a particular month would give a reliable value of I_{F_2} . There is an obvious risk in using such a small number of stations since if, for any reason, one station were to cease to operate, or if its data were to deteriorate in quality, the index values based on the data from the remaining two stations would be much less reliable.

To minimize this risk, Minnis and Bazzard (1960b) recalculated the index I_{F_2} using the data from eleven stations for which adequate F_2 layer measurements were available from 1942 onwards. It is important to remember that the accuracy with which the parameters of the f_0F_2-R regression lines can be calculated depends on the number of years for which f_0F_2 data are available. This consideration limits the number of stations whose data can be used to calculate such indices. For the eleven stations selected by Minnis

and Bazzard, the data available were nearly complete and they covered a period of 18 years up to 1959. The new I_{F_2} index was the median of the eleven component indices (R') and it seemed advisable to check that none of the stations gave R' values which tended to be consistently far above or far below the monthly median value. This check was made by counting the number of months (Na , Nb) in which each station was responsible for: (a) one of the two highest or the two lowest values of R' ; (b) one of the four values having the smallest departures above and below the monthly median. The ratio Na/Nb was used as an indication of the variability of the R' values for each of the individual stations and the values of the ratio are given in Table I.

TABLE I. *Variability Index (Na/Nb)*

Station	Na/Nb
Washington	0.45
Tokyo	0.57
Churchill	0.65
San Francisco	0.75
Slough	0.80
Fairbanks	0.85
Puerto Rico	0.87
Delhi	0.93
Huancayo	1.04
Canberra	1.06
Godley Head	1.08

Since the variability of the F_2 layer is approximately the same at the stations in the lower part of the table, it was decided to include the data from all the listed stations in the calculation of I_{F_2} . A similar check ought to be made if, at some time in the future, it is decided to recalculate I_{F_2} and if the possibility of including data from additional stations is considered.

The standard deviation of the differences between the individual values of R' for a given month and corresponding value of I_{F_2} was found to be 11.5 units at $I_{F_2} = 9$, and 17.3 units at $I_{F_2} = 161$. Minnis and Bazzard (1959a) have shown that extrapolation down to zero of the fluxes both of the E layer ionizing radiation, as defined by the character figure, and of 10 cm solar radio noise leads to the conclusion that both would probably be very near zero for $I_{F_2} = -160$. If, therefore, $(I_{F_2} + 160)$ is assumed to be very roughly proportional to the flux of the F_2 layer ionizing radiation, the standard deviations quoted above for R' correspond to about 6 per cent of the flux at both minimum and the maximum phases of the solar cycle. Since I_{F_2} is now based on eleven values of R' , its standard error may therefore be regarded as equivalent to approximately 2 per cent of the radiation flux at all stages of the solar cycle.

A great many fairly recently established stations were actually in existence in 1959, but many of them had been in operation for an insufficiently long

period to enable accurate regression lines to be calculated from their ionospheric data. Many of these new stations commenced operation in 1957 at the beginning of the IGY and if some of these continue in full operation until the next peak in the solar cycle in about 1968, it would be possible, but not necessarily worthwhile, to make a new revision of I_{F_2} based on a much larger number of stations than is at present available. For the next few years, however, it is probably not worthwhile to consider the inclusion of data from new stations, but this opinion must be based on the suitability of the present index for the applications in which it is to be used. This subject is discussed in Section IV, F in relation to the use of I_{F_2} in making ionospheric predictions.

D. APPLICATIONS OF F_2 LAYER INDICES

There are two main applications of an index, such as I_{F_2} , that is based on F_2 layer data. Studies of the behaviour of the F_2 layer are complicated by the fact that the changes in the characteristics of the layer that are attributable to seasonal effects are always distorted to some extent by simultaneous short- and long-term changes in solar activity. The availability of an ionospheric index of solar activity would, for example, enable the ionospheric data obtained over a long period of years to be reduced to a form in which the annual changes could be calculated for any required number of different fixed levels of solar activity.

The second application of an F_2 layer index is in the field of radio communications where there is a requirement for an index that can be used in making predictions of the future values of f_0F_2 and of other parameters that are important in the control of the frequencies used in radio communications, and especially in the high-frequency waveband. The application of the index I_{F_2} in this way has been discussed by Minnis (1957).

In both these applications it is desirable to have an index which extends back over as many years as possible in order to provide enough data to permit its use in various statistical processes. It is also desirable that the correlation coefficient between the index and the most important ionospheric parameters should be as high as possible. The linear correlation between the monthly median noon values of f_0F_2 and the index I_{F_2} has been investigated by Minnis and Bazzard (1960a) and found to be 0.986 (see Section IV, F).

E. INDICES DEPENDING ON IONOSPHERIC DATA ALONE

1. *Introduction*

The F_2 layer indices that have been discussed in the preceding sections have all been based on empirically determined relations between f_0F_2 and some primary index of solar activity such as the sunspot number or the calcium character figure. The introduction of the primary index, which is assumed to contain no annual component due to seasonal effects, is necessary in order to provide a reference which, in effect, allows the seasonal variations in f_0F_2 to be eliminated.

It must be admitted that, in principle, it would be preferable to derive an F_2 layer index from the ionospheric data alone; such a method would avoid the complication which arises from the introduction of an auxiliary primary index. Two possible methods of achieving this have been proposed and they are discussed in the following sections.

2. The Critical Frequency Ratio

Allen (1948) has suggested the use of the "relative critical frequency" (A_{F_2}) as an F_2 layer index of solar activity. This index is analogous to the index (A_E) discussed in Section II, F. It is defined by

$$A_{F_2} = f_{F_2}(m, R)/f_{F_2}(m, 0) \quad (23)$$

and hence, if f_{F_2} is assumed to be a linear function of the index R such as:

$$f_{F_2} = a_m + b_m R \quad (24)$$

A_{F_2} can be expressed in the form

$$A_{F_2} = 1 + b_m R/a_m \quad (25)$$

Thus, the variation of A_{F_2} with time depends not only on solar activity as denoted by R , but also on the annual variation in the ratio b_m/a_m at the station from which the measured values of f_{F_2} were obtained. This ratio varies from about 0.20×10^{-2} to 1.00×10^{-2} and there are corresponding variations in A_{F_2} . A sample of values of A_{F_2} corresponding to a sunspot number of 100 is given in Table II.

TABLE II. Values of A_{F_2} for $R = 100$

Station	March	June	December
Slough	1.98	1.35	1.90
Tokyo	1.51	1.41	1.49
Huancayo	1.55	1.52	1.39
Godley Head	1.29	1.95	1.20
Mean	1.58	1.56	1.50

Although the index varies considerably from station to station and from month to month, these variations can be reduced by appropriately selecting the stations and taking the mean value for the sample as shown in Table II. Allen, in fact, used ten stations in his calculation of A_{F_2} , but Minnis and Bazzard (1959a) found that although the residual annual variation in A_{F_2} is small near $I_{F_2} = 50$, it is quite large when solar activity is greater or less than that corresponding to this value.

In addition to the difficulty just referred to, there is the additional problem of determining $f_{F_2}(m, 0)$. As in the determination of $f_E(m, 0)$, referred to in Section II, F, Allen's values for $f_{F_2}(m, 0)$ are too high in northern winter.

3. The 24-h Mean Critical Frequency

The difference between the winter and summer or the day and night values of f_0F_2 is often very great, especially at medium latitude stations. These short-term changes are so large that they tend to obscure the slow long-term changes in f_0F_2 which are attributable to solar cycle changes.

Rawer (1944) found that the mean value of f_0F_2 for all the 24 hours of the day contained a much smaller seasonal variation than the value of f_0F_2 for a single hour. The parameter calculated by Rawer was, in fact, proportional to the mean electron density during the whole day at the peak of the F_2 layer and was defined by

$$Q = \sum_0^{23} (f_0F_2)^2 / 24 \quad (26)$$

Monthly mean values of Q for Kochel for the years 1940–1944 are tabulated by Eyfrig *et al.* (1948), together with the corresponding 13-month running mean values, Q_{13} .

It is reasonable to assume that Q_{13} does not contain any appreciable residual annual component attributable to seasonal effects, and that its variation with time represents the smoothed trend of the solar cycle. The monthly values of the ratio Q/Q_{13} for Kochel do, however, contain a seasonal component whose magnitude was determined statistically using data which were available covering a period of several years. The median values (I) of Q/Q_{13} for the years 1940–1944 have been tabulated by Eyfrig *et al.* and they vary from 0.78 in January to 1.11 in June. Once the values of I for all months have been determined, they can be used as correction factors to remove the seasonal variation from Q . A table of $(Q/I)^{\frac{1}{2}}$ has been tabulated by Eyfrig *et al.* for Kochel; this index is nominally free from seasonal variations and has the dimensions of frequency.

Unfortunately, nothing further has been published on the use of $(Q/I)^{\frac{1}{2}}$ as an F_2 layer index, or on how the corresponding values for other locations agree with those for Kochel, and for Freiburg which later replaced Kochel. In a later paper, Gallet and Rawer (1950) tabulated values of Q_{13} for thirteen stations for the years 1944–1947 and discussed its relation with R_{13} .

IV. SOLAR ACTIVITY INDICES AND IONOSPHERIC PREDICTIONS

A. IONOSPHERIC PREDICTION SERVICES

Important advances have been made in recent years in the techniques of microwave transmission and reception but, in spite of this progress, the high-frequency (HF) waveband (3–30 Mc/s) continues to provide most of the facilities required for the international network of long-distance radio communication systems which covers the world. Radio links that operate in the HF waveband depend for their success on the trapping, between the ground and the ionosphere, of the energy radiated from the transmitter, but this can occur only if the radio frequency used is correctly chosen and if it lies between certain upper and lower limits. When the frequency used is too high, the radiation penetrates the ionosphere and is lost in space; when it is

too low, the energy emitted is nearly all absorbed during its passage through the lower layers of the ionosphere and, in consequence, the field strength at the receiving station may be too low to permit effective operation. These restrictions on the choice of a radio frequency that will provide a satisfactory HF link between two points have led to the establishment of ionospheric prediction services in those countries which maintain large HF radio communication services.

Ionospheric prediction services would obviously be unnecessary if the characteristics of the ionosphere remained constant. As is well known, however, the parameters which define the reflecting and absorbing characteristics of the ionosphere vary from one location to another, and also with the month and the local time of day. These variations, if they occurred alone, would not justify the existence of prediction services because the same conditions in the ionosphere would recur regularly each year and it would be possible to use the same operating frequencies on the same date year after year.

The need for ionospheric prediction services arises as a result of the 11-year cycle of solar activity which leads to rather irregular changes in the ionosphere which are superposed on the regular diurnal and annual changes. Although the length of the solar activity cycle is nominally 11 years, in fact it varies considerably; moreover, the rates of rise and fall of activity during a cycle, and the level of activity reached at the peak, all vary from one cycle to another in a way which cannot be predicted with any great accuracy more than a year or two ahead.

The first requirement of an ionospheric prediction service is, therefore, to find some means of following and predicting the variations in solar activity that are associated with the solar cycle. To do this, it is necessary to adopt an index of solar activity that can be followed regularly and that can be related to the ionospheric parameters for which predictions are required. The factors that determine the choice of such an index can be better appreciated by considering how the ionosphere varies with time.

B. CLASSIFICATION OF IONOSPHERIC VARIATIONS

The variations in the characteristic features of the ionosphere at a given location can be divided into five types:

Type A. Daily and annual variations which are controlled respectively by the zenith angle and the declination of the sun.

Type B. Long-term variations which follow the main trend of the solar cycle and have a period of about 11 years.

Type C. Short-term variations which are due to irregular changes in the main trend of the solar cycle and which frequently have quasi-periods of roughly 1 year.

Type D. Variations which have a period of 27 days and which are caused by the rotation of the sun on its axis.

Type E. Variations which are due to ionospheric disturbances caused by unusual outbursts of radiation from the sun and which usually last for several days.

As already explained, the variations of Type A would not, by themselves, warrant the establishment of prediction services; the need for these services arises from the existence of the irregularities in the variations referred to as Types B, C and D and from the erratic variations which are associated with the occurrence of ionospheric disturbances, Type E.

C. CLASSIFICATION OF IONOSPHERIC PREDICTIONS

The prediction services which are in actual operation vary from one country to another, but the predictions provided usually fall into three categories, which may be described briefly as follows:

1. *Long-range Predictions*

The aim is to make approximate predictions of the radio frequencies that will be required one or more years ahead. Such predictions are needed in order to make plans for the future availability of equipment at radio transmitting and receiving stations.

2. *Short-range Predictions*

These are usually made about 6 months ahead and the intention is to predict, as accurately as possible, the monthly median values of selected ionospheric parameters. These predictions provide the information needed for the optimum use of the frequency allocations which have been made available to the operating organization.

3. *Disturbance Forecasts*

These provide advance information a few days, or perhaps weeks, ahead on the probable day-to-day changes in ionospheric characteristics.

Long-range predictions refer only to the variations of Type B, since only the main trend of the solar cycle can be predicted for periods more than about 1 year ahead. Short-range predictions are intended to take into account not only the main trend but also the short-lived irregularities of Type C. Since short-range predictions refer only to the monthly median values of ionospheric characteristics, they cannot provide any information about the day-to-day variations above and below the median which are referred to as Types D and E. For prediction purposes, it is probably best to regard both Types D and E as disturbances and to attempt to predict them together; such predictions can then be regarded as providing some more recent information on how the previously issued monthly median short-range prediction may have to be modified on certain days during the month in question.

D. THE CHOICE OF AN INDEX FOR IONOSPHERIC PREDICTIONS

It is now possible to see how the choice of a solar activity index will be determined by the type of prediction to be made.

1. *Long-term Predictions*

When it is required to predict the trend of solar activity a year or more ahead, or to predict the probable degree of activity during the next maximum,

the only satisfactory index which is available for use is the 12-month running mean of the Zürich sunspot number. The sunspot number is available as a continuous series of values extending back for 200 years and the data are sufficiently numerous to permit extrapolation by mathematical and statistical methods. The accuracy provided by such predictions is not high since, in fact, the 200 years represent only 20 solar cycles. Such a small sample is insufficient to allow accurate predictions to be made but, since no index other than sunspot number would lead to better results, it is difficult to see how the accuracy of long-term predictions can be improved in the foreseeable future.

2. *Short-term Predictions*

For short-term predictions, which are usually made 6 to 12 months ahead, the monthly mean sunspot number is unsatisfactory. This is because the number tends to fluctuate in a rather erratic manner which is often not matched by corresponding changes in the ionosphere. These erratic changes are, therefore, not always relevant to ionospheric predictions and, since they obscure the short-term trend, it is difficult to extrapolate the trend of the monthly mean sunspot number. The smoothing referred to under long-term predictions is not acceptable for short-term predictions because it smooths out not only the unwanted fluctuations but also the real short-term changes which are reproduced in the ionosphere and which ought to be taken into account when short-term predictions are made.

Indices, other than the monthly mean sunspot number, which are actually available at present and which could be used for short-term predictions, include the flux of solar noise near 10 cm (ϕ), the F_2 layer index (I_{F_2}), and the 3-month weighted mean (1 : 2 : 1) sunspot number (R_3). The relative merits of these indices for use in short-term ionospheric predictions are discussed briefly in the next section.

E. THE CHOICE OF AN INDEX FOR SHORT-TERM PREDICTIONS

The process of making an ionospheric prediction consists of two independent steps: (1) the prediction of the value of the index for the date in question; (2) the conversion of the predicted index value into the corresponding values of the required ionospheric parameters.

For the first step, the ideal index would be one in which the variations were entirely due to the solar cycle variations referred to as Types B and C in Section IV, B. It ought not to contain large erratic fluctuations or annual or semi-annual components such as could arise from the incomplete removal of seasonal components from the original data; all these would add to the difficulties of extrapolating the index.

The second step requires a knowledge of the statistical relation between the index and the parameter to be forecast. Such relations can be established with reasonable precision only after observations of both the index and the parameter have been made for at least one solar cycle. Once the statistical relation is known, the accuracy with which any single prediction of the index

can be converted into the equivalent value of the ionospheric parameter depends on the correlation coefficient between the index and the parameter.

Hence, tables of values of an index which is to be used for short-term predictions ought to be available for at least 10 and preferably 20 years; in addition, the index ought to be highly correlated with the most important ionospheric parameters. It is also worth remembering that it would be helpful to those who are responsible for making the actual radio frequency predictions if the index were linearly related to the principal ionospheric parameters. This last criterion is probably of greatest importance where digital computers are used to calculate maximum usable frequencies and where it is necessary to store the data which define the regression lines.

F. RELATIVE MERITS OF INDICES FOR SHORT-TERM PREDICTIONS

The most important ionospheric parameter for which predictions are required is the monthly mean value of f_{F_2} , which determines the maximum radio frequency which can be used in communicating between two points. For this reason, the correlation coefficient between the index and monthly median value of f_{F_2} is frequently used as a criterion of the merit of an index. These coefficients have been calculated by Minnis and Bazzard (1960b) for eight locations for each of a number of possible indices and are shown in Table III. The histograms in Fig. 10 illustrate the variability of the correlation coefficients for three indices.

TABLE III. *Correlation between f_0F_2 at Noon and Indices of Solar Activity*

Index	Linear correlation coefficient
I_{F_2}	0.986
R_3	0.967
R_1	0.960
ϕ	0.945

Key

- I_{F_2} The F_2 layer index based on data from 11 stations (Section II, C).
- R_3 The 3-month weighted mean (1 : 2 : 1) sunspot number.
- R_1 The monthly mean sunspot number.
- ϕ The monthly mean solar radio noise flux at 10.7 cm.

The relation between I_{F_2} and f_{F_2} is nearly always very close to a linear one, whereas the corresponding relations with ϕ tend to be slightly curved according to evidence presented by Minnis and Bazzard (1959a). It is possible that this non-linear relation may account for the low correlation coefficient for ϕ .

At its Xth Plenary Assembly in 1963, the CCIR recommended the use of the 12-month running mean sunspot number for long-range predictions of

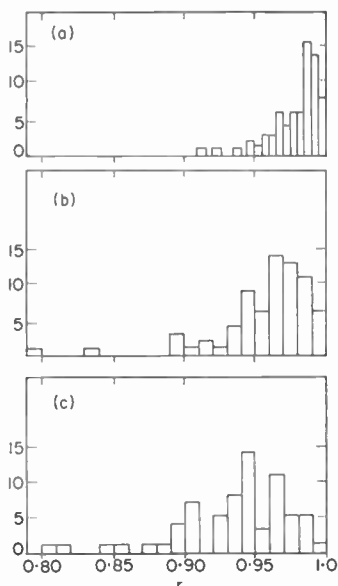


FIG. 10. The distribution of linear correlation coefficients at noon.

(a) $f_0F_2 - I_{F_2}$,

(b) $f_0F_2 - R_3$,

(c) $f_0F_2 - \phi$.

(After Minnis and Bazzard, 1960a.)

the frequencies to be used in radio communications. For short-range predictions, the index I_{F_2} was recommended (CCIR, in press).

It would probably not be worthwhile to search for an index that had a much greater mean correlation coefficient with f_0F_2 than I_{F_2} . The practical limit to the correlation between I_{F_2} and f_0F_2 is determined by the correlation between values of f_0F_2 at stations in different parts of the world. This correlation is not perfect and, at high latitude stations in particular, the effects due to the particle streams discussed in Section V, A may reduce the correlation. This difficulty has been described by Kerblai and Kovalevskaya (1960).

V. OTHER IONOSPHERIC INDICES

A. PARTICLE STREAMS

The ionospheric indices which have been described in Sections II and III depend primarily on the state of the E and F_2 layers under average conditions which are determined mainly by the flux of ultra-violet and X-radiation from the sun. From time to time streams of charged particles are emitted from the sun and some of these streams later impinge on the earth's atmosphere where they give rise to auroral displays, magnetic storms, ionospheric disturbances and other phenomena. The recording of auroral

phenomena and the derivation of the many types of indices which are used to denote variations in magnetic activity are subjects which are not relevant to this review, even though such observations form a useful indication of one type of solar activity.

The ionospheric disturbances which have just been mentioned are caused by the arrival in the atmosphere of particle radiation from the sun. For this reason, they have long been regarded as qualitative indices of solar particle emission. The two main types of ionospheric disturbance which are useful in this respect are the large increases in D layer ionization, which give rise to radio blackouts at stations in polar latitudes, and the sudden increases and decreases in the critical frequency of the F_2 layer. The main reason for trying to reduce these types of observation to numerical index form is that in attempts to understand the normal undisturbed ionosphere it is often necessary to know how much disturbance is present on a given day and to make corrections for this. The derivation of such indices and indeed the study of ionospheric disturbances in general also has a bearing on the prediction of the Type E disturbances referred to in Section IV, C.

The analysis of the geophysical data obtained during the IGY lent impetus to the development of indices of the flux of particles from the sun. Unfortunately, it is not possible to link the phenomena which can actually be observed with the characteristics of the stream of particles because the mechanism of the interaction of the stream with the atmosphere is not well understood. The only possibility at present is to interpret the observations subjectively.

Piggott (1960a) has tabulated a daily polar blackout index for the period April 1957–December 1958. This index is based on the number of hours of blackout at twenty-seven polar ionospheric stations. The index runs from 0–9 and values are tabulated for the northern and southern hemispheres. In addition, a weighted index for the whole world is given. It is important to note that the stations have been selected to cover, as far as possible, the whole range of geomagnetic longitudes. The index is designed so as to exclude the effects of blackout over the polar cap itself since this condition is mainly associated with quiet conditions.

A daily F_2 layer disturbance index has been tabulated by Piggott (1960b) for the period July 1957–December 1958. This index is based on nine observable characteristics of the F_2 layer which can be deduced from f -plots or from original ionograms. The data from eighteen well-distributed stations were used to derive the index which runs from 0 to 5. Even though these two indices depend on totally different types of ionospheric data, and in spite of the difficulties of assigning numbers based on subjective interpretation of the data, it is satisfactory to note that the two indices seem to agree very well with each other.

B. D LAYER ABSORPTION

Appleton and Piggott (1954) have described a long series of measurements covering about two solar cycles of the absorption of radio waves in the D layer of the ionosphere. This layer lies below the E layer and its ionization is caused by components of the solar radiation which have passed through

the upper levels of the atmosphere without being absorbed. There is a close resemblance between the variations of the absorption and of solar activity as indicated by the sunspot number when monthly mean values of both

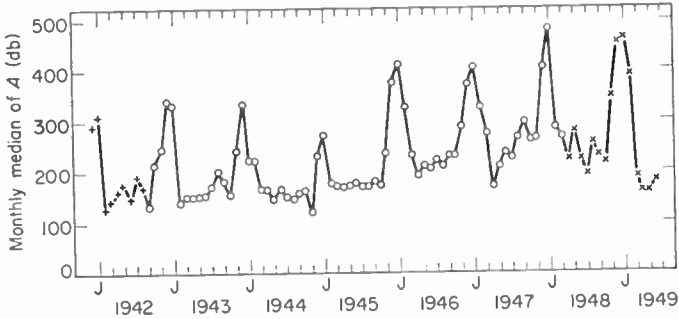


FIG. 11. A D layer absorption index for Slough which shows the anomalous high values in local winter. (After Appleton and Piggott, 1954.)

quantities are compared. The absorption values in winter are greater than would be expected by comparison with the summer values and this so-called winter anomaly, the origin of which is not known, detracts from the value of the data as a simple index of solar activity (Fig. 11).

APPENDIX I

THE ROLE OF THE SUNSPOT NUMBER IN THE DERIVATION OF THE INDEX I_{F_2}

A. We shall assume that for month m , the median value of f_0F_2 at a given time of day can be represented as a linear function of some ideal solar index, $A(t)$, which varies with time t . Hence we can write:

$$f_0F_2 = f(m, t) = a(m) + b(m)A(t) \quad (1)$$

We shall choose two reference values of the index, A_0 and A_1 , which correspond approximately to the minimum and the maximum values attained during the solar cycle.

Consider the ratio $\gamma(t)$ defined by:

$$\gamma(t) = \frac{f(m, t) - f(m, A_0)}{f(m, A_1) - f(m, A_0)} \quad (2)$$

When equations (1) and (2) are combined, we find

$$\gamma(t) = \frac{A(t) - A_0}{A_1 - A_0} \quad (3)$$

Hence, provided that the constants $f(m, A_0)$ and $f(m, A_1)$ can be determined for all values of m , that is for all months of the year, $\gamma(t)$ can be regarded as an index which is characteristic of the epoch t and which depends only on a

single measured value $f(m, t)$ of the critical frequency. Equation (3) shows that $\gamma(t)$ is independent of m ; that is, its variation with time contains no annual component, and hence its magnitude depends only on that of the ideal index A . The index $\gamma(t)$ obviously runs from near 0 at sunspot minimum to approximately 1 at sunspot maximum and it represents the degree of solar activity at any epoch as a fraction of the total range of values represented by $A_1 - A_0$.

B. We shall now make the arbitrary assumption that throughout the years 1954 and 1958, $A(m)$ remained close to the reference values A_0 and A_1 respectively, and that the departure of the actual value from the reference value in any month can be represented by $\delta A(m)$. It follows that:

$$A_{54}(m) = A_0 + \delta A_{54}(m) \tag{4}$$

$$A_{58}(m) = A_1 + \delta A_{58}(m) \tag{5}$$

$$f(m, A_0) \simeq f(m, 54) \tag{6}$$

$$f(m, A_1) \simeq f(m, 58) \tag{7}$$

If the approximate values of $f(m, A_0)$ and $f(m, A_1)$ given by equations (6) and (7) are inserted in equation (2) together with the measured value of $f(m, t)$, it can easily be shown with the help of equation (1) that:

$$\gamma(t) = \left(\frac{A(t) - A_0}{A_1 - A_0} \right) \left(\frac{1 - \delta A_{54}(m) / (A(t) - A_0)}{1 - \{ \delta A_{58}(m) - \delta A_{54}(m) \} / (A_1 - A_0)} \right) \tag{8}$$

Unless both $\delta A_{54}(m)$ and $\delta A_{58}(m)$ are always zero, the second term in equation (8) will vary with m . This means that any month-to-month variations in A that may have occurred during one or both of the two reference years will be reflected in all future values of $\gamma(t)$. In other words, any series of values of $\gamma(t)$ which covers a period of years will contain a spurious annual component which will modulate the correct sequence of values by an amount represented by the second term in equation (8). It is not difficult to see that, in order to remove this modulation, it is necessary to find some method of determining how $f(m)$ varies during the year for a constant value of A . If this can be done, it is possible to obtain the values of $f(m, A_0)$ and $f(m, A_1)$ which are required in equation (2). Since, in fact, A never remains constant for 12 months, $f(m, A)$ can never be determined by direct experiment.

C. It is not immediately obvious what is meant in practice by a constant level of "solar activity" and the term can, in fact, be defined only after the adoption of some already available index, the magnitude of which is assumed to be a measure of "solar activity" alone and to be independent of terrestrial influences. It is reasonable to assume that the so-called "primary indices" such as the Zürich sunspot number, 10 cm solar radio noise flux, and others which depend also on the direct measurement of physical characteristics of the sun, are measurements of "solar activity" alone. The justification for this assumption is that the measurements on which these indices are based

are of such a kind that they are unlikely to be subject to any terrestrial influence which could introduce an important annual variation into the magnitude of the index.

We shall assume that the sunspot number R has been selected as the measure which is to be used to define constant solar activity, and that the two values R_0 and R_1 have been chosen to represent A_0 and A_1 , the two reference levels that have been referred to earlier. Hence we put:

$$f(m, A_0) = f(m, R_0) \quad (9)$$

and

$$f(m, A_1) = f(m, R_1) \quad (10)$$

For each month of the year, the monthly mean values of $f(m)$ can be plotted against those of R and, using the least squares method, a regression line can be drawn which enables the most probable value of f to be determined for any given value of R . By this means the twenty-four values of f which correspond to R_0 and R_1 in each of the 12 months of the year can be determined; these values will be written $f_L(m, R_0)$ and $f_L(m, R_1)$ and used instead of $f(m, A_0)$ and $f(m, A_1)$ respectively. Substitution of these values for $f(m, A_0)$ and $f(m, A_1)$ in equation (2) gives:

$$\gamma(t) = \frac{f(m, t) - f_L(m, R_0)}{f_L(m, R_1) - f_L(m, R_0)} \quad (11)$$

As already indicated by equations (2) and (3), this ratio can be regarded as an index which represents the level of solar activity expressed as a fraction of the range between minimum and maximum activity.

D. The index $\gamma(t)$ depends only on ionospheric measurements, but it is more convenient to convert it to a scale of numbers which corresponds to the sunspot number scale. The reason for this is that the general behaviour and the statistical characteristics of R are well known and it is often useful to make direct comparisons between R and a new index which denotes long-term changes in the ionosphere. This conversion gives:

$$Z(t) = R_0 + \gamma(t)[R_1 - R_0] \quad (12)$$

The substitution in equation (12) of the expression for $\gamma(t)$ which has been given in equation (11) leads to:

$$Z(t) = R_0 + \frac{f(m, t) - f_L(m, R_0)}{[f_L(m, R_1) - f_L(m, R_0)](R_1 - R_0)} \quad (13)$$

$$= R_0 + \frac{f(m, t) - f_L(m, R_0)}{\frac{df(m)}{dR}} \quad (14)$$

If the value of R_0 is chosen so as to represent the lowest solar activity possible, then $R_0 = 0$ and equation (14) becomes

$$Z(t) = \frac{f(m, t) - f(m, 0)}{\frac{df(m)}{dR}} \quad (15)$$

But this is the definition of R' , the basic parameter which is used in calculating the index I_{F_2} which is the median value of R' for a number of long-established ionospheric observatories for which sufficient data are available to allow $f(m, R_0)$ and $df(m)/dR$ to be determined with a reasonable degree of accuracy.

E. It is concluded that the essential role of the sunspot number in the derivation of I_{F_2} is to provide a definition of constant solar activity. Once this has been done, the constants $f(m, A_0)$ and $f(m, A_1)$, which are needed in the calculation of $\gamma(t)$ using equation (2), can be determined. Unless the sunspot number or some other primary index is used to define constant solar activity, there is no means by which the values of $\gamma(t)$ for different months of the year can be related to each other.

ACKNOWLEDGMENT

The author acknowledges with thanks the permission of the publishers to reproduce the following figures:

Figure 1. *Philosophical Magazine* (Taylor and Francis Ltd., London).

Figures 2, 6, 7, 10 and 11. *Journal of Atmospheric and Terrestrial Physics* (Pergamon Press Ltd., Oxford).

Figure 8. *Proceedings of the Institute of Radio Engineers* (The Institute of Electrical and Electronic Engineers Inc., New York).

REFERENCES

- Allen, C. W. (1948). *Terr. Magn. atmos. Elect.* **53**, 433.
 Appleton, E. V., and Naismith, R. (1939). *Phil. Mag.* **27**, 144.
 Appleton, E. V., and Piggott, W. R. (1954). *J. atmos. terr. Phys.* **5**, 141.
 Appleton, E. V., Lyon, A. J., and Turnbull, A. G. (1955). *Nature, Lond.* **176**, 897.
 Bazzard, G. H. (1960). *J. atmos. terr. Phys.* **18**, 290.
 Bazzard, G. H. (1961a). *Nature, Lond.* **189**, 47.
 Bazzard, G. H. (1961b). *J. atmos. terr. Phys.* **21**, 193.
 Beynon, W. J. G., and Brown, G. M. (1956). *Nature, Lond.* **177**, 583.
 Beynon, W. J. G., and Brown, G. M. (1959a). *J. atmos. terr. Phys.* **14**, 138.
 Beynon, W. J. G., and Brown, G. M. (1959b). *J. atmos. terr. Phys.* **15**, 168.
 Burkard, O. (1947). *Acta. phys. austr.* **1**, 98.
 Chapman, S. (1931). *Proc. Phys. Soc. Lond.* **43**, 26 and 483.
 Chapman, S. (1940). In "Geomagnetism" (S. Chapman and J. Bartels), p. 215.
 CCIR (1959). Documents, IXth Plenary Ass. CCIR, 1959 (International Telecommunications Union, Geneva).
 CCIR (in press). Documents, Xth Plenary Ass. CCIR, 1963 (International Telecommunications Union, Geneva).
 CSAGI (1962). *Ann. IGY*, Vol. XVI.
 Denisse, J. F., and Kundu, M. R. (1957). *C. R. Acad. Sci., Paris* **244**, 45.
 Eyfrig, R. (1960). *Geofis. pur. appl.* **45**, 179.
 Eyfrig, R. (1962). *Nature, Lond.* **196**, 758.

- Eyfrig, R., Gallet, R., and Rawer, K. (1948). *Rapp. Serv. Préviation Ionosphérique Marine*, no. SPIM-R2.
- Gallet, R., and Rawer, K. (1950). *Ann. Géophys.* **6**, 104 and 212.
- Goodall, W. M. (1939a). *Nature, Lond.* **143**, 977.
- Goodall, W. M. (1939b). *Proc. Inst. Radio Engrs, N.Y.* **27**, 701.
- Harnischmacher, E. (1950). *C. R. Acad. Sci., Paris* **230**, 1301.
- Harnischmacher, E. (1955). *C. R. Acad. Sci., Paris* **240**, 553.
- Kerblai, T. S., and Kovalevskaya, E. M. (1960). *Ionospheric Researches*, Moscow, no. 3, p. 22.
- Medd, W. J., and Covington, A. E. (1958). *Proc. Inst. Radio Engrs, N.Y.* **46**, 112.
- Minnis, C. M. (1955). *J. atmos. terr. Phys.* **7**, 310.
- Minnis, C. M. (1957). *Ann. Télécomm.* **12**, 164.
- Minnis, C. M. (1960a). *URSI Inform. Bull.* no. 120, p. 10; no. 121, p. 10.
- Minnis, C. M. (1960b). *Proc. XIIIth Gen. Assy. URSI*, Vol. XII, Part 3, p. 10.
- Minnis, C. M. (1961). *URSI Inform. Bull.* no. 124, p. 47.
- Minnis, C. M. (1964). *Nature, Lond.* in press.
- Minnis, C. M., and Bazzard, G. H. (1958). *Nature, Lond.* **181**, 1796.
- Minnis, C. M., and Bazzard, G. H. (1959a). *J. atmos. terr. Phys.* **14**, 213.
- Minnis, C. M., and Bazzard, G. H. (1959b). *J. atmos. terr. Phys.* **17**, 57.
- Minnis, C. M., and Bazzard, G. H. (1960a). *J. atmos. terr. Phys.* **18**, 297.
- Minnis, C. M., and Bazzard, G. H. (1960b). *J. atmos. terr. Phys.* **18**, 306.
- Phillips, M. L. (1947). *Terr. Magn. atmos. Elect.* **52**, 321.
- Piggott, W. R. (1960a). In "Some Ionospheric Results of the IGY" (W. J. G. Beynon, ed.), p. 94, Elsevier, Amsterdam.
- Piggott, W. R. (1960b). *ibid.* p. 116.
- Rawer, K. (1944). *Deutsche Luftfahrtforschung FB*, no. 1943 (see *Rev. sci., Paris*, 1947, **85**, 234).
- Rawer, K. (1959). *Geofis. pur. appl.* **43**, 218.
- Shimazaki, T. (1959). *J. Radio Rad. Lab. Japan.* **6**, 109.

ANTENNAS AND RECEIVERS FOR RADIO ASTRONOMY

JOHN W. FINDLAY

*National Radio Astronomy Observatory †
Green Bank, West Virginia, U.S.A.*

Introduction	37
I. Receivers for Radio Astronomy	38
A. Introduction	38
B. Low-noise Radiometers	45
C. Radiometer Stability	56
D. Radiometer Calibration	70
E. Radiometers for Special Purposes	71
II. Parabolic Reflector Antennas	72
A. Introduction	72
B. The Choice of Antenna Specifications	72
C. The Performance of a Parabolic Dish Antenna	74
D. Characteristics of Some Specific Antennas	80
III. Other Types of Radio Astronomy Antennas	93
A. Introduction	93
B. Reflector Antennas	93
C. 2-element Interferometers	98
D. Unfilled Apertures of High Resolution	104
E. The Technique of Aperture Synthesis	108
References, Section I	112
References, Section II	115
References, Section III	116
References, General	119

INTRODUCTION

Radio astronomy is the study of the radio waves naturally emitted by astronomical objects such as the sun, moon, and planets, our own galaxy and other galaxies and clusters of galaxies far distant from our own. The amounts of radio energy received on earth from even the most powerful sources are very small. The science has grown, therefore, mainly because experimenters have built antennas of very large collecting area, and have observed with receivers of very high sensitivity and stability.

It is the purpose of this review to describe the principles behind the design of such antennas and receivers, and to show how such instruments have been built and used in recent years. In writing this review the author has been influenced both by his own interests, which lie very much toward the experimental approach to building instruments, and by the existence in print of the article by Bracewell (1962) in the *Handbuch der Physik*. It is hoped that

† The National Radio Astronomy Observatory is operated by the Associated Universities, Inc., under contract with the National Science Foundation.

this present review may complement that of Bracewell to some extent, and so it has omitted the consideration of some subjects where reference to Bracewell will provide the necessary description.

It will also be evident that the collections of articles in the January 1958 issue of the Institute of Radio Engineers, the January 1961 issue of the I.R.E. *Transactions on Antennas and Propagation*, and the February 1963 issue of the *Proceedings of the Australian Institution of Radio Engineers* have provided many of the references throughout this article.

The author is indebted to Dr. E. G. Bowen for permission to use the plate of the 210-ft telescope, and to Dr. J. D. Kraus for permission to use the photograph of his telescope. He has also received much help from the staff of the National Radio Astronomy Observatory.

I. RECEIVERS FOR RADIO ASTRONOMY

A. INTRODUCTION

A radio astronomy receiver or radiometer is the device which measures the radio frequency power available from the antenna system. The receiver amplifies the power over a range of frequencies centered on the frequency being used, detects the power, and integrates or filters the result before recording it. Figure 1 shows in its simplest form the general elements of

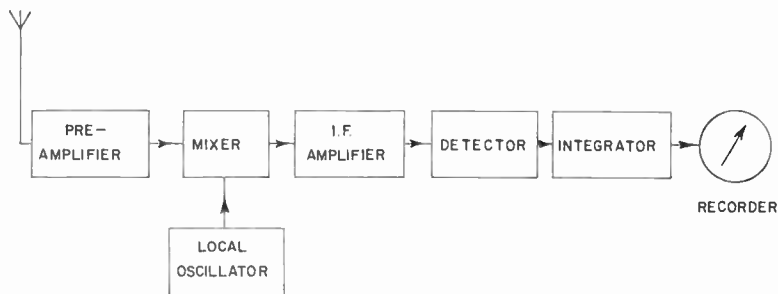


FIG. 1. The block diagram of a radiometer.

such a receiver, and the principles of receivers are well described in standard texts (Pawsey and Bracewell, 1955; Shklovsky, 1960, for example). We will define some of the important parameters of the receiver, referring to Bracewell (1962) for fuller descriptions.

1. Main Parameters of Receivers

a. *Central Frequency* (f Mc/s). The output of the antenna (Fig. 1) is fed to the preamplifier, which provides gain over a range of radio frequencies. The central frequency is the frequency at which observations are being made and is usually at the center of the preamplifier frequency response.

b. *Gain* (G). The receiver is intended to convert the very small change in power (perhaps only about 10^{-17} W) due to a radio astronomy source in the antenna beam into a power capable of being recorded. It is seldom of

interest to refer to the overall gain of a receiver, although this could be simply defined as

$$G_{\text{total}} = \frac{\text{Output power to recorder}}{\text{Input power to receiver}} \quad (1)$$

Since about 10^{-3} W will operate a conventional pen recorder, G_{total} might be 10^{14} expressed as a ratio, or 140 db. The total gain of the receiver is usually provided before the detector by the preamplifier and the IF or main amplifier and after detection by low-frequency or direct current-amplifiers. G will depend on the radio frequency fed to the receiver, and is often a function of the size of the input signal to the receiver.

c. Bandwidth (B Mc). The gain of the whole receiver is large only over a relatively narrow range of frequencies, known as the bandwidth, normally symmetrically placed with respect to the central frequency. In a receiver such as Fig. 1, the bandwidth would probably be determined by the intermediate frequency amplifier, although receivers with the bandwidth set by the properties of the signal frequency amplifier are known. The bandwidth B (sometimes known as the pre-detector bandwidth) is always determined at some point in the receiver before the signal reaches the detector.

d. Time Constant (τ sec). The signal leaving the detector is still fluctuating with time, and it is necessary to smooth out the fluctuations before recording the signal. In its simplest form, this smoothing may be done by a resistor and capacitor network forming a low-pass filter or by making a time integral of the detector output over a fixed integration time. Whatever means of smoothing is adopted, the result is to provide a number of statistically independent measures of the detector output per second of time. The reciprocal of this number we will refer to as the time constant (τ) of the integrator. It is related to the characteristics of the integrator (Bracewell, 1962, p. 50).

e. Effective Input Noise Temperature (T_e °K). We have now stated the important characteristics of a noise-free radiometer. Practical receivers always generate noise within themselves and the antenna also may generate or receive unwanted noise. A good radiometer is one which allows radio astronomical signals to be detected most easily and measured most accurately in the presence of such noise. In order to describe this noise consider the behavior of a simple receiver (Fig. 2a). Assume first that the receiver generates no noise, and that it is connected not to an antenna but to a matched resistor in an enclosure at T °K. The available noise power which such a resistor can deliver to the receiver within its bandwidth B is

$$P = kTB \text{ watts} \quad (2)$$

where k is Boltzmann's constant (1.38×10^{-16} erg/deg) and the output meter will show a deflection due to this input power. Equation (2) is, of course, derived from Nyquist's formula for the thermal noise power generated in a resistor. If the temperature of the resistor were reduced to 0°K no noise power would be delivered to the noiseless receiver (Fig. 2b), and the output meter deflection would be zero. Under these same conditions, assume the

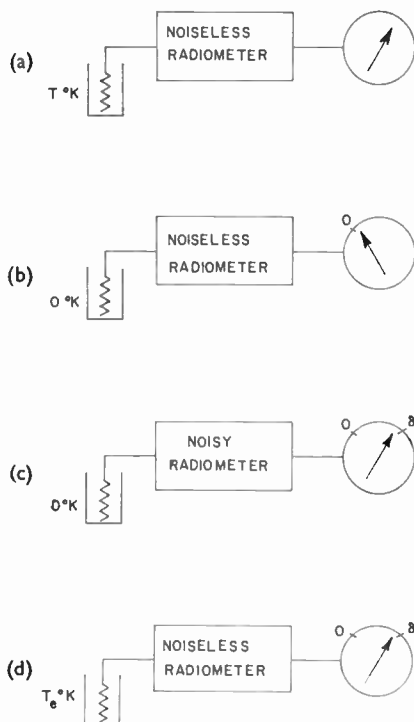


FIG. 2. The noise temperature T_e of a radiometer.

receiver now to become noisy (Fig. 2c), generating its own noise power and thus deflecting the recorder by an amount δ . Then imagine the receiver returned to its noise-free state and the temperature of the resistor increased to a value T_e so that the same deflection δ occurs (Fig. 2d) as with the noisy receiver. T_e is defined as the effective input noise temperature of the noisy receiver.† This definition of the internal noise of a receiver in terms of an equivalent noise input power is related to the well-known noise factor (F) of the receiver by the relation

$$T_e = (F - 1) \times 290^\circ \text{K} \quad (3)$$

For a standard definition of terms describing the noise performance of amplifiers and receivers, see Haus (1963).

2. The Radio Astronomy Signal

a. The Nature of the Signal. To complete the preliminary survey of the use of radiometers a brief description of the signal received in radio astronomy will now be given. As a rough first approximation it can be said that all radio

† T_e should be written $(T_e)_{av}$ throughout to conform to Haus (1963) and the IRE specification. We will often also omit the words "effective input" and call T_e the noise temperature.

astronomy signals are “white” noise, which has the following characteristics:

- (i) Its power spectral density function is constant over all frequencies, or
- (ii) Its autocorrelation function is a constant times the unit impulse function.

However, even if the radio astronomy signal were truly white noise as it impinges on the antenna, its characteristics would be modified by the antenna and receiving system. Before the noise signal reaches the detector, it has been forced to pass through various parts of the receiver. By the time this incident noise power has passed through the predetector bandwidth, the noise power has been modified,† and it is now much more nearly true to describe the noise power as “bandwidth-limited white noise”. The degree to which this approximation approaches the truth depends on:

- (i) The power spectral density function of the noise before it reaches the antenna.
- (ii) The width of the predetector bandwidth.

Experimental evidence on (i) can be derived by measuring the power received from a radio source within a finite bandwidth whose center is placed at various frequencies throughout the usable radio spectrum. The kind of spectra measured are illustrated in Fig. 3. This figure illustrates the fact that though no radio source is truly a white noise emitter, the noise power received from such sources can be accurately described as bandwidth-limited white noise so long as the predetector bandwidth is chosen to be so small that the spectral density function of the source is approximately constant over the chosen bandwidth. For various measurements, therefore, different bandwidths are chosen. The condition is obviously met in cases (a)–(c) of Fig. 3 if bandwidths of a few Mc/s are used. For the study of neutral hydrogen (Fig. 3d) bandwidths of 10–20 kc/s usually are used. We shall, therefore, in what follows, assume that the characteristics of the radio astronomy noise powers to be measured are those of bandwidth-limited white noise.

Such signals must be measured in the presence of noise originating in the atmosphere, the antenna and the whole receiver system. It is quite adequate to describe all these unwanted noise powers also as bandwidth-limited white noise, unless the receiver is subjected to interference from man-made or similar types of noise disturbance. In these latter types of noise, the power spectral density function often departs very considerably from even the bandwidth-limited white noise approximation. For other reasons, radio astronomy observations cannot usually be made in the presence of man-made interference, and so we can avoid the discussion of the problem of such noise.

b. Antenna Temperature (T_A °K). When a radio astronomy signal is received, a convenient measure of the available power from the antenna

† The signal as it passes from the antenna through the receiver suffers several other changes which are well illustrated in Pawsey and Bracewell (1955, p. 36).

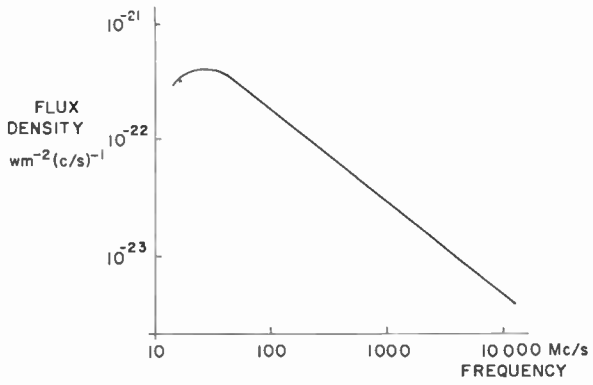


FIG. 3a. The radio source Cas A.

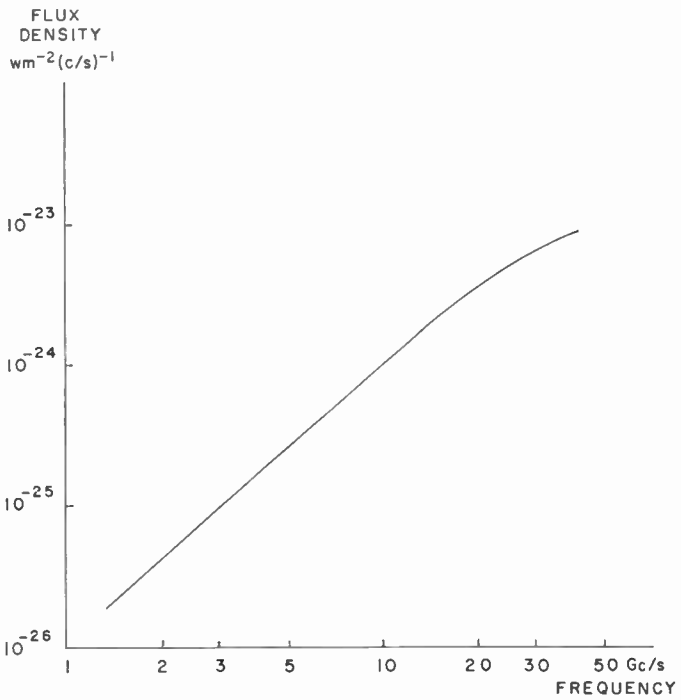


FIG. 3b. The planet Venus when its disk semi-diameter is $30''$ of arc.

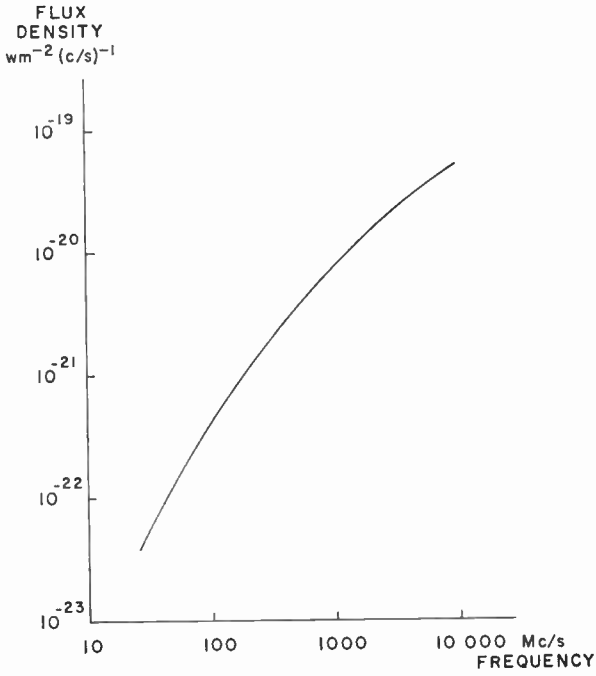


FIG. 3c. The quiet sun at sunspot maximum.

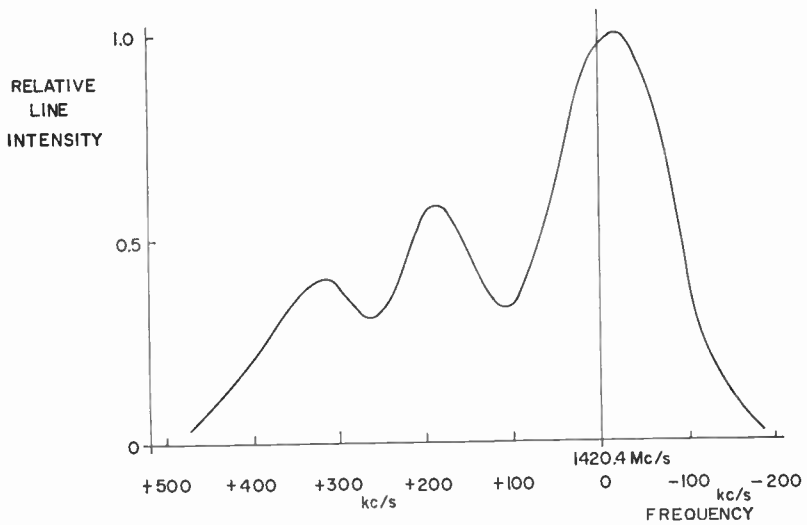


FIG. 3d. Neutral hydrogen in the galaxy. (van der Hulst *et al.*, 1954.)

FIG. 3. Spectra of some typical radio sources.

terminals is that of antenna temperature. Just as the thermal power available from a resistor is related to the absolute temperature of that resistor (equation (2)), so may the power available from the antenna be related to a corresponding antenna temperature T_A .

$$\text{Available power} = kT_A B \quad (4)$$

The methods of using and calibrating a radiometer generally result in a knowledge of the change of T_A due to the radio astronomy signal, so that the concept of antenna temperature is convenient to use throughout as a measure of the power delivered to the receiver.

3. Desirable Radiometer Characteristics

Having reviewed the various parameters of a radiometer, we can now state generally what are its desirable characteristics. Simply to detect the smallest signals the radiometer must be sensitive; to measure these signals accurately it must be stable. This statement is of course over-simplified, in that some stability is needed even to detect a source, but it conveniently divides the scope of the techniques which must be used.

a. Sensitivity. The sensitivity of a radiometer is measured by the smallest change in T_A which the instrument can detect. Even if the stability of a radiometer were perfect, the total noise made up from noise from the radiometer T_e , together with antenna noise and atmospheric noise, limits the sensitivity of the instrument. If the total noise in the radiometer system be represented by T_{op} °K (T_{op} is called the system or operating noise temperature), then it is well known that the r.m.s. fluctuations of the radiometer output signal (ΔT_A), measured in terms of changes of antenna temperature, can be written

$$\Delta T_A = c \frac{T_{op}}{\sqrt{\tau B}} \quad (5)$$

This expression was first given by Dicke (1946). In equation (5), c is a constant of the order of unity and τ is the time constant or integration time used. For the present we will not discuss the values which c may have in various kinds of radiometer systems but for simplicity take $c = 1$. It is seen at once that for high sensitivity T_{op} should be reduced, while B and τ should be increased. These latter two quantities cannot, however, be adjusted at will since they are to some extent determined by the observing program. The reduction of T_{op} by the development of low-noise receiving techniques is one of the main advances in radio astronomical techniques which must be considered in some detail.

b. Stability. The requirement for good stability cannot be stated quite so simply. Changes of the gain, the bandwidth, or the noise temperature of the radiometer during observations are examples of possible unstable behavior. The techniques of improving stability by good design and construction of circuits, the use of switched radiometer systems and other devices forms the second area of technical advances to be described.

B. LOW-NOISE RADIOMETERS

We will first describe the progress which has been made in achieving low noise temperatures for radiometer systems. The overall noise temperature of a radiometer is normally determined by the noise generated in the pre-amplifier and the components between it and the antenna. The reason for this can be seen from the expression for the noise temperature of a system of cascaded amplifiers

$$T_e = T_{e1} + T_{e2}/G_1 + \frac{T_{e3}}{G_1 G_2} + \dots \tag{6}$$

where T_e is the overall noise temperature due to amplifier stages with noise temperatures T_{e1} , T_{e2} , etc., and gains G_1 , G_2 , etc. Equation (6) expresses the fact that the noise in the first amplifier appears directly with the signal, but noise in later stages is of less importance since the signal and first-stage noise have been amplified by the earlier stages. Since power gains of about 100 (20 db) are usually achieved in the first stage of a receiver, the contributions to T_e from later stages become small and can often be neglected.

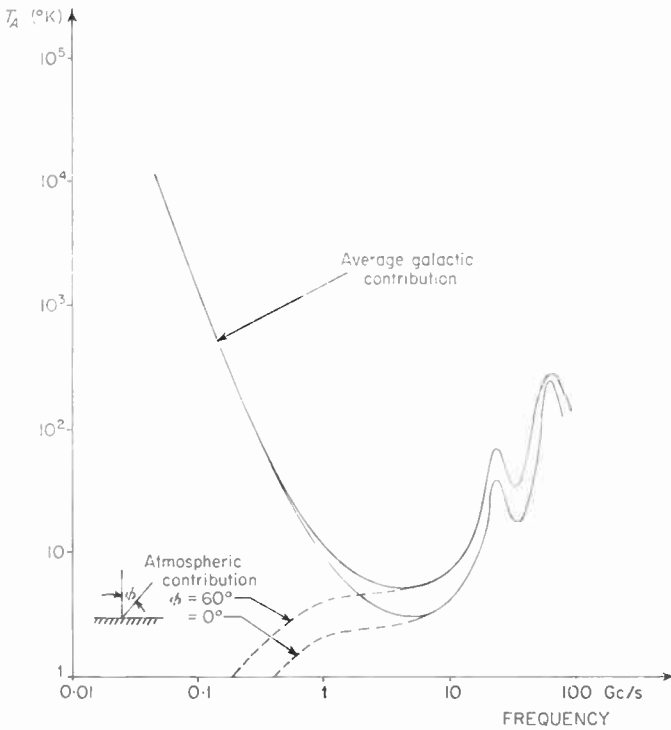


FIG. 4. Average values for the contribution to the temperature of an antenna due to radiation from the galactic background and from the atmosphere.

The types of preamplifier, or "front-ends" as they are often called, which have been successfully used in radiometers are:

- (i) Crystal mixer superheterodynes
- (ii) Travelling wave tubes
- (iii) Parametric amplifiers, using varactor diodes or electron beam devices
- (iv) Ruby masers
- (v) Tunnel diodes

The above list does not include the use of simple vacuum tube front-ends, although these can give quite low values for T_e at the lower frequencies (20 Mc/s to 200 Mc/s). At these frequencies, however, the contribution of the sky background noise is usually considerably greater than the T_e 's which can be achieved, so that the use of good standard vacuum-tube practice in the design of the front-end meets the radio astronomer's needs quite well. This fact is illustrated in Fig. 4, which shows how the noise due to the galactic background and the earth's atmosphere contributes to the antenna temperature at various frequencies.

1. *Crystal Mixer Front-ends*

The crystal mixer has proved itself to be a very valuable front-end in the frequency range up to about 1500 Mc/s, and has also been used extensively at much higher frequencies. This is due to the excellence of the mixer crystals available and to the very low noise contributions which can now be achieved in the intermediate frequency preamplifiers which immediately follow the mixer. Figure 5a shows the block diagram of a front-end including the mixer, local oscillator and IF preamplifier. All these components may contribute to the noise temperature of the radiometer and their total gain is normally high enough for the subsequent parts of the radiometer not to effect the value of T_e .

a. T_e for a Crystal Mixer. A crystal mixer is normally sensitive to signals at both the "signal" and "image" frequencies, so that the overall band-pass characteristic is as shown in Fig. 5b.† For many radio astronomy observations in the continuum it is no disadvantage for both signal and image bands to be available for reception, since they are spaced only twice the intermediate frequency apart and this is generally a small separation compared to the frequency of observation. For example, f_{IF} might be 30 Mc/s and $f_{LO} = 1400$ Mc/s, so that if the radio astronomy signal spectrum is linear over 60 Mc/s around 1400 Mc/s a good continuum observation can be made.

For observations of a line radiation, such as that at 1420 Mc/s from galactic hydrogen, the energy only occupies somewhat less than 1 Mc/s of bandwidth and thus falls only within either the signal or the image band. This can be thought of as effectively increasing the T_e of the radiometer in that a given signal power is more difficult to detect. In fact, for the crystal mixer of Fig. 5a, provided the two pass-bands are identical in gain and

† The choice of the higher frequency band as the "signal" band is of course arbitrary.

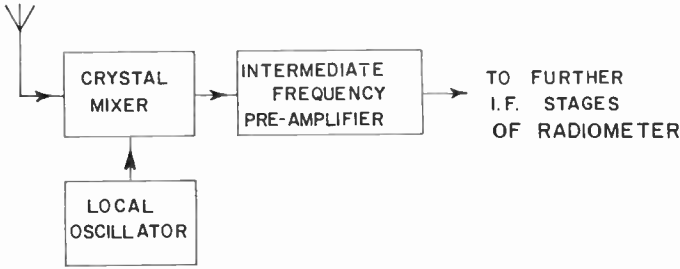


FIG. 5a. The crystal mixer front-end.

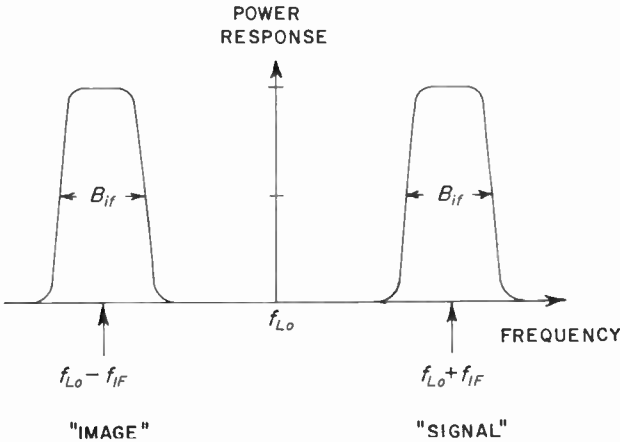


FIG. 5b. The band-pass characteristic of the crystal mixer.

provided they are both fed from sources of the same impedance, we can relate the noise temperature of the system T_e to that measured by a standard technique using a white-noise source T_e (W.N.S.) by

$$\left. \begin{aligned} \text{Double channel system } T_e &= T_e \text{ (W.N.S.)} \\ \text{Single channel system } T_e &= 2T_e \text{ (W.N.S.)} \end{aligned} \right\} \quad (7)$$

For a full statement of the standards for the noise performance of single and multiple response receivers see Haus (1963). In quoting noise temperatures achieved with mixers we will give the “double channel” figure, often called the “radio astronomer’s noise temperature”, which as equation (7) states is the figure measured with a white-noise source.

It is interesting to note the importance of the various contributions to the values of T_e for crystal mixers. The crystal mixer itself may be thought of as an element having a power loss L measuring the ratio of the power available from the mixer at the IF to that fed equally to both the signal and image channels at the input. So defined, L is of course > 1 . The crystal mixer is also treated as a lossy element at a temperature T_{mix} . This temperature will be greater than its actual temperature due to noise generated in the

crystal and possibly coupled also from the local oscillator. The first stage of the IF preamplifier has a noise temperature T_{if} . Then, using the expression for the noise temperature of a receiver with a lossy element at T_{mix} ahead of it, we get

$$T_e = (L-1)T_{mix} + L \cdot T_{if} \quad (8)$$

For a good IF preamplifier T_{if} may be as low as 50°K. L is about 1.5 and T_{mix} about 320°K, so that $T_e = 235°K$. As we shall see, such figures are achieved, but only because of the low loss and low noise of available mixer crystals and at the expense of considerable care in reducing the IF noise temperature to the 50°K region.

b. Crystal Mixer Performance. The performance of the crystals now available is very good. Many workers use a 1N21F mixer crystal for receivers in the 400 Mc/s to 1500 Mc/s range. When this is combined with a good IF preamplifier, noise temperatures (double channel) of 250°K to 500°K are achieved. Balanced mixers are an advantage both in requiring less local oscillator power and in giving protection against local oscillator noise entering the mixers.

The improvements in crystals have also resulted in better noise characteristics at lower frequencies, so that intermediate-frequency amplifiers with center frequencies in the 10 Mc/s range, giving a corresponding improvement in T_{if} , have been successfully used. It is difficult to make an exact comparison between the performance of various radio astronomy groups in the exact values of T_e which have been achieved, since "noisemanship" (Greene, 1961) may occur and different noise contributions may arise from components such as switches, directional couplers or isolators before the mixer, but the following Table I gives some figures for the noise temperatures achieved by mixer radiometers. The figures include contributions from circuit elements between the mixer and the antenna, but not from the antenna itself.

TABLE I. *Double Channel Noise Temperatures of Crystal Mixer Radiometers*

Center frequency	Intermediate frequency	T_e°	Reference
960 Mc/s	10 Mc/s	290°K	Harris and Roberts (1960)
About 1000 Mc/s	10 Mc/s	250°- 300°K	Cooper (1963)
1400 Mc/s	30 Mc/s	450°K	NRAO (unpublished)
8000 Mc/s	30 Mc/s	500°K	NRAO (unpublished)

The design of the IF preamplifier and the coupling of the mixer to the preamplifier have both been the subject of considerable technical advance.

The principles to be followed are available in standard texts (Valley and Wallman, 1948). In applying these principles, considerable care has to be taken in choosing the best form for the output filter section of the mixer and the optimum low-loss coupling circuit between the mixer and the first tube of the preamplifier. The cascode circuit of two tubes is still the most used. The first tube usually requires careful neutralizing. The choice of the tubes for this circuit is most important. Good results have been achieved using cascode circuits of a 437A followed by a 417A, and also by using the ceramic tube 7768 in both cascode stages.

2. Travelling Wave Tube Radiometers

For observations in the frequency range between 2500 Mc/s and 10 Gc/s, radiometers which use travelling wave tubes to provide all the radio frequency gain have proved very valuable. Drake and Ewen (1958) describe such an instrument working at a center frequency of 8000 Mc/s, with a bandwidth of 1000 Mc/s. It is of course the large available bandwidth of such radiometers rather than the noise properties of the first tube which permits the achievement of high sensitivity. In the 8000 Mc/s radiometer at the NRAO the first tube, including the losses in the ferrite switch and the directional coupler needed for noise compensation and calibration signals, gives a measured T_e of 3000°K. This in turn should lead to r.m.s. fluctuations at the output of about 0.01°K when time constants of 100 sec can be used. In practice, due to atmospheric and other disturbing effects and the use of shorter time constants, observations with the receiver show r.m.s. fluctuations of about 0.1°K. A similar receiver † working at a central frequency of 3000 Mc/s with a bandwidth of 200 Mc/s has also been extensively used at NRAO. The performance of the travelling wave tube at this frequency is considerably better, and the corresponding figure for the noise temperature is 1200°K. Typical observations with the receiver show r.m.s. fluctuations in the results of 0.09°K with a $\tau = 30$ sec (Drake, 1962). Travelling wave tube receivers have also been used by workers in Russia (Apushkinskii, 1960) and elsewhere, and so long as occupancy of the spectrum allows this large bandwidth to be used they will continue to be valuable radiometers of high sensitivity.

3. Parametric Amplifiers

The theory of parametric amplifiers is already well known (see, for example, Louisell, 1960; Blackwell and Kotzebue, 1961), and a good survey has been given by Robinson (1963) of their applications and use in radio astronomy. In this paragraph we will therefore include only a discussion of the theory and practice of the two types of parametric amplifier which have so far proved of great value to radio astronomy—the semiconductor diode amplifier in its various forms and the fast cyclotron mode parametric amplifier. A full survey of the use made of parametric amplifiers at many observatories has

† Both these receivers were supplied to the Observatory by the Ewen-Knight Corporation, Natick, Massachusetts.

been published by Jelley (1963). The idea of a parametric amplifier may be traced back as far as Faraday in so far as mechanical systems are concerned, and devices depending on variable inductances have been known for many years. Van der Ziel (1948) showed that non-linear capacitors could be used for a low noise amplifier, and Adler (1958) introduced the fast cyclotron wave amplifier.

The chief interest of parametric amplifiers in radio astronomy is their promise of low effective noise temperatures, and it is unfortunate that the theory of the noise temperature of the semiconductor diode amplifier is somewhat complex (Heffner and Wade, 1958; Uenohara, 1960; Robinson, 1961; Heinlein and Mezger, 1962), but it leads to estimates, which measurements confirm, of double side-band noise temperatures in the range 75°K to 150°K for amplifiers operated at room temperature. The theory for the Adler tube is also difficult (Wade *et al.*, 1954), but the results achieved (Adler *et al.*, 1959) show noise temperatures of about 120°K at frequencies near 500 Mc/s. Thus either kind of amplifier offers a considerable reduction of T_e for radiometers. The results achieved in practice will now be reviewed.

a. Variable Capacitance Diode Amplifiers. Two types of amplifiers have been used in radio astronomy, the regenerative amplifier and the so-called "up-converter". The class of regenerative amplifier more often used has been that in which the input and output signals are at the same frequency and the pump frequency is twice the signal frequency. We will refer to this as the "degenerate" amplifier and use the term "nondegenerate" to describe amplifiers where the pump frequency is considerably higher than twice the signal frequency which also have been used in radio astronomy. Table II illustrates some results so far achieved and the article by Jelley (1963) gives a list of parametric amplifier installations.

Of the various types of amplifier shown in Table II, only the upper side-band up-converter type is relatively insensitive to changes in the pump power and the impedances presented by the antenna and the following amplifier stages at the parametric amplifier parts. The gain of the up-converter is, of course, limited to a value set by the ratio of the output frequency f_2 to the input frequency f_1 , and this in turn limits the upper frequency at which it is practical to use the up-converter. Although high pump frequencies can be used, the increase of the output frequency generally results in the use of a following stage with a higher T_e and so an overall improvement in noise temperature is difficult to attain. In the up-converter two-stage amplifier quoted, the up-converter has a measured gain of only 1.3 (compared to $f_2/f_1 = 1.69$), but it is followed by a low-noise stage and is also valuable as a tunable frequency-comparison switch for the hydrogen-line radiometer on which it was used.

The other types of parametric amplifier are all negative resistance devices and are thus sensitive to variations of impedance presented at the amplifier ports. They all show the property that the gain-bandwidth product is constant, so that at higher gains the bandwidth becomes small and the potential instability greater. Even with the best circulators available, stabilizing against input impedance changes is difficult; so also is stabilizing

TABLE II. Performance of Variable Capacitance Parametric Amplifiers

Type of amplifier	Frequency	Bandwidth B Mc/s or gain G db, or gB where g = voltage gain	Variable capacitance used	Noise temperature of amplifier and succeeding stage	Reference
Degenerate	408 Mc/s	$gB = 25$ Mc/s	Hughes IN 2629	105°K	Robinson (1963)
Degenerate—cooled to 78°K	1410 Mc/s	$gB = 250$ Mc/s	Hughes IN 2629	55°K, including input isolator and circulator	Gardner and Milne (1963)
Upper sideband up-converter followed by degenerate amplifier at 2400 Mc/s	1420 Mc/s H-line	Tunable 1380–1440 Mc/s $G = 21$ db	Texas Instruments XD 502	140°K	Robinson (1963) Robinson and de Jager (1962)
Degenerate (being developed)	2700 Mc/s	$gB = 500$ –1000 Mc/s	MS 3062	~ 60°K	Robinson (1963)
Degenerate (wide band)	3300 Mc/s	$B = 190$ Mc/s $G = 16.5$ db	Microwave Associates varactor	150°K (amplifier and circulator)	Little (1961)
Lower sideband up-converter	961 Mc/s	$B = 20$ Mc/s $G = 22$ db	Silicon p - n junction	125°K, including isolator	Uenohara and Seidel (1961)
Non-degenerate two stage	1420 Mc/s	Tunable 1300–1450 Mc/s	Texas Instruments XD 502	120°K	Mezger (1963)
Non-degenerate single stage	1420 Mc/s	Tunable 1390–1420 Mc/s $B = 20$ Mc/s $G = 20$ db	Microwave Associates varactor MA 4557	150° with second stage $T_e = 710$ °K	NRAO† (unpublished)

† Supplied by Airborne Instruments Laboratory, Deer Park, Long Island, New York.

against changes in pump power, although a method (Robinson *et al.*, 1960) has been devised by which the current through the diode is used to monitor and adjust the pump power to give good gain stability of the amplifier. Various workers are now making and using amplifiers with the diode cooled by liquid nitrogen and helium to reduce the noise temperature.

b. The Fast Cyclotron Wave Amplifier (Adler Tube). This amplifier is described by Adler *et al.* (1959), and has proved successful in radio astronomy, particularly at frequencies near to 400 Mc/s and 1420 Mc/s. In principle, the signal to be amplified is impressed as a fast-travelling cyclotron wave on an electron beam moving along a longitudinal magnetic field. The phase velocity of the cyclotron wave is infinite if the magnetic field is chosen so that the signal and cyclotron frequencies are equal. When the signal is impressed onto the beam, it may be amplified by pumping the beam as it passes through a quadrupole structure at a radio frequency twice the cyclotron frequency. The amplified signal is removed from the beam after it has passed through the quadrupole structure.

The possible advantages of this type of amplifier are notable. By using a correct design of the coupler by which the signal is impressed on and removed from the electron beam, it is possible for the input coupler to remove the noise from the beam while the signal is being inserted. The gain and bandwidth can be considerable, the device is directional in the sense that an isolator is directional and the gain should be stable. The results obtained by Adler *et al.* (1959) at 420 Mc/s ($T_e \sim 120^\circ\text{K}$) and later (Adler *et al.*, 1960) of about $T_e = 75^\circ\text{K}$ at 425 Mc/s and 780 Mc/s, and of Ashkin (1961) of about $T_e = 60^\circ\text{K}$ at 4137 Mc/s show that good low-noise performance can be achieved. Although the noise temperature falls off at the edges of the bandpass curve, tuning ranges of 30 Mc/s at 420 Mc/s are possible with gains of 30–40 db. Adler tubes have been used at the observatories listed in Table III.

TABLE III. *Reports of Adler Tube Radio Astronomy Observations*

Observatory	Frequency	Pump frequency	System noise temperature	Reference
Cambridge, England	408 Mc/s	816 Mc/s	190°K	Wielebinski <i>et al.</i> (1962)
Manchester, England	408 Mc/s	820 Mc/s	200°K	Thompson <i>et al.</i> (1961)
Penticton, B.C., Canada	1420 Mc/s	2840 Mc/s	155°K	Jelley (1963)
NRAO, U.S.A.	1420 Mc/s	2840 Mc/s	150°K (amplifier alone)	Unpublished

4. *The Maser*

The maser itself is a very low-noise amplifier and is by now well described in standard texts (Singer, 1959; Troup, 1960). Its uses, both as a negative resistance amplifier and as a travelling wave amplifier, have been appreciated for some time by radio astronomers. The first radio astronomy measurements with a maser were made by Giordmaine *et al.* (1959) using an X-band ruby maser mounted on the Naval Research Laboratory 50-ft dish in Washington, D.C. Since that time several observatories throughout the world (see Jelley, 1963, for a summary) have been using masers. The maser can, of course, also be used as an oscillator, but this application is not yet of much practical astronomical interest; although the development (Kleffner *et al.*, 1962) of the atomic hydrogen maser giving a very stable hydrogen-line oscillator will have important applications in the future. We will illustrate the use of the maser by choosing examples of the three-level cavity maser and the travelling wave maser.

a. The Three-Level Solid-State Cavity Maser. The principle of operation of the three-level maser (Bloembergen, 1956) relies on finding a crystal in which two energy levels exist whose energy difference corresponds to the frequency to be amplified, while a third energy level also can be found, so that by supplying radio frequency power (pumping) to the crystal the energy level population can be changed from the normal population set by thermal processes. For maser action the population ratio between the upper and lower energy levels corresponding to the frequency to be amplified must be so arranged that, when this radio frequency is applied to the crystal, stimulated emission from the upper to the lower level occurs and the resulting energy release increases the applied signal. For these conditions to be met, the pump frequency, the magnetic field on the crystal and its orientation with respect to the crystal axes, and the signal frequency all have to be correctly chosen. To achieve the required population inversion the crystal must be at a low temperature, and either liquid helium at 4.2°K, or sometimes liquid helium at reduced pressure is used in the cryostat surrounding the crystal. Figure 6 shows the way in which the three energy levels 1, 2 and 3 in order of increasing energy, can be used in a three-level maser. The pump frequency matches the energy difference between 1 and 3, and the populations of these two levels are approximately equalized by a balance between the pumping $1 \rightarrow 3$ and the stimulated emission and thermal processes leading to $3 \rightarrow 1$. In thermal equilibrium at low temperature 1 is much more populated than 3, so that the increase in the population of 3 when pumped is considerable. Stimulated transitions $3 \rightarrow 2$ can now occur, and if the energy difference between 3 and 2 corresponds to the signal frequency the maser will provide gain. The energy levels of Fig. 6 were those used by Giordmaine *et al.* (1959). It is not the only way the three-level maser can work, but is sufficient to describe the principle.

(i) *The three-level maser at Harvard College Observatory.* A different level scheme for ruby, with the pump and signal frequencies of 11.27 Gc/s and 1420 Mc/s, was used by Jelley and Cooper (1961) in a maser which has been used extensively on the 60-ft antenna at the Agassiz station of the Harvard

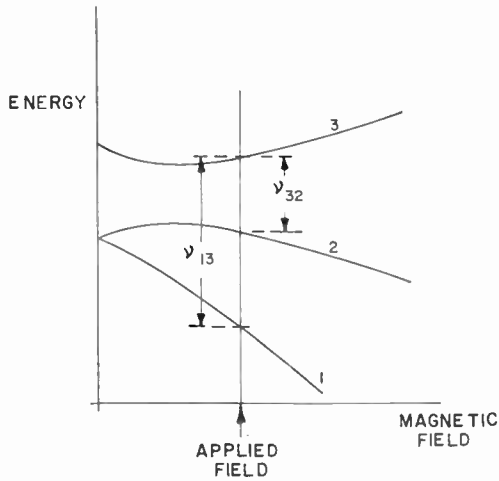


FIG. 6. Energy levels in a three-level ruby maser.

ν_{13} = Pump frequency
 ν_{32} = Signal frequency

College Observatory. With its observations of the neutral hydrogen content in twenty-one of the nearer galaxies have been made (Roberts, 1963).

It is interesting to note the contributions to the total measured system noise temperature T_{op} °K of $(85 \pm 5^\circ)$ K which Cooper and Jelley estimate. The antenna spillover measured as the effect of radiation from the ground and surrounding objects with the antenna pointed to the zenith was 20° K. Losses in cables, a directional coupler and a circulator, all at ambient temperature, introduced a further 52° K. The following amplifier stage with a T_e of 1000° K and a maser gain of 20 db introduced 10° K, and the maser itself only added perhaps 2° – 3° K. The cable loss was later reduced; but the magnitude of the various contributions demonstrates very well the care which is needed in antenna design and maser engineering and installation to reduce system noise temperatures below 50° K. Two systems were used to stabilize the gain of the radiometer, the second of which (Cooper, 1961) proved more useful.

b. The Travelling Wave Maser. The single-cavity maser suffers from the disadvantages that it requires a circulator to isolate the input from the output and that the gain and bandwidth are mutually dependent. DeGrasse *et al.* (1959) describe a travelling wave maser where these difficulties can be overcome. In principle, the signal to be amplified is still impressed on a pumped crystal in a magnetic field. However, the crystal is part of a slow-wave structure arranged so that the signal effectively couples with the crystal, and also designed so that propagation along the structure takes place in only one direction. Then, if the crystal is pumped to give gain, the slow wave moving along the structure gains exponentially in amplitude. The bandwidth

of the device, as for all travelling wave systems, can be considerable compared with that of a single-cavity maser, and the directional properties of the structure make it unnecessary to use additional circulators or isolators.

A comb slow-wave structure is normally used, and the non-reciprocal behavior to eliminate the backward-moving wave is achieved by incorporating ferrimagnetic isolator material into the structure. DeGrasse *et al.* (1961) describe the construction and use of such a maser at 2390 Mc/s for the Echo satellite observations. Their maser, cooled to 1.8°K , gave $T_e = 8 \pm 1^\circ\text{K}$; gains of 33 db and 36 db (two masers were built in the same package) and a bandwidth of 13 Mc/s with a tuning range of ± 10 Mc/s were achieved. Masers of this type are already available at several observatories (Jelley, 1963).

The travelling wave maser † at NRAO, which has been installed on the 85-ft telescope and tested, has the characteristics given in Table IV.

TABLE IV. *Summary of the NRAO Travelling Wave Maser*

Operating center frequency	4995 Mc/s
Bandwidth	25 Mc/s
Pump frequency	32.77 Gc/s
Gain	25 db
Magnetic field	3770 G
Noise temperature T_e °K	
<i>a.</i> TWM alone	28°K
<i>b.</i> Including Dicke switch and calibration equipment	68°K
Second stage	Balanced mixer T_e (single channel) = 1500°K
Dewar capacity	
<i>a.</i> Nitrogen	7 l
<i>b.</i> Helium	3.5 l
Holding time	24 h

The system incorporates a Dicke switch cooled to helium temperature; an external comparison load or a load in the helium may be used. When the instrument is mounted on the telescope the total system temperature is about 100°K .

5. Tunnel Diodes

Although the tunnel diode (Esaki, 1958) is known to be a possible low-noise amplifier, progress so far has not led to extremely good noise temperatures. Nevertheless, the possibilities of an amplifier which requires only a small dry cell to provide power, which gives a wide bandwidth and which has quite a low single-channel noise temperature, is obviously attractive to radio astronomers. Two such amplifiers ‡ have been used at the NRAO,

† Supplied to NRAO by Airborne Instruments Laboratory, Deer Park, Long Island, New York.

‡ Supplied to NRAO by Micro State Electronics Corporation, Murray Hill, N.J.

one as the first stage of a 1400 Mc/s continuum receiver on the 300-ft telescope and one for observations at 750 Mc/s on the 85-ft telescope of the polarization of the sky radiation. The amplifiers have proved to be both stable and convenient to use. Table V gives the characteristics of the amplifier used at 1420 Mc/s. It is clear that as diode performances improve the amplifier will be a very attractive radiometer front-end (Armstrong, 1962).

TABLE V. *A 1420 Mc/s Tunnel Diode*

Operating center frequency	1420 Mc/s
1 db bandwidth	70 Mc/s
Gain	16.5 db
Single channel noise temperature	
<i>a.</i> Tunnel diode only	375°K
<i>b.</i> System on telescope	500°K

C. RADIOMETER STABILITY

The problem of stabilizing radiometers can be discussed in the light of equation (5), which gives the approximate value that ΔT_A , the r.m.s. noise fluctuations, should have for a given T_{op} , bandwidth and time constant. It would obviously be desirable that observations should be limited only by ΔT_A , but in practice the changes in gain, noise temperature or bandwidth of the radiometer may in fact be the limiting factor in radio astronomy observations. There are many ways in which the effect of these changes has been minimized, but it should still be recorded that in practice very few radiometers operated on radio telescopes give fluctuations in their outputs as low as those indicated by (5).

It is first evident that the overall gain of the system must be stable to a high degree. If no means were adopted to remove the effects of the operating noise temperature T_{op} , any gain change ΔG would cause a change at the output corresponding to a ΔT at the input of $T_{op} \frac{\Delta G}{G}$. With the older receivers where T_{op} was about 1000°K, this required gain stability of 0.1 per cent to keep ΔT down to 1°K, while even with these receivers the r.m.s. noise fluctuations ($B = 10$ Mc/s, $T = 10$ sec) could be only 0.1°K. When T_{op} is reduced with the newest receivers there is promise of correspondingly low noise fluctuations, and to take fullest advantage of the reduced fluctuation noise still requires an equivalent fractional gain stability. The means by which this stability is achieved may be listed as follows:

1. Total power radiometers.
2. Dicke radiometers.
3. D-C comparison radiometers.
4. Frequency-switched radiometers.
5. Phase-switched radiometers.
6. Correlation radiometers.

1. The Total-Power Radiometer

In this simplest radiometer (Fig. 7) great care must be taken to keep the gain, T_e , and bandwidth constant by careful circuit design. The rectified signal at the detector output due to the noise of the receiving system is balanced against a constant voltage and the difference signal amplified at

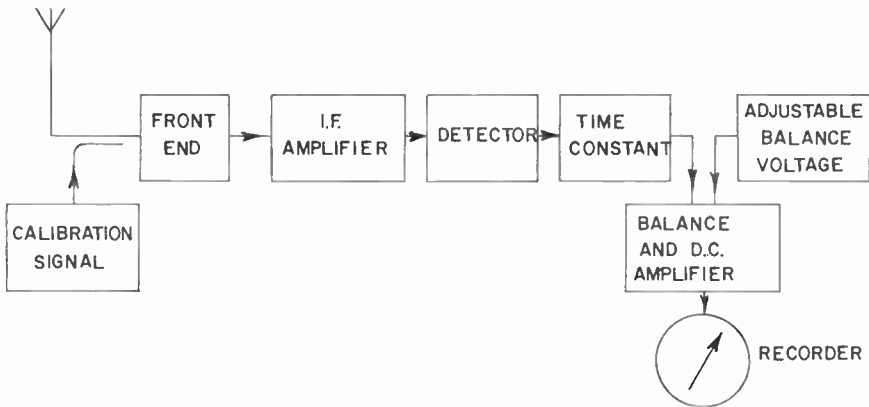


FIG. 7. The total-power radiometer.

DC before recording. Stable supplies to both heaters and anodes of vacuum tubes, the inclusion of large cathode resistors to a negative supply, careful temperature control, and the use of temperature-insensitive tuned circuits have all been employed. See Seeger *et al.* (1959) for an example of such a design. The results can be surprisingly satisfactory, with gain stabilities of 0.1 per cent maintained over several hours, and reasonable periods existing when the stability is perhaps even five times better. The total-power radiometer observes the source continuously, which is not true for most switched radiometers, so that for a given duration of observing time the noise fluctuation is lower than for the switched system.

2. Dicke Radiometers

a. General Description. This type of radiometer (Dicke, 1946), shown in diagram form in Fig. 8, is in one or other of its variants the most widely used radiometer. The input of the receiver is switched between the antenna and a constant comparison source of noise power, usually simply a resistance maintained at a constant temperature. To a first approximation the receiver noise is the same in both switched positions, so that the output of the detector is a signal corresponding to the constant system noise carrying on it a square wave modulation of peak-to-peak amplitude corresponding to the difference ($T_A - T_C$) between the antenna temperature and the comparison-noise-source temperature. This signal is applied to the phase-sensitive detector, fed also with a square wave at the switch frequency, and the output of this detector, smoothed, amplified and recorded, is a measure of the difference between the antenna and noise-source temperatures.

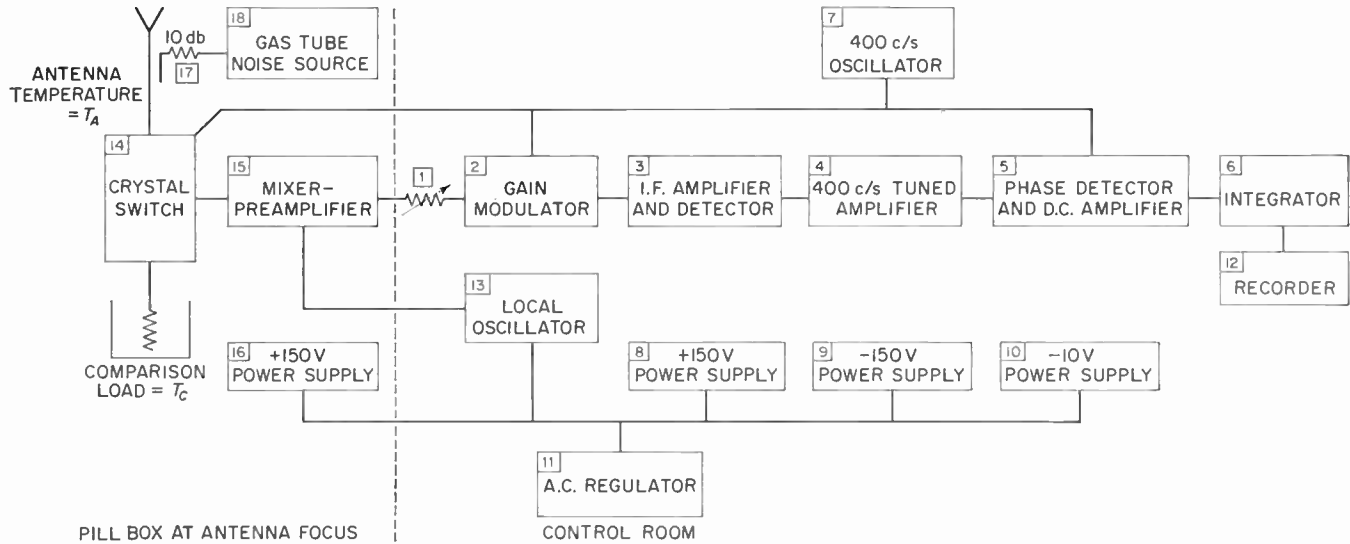


FIG. 8. A switched-load radiometer.

It is at once obvious that the radiometer is less affected by gain changes than the total-power radiometer, since such gain changes affect only $(T_A - T_C)$ and not the total system noise. The radiometer is of such value that it requires more detailed analysis to show how its performance depends on various possible instabilities. Before giving the results of this analysis we can note the obvious desirability of keeping the temperatures of the antenna and noise source the same, as far as possible. This can be done, for example, by varying the noise-source power to keep the receiver output zero (Ryle and Vonberg, 1948), and measuring the antenna temperature by measuring the noise source power. This is a valuable technique and has not, perhaps because of technical difficulties of making a good variable power noise source of low effective temperature, been sufficiently used at the higher frequencies where antenna temperatures are well below room temperature (Haneman and Bridgeman, 1959).

Another method by which the noise powers at the two inputs can be approximately equalized is by adding noise by a directional coupler into the antenna arm (Drake and Ewen, 1958). This is useful only when the resulting increase of system noise is not important. The same effect can be simulated by modulating the gain of the receiver at the switch frequency so that through most of the receiver the noise powers from the antenna in the absence of a radio astronomy signal and from the comparison source are equal. This "gain-modulator" technique has been used successfully in many receivers.†

b. Discussion of the Instability of a Dicke System. The receiver with the block diagram of Fig. 8 was analyzed by Orhaug and Waltman (1962). It is a simple Dicke system, except for the assumption that the gain can be modulated at the switch frequency to give gains G_A and G_C for the "antenna" and "comparison" switch positions. A loss L at temperature $T^\circ\text{K}$ is assumed to be included in the antenna line so that the comparison switch loss can be allowed for.

The analysis leads to the following conclusions:

(i) *Gain variations.* A change ΔG in the overall gain G of the system will not cause a change in output provided

$$\frac{G_C}{G_A} = M = \frac{T_A + T_e}{T_C + T_e} \quad (9)$$

M is the gain modulator ratio and T_e the noise temperature of the receiver after the switch. Thus without a gain modulator T_A and T_C should be the same, as was discussed above, but with a gain modulator they can still be different and yet the radiometer can have good stability against small gain changes.

(ii) *Changes in T_e .* A change in receiver noise temperature will give a change in receiver output in all practical conditions unless $T_A = T_C$ (the inputs are balanced) and thus $M = 1$. Even this condition cannot easily be achieved in a normal Dicke receiver because the gain of the receiver is usually

† The use of a gain modulator is believed to originate with the Ewcn-Knight Corporation, Natick, Mass.

somewhat different in the two switch positions due to the small impedance difference presented by the antenna and the comparison source to the receiver input.

(iii) *Changes in noise bandwidth B.* Provided the receiver is balanced or that equation (9) is satisfied in the gain modulator case, small changes in B do not affect the output.

(iv) *Changes in gain modulator ratio M.* When M is adjusted for balance any change ΔM gives a change in output proportional to $L (T_A + T_e) \frac{\Delta M}{M}$.

Thus the gain modulator must give a very constant value for M . This can generally be achieved easily, since M can be determined almost entirely by the properties of resistive elements and only to a much lesser extent by the characteristics of the switching diodes. Any variation of the symmetry of the switch wave form applied to the modulator also may change M .

c. *The Detector Law.* The foregoing discussion has been concerned with the stability of a Dicke radiometer in the absence of an added radio astronomy signal in the antenna, and so it has been possible to omit a consideration of the law of the envelope detector. If V , the DC output from the detector, is related to the input power P by

$$P = CV^z \quad (10)$$

then it can be shown (Orhaug and Waltman, 1962) that for a small increase ΔT of input temperature an output change ΔV occurs given by

$$\left(\frac{\Delta T}{T_A + T_e} \right)_{\Delta T \rightarrow 0} = \frac{\alpha}{V} \Delta V \quad (11)$$

By calibrating with a suitable noise source α can be found for any detector, and the range over which α can be assumed to be constant can also be found. Then a correction factor necessary when finite changes of input level are used can be found and expressed in terms of α and $\frac{\Delta T}{T_A + T_e}$. This correction factor is then used to allow for the law of the detector (Seeger *et al.*, 1959). For a truly square-law detector $\alpha = 1$ and no correction factor is needed; in practice, α may be about 1.6 or 1.7 and when $\frac{\Delta T}{T_A + T_e}$ is 10 per cent the detector-law correction will be about 2 per cent.

Thus two effects are of importance when the signal to be measured represents an appreciable increase in the noise in the system. First, the radiometer gain, irrespective of the switching, must be constant enough for the signal to be measured and compared with a calibration, and, second, the detector law must be known well enough for a sufficiently accurate correction to be made for it.

d. *Experimental Results.* Orhaug and Waltman (1962) give the results which are shown in Fig. 9 of tests on a radiometer similar to that of Fig. 8. The top record shows the performance of the radiometer unswitched operating as a total-power device. The middle record shows the improvement due

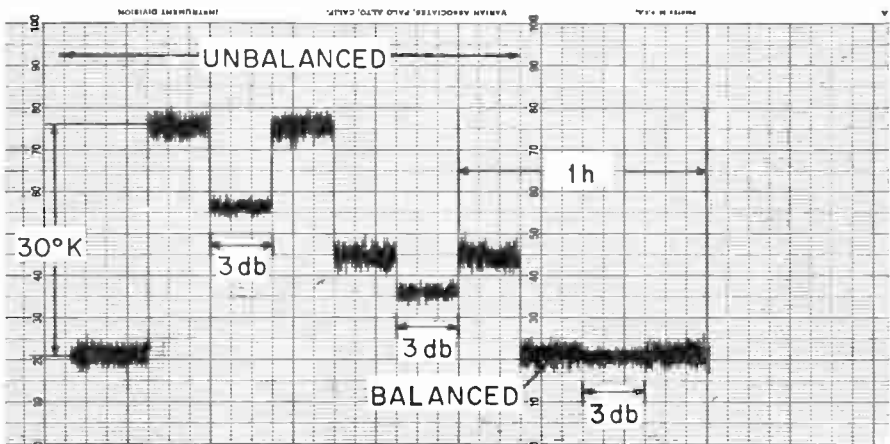
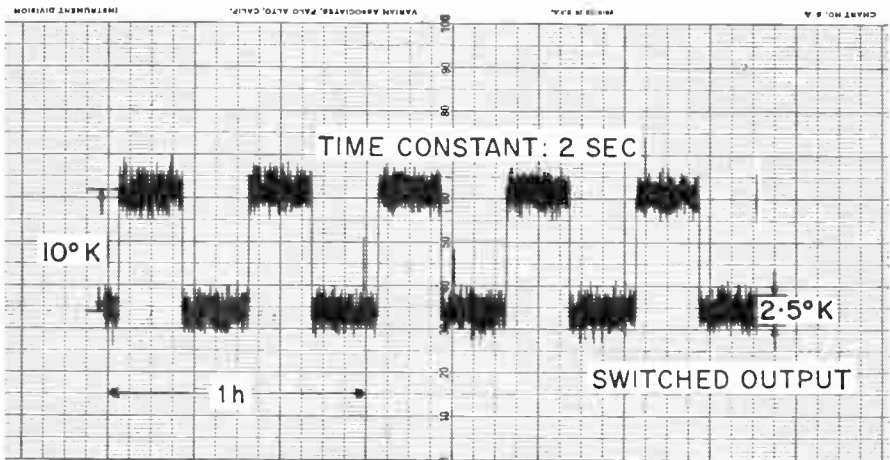
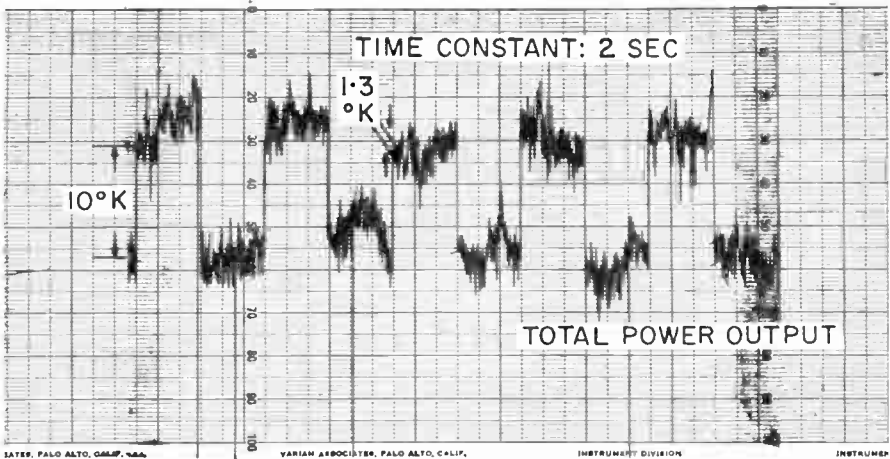


FIG. 9. Total power and switched-load radiometer records, and the effects of an unbalanced input.

to switching, while the lower record shows the output changes when a large (3 db) gain change is made. When the input is unbalanced, large changes in output occur, but for a balanced input only a reduction in the r.m.s. noise is seen.

Figure 10 shows some further work by Orhaug (unpublished) on the same radiometer. The radiometer was run first in a balanced condition with

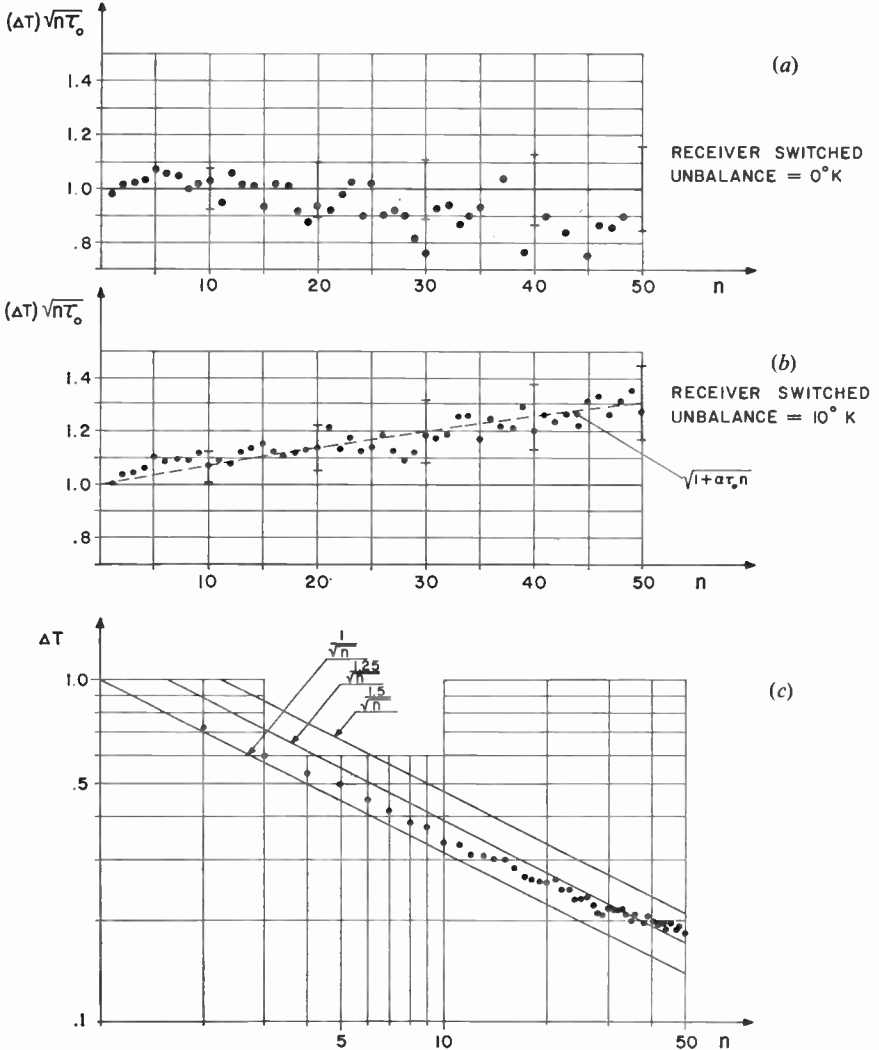


FIG. 10. Analysis of the output of a switched-load radiometer.

FIG. 10a. Receiver balanced.

FIG. 10b. Receiver with a 10°K unbalance.

FIG. 10c. Receiver with a 10°K unbalance.

$T_A = T_C$ (Fig. 10a) and then with a 10°K unbalance between T_A and T_C (Fig. 10b). A run of more than 3 h was made for each condition; the output of the receiver was averaged for $\tau_0 = 5$ sec and these average values of the output were recorded every 5 sec throughout each run. This gave about 2500 independent values of the receiver output for both the balanced and the unbalanced condition of the receiver. The r.m.s. fluctuation ΔT for an integration time of $\tau_0 = 5$ sec was derived from these readings of the receiver output. Values of the r.m.s. fluctuation for longer integration times $n\tau_0$ were derived from the same data by combining the observations into groups with $n = 2, 3, 4 \dots$

If only thermal noise having an essentially flat spectrum over the effective output filter bandwidth $1/\tau_0$ were present, then $\Delta T\sqrt{n\tau_0}$ should be a constant as n varies. Figure 10a confirms that this is true for the balanced receiver and thus also shows that gain changes are not contributing to the fluctuations. If the fluctuations do have a contribution from the gain instabilities, then it can be shown that

$$\Delta T\sqrt{n\tau_0} \propto \sqrt{1 + \alpha n\tau_0}$$

where α is determined by the ratio of the power in the instability fluctuations to the power in the thermal fluctuations. Figure 10b shows that this is in fact the case for the unbalanced receiver, in which gain instability is certainly contributing to the output fluctuations. The same effect is shown in Fig. 10c, where the same results for the unbalanced receiver are plotted as the value of the r.m.s. fluctuation ΔT as a function of integration time n . It is seen that for large integration times (250 sec) the points depart from the theoretical $1/\sqrt{n}$ law and approach the $1.5/\sqrt{n}$ law. This again shows how the gain changes cause noise-like fluctuations. It is also evident that for the long integration times fluctuations are relatively greater than would be deduced from the effective temperature of the receiver, and correspond to the fluctuations which would be produced by a receiver with about a 30 per cent higher effective temperature.

The above treatment of the stability of the Dicke radiometer is by no means exhaustive. For further work see Strum (1958), and a long discussion by Calvin (1961).

3. The D-C Comparison Radiometer

This instrument (Selove, 1954) has been successfully used by some workers for observations of hydrogen-line radiation. It resembles the total-power radiometer, but derives the comparison voltage from the noise received in a band of frequencies close to the band containing the line being observed. Gain changes and changes of noise temperature affecting both the signal and the comparison bands identically should have no effect on the output provided that no changes occur in the bandpass characteristics of the two channels.

4. Frequency-Switched Radiometers for Line Observations

a. Swept-Frequency Radiometers. The requirement for accurate measurements of the 1420 Mc/s radiation from neutral hydrogen in our own galaxy and in external galaxies has led to the development of special radiometers for the purpose. One of the first and best may be taken as an example of the technique of frequency switching (Müller, 1956). Figure 11 shows a block diagram of the radiometer in its simplest form—later developments have added more channels and reduced the bandwidth of the channels.

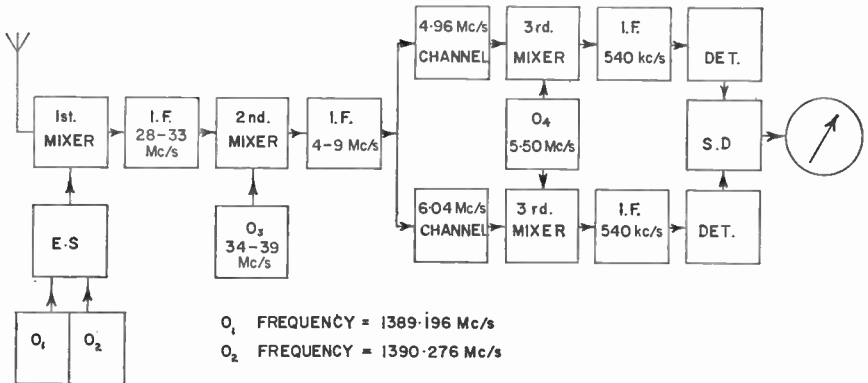


FIG. 11. The frequency-switched hydrogen-line radiometer.

The first stage of the receiver is a crystal mixer, and the frequency switching is accomplished by supplying a local oscillator signal alternately 400 times per sec through an electronic switch ES from the two crystal-controlled sources O_1 and O_2 . The frequencies of O_1 and O_2 supplied to the mixer differ by 1.08 Mc/s.† The output of the mixer after IF amplification at 28–33 Mc/s passes to the second mixer, the local oscillator of which O_3 can be swept in frequency from 34–39 Mc/s. The output after amplification over 4–9 Mc/s is fed to two separate channels, one centered on 4.96 Mc/s, the other on 6.04 Mc/s. The difference frequency between these is chosen to be 1.08 Mc/s—the same as that between O_1 and O_2 . These two channels give outputs (through a third mixer and 540 kc/s amplifiers) over a bandwidth of 35 kc/s to the detectors and synchronous detector SD, which is also supplied with the 400 c/s switching wave.

If a 1420 Mc/s signal is traced through the receiver it will be seen to emerge through the 4.96 Mc/s channel when O_1 is the LO, and through the 6.04 Mc/s channel when O_2 is the LO; O_3 is assumed to be set at 35.764 Mc/s for this to occur. With the same value for the O_3 frequency the signal frequencies passing through the channels are shown in Table VI.

† This frequency difference is adequate for measurements of galactic hydrogen. For the wider spread of frequencies from hydrogen in other galaxies a greater difference would be needed.

TABLE VI. *Signal Frequencies Observed in the Switched-Frequency Receiver*

Local oscillator in use	Signal frequency emerging from 4.96 Mc/s channel	Signal frequency emerging from 6.04 Mc/s channel
$O_1 = 1389.196 \text{ Mc/s}$	1420 Mc/s	1418.920 Mc/s
$O_2 = 1390.276 \text{ Mc/s}$	1421.080 Mc/s	1420 Mc/s

It will be seen that if 1420 Mc/s is the required frequency it is always available at one of the two channels while the other channel gives a 35 kc/s wide band 1.08 Mc/s above or below 1420 Mc/s. Thus the synchronous detector output is a measure of the difference between the noise power at 1420 Mc/s and the mean of the noise power at frequencies equally spaced above and below 1420 Mc/s. Figure 12 shows how these bands lie with

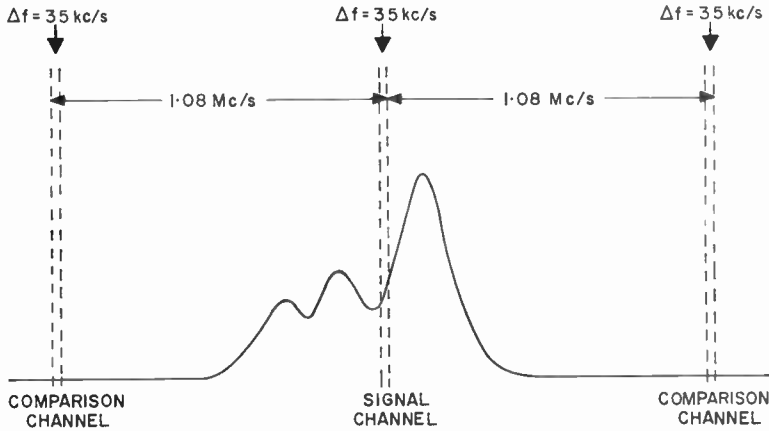


FIG. 12. The signal and comparison channels in a frequency-switched radiometer.

respect to a hydrogen profile to be observed. It is also obvious that by tuning O_3 across the band, the sensitive band of the receiver may be swept across the hydrogen-line profile.

There have been several later improvements in this basic receiver technique, but the above description will be sufficient to explain the radiometer. It is clear that, as in the Dicke radiometer, the switching technique will improve the overall receiver stability since the effects of receiver noise are, to a first approximation, eliminated. The switching system described also has the advantage that the line is observed in both switch positions so that no sensitivity is lost. There are many instrumental difficulties in building and

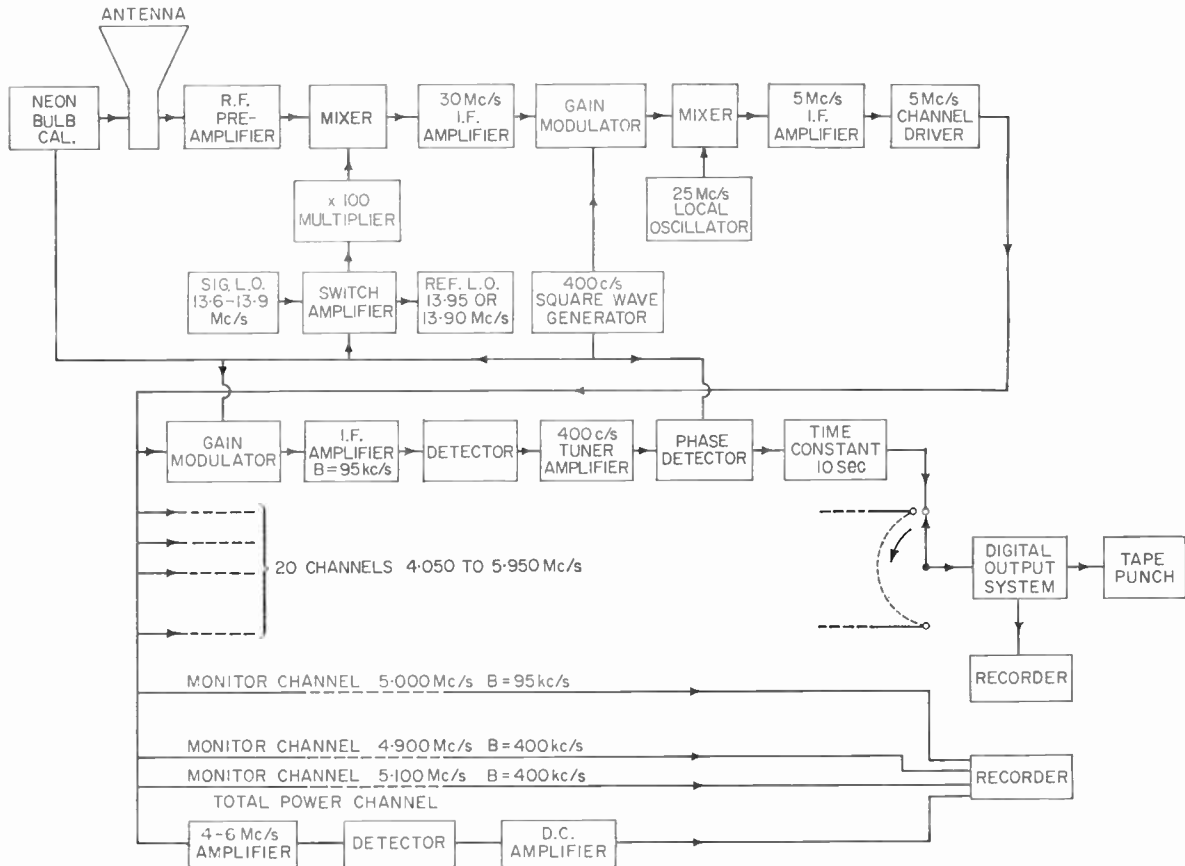


FIG. 13. A multichannel hydrogen-line radiometer.

using these switched radiometers; for details the paper by Müller already mentioned, and by Hogland and Radhakrishnan (1959) should be consulted.

b. Multichannel Radiometers. The principle of frequency switching, together with the sampling of the whole frequency range within which the line profile lies by means of a bank of filters, has been used by several workers (Burke *et al.*, 1959; Adgie, 1959; McGee and Murray, 1963). A block diagram of such a receiver which has been built at the NRAO is given in Fig. 13. Frequency switching is used to improve stability; the noise power in the signal channel is then fed into the bank of twenty filters, each with its own detector, synchronous detector and time constant. After a period of observation the outputs of all filter channels are sampled and recorded in digital form to give a record of the line profile. The receiver of Fig. 13 was designed for the study of hydrogen in other galaxies, where the hydrogen profile may extend over 2 Mc/s. Twenty channels, each 95 kc/s wide, are used. For galactic hydrogen more channels of narrower bandwidth are required. The care and skill needed to build a stable multichannel radiometer are considerable, and in fact only a few such receivers have been made and used successfully.

5. The Phase-Switched Radiometer

The use of phase switching is very well known (Ryle, 1952) and is illustrated in Fig. 14 for a two-element interferometer. The phase switch in one of its two switch positions introduces an extra half-wavelength of cable into the line from one antenna to the receiver, thus changing the phase of the signal from that antenna by 180° . The phase-sensitive detector is driven in synchronism with the phase switch. The phase switching results in a movement on the sky at the switch frequency of the lobes of the interference pattern (Fig. 15), so that if a point source is being observed against a uniform sky background only the power from the point source contributes to the recorded fringe pattern. However, it is also well known that in the case of an extended source, the amplitude of the recorded trace is proportional to one term of the Fourier transform of the angular distribution of the intensity across the source. For these two reasons the practice of phase switching has been extensively used in radio astronomy. It is also clear that the operation of phase switching removes from the output any contributions from the receiver noise as well as from a uniform sky background, so that the system has the additional stability associated with this characteristic.

6. Correlation Radiometers

The phase-switched interferometer gives a radiometer output proportional to the product of the powers P_1 and P_2 from the two antennas and to the cosine of the phase angle between the phases of the two signals. A similar result could be obtained by suitably multiplying the two signals, and in principle this is the method adopted in correlation receivers. Figure 16 is a simple example of a two-element interferometer with crystal mixer front-ends used as a correlation radiometer.

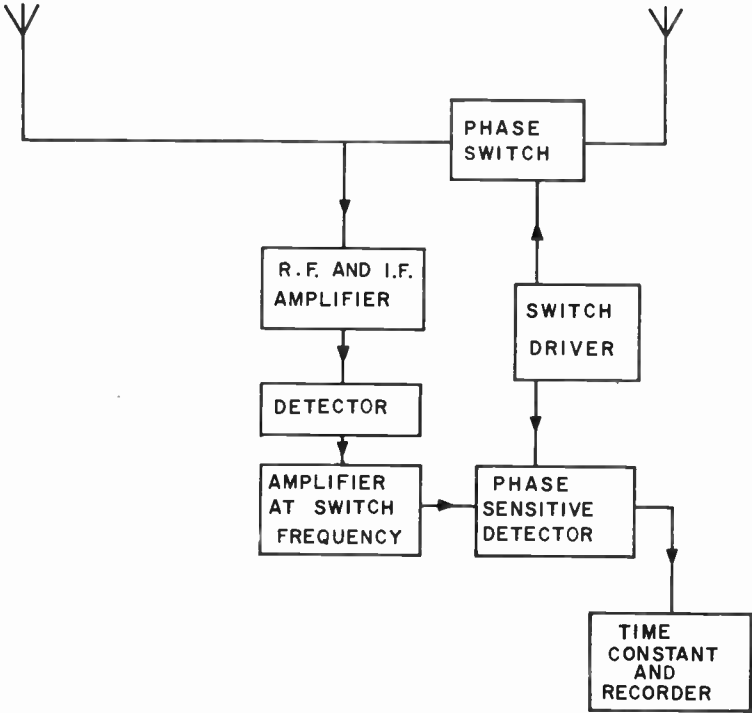


FIG. 14. The phase-switched interferometer.

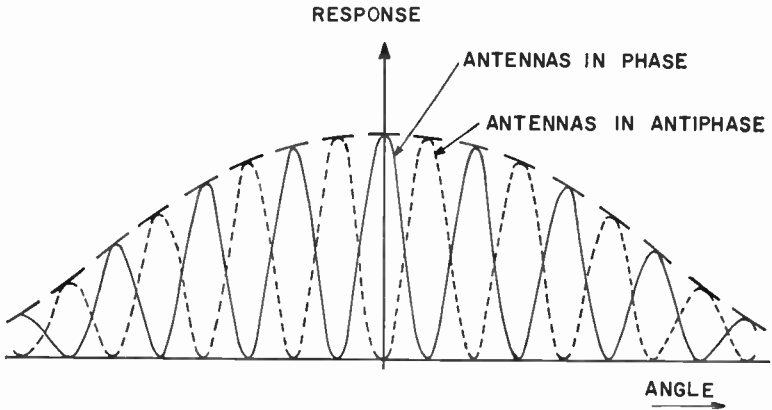


FIG. 15. The response pattern of two antennas in a phase-switched interferometer.

Suppose V_1 and V_2 are the outputs from the two intermediate-frequency amplifiers. The correlation coefficient ρ of V_1 and V_2 may be defined

$$\rho = \frac{\overline{V_1(t) V_2(t)}}{\overline{V^2}} \quad (12)$$

where $\overline{V^2}$ is the mean value of $[V_1(t)]^2$ and $[V_2(t)]^2$.

When the voltages $V_1(t)$ and $V_2(t)$ are completely correlated (for example, identical functions) $\rho = 1$. When they are quite uncorrelated $\rho = 0$. It is

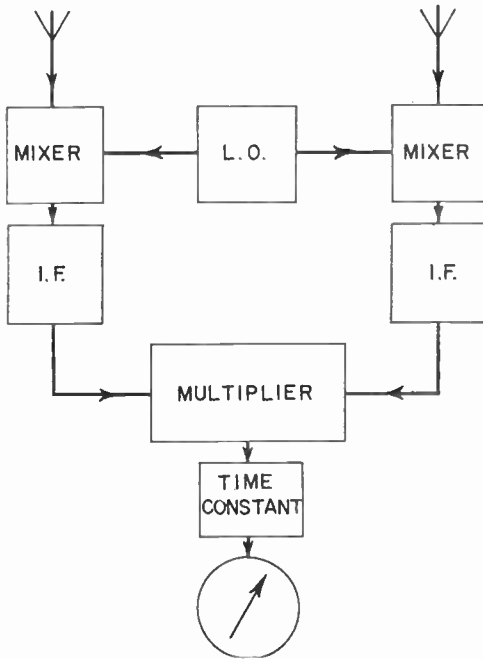


FIG. 16. The correlation radiometer.

clear that a multiplier as shown in Fig. 16, with appropriate smoothing to give the average value and normalizing, will provide a measure of ρ .

The original concept of the use of correlation may be seen in papers by Goldstein (1955) and Tucker (1955, 1957), while Blum (1959) has dealt with the sensitivity of correlation radio telescopes and receivers. The fact that a measurement of the correlation is equivalent to measurements with a phase-switched system is shown in the paper by Goldstein, and the sensitivity of the system in the presence of noise is shown to be similar, though not identical, in the same papers. Only a few workers have used correlators so far. The Nançay and California Institute of Technology groups, whose work is described in Section III, are among these.

D. RADIOMETER CALIBRATION

Generally the basis for calibrating any radiometer is a comparison between the deflection of the output recorder when a radio source is observed and a deflection when the radiometer is fed with a known noise power. This calibrating noise power could in principle be derived from a suitably designed thermal source by changing the temperature of such a source by a known amount from $T_1^\circ\text{K}$ to $T_2^\circ\text{K}$. The noise power change fed to the radiometer would be

$$P = k(T_2 - T_1)B \quad (13)$$

where k is Boltzmann's constant. In fact, a knowledge of the antenna temperature change due to the radio source is all that is usually required, so a calibration of the output recorder in terms of $(T_2 - T_1)^\circ\text{K}$ is sufficient.

There are practical difficulties in carrying out such a measurement, although in fact it always has to be made in order to calibrate secondary noise standards. At the higher frequencies (above a few hundred Mc/s) a secondary calibration noise standard in the form of a gas discharge tube, either of argon or neon, is built into the radiometer so that a known calibration signal can be inserted onto a record at will by firing the tube. The gas discharge tube may be mounted in a waveguide (normal at 3000 Mc/s and above) or in a coaxial mount (usual at 1420 Mc/s and below). The noise from the tube is fed into the antenna line as in Fig. 7 through a directional coupler and attenuator. This directional coupler adds a small loss in front of the receiver which may contribute 15–20°K to the radiometer noise temperature. An argon tube behaves like a thermal source of 10 500°K, so that a 20 db directional coupler and 10 db of attenuation give a convenient calibration signal of about 10°K.

Although the temperatures of gas tubes have been measured directly against thermal sources (Hughes, 1956; McNeill, 1961), the results of such measurements are not normally used in calibrating a radiometer, since to do so would still require the measurement of about 30 db of attenuation to a high accuracy. Usually the built-in calibration signal is compared with the signal from a thermal source connected directly to the radiometer input in place of the antenna. The temperature of the thermal source is varied by an amount about equal to the calibrating signal. Such a thermal calibration is made only occasionally, and reliance placed on the stability of the gas tube and its associated attenuation to preserve the calibration. In using a thermal source care must be taken to ensure that possible errors due to losses in connecting cables, temperature gradients along the cables and impedance changes of the source with temperature are negligible, or means must be devised to allow for these effects.

As an example of the care needed even to provide a thermal load at a constant temperature see Stelzried (1961) and for further details of calibration see Mezger (1962). Some receivers are particularly sensitive to small impedance changes at the input, and the changes of impedance of thermal sources may introduce serious errors in the calibration procedure. For example, it is estimated in Altenhoff *et al.* (1960) that in calibrating a receiver with

$T_e = 2450^\circ\text{K}$ errors up to 50 per cent might result if the impedance of the source changed by only 5 per cent. It is often possible to avoid such errors by using a good isolator between the calibrating source and the radiometer. At the lower frequencies, where diode noise sources may safely be used, radiometers may be calibrated by using the diode noise source as a primary standard.

The calibration of hydrogen-line radiometers presents difficulties due to the lack of an absolute standard noise source in the form of an artificial spectral line. It is therefore necessary to measure the radiometer noise temperature and various receiver constants. This indirect method is applied to determine the intensity of a hydrogen-line profile from one standard point in the sky, and the intensity of other profiles is then compared with that of the standard profile. Alternative methods of inserting noise from a broadband noise tube or a small gas discharge lamp into the antenna arm and firing the noise source in synchronism with the switch frequency have also been used, but mainly to provide secondary reference calibrations.

E. RADIOMETERS FOR SPECIAL PURPOSES

1. *Solar Observations*

Many observations of the sun are made with radiometers of the kinds already described, but there remains the important class of observation in which the intensity of solar radiation is observed as a function of time over a very wide range of frequencies. The first observations with this technique by Wild and McCready (1950) were made over the frequency range 70–130 Mc/s, and since that time many workers in the field have extended the techniques to wider frequency ranges and to the measurement of the polarization of the radio waves and the precise position of the active regions on the sun. Some recent references to the extensive techniques are given in the paper by Sheridan (1963), Goodman and Lebenbaum (1958), Maxwell *et al.* (1958) and Casey and Kuiper (1961).

2. *Autocorrelation Radiometers*

An interesting alternative approach to the problem of spectral line observations, which has potential applications to other branches of radio astronomy, has been described by Weinreb (1961). He has applied this technique to observations setting a limit to the galactic deuterium-hydrogen ratio (Weinreb, 1962) and to a search for Zeeman splitting of the hydrogen radiation. When applied to a measurement of the profile of a line the method works as follows. A radiometer, which is switched to give stability, delivers at its output the noise in a bandwidth sufficient to cover the entire line profile. It is well known that if this signal were recorded and its autocorrelation function measured then the Fourier transform of the autocorrelation function would be the power spectrum of the signal. This, of course, is the desired line profile. In applying the method it is assumed that the noise signal has Gaussian statistics, and on this assumption the autocorrelation function can be obtained by digital methods in real time. The Fourier

transform of this function can be calculated within the radiometer or later in a computer. The method gives good stability together with the opportunity to collect and integrate data over many hours of observing time.

II. PARABOLIC REFLECTOR ANTENNAS

A. INTRODUCTION

The most versatile and valuable antenna in radio astronomy is the parabolic reflector. Such instruments, of diameters up to 300 ft, have been built on a variety of mountings. In this section we will describe these antennas by outlining the choices which lead to the design of such an instrument, and we will describe some typical antennas which have already been built and tested.

B. THE CHOICE OF ANTENNA SPECIFICATIONS

Parabolic antennas are good general-purpose antennas for radio astronomy. They can be used for a wide range of research problems extending over quite a wide range of frequencies. In choosing specifications for an antenna, the work to be done with it will generally lead to choice of the following characteristics which have to be specified before the antenna is designed.

1. *Reflector Diameter (D)*

The choice of reflector diameter is governed largely by economic considerations. For a given type of antenna mount, and for a given upper frequency limit at which the antenna will work, experience has suggested that the cost of the antenna will vary roughly as D^3 . Such a relation only holds for diameters between perhaps 30 ft and 300 ft.

2. *Frequency Range*

The lower frequency at which a parabolic dish will be used is decided mainly by the fact that the antenna gain becomes low at long wavelengths. Thus, in practice other types of antenna become more economical. The upper frequency at which the dish will work is set either by the perfection of the parabolic reflector surface or by the size of the holes in the reflector material. The degree of perfection of the paraboloid is determined by the manufacture of the surface itself, or by the rigidity of the supporting structure. In the best practice for very large paraboloids the deflections of the structure generally set the upper frequency limit of the instrument, and the mesh size and the smoothness of the reflector surface are so chosen that they do not themselves reduce this upper frequency limit. The relationship of the gain, beamwidth and sidelobe performance to the imperfections of the paraboloid are of great importance and are treated more fully in Section II, C.

3. *Focal Length (f)*

There is no satisfactory agreement among designers and radio astronomers as to the best method of choosing the focal length for a parabolic dish. The trend is towards an f/D ratio of about 0.3 to 0.4 for the dish with its feed at

the primary focus. The Jodrell Bank dish, 250 ft in diameter, has its feed in the aperture plane ($f/D = 0.25$). Such deep dishes may give less spill-over (Pauliny-Toth *et al.*, 1962), but are more difficult to feed correctly. They gain also in focal point stability, but may suffer from less satisfactory polarization performance.

The Cassegrain antenna is just coming into use as a radio astronomy antenna, although none larger than 85 ft in diameter have so far been built. The Lincoln Laboratory of Massachusetts Institute of Technology 120-ft Cassegrain antenna (Haystack) will be the first large high-precision antenna of this kind used in radio astronomy. These antennas have the obvious advantage of placing the quite considerable weight of electronic instruments required at the focus at or near the vertex of the dish. They suffer from some difficulties in the feed design, since the feed must illuminate the sub-reflector quite efficiently, and in the blocking effects of the sub-reflector. They have, however, been shown to be very effective as low-noise antennas (Potter, 1962) since the main spill-over effect is caused by radiation from the cold sky entering the feed horn past the edge of the sub-reflector.

4. *Type of Mounting*

Almost all parabolic dishes built for radio astronomy have either a polar or an azimuth-elevation (Az/EI) mounting. The smaller instruments, up to 85 ft in size, can be built for about the same cost on either type of mount. The polar-mounted 85-ft dish with its simple drive and control system is an excellent telescope for radio astronomy. The larger dishes are cheaper if they are on Az/EI mounts, and cheapest of all on a simple meridian transit mount. Coordinate converters, which may be mechanical or optical or which may use either analogue or digital computer techniques, have all been used in existing radio telescopes to convert from Az/EI to polar coordinates, and to permit the telescopes to be moved and pointed in the celestial coordinate system. The drives for such Az/EI telescopes must, of course, be servo mechanisms of high performance.

5. *The Drive and Position-Indicator System*

The most important characteristics which are required of the drive and indicator system are that it can direct the antenna beam to the chosen direction in space and move the beam either to track the apparent motion of a radio source or to scan a selected area of the sky. Generally in radio astronomy the accuracy with which the telescope can be pointed or moved has been defined in terms of the beamwidth of the telescope, and pointing or guiding accuracies of one-twentieth of the half-power beamwidth are considered to be satisfactory. For an instrument which will be used over a range of frequencies, the smallest beamwidth, associated with the highest usable frequency, sets this pointing and guiding accuracy. Radio astronomers, in the search for large instruments, have accepted the fact that the telescopes will deflect under their structural dead load, and so large telescopes have to be calibrated to determine the effect of these deflections on the drive and positional accuracy.

6. Environment

All parabolic dishes so far primarily used for radio astronomy have been built to withstand the local weather environment. "Haystack" will be one of the first to be operated within a radome, although many antennas used for radar and communications are so housed. Some savings of cost have been made by requiring precise operation of the radio telescope in winds only up to about 25 m.p.h., and so accepting the fact that observations may have to be suspended in high winds. Survival conditions are chosen to suit the particular telescope location: for example, winds up to 85 m.p.h. and snow or ice loads of 20 lb/ft² might have to be resisted with the telescope in a specially chosen stowed position.

C. THE PERFORMANCE OF A PARABOLIC DISH ANTENNA

In the preceding section we have outlined the main characteristics which have to be chosen in a radio astronomy antenna. Although all these factors bear on the ultimate performance of the instrument, it is generally in the behaviour of the parabolic reflector that the radio astronomer is chiefly concerned. In this section we will summarize what has been achieved in the performance of parabolic dish antennas.

1. The Antenna Gain

Antenna theory permits of the calculation of the gain of a perfect parabolic antenna if the characteristics of the feed at the focus of the antenna are known. The steps necessary in making such a calculation are given, for example, by Silver (1949, pp. 415–433). Such calculations usually overestimate the gain and so have not been used in practice to determine the gain of radio telescopes. The radio astronomer is concerned to achieve adequate gain, satisfactory beamwidth and low spill-over and sidelobes from his antenna. The greatest gain for a perfect parabolic dish would be achieved with a uniform illumination by the feed horn across the dish aperture and no illumination outside the aperture. Such a feed design cannot be achieved, and most paraboloids have used feed horn patterns which diverge considerably from this maximum-gain criterion. Compromises have to be made between the need for gain and the desire to reduce the sidelobes and spill-over in the antenna. Figure 17 shows a typical primary feed pattern which has been used on an 85-ft dish with an f/D ratio of 0.43. With such primary feed patterns the measured aperture efficiency of the dish is about 60 per cent, and the spill-over, when the antenna is directed towards the zenith (so that the feed points towards the ground), represents an increase of antenna temperature of about 25°K. The main beam of the 85-ft reflector using the feed of Fig. 17 is shown in Fig. 18.

The main departures from perfection in practical parabolic antennas arise from the irregularities of the reflector surface, partial transmission through the surface, and blocking of the total antenna aperture by the feed support legs and the equipment near the focal point of the telescope. All these imperfections lead to a loss of gain of the instrument. The effect due to

transmission through the reflector is kept small by using closely spaced mesh or solid-surface reflectors. The criterion accepted for transmission is generally that less than 1 per cent of the energy incident on the reflector surface should be transmitted. This in turn has led to choices of solid-surface reflector materials for antenna reflectors designed to work at 10 Gc/s and of expanded aluminum material for lower frequencies.

The effects of aperture blocking have not been investigated generally for parabolic radio telescopes. Simple diffraction theory can be applied to this problem (Silver, 1949, p. 190) if the obstacles to the wave front are large

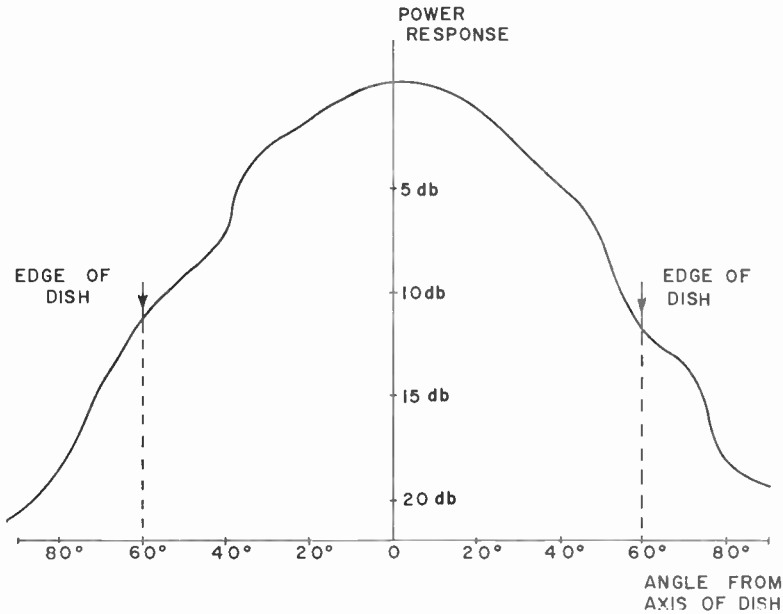


FIG. 17. The primary feed pattern of a horn feed at 7600 Mc/s suitable for an 85-ft dish with $f/D = 0.43$.

compared with the wavelength used, and if the blocking is all assumed to be a geometrical obstruction both of the plane wave front entering the telescope aperture and of the ray paths from the surface of the dish to the feed. The aperture blocking may then be represented as a reduction to zero of the field over the obstructed part of the aperture, and the gain and pattern of the antenna may be calculated for this aperture illumination. A simple calculation of this type made for the case of an aperture blocked by a tetrapod feed support and a circular electronics canister at the focus showed a loss of gain of 0.5 db. The antenna pattern was also modified by the blocking in that the first sidelobes were slightly increased in size and the next slightly decreased.

It can be important to know the effect on the gain of a parabolic antenna of irregularities in the reflector surface. This problem has been discussed

theoretically by Spencer (1949), Ruze (1952) and Robieux (1956), and is summarized by Jasik (1961). A theoretical analysis of the problem can be made in the case where only small random phase errors are produced in the wave front due to irregularities of the reflecting surface. These irregularities will be correlated over finite distances across the surface of the reflector. The theory gives simple expressions for the cases where the correlation interval (c), the distance at which on the average the errors become independent of one another, is much greater or much less than the wavelength used (λ). In large radio astronomy dishes c is always much greater than λ and the expression for the gain (G) compared to that for a perfect surface (G_0), is, for small phase errors:

$$G/G_0 \simeq 1 - \overline{\delta^2} \quad (14)$$

where $\overline{\delta^2}$ is the mean square phase error in radians squared. Equation (14) is compared with measurements made on the 300-ft NRAO paraboloid in Table VII. Gain measurements were made at two frequencies and compared with the gain of a perfect paraboloid using the same aperture illumination. The surface errors were measured by photogrammetric methods.

TABLE VII. *Experimental Verification of the Loss of Gain of a 300-ft Paraboloid Dish due to Surface Irregularities*

Wavelength	Measured aperture efficiency	Measured r.m.s. surface errors	Mean square phase error	Calculated aperture efficiency from equation (14)
40 cm	0.59	1.07 cm	0.12 (rad) ²	0.58
21.4 cm	0.40	1.07 cm	0.42 (rad) ²	0.38

In calculating the aperture efficiency for the last column of Table VII, the estimate of 0.66 for the aperture efficiency of a smooth 300-ft dish with the same aperture illumination was used.

Other tests of the value of equation (14) have been given by Bowen and Minnett (1963) for the 210-ft Australian radio telescope, where they show that the gain of the instrument measured at 10 cm and 20 cm wavelengths fits a curve corresponding to a 5 mm r.m.s. surface accuracy, and by Altenhoff *et al.* (1960) for the Bonn 25-m radio telescope at Stockert. It may be concluded, therefore, that the expression (14) gives a valuable practical estimate of the loss of gain of large parabolic antennas due to surface irregularities.

2. The Antenna Pattern

It is necessary in radio astronomy that the radiation pattern of the parabolic dish be well known, and that it does not show certain undesirable features. The main requirements which have generally been met in practice with the best dishes are:

(a) The main beam should be as narrow as the physical size of the dish permits. Some slight widening of the main beam is acceptable if this is accompanied by reductions in the level of sidelobes and in the amount of radiation received by the antenna from surrounding objects.

(b) The level of the sidelobes should be low. Those close to the main beam are normally kept to 25 db below the main beam in power. The distant sidelobes should be about 50 db below the main beam in power.

(c) The spill-over radiation should be low enough so that the noise contribution added by it is a small fraction of the total system noise of the antenna and receiver.

(d) If the antenna is to be relied on for polarization measurements, the antenna pattern should be closely similar for all planes of polarization of the primary feed horn.

One considerable experimental difficulty encountered is in the measurement of the antenna patterns for large parabolic radio telescopes. To make such a measurement requires the use of a source of radio frequency power which has an angular size small compared with the telescope beamwidth, which radiates sufficient power to be detected even in the relatively insensitive sidelobes of the telescope, and which is more than the "Rayleigh distance" from the telescope. This Rayleigh distance requirement states that the antenna whose pattern is required should be illuminated by an essentially plane wavefront, and this is normally taken to mean that a spherical wave can be used if the difference between paths from the source to the edge and center of the antenna aperture is not greater than $\lambda/16$. The point source must thus be at the Rayleigh distance R from the antenna, where

$$R \geq \frac{2D^2}{\lambda} \quad (15)$$

for this criterion to be satisfied. Phase path errors larger than $\lambda/16$ can be tolerated, but deformed radiation patterns result (Jasik, 1961, p. 34-15). R becomes impractically large for man-made sources to be used to measure patterns of large radio telescopes. Both the Australian 210-ft and the NRAO 300-ft only move from the zenith to an elevation angle of 30° . The values of R for these instruments near their shortwave limits (10 cm and 21 cm respectively) are both about 50 miles, and at 30° elevation an artificial source would have to be at a height of 25 miles.

The use of the stronger radio astronomical sources is possible, provided those of small enough angular diameter are chosen. The sun, for example, is both too large and too variable in intensity for reliable pattern measurements of large dishes. The most intense of the other radio sources give adequate power for good measurements of main beam shape. As an example of current practice some measurements of the main beam shape of the NRAO 85-ft at 7.6 Gc/s are shown in Fig. 18. The experimental observations were derived from a number of scans across the Cas A radio source in right ascension. The smooth curve is of gaussian shape with a half-power beamwidth of 6.95' of arc. The source itself has a finite angular size (about 3' of arc), so that in a result such as is given in Fig. 18 even this rather small source

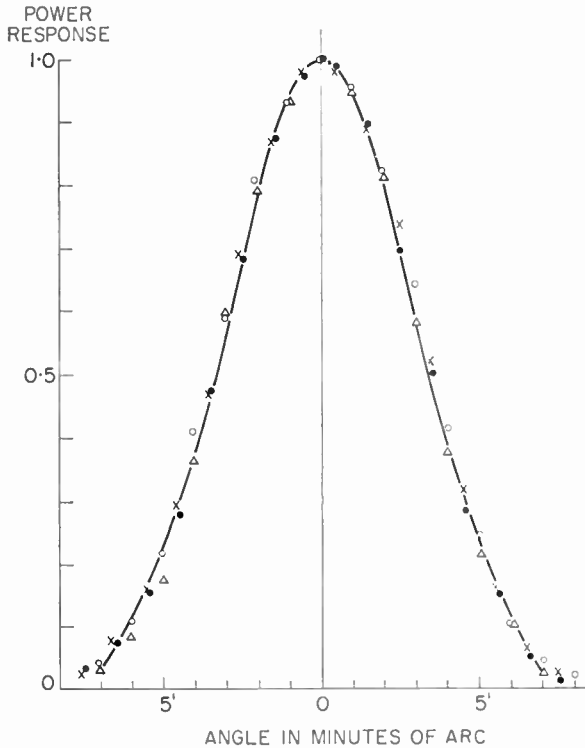


FIG. 18. The shape of the main beam of the 85-ft dish when the feed of Fig. 17 is used at 7600 Mc/s.

diameter is contributing to the width of the antenna response. If allowance is made for this, the measured half-power beamwidth of the 85-ft telescope at 7.6 Gc/s is 6.3' of arc with the illumination of Fig. 17. The resultant relation between antenna diameter, wavelength and half-power beamwidth (HPBW) in radians is:

$$\text{HPBW} = 1.20 \frac{\lambda}{D}$$

The same relationship for a uniformly illuminated circular aperture is

$$\text{HPBW} = 1.02 \frac{\lambda}{D}$$

It is difficult, even with the largest dishes, to observe the lower intensity sidelobes. Cas A, for example, gives for the 300-ft dish at a wavelength of 21 cm an antenna temperature of about 2500°K. Sidelobes which are greater than 40 db below the main beam give antenna temperatures of 0.25°K and

become difficult to measure. The sidelobes which lie at considerable angular distances from the main beam cannot be measured, although qualitative information shows they exist. Observations with the 300-ft telescope during the daytime have shown the existence of solar radiation entering sidelobes which are about 50 db below the main lobe. A series of qualitative measurements made at 21 cm on the NRAO 85-ft dish with a feed illumination pattern about the same as that of Fig. 17, using a ground-based transmitter on a mountain top 6 km away, showed that at angles of more than 30° away from the main beam no sidelobe exceeds the level which would be received in an isotropic antenna. The gain of the antenna at this frequency is 50 db above isotropic.

The presence of low-level sidelobes is already limiting the ultimate sensitivity of large parabolic dishes during the daytime, since the sun is such a powerful source; and the most accurate observations are made at night. The increase of antenna temperature due to spill-over is also becoming significant with the use of low-noise receivers, as can be seen from the figures quoted in Section I, B, 4a. Efforts have been made with both conventional parabolic dishes and with Cassegrain dishes to reduce the spill-over contribution. For conventional dishes, with the feed at the prime focus, quite low spill-over can be achieved with short focal length dishes. Pauliny-Toth *et al.* (1962) report a contribution of only 1°K from radiation from the ground into a 27-ft diameter dish ($f/D = 0.23$) used at 404 Mc/s at the zenith. The aperture efficiency of the dish was 55 per cent. Similar results can be achieved with well-designed Cassegrain systems. Such a system on an 85-ft parabolic dish used for radio astronomy and for tracking deep space probes is described by Potter (1962). After careful design of the sub-reflector system, including a conical extension flange to minimize spill-over, he estimates that at 960 Mc/s, with the antenna pointing to the zenith, the contribution of spill-over to the system temperature was 3°K . The measured aperture efficiency of the telescope was 50 ± 8 per cent (compared with a calculated value of 58 per cent). The main dish had a primary focal length of 36 ft.

It is possible, of course, to modify the primary feed radiation pattern for a conventional paraboloid of longer focal length so that spill-over is minimized. Schuster *et al.* (1962) describe the performance of an 85-ft dish identical with that used by Potter, when various feeds are used at the prime focus of the telescope at both 960 Mc/s and 2388 Mc/s. The technique of measuring the antenna temperature is also described in this article. Tests were made using horn feeds and a specially designed shaped beam feed which consisted of a small-aperture square horn set in a large ground plane. The ground plane reduces unwanted wide-angle and backlobe radiation from the feed. With this feed at 2388 Mc/s the spill-over was about 5 per cent, which corresponds to a contribution of 15°K at most to the antenna temperature, and the aperture efficiency of the dish was 55 per cent. Further development work on primary feeds with shaped patterns is continuing, and the evidence suggests that spill-over as low as 1 per cent (corresponding to 3° contribution from the ground to the system temperature) may be achieved.

3. *The Polarization Performance*

In the last few years measurements of the polarization of radio waves emitted by the sun, by discrete radio sources and by the diffuse sky background have assumed very considerable importance. The results of such measurements are given in many papers, of which those by Cohen (1958b), Mayer *et al.* (1957), Westerhout *et al.* (1962), Cooper and Price (1962), and Morris and Radhakrishnan (1963) are only a selection. Such measurements set very rigorous requirements on the performance of the antenna system used.

For a complete knowledge of the state of polarization of the incoming radio waves, it is necessary to observe properties of the waves equivalent to the determination of the four Stokes parameters (Cohen, 1958a), and this has been done by some observers. However, most observations so far of the polarization of the discrete radio sources and of the galactic background have been restricted to determinations of the percentage plane polarization of the incoming wave and to the position angle of the plane-polarized component of the partially polarized wave.

When polarization measurements are to be made with a parabolic antenna it is essential that the effects of the antenna itself be measured. The simplest polarization measurement uses a plane-polarized feed horn or dipole which is slowly rotated about the dish axis. If dish and feed were perfect, the signal received by this feed from a completely unpolarized source would not vary with the position angle of the feed. In practice, even with very good parabolic dishes, there is a variation of up to about 1 per cent in the signal collected by the feed as it rotates. In practice, also, there is an additional contribution to the instrumental effects if the antenna is collecting noise power from the surrounding ground. The ground, being a dielectric, radiates differently for orthogonal polarizations, and thus any ground radiation in the antenna will be partially plane polarized. This contributes to the antenna effects.

Despite these instrumental difficulties, the results of observations of the polarization of radio sources made with parabolic dishes have already been most successful. Effects of the change of the polarization angle with frequency have been observed (Cooper and Price, 1962) and it is evident that radio astronomy is now entering a new and very productive field of research. A very similar state exists in measurements of the polarization of the background radiation from our own galaxy. Westerhout *et al.* (1962) published the results of a survey in a paper which is interesting both for the results themselves and also for understanding of the effects of the radio telescope on the polarization measurement. When the sky background measurements are attempted, the overall antenna pattern and its polarization characteristic become more important, and these effects are discussed in the paper.

D. CHARACTERISTICS OF SOME SPECIFIC ANTENNAS

Many different types of parabolic antenna have been built in recent years and only selected examples will be described here: these are a medium-size

polar-mounted antenna, a large azimuth-elevation mounted antenna and a large transit antenna, which will serve to illustrate various aspects of the design and performance of antennas.

1. *The 85-ft Polar-Mounted Antenna at NRAO*

This instrument was completed in the early part of 1959, and has performed very satisfactorily since that time. A brief specification of the instrument follows:

- Dish diameter: 85 ft.
- Focal length: 36 ft ($f/D = 0.424$).
- Surface: Aluminum sheet panels.
- Sky coverage: 6^h east to 6^h west in hour angle, except as limited by the horizon. Declination motion is from the North Pole to within 2° of the south horizon, i.e. $+90^\circ$ to -50° .
- Drive system: Electric motor drive in slew, scan, and track about the polar axes; slew and scan about the declination axes.
- Indicator system: A geared synchro system reading to $30''$ of arc is generally used. A high precision ($3''$ of arc) inductosyn system is available for special work.
- Constructed by: Blaw-Knox Equipment Division, Pittsburgh, Pennsylvania.

The general design of the antenna is shown by Fig. 19. The polar motion is provided through the polar gear, 48 ft in diameter, and the declination motion through a gear 20 ft in diameter. The drive system permits the telescope to be moved fairly rapidly (slewed) in hour angle and declination at $20^\circ/\text{min}$ to move it from one observing position to another. The fine setting of the telescope is controlled by drives with speeds variable up to $8^\circ/\text{min}$, and these same drives are used to scan the telescope across the small area of sky being examined. The telescope may also be moved from east to west hour angles by constant speed drives at either the solar or the sidereal rate; in the latter case the telescope remains pointed at the same area of sky.

Observations with such a telescope are often made by keeping the telescope fixed in hour angle and declination, and allowing the radio source to move through the beam. Areas of sky may be observed in this way also, or by moving the telescope at the sidereal rate in hour angle but scanning in declination at a uniform speed. The rate at which the telescope moves during an observation must be chosen to allow for adequate integration time being used in the receiver to achieve the sensitivity that the observations require. For observations of very weak sources, long integration times of a minute or so are used, and for them the telescope is set either to track the source or to move at a rate very nearly the sidereal rate so that the apparent drift of the source through the beam is slow.

The 85-ft telescope was designed for use at frequencies as high as 10 Gc/s and very many observations have been made with it at a frequency of 8 Gc/s (3.75 cm). The surface of the reflector was carefully set to approximate as

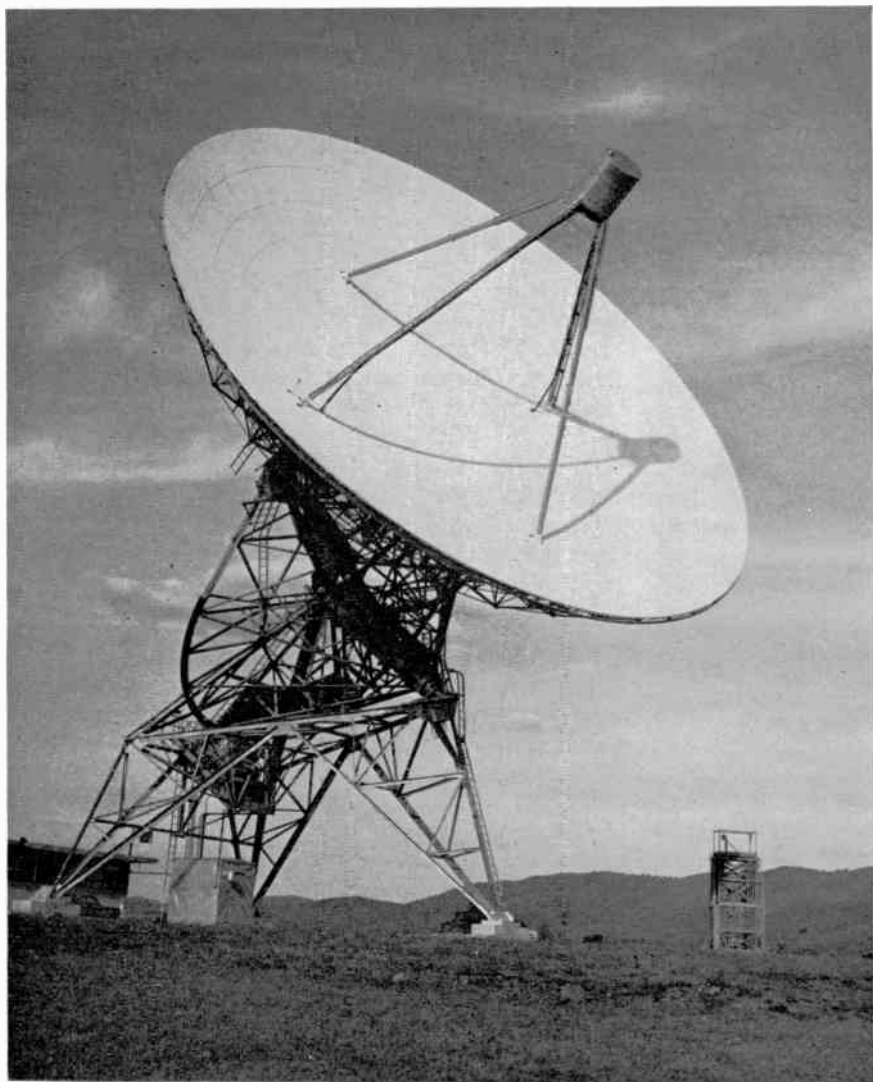


FIG. 19. The 85-ft Howard E. Tatel radio telescope at the NRAO.

closely as possible to its correct parabolic shape when the dish was pointing toward the zenith. This setting was made by using measurements of the surface position by an accurate theodolite and a surveyor's steel tape. A check of the accuracy of the setting of the surface and of the stability of this setting with time and of the way the surface deflects as the dish is tilted is provided in Fig. 20. This figure shows the contours of equal deviation of the surface from a best-fit parabolic surface when the dish is pointed towards

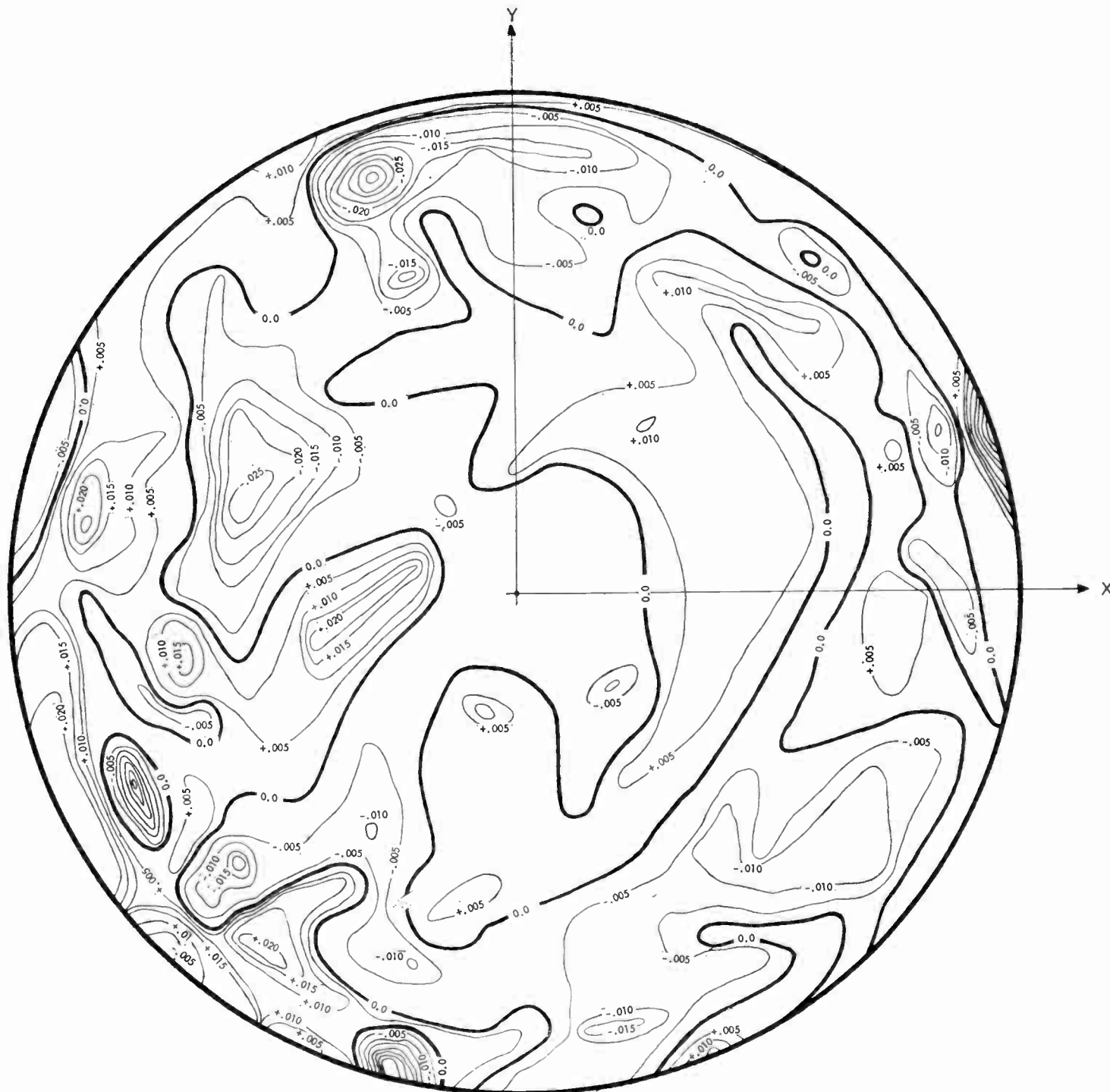


FIG. 20. Photogrammetric measurements of the surface of the NRAO 85-ft telescope. The contour interval is 0.005 ft or 1.52 mm.
 FIG. 20a. Dish pointing to the zenith.

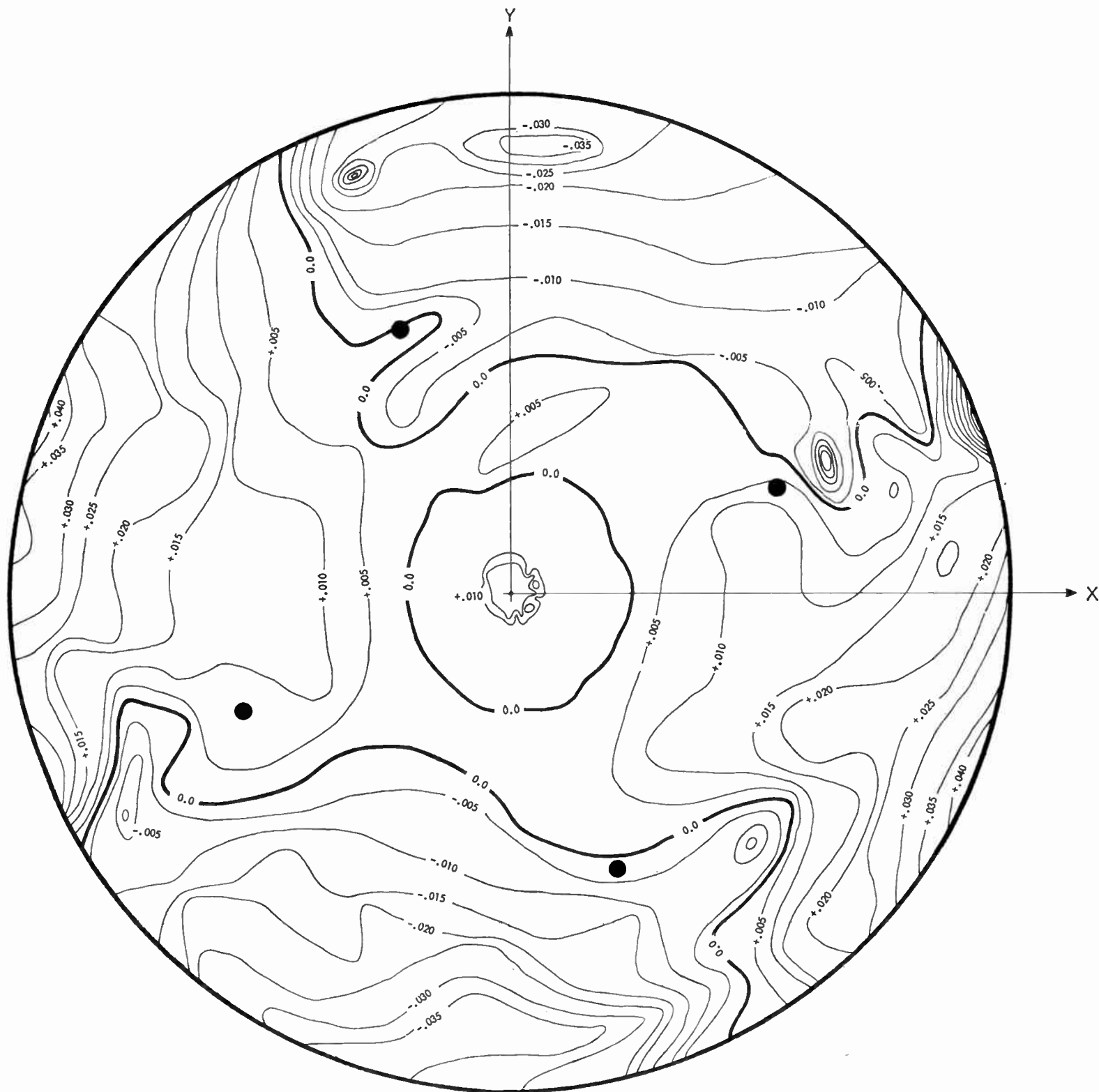
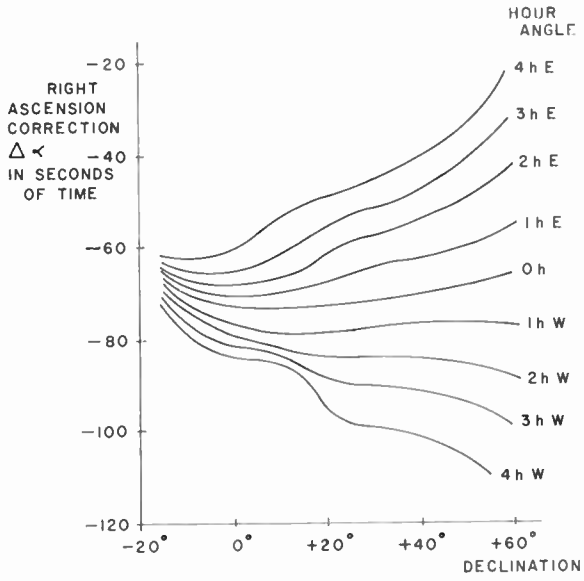


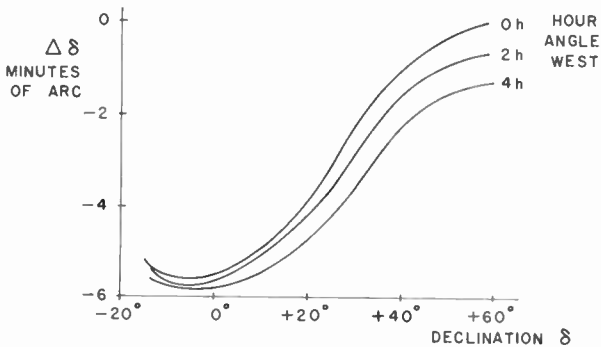
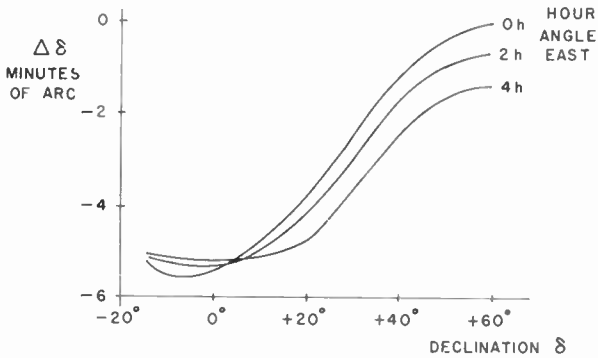
FIG. 20b. Dish pointing to the horizon.

FEED SUPPORT ●



$$\alpha_{\text{INDICATED}} = \alpha_{\text{TRUE}} + \Delta \alpha$$

FIG. 21a. The corrections in right ascension.



$$\delta_{\text{INDICATED}} = \delta_{\text{TRUE}} + \Delta \delta$$

FIG. 21b. The corrections in declination.

FIG. 21. Pointing calibration curves for the NRAO 85-ft telescope.

the zenith (Fig. 20a) and towards the horizon (Fig. 20b). They were obtained from a photogrammetric survey of the telescope surface made in late 1962. The surface panels had previously been adjusted by the tape and theodolite method in 1960. These photogrammetric results are summarized in Table VIII.

TABLE VIII. *Summary of Measurements of the Surface of the 85-ft Telescope*

Position of dish zenith distance	Greatest departure from best-fit paraboloid	r.m.s. departure from best-fit paraboloid	Focal length of best-fit paraboloid
0°	1.7 cm	0.32 cm	35.883 ± .006 ft
90°	1.6 cm	0.57 cm	35.748 ± .0015 ft

Measurements of this kind show several points of interest in the structural behavior of a parabolic dish. The greatest departure of the surface from the best-fit surface is clearly due to an error in setting the surface, since it occurs in the same area of the dish at both zenith distances. (It can be seen at the right-hand side of the dish in Figs. 20a and 20b just above the X-axis.) The fact that the r.m.s. departure is almost twice as great with the dish at the horizon as at the zenith agrees with the fact that the dish surface was originally set at the zenith position. The dish and its supporting structure deflect in moving from zenith to horizon, but there is still a reasonable adherence of the dish surface to a best-fit paraboloid. This paraboloid also changes in focal length as the dish moves from zenith to horizon, as the last column of the table shows.

In summary, to a first order the main effect of the structural deformations of the dish shows as a movement of the best-fit paraboloid axis with respect to the apparent movement of the telescope, as shown by its indicator system, and a change in focal length of the dish. To these deformations must be added the movement of the feed horn of the telescope as the feed-support legs also deflect.

It is of course practically possible to calibrate the deflections of such a telescope so as to make first-order corrections to the telescope position as shown on the indicator system. Such calibrations are always made for parabolic dish antennas by making observations of radio sources whose positions in the sky have already been well determined. In the case of the 85-ft dish, it has been possible to detect the radio radiation from planets at the higher frequencies, and to use the known planetary positions to provide the necessary reference system of very high accuracy. Drake (1960) has reported the use of the telescope to measure a number of source positions to accuracies of 10" of arc. For general use, positional calibration to 30" of

arc is adequate, and for this purpose calibration curves are drawn showing the corrections to be applied to the indicated positions. An example of such curves for the 85-ft telescope is given in Fig. 21. Some of the change in beam position is due to feed-support deflection and, since this depends on the load carried at the focus of the instrument, it is necessary to recheck the pointing calibration of such a telescope when major instrumental changes are made. It is necessary to recheck the pointing calibration when new feeds are used, since it is not possible to position the phase centers of all feeds in the identical position with respect to the axis of the parabolic dish.

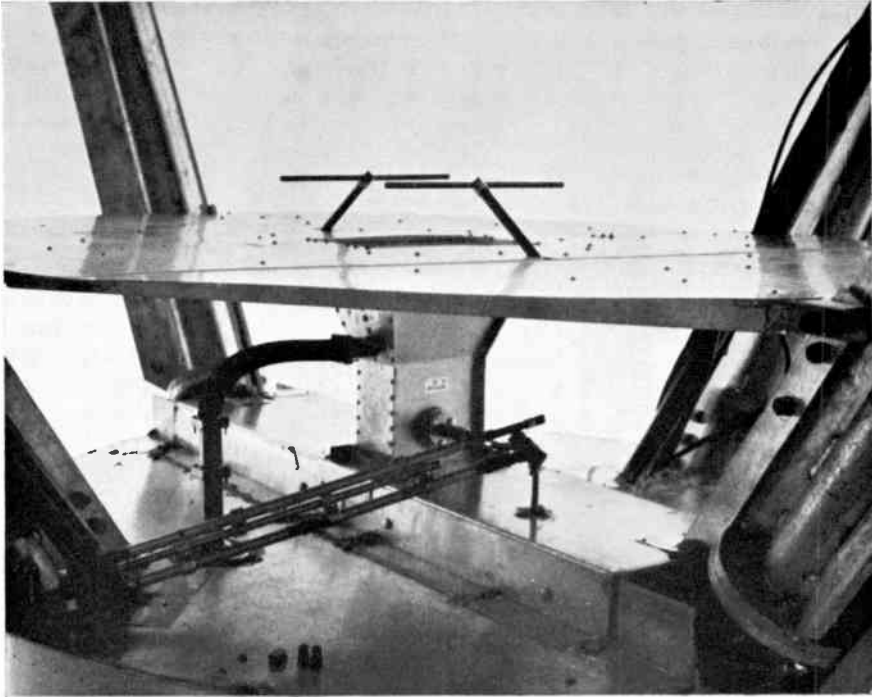


FIG. 22. The three-frequency feed used on the NRAO 85-ft telescope.

A wide variety of feed systems have been used on the 85-ft antenna, ranging in frequency from 440 Mc/s to 8 Gc/s. One of the more interesting composite feeds is shown in Fig. 22. This consists of three concentric confocal feeds, which can be used simultaneously if necessary. The pair of dipoles and ground plane is a 440 Mc/s feed. The horn feed covered by a radome is used from 1350–1450 Mc/s, and within this horn is another horn which can be used over the frequency range of 7–9 Gc/s. Generally, scientific programs do not require the simultaneous use of such a cluster of feeds, but various programs can be carried out with separate receivers connected to the feeds with no delay in changing from one program to another.

2. *The 210-ft Telescope at the Australian National Radio Astronomy Observatory*

The group of the Division of Radiophysics at the C.S.I.R.O. in Sydney, Australia, has developed several novel antenna systems for radio astronomy, and also has recently completed building the 210-ft steerable parabolic dish (Fig. 23). Full descriptions of this instrument are given by Bowen and

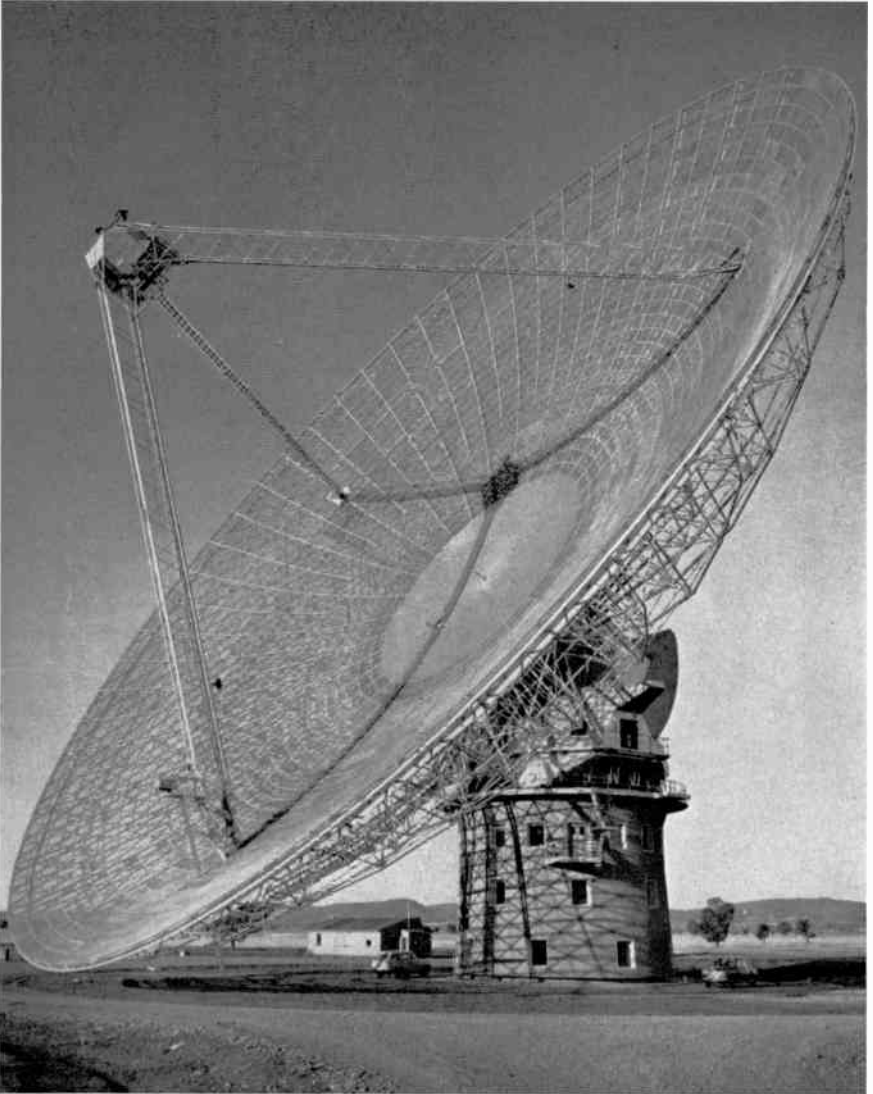


FIG. 23. The 210-ft steerable radio telescope of the Australian National Radio Astronomy Observatory at Parkes, N.S.W. This telescope is operated by the CSIRO Division of Radiophysics.

Minnett (1963) and Minnett (1962), and the first results obtained with the telescope are given by Kerr (1962) and Bolton (1963).

The principal specifications of the telescope are:

- Dish diameter: 210 ft.
- Focal length: 86 ft ($f/D = 0.41$).
- Surface: Central 55-ft diameter is welded steel plate; remainder is $\frac{5}{16}$ -in galvanized steel mesh.
- Mount: Azimuth/Elevation.
- Sky coverage: Complete in azimuth, in elevation moves 60° from the zenith.
- Drive system: Electric servo motors.
- Positioning system: The Az/El mount is guided in equatorial coordinates by means of a master equatorial unit.
- Designers: The original feasibility study, design and engineering were by Freeman Fox & Partners, London, England. The staff of C.S.I.R.O. worked closely with them throughout the project.

Although the 210-ft dish was not the first large fully steerable parabolic antenna to be built, since it was preceded by the Jodrell Bank 250-ft telescope (Lovell, 1957; Husband, 1958), it serves as an excellent example of a large accurate instrument incorporating modern and novel techniques.

The required performance of the telescope was stated with considerable care before design work started. The size of the dish was chosen only after a careful study had shown how the cost and complexity of the instrument would vary with its size. The surface accuracy of the dish was specified in terms of the departures of the actual surface from the paraboloid of revolution which best fitted the surface. Good performance at 21-cm wavelength was regarded as essential, and in fact the instrument operates satisfactorily at 10 cm wavelength. The area of sky covered by the instrument was chosen to exclude the 30° of elevation angle immediately above the horizon, a region where irregularities of atmospheric refraction and possible absorption in and radiation from the atmosphere become noticeable. The telescope was not required to operate in average winds greater than 20 m.p.h., nor would it have to withstand ice and snow. Choosing such realistic design criteria allows for a good but quite economical structure to be built, and the consequent slight loss of observing time or sky cover is more than outweighed by the economy of the total instrument. The full description of the telescope is given in the articles already quoted. The main novelties in the design lie in the system of coordinate conversion and control of the instrument. It also has been fitted with many good receivers and with a large cabin at the focus to house a variety of electronic equipment. The feeds can be rapidly exchanged and are mounted on a rotating support so that the plane of polarization can be varied at will.

The control system for an Az/El telescope used in radio astronomy should allow the telescope to be moved and set in celestial coordinates. The necessary coordinate transformation can be done by an analogue coordinate con-

verter, or by a digital computer running fast enough so that the errors due to computer time are small. The problem is solved for the 210-ft dish by using an analogue optical coordinate converter suggested by Dr. Barnes Wallis (1955). In principle, a small precise optical telescope is set on an equatorial mount at the point where the azimuth and elevation axes of the radio telescope intersect. This "master equatorial" is driven from the control room to point at the desired part of the sky, or to track or scan in the desired way. By an optical link, the radio telescope is forced to follow the pointing of the master equatorial. The optical link is a beam of light projected from the radio telescope structure and reflected from the mirror of the master equatorial back to a two-axis error detector. Any errors in the position of the reflected light beam cause the main Az/EI drive motors to run until the errors are reduced to zero. The whole system, including the master equatorial and the drive motors, represents a servo mechanism of high performance. The master equatorial is mounted on a column structurally independent of the main load-bearing tower of the telescope. The system of coordinate conversion reduces the magnitude of the pointing errors which in more conventional systems may arise from gear imperfections, gravitational structural deflections and bearing irregularities.

3. *The 300-ft Transit Telescope at Green Bank*

This instrument was designed and constructed in a short time for a rather modest cost in order to fill some definite needs in radio astronomical research. It is described more fully by Findlay (1963). The following is a brief specification of the instrument:

Dish diameter:	300 ft.
Focal length:	128.5 ft ($f/D = 0.428$).
Surface:	Expanded aluminum mesh (Squarex) 0.625 in \times 0.091 in.
Mount:	Meridian transit.
Sky coverage:	From the North Pole through the zenith to 60° south of the zenith. (Declination range +90° to -21°.)
Drive system:	Two-speed electric drive through quadruple roller chain giving positioning speeds of 10°/min and 2.5°/min.
Indicator system:	A digital encoder disk giving a 10"-of-arc digit interval operating a declination display and also providing printed and punched tape outputs.
Designers:	Robert D. Hall and Edgar R. Faelten.

The astronomical problems required that the telescope perform well at wavelengths of 21 cm and longer, and it was realized that it would be difficult and costly to achieve an accuracy compatible with this in the whole steel structure. The main structure was therefore designed to be fabricated and erected to the accuracies normally achieved in standard engineering practice, and the surface was designed so that it could be fitted to the required accuracy onto the steel supporting members. To reduce the cost and size of the project, it was also agreed to accept the limitations of a transit mount, the

fact that precise operation would only be possible in winds up to 15 m.p.h. and that the 30° of sky above the southern horizon would not be observed by the telescope. The instrument, which is shown in Fig. 24, was completed in 23 months from the start of design work at a cost of about \$850 000.

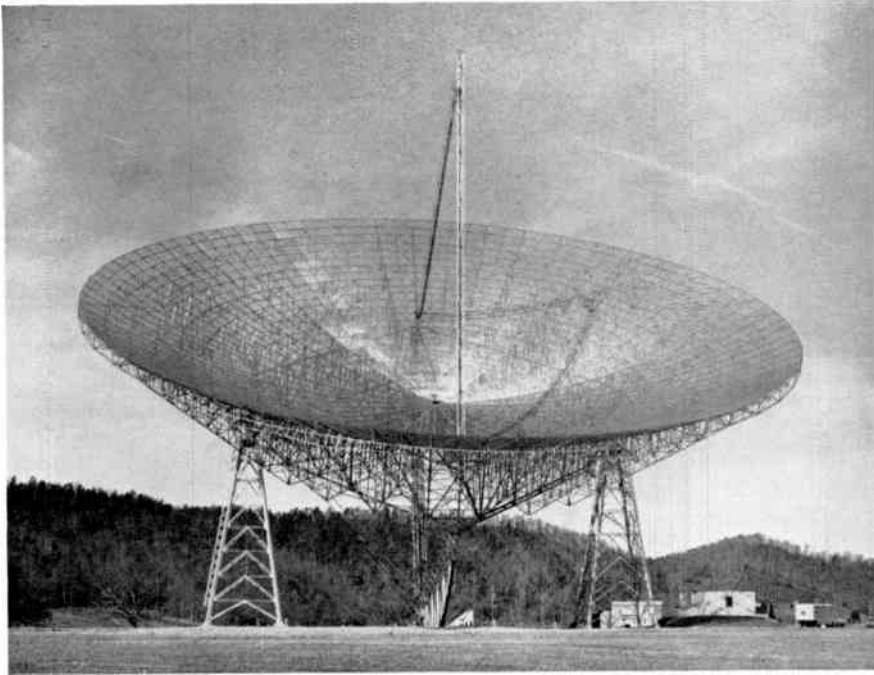


FIG. 24. The 300-ft transit radio telescope at the NRAO.

The principle features of interest in such a telescope are the relationships between the structural behaviour of the dish and its supporting structure, and the radio performance of the telescope.

Table VII summarizes the way in which the gain of the instrument varies as the radio frequency changes, and also shows how the changes of gain may be related to the surface irregularities of the dish. The surface measurements were made by photogrammetric methods, in the same survey described in Section II, C, 1 for the 85-ft dish. Three hundred and five photographic targets were fixed to the 300-ft dish surface in a regular pattern, and these were photographed by a special camera using ultra-flat glass plates coated with a fine-grain but fast emulsion. Three good photographs of the targets were obtained with the telescope at the zenith and three more with it 30° from the zenith. These photographs were taken from a helicopter. One similar aerial photograph and one ground-based photograph were used when the telescope was $51^\circ 24'$ from the zenith. The plates were measured and after

various corrections had been applied the coordinates of the target points with respect to the parabolic surface which best fitted the target points were determined. The results are given in Fig. 25 in the form of contour diagrams showing the departures of the surface from the best-fit paraboloid. The results are also summarized in Table IX below.

TABLE IX. *Summary of Measurements of the Surface of the 300-ft Telescope*

Position of dish, zenith distance	Greatest departure from best-fit paraboloid	r.m.s. departure from best-fit paraboloid	Focal length of best-fit paraboloid
0°	3.3 cm	1.07 cm	128.145 ± .012 ft
30°	2.8 cm	1.27 cm	127.980 ± .011 ft
51° 24'	3.4 cm	0.95 cm	127.782 ± .009 ft

This table shows how the focal length of the best-fit paraboloid decreases as the telescope goes from the zenith towards the horizon; an effect similar to that seen for the 85-ft dish. The r.m.s. surface errors of the instrument vary irregularly at the greater zenith distance. The structural deflections, both of the dish and of the feed support, show again in the calibration curves of the instrument (Fig. 26). The plot of indicated-minus-true declination against declination shows that as the telescope moves from the zenith through 60°, the radio beam moves through an angle about 7' of arc less than that indicated at the elevation axis. This is due to the feed support deflecting downward through a larger angle than the angle through which the axis of the best-fit paraboloid moves. The plot of the right-ascension calibration curve shows mainly that the bearing axis of the telescope is not exactly on a true east-west line—in fact, it can be deduced from the calibration curve that the dish points about 3' of arc west of the meridian when it is at its greatest southern declination.

Figure 27 shows the contour maps of the beam shape when measured at 1400 Mc/s and 750 Mc/s. The measured beamwidths at half power (10' and 18.5' of arc respectively) are closely similar to those predicted from the dish size and the known primary feed patterns. There is more distortion and there are greater sidelobes at 1400 Mc/s, since at this frequency the surface accuracy of the dish is showing its effects both on the gain and the pattern of the dish. Some of the pattern irregularity may be due to the steel cables which give lateral support to the bipod feed support. A total of ten cables, each $\frac{5}{8}$ -in steel aircraft cable, provide this support.

The telescope has been used for extensive observations at and near 1420 Mc/s. For some of these, a moving feed has been used so that a fixed point in the sky could be tracked for a short time through the transit. The

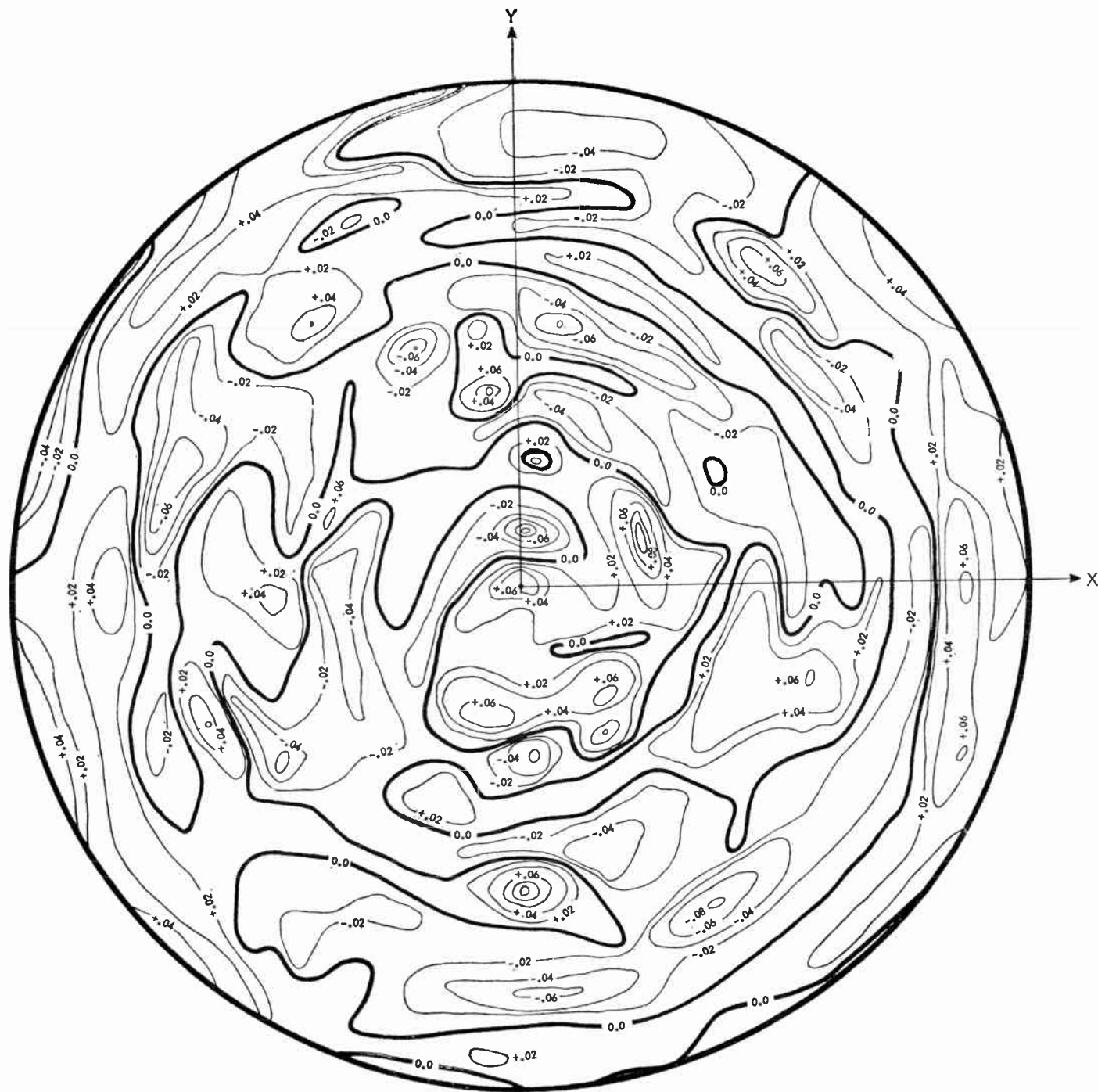


FIG. 25a. Dish at the zenith.

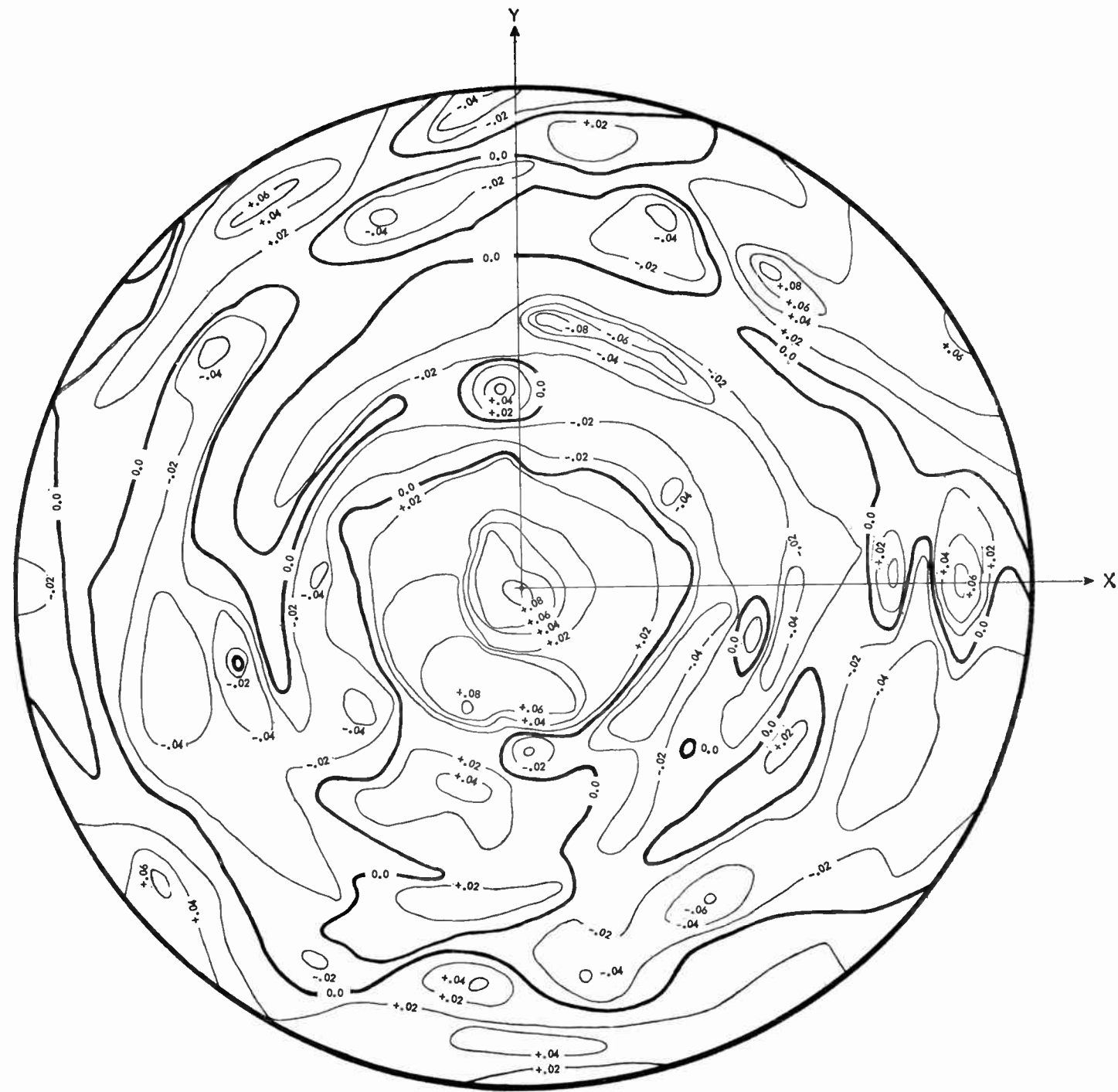


FIG. 25b. Dish at a zenith angle of 30°.

FIG. 25. Photogrammetric measurements of the surface of the NRAO 300-ft telescope. The contour interval is 0.02 ft or 6.1 mm.



FIG. 25c. Dish at a zenith angle of $51^{\circ} 24'$.

total beam movement obtained was three beamwidths (30' of arc) on either side of the dish axes. The telescope has also been used for a large number of polarization measurements of sources, and its characteristic polarization effects have been measured and shown to be reproducible.

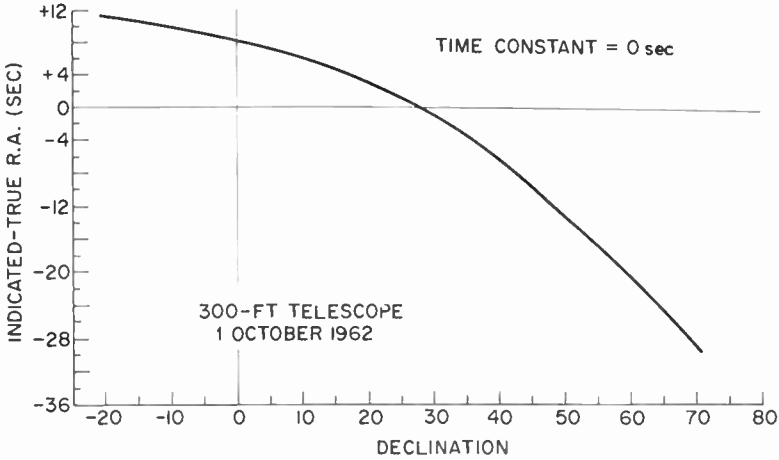


FIG. 26a. Right ascension.

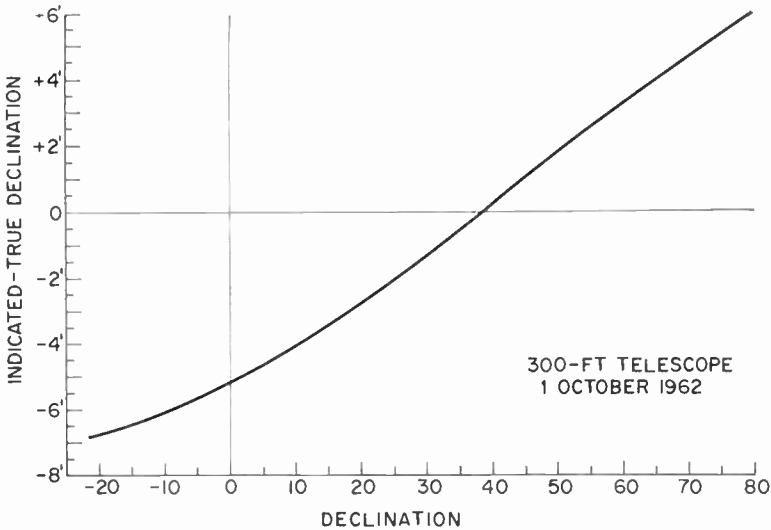


FIG. 26b. Declination.

FIG. 26. Pointing calibration curves for the NRAO 300-ft telescope.

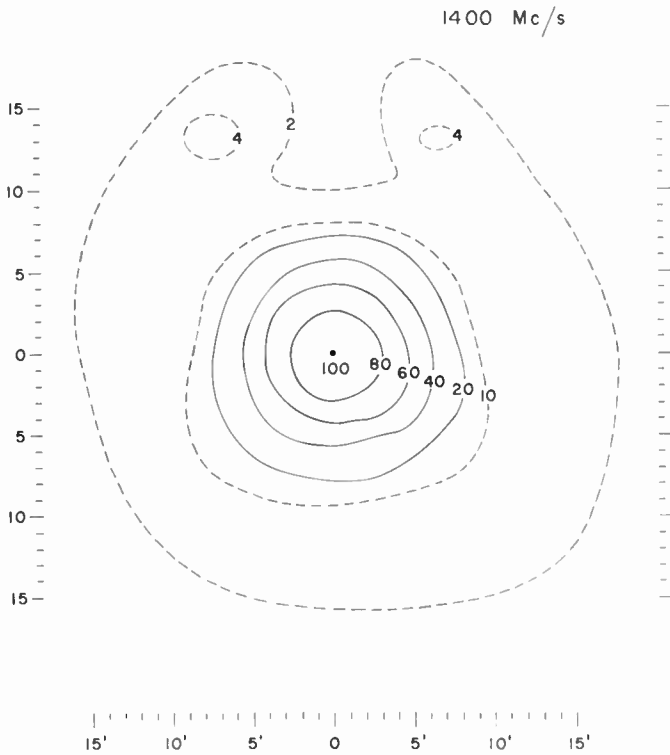
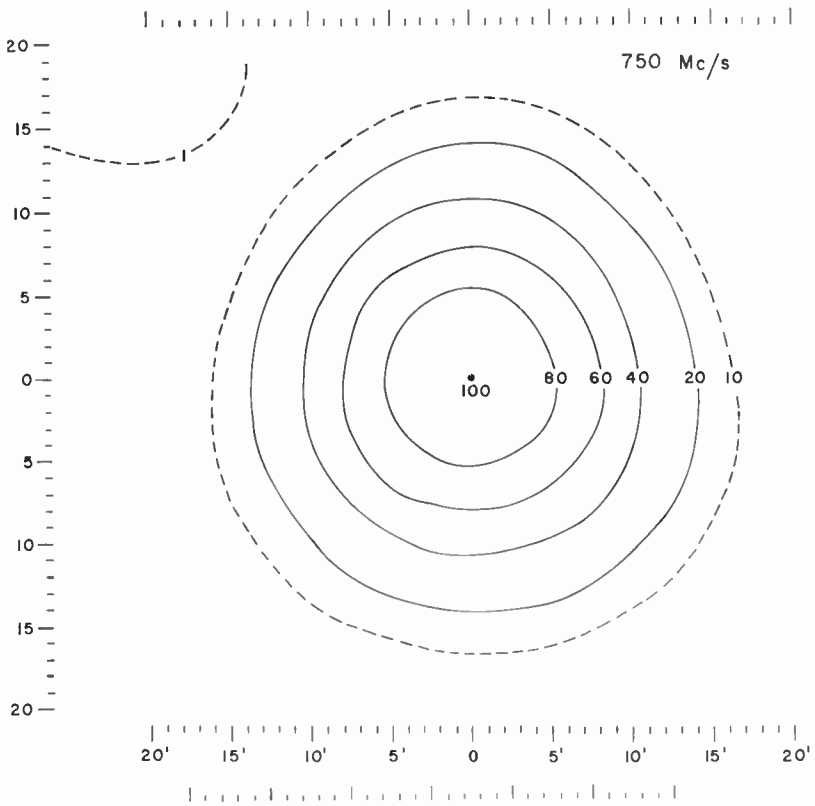


FIG. 27. The intensity contours of the beam shape of the 300-ft telescope.
(a) at 750 Mc/s; (b) at 1400 Mc/s

III. OTHER TYPES OF RADIO ASTRONOMY ANTENNAS

A. INTRODUCTION

Although the parabolic reflector antenna because of its simplicity and wide usefulness is the most important single type of antenna used in radio astronomy, it is true to say that a large portion of radio astronomical research has been carried out using other types of instruments. It is difficult to divide them into suitable categories, so that in the following section they will be treated in approximately the order in which they depart from filled-aperture antennas. Developments are rapid, and antenna systems are being studied and developed continuously. The present account is restricted to antennas which are already operating or sufficiently far advanced in construction for their main characteristics to be known.

B. REFLECTOR ANTENNAS

There are three main types of reflector antenna, which may be described as cylindrical parabolic antennas, spherical surface reflectors, and antennas of the tilted plate type. All these reflector antennas have been developed with the intention of keeping as large a part of the reflector surface fixed as firmly as possible to the ground as its main support. In this way large fixed reflectors of considerable accuracy can be built at fairly low costs. The requirement to move the beam of the telescope is met by different means in the various types of instruments; the relative advantages of each depends to a considerable extent on the kind of research for which it is required. The three main types of antenna can be described by means of specific examples.

1. *The Parabolic Cylinder Antenna at the University of Illinois*

This antenna, described by Swenson and Lo (1961), has for its main objective the determination of the intensities and positions of as large a number of radio sources as possible; and the instrument is very well suited for such a task. Its main characteristics are summarized below.

General type:	Meridian transit.
Aperture shape and size:	400 ft (EW) × 600 ft (NS).
Focal length:	153 ft.
Frequency of operation:	611 Mc/s (49 cm wavelength).
Half-power beamwidth:	19' of arc.
Beam movement:	By phase adjustment of the feed from +10° to +70° in declination.
Polarization:	Circular.

The various practical points of interest are treated in the article referenced. The feed system and its phasing deserve specific mention, since a straight-forward linear feed using elements closely spaced enough to avoid the appearance of a secondary major beam within the working range of declination of the telescope would have required about 400 individual elements. Each would have needed its own phase shifter. In fact, by using circularly

polarized feed elements and by rotating these to change the phase, considerable economy resulted, although a strict requirement is then placed on the perfection of the circular polarization of the element. If, in fact, this feed element were slightly elliptically polarized the whole antenna would suffer from a secondary lobe which would be moved in declination in a regular way when the primary beam is moved. This difficulty was overcome in the antenna design by combining the phase shift due to the transmission line to an element with the phase shift due to the rotation of the element so that the required main beam of the telescope was correctly formed from the in-phase contributions while the unwanted lobe was not formed since the contributions to it from the various feed elements were in random phase.

To reduce the number of individual feed elements, non-uniform spacing of these elements along the focal line was adopted, together with some weighting of the power collected from the central group of elements. Extensive calculations led to a successful design for the current weighting and spacing of the elements. The individual elements themselves were carefully-designed equiangular spirals wound on a conical surface (Dyson, 1959), giving a low axial ratio and excellent wide-band frequency characteristics. Against the advantage of the low cost per unit area of collecting surface for this type of antenna must be weighed the difficulties in forming a good beam with low sidelobes, of steering this beam, and in changing the antenna operating frequency.

2. *The Spherical Reflector Antenna*

The possibilities of using a spherical reflector which remains fixed and a suitably corrected feed which moves to steer the beam have attracted various workers for some time. Earlier work, such as that by Ashmead and Pippard (1946) for example, mainly considered the situation where the necessary corrections for the spherical aberration of the system were small. Spencer *et al.* (1949) showed one way in which this spherical aberration could be corrected by using a phase correcting line source, and Head (1957) suggested using an auxiliary reflector around the feed. Other methods of correction using lenses or multiple feeds have been proposed. Love (1962) describes a practical phased line source used in a series of experimental tests with antennas working from 8.3 to 34.6 Gc/s. Further theory of the spherical reflector antenna is given by Schell (1963).

The phased line source appears to be the most attractive solution to the problem of correcting for the aberration. Simple geometrical optics (Spencer *et al.*, 1949) shows that, of all the parallel rays which enter a spherical mirror, the marginal rays such as MP (Fig. 28) cross the axis at F' and rays lying close to the axis cross at F . F is the paraxial focus and FO is half the radius of curvature of the mirror. Thus a line feed lying along FF' can in principle collect all the energy incident on the mirror, and if this energy is correctly combined in phase by the feed the spherical aberration will be zero. It is possible to combine the total energy at F if means can be found to adjust the phase velocity of the paths within the line feed between F' and

F; and this can, for example, be achieved by using waveguide of such dimensions that the phase velocity varies in the correct manner along the guide. The practical design of such feeds is more complicated. In addition to giving the correct phase correction, they must have the correct directivity;

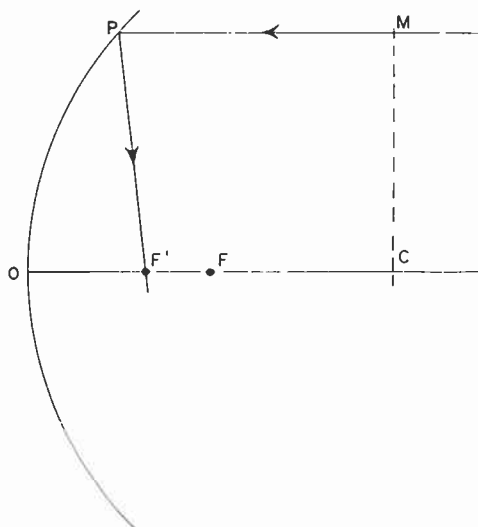


FIG. 28. The geometry of a spherical reflector.

for example, the part of the feed at F must act as an end-fire receiver looking at O, while at F' it must be almost a broadside antenna. Ways of achieving this are summarized by Love (1962). Such feeds also can generally be designed to work only over a relatively narrow band of frequencies.

a. The 1000-ft Arecibo Reflector. A most interesting example of a very large spherical reflector with a corrected line feed has been built in a natural fairly spherical depression in the earth near Arecibo, Puerto Rico. The antenna was designed by members of the Cornell University Center for Radiophysics and Space Research, and the project is sponsored by the Advanced Research Projects Agency of the U.S. Air Force. Although the primary functions of the antenna (Gordon and LaLonde, 1961) are ionospheric research and radar astronomy, it will also be capable of carrying out many radio astronomical studies.

A brief specification of the instrument is:

General type:	Fixed zenith pointing reflector with moving feed.
Aperture size and shape:	1000 ft diameter part of sphere.
Focal length:	Paraxial focal length 435 ft ($f/D = 0.435$).
Frequency of operation:	430 Mc/s (70 cm wavelength). The bandwidth of the feed is 10 Mc/s at the 3 db points.

Half-power beamwidth:	10' of arc.
Beam movement:	By moving the feed the beam can move anywhere within a cone of semi-angle 20° centered on the zenith.
Polarization:	Two orthogonal linear polarizations may be used.
Transmission:	The feed may be used for transmission and reception.

A radio telescope of such size raises many structural, mechanical and electrical problems. The practical realization of the line feed in the form of a slotted waveguide 96 ft long is described by Kay (1961); and the strict structural, as well as mechanical, requirements for the feed are described. The support system by which the feed is positioned to the necessary accuracy above the dish surface consists of steel cables from the tops of three towers carrying a central triangular structure on which rotates an azimuth truss. This truss carries the feed on a movable carriage, so that it can point to the required direction in the dish. The feed can illuminate the whole dish, and when used in this way the gain of the instrument will fall and the beamwidth increase as the beam moves away from the zenith. Less of the surface could be used by a change in feed illumination so that these changes would not occur as the beam is steered.

Such a telescope has the great advantages of large size with a relatively modest cost. Against this must be weighed the limited sky coverage, the cost of new feeds for different frequencies, and the rather small bandwidth achieved for any single feed. It is interesting to note that fairly soon beamwidths of almost exactly 10' of arc in pencil beam instruments will be available to radio astronomers at 430 Mc/s (Arecibo), 1400 Mc/s (NRAO 300-ft), 3 Gc/s (NRAO 140-ft) and 6 Gc/s (NRAO 85-ft); so that mapping of areas of the sky with scaled antennas over a wide range of frequencies becomes possible.

3. *The Tilted Plate Antenna*

Two examples of this type of antenna which have been built and used for radio astronomy are based on the design proposed by Kraus (1955). A fixed vertical reflector surface which is a section of a paraboloid with its focus near the ground is used, and rays arriving from a particular declination are directed onto this reflector by a large tiltable flat plate. The purpose of the design is to achieve large collecting area, good resolution and reasonable sky coverage with an instrument, the main reflecting areas of which can be built on the ground. The telescope built and described by Kraus *et al.* (1961) and Kraus (1963) is at the Ohio State University, and a very similar telescope has been built at the Nançay Station of the Paris Observatory by Denise and his group (Blum *et al.*, 1963). Both these projects take advantage of the fact that this type of antenna can be extended, and in both cases the central sections of the instrument were built and tested first, and lateral extensions were planned for the future.

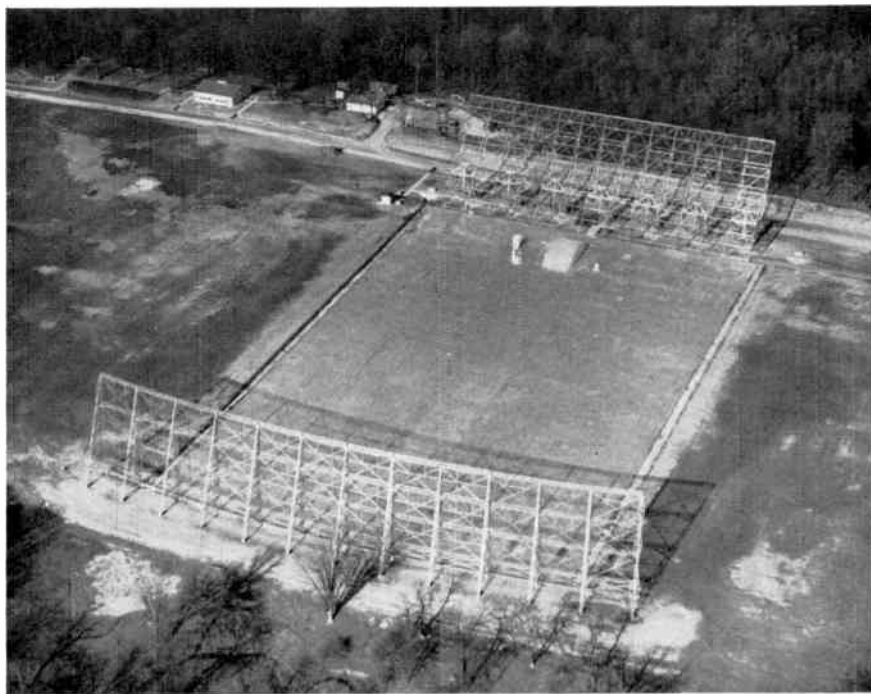


FIG. 29. The radio telescope at Ohio State University.

a. The Ohio State University Telescope. The general appearance of this instrument is shown in Fig. 29, which shows the three main components of the instrument, the standing parabola, the tiltable plane reflector and the horizontal ground plane. The general specifications of the instrument are:

General type:	Meridian transit with limited ability to track in hour angle.
Aperture size and shape:	Parabolic reflector 360 ft long by 70 ft high which can be extended to 720 ft \times 70 ft. Flat reflector 100 ft wide \times 260 ft long; this also can be extended.
Focal length:	420 ft.
Frequency range:	Usable from 30 Mc/s to 2 Gc/s.
Half-power beamwidth:	

Frequency	Right ascension	Declination
100 Mc/s	2.5°	10°
1 Gc/s	0.25°	1.0°
2 Gc/s	0.13°	0.5°

Sky coverage:	In declination from the pole through the zenith towards the southern horizon. The effective aperture is a function of declination.
Feeds:	Aperture blocking is small. Multiple feeds using various frequencies or polarizations may be used.

The performance of the instrument is limited at the higher frequencies since the parabolic reflector screen has 1 in spacing between the wires over the central 180 ft and 1.5 in spacing beyond. Improvements in the screen wire can easily be made. The surface of the ground between the tiltable plate and the parabolic reflector is transformed by making it a flat conducting surface into an image plane. This in turn gives a reduction in the height of the feed horn needed to illuminate the parabolic reflector and reduces the noise from the ground entering the receiver system.

b. The Pulkovo Telescope. A second type of tiltable plate telescope is that built at the Pulkovo Observatory and described by Kalachov (1963). In this instrument ninety rectangular flat elements are arranged on the ground so that the energy striking them is reflected and focused onto a feed also on the ground. The ninety plates can be tilted and moved to form a section of a paraboloid, so chosen that at transit the required source is observed at the focus. The telescope has been used at wavelengths as short as 3 cm. The main characteristics of the instrument are summarized below:

General type:	Meridian transit.
Aperture size and shape:	Ninety reflector elements, each 1.5 m × 3 m in size, arranged around an arc 100 m in radius. Total area = 405 m ² .
Focal length:	100 m.
Frequency range:	Up to 10 Gc/s.

C. TWO-ELEMENT INTERFEROMETERS

Much of the earliest radio astronomy carried out after 1945 was done with simple interferometer antennas. The use of the phase-switched interferometer (Ryle, 1952) and the realization that interferometer observations could give a method of determining the brightness distribution across radio sources (McCready *et al.*, 1947) have led to a very extensive use of these instruments. They have been used for surveys of the positions, intensities and polarizations of radio sources and for the determination of the angular sizes and brightness distributions of radio sources as well as for the examination of the sources of radio noise on the sun. The recent developments in the use of interferometry of greatest interest have been in the use of two-element systems for measuring accurate positions, angular size and brightness distribution of sources.

1. *Theory of the Two-Element Interferometer*

The theory of the interferometer may be found in general works such as Pawsey and Bracewell (1955) and Bracewell (1962), while the reasoning

which leads to the statement that observations of the complex visibility of the interference pattern can provide the Fourier transform of the source distribution may be found in Bracewell (1958). It is worth describing what is meant by an observation of the complex visibility of an interference fringe pattern. The term "visibility" is taken from the optical terminology, where, if I_{\max} and I_{\min} are the intensities at the maximum and minimum of an interference fringe system produced by a two-beam optical interferometer, the visibility V is defined by

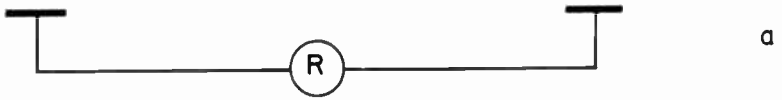
$$V = \frac{I_{\max} - I_{\min}}{I_{\max} + I_{\min}} \quad (16)$$

The same concept of visibility in the radio interferometer case can be extended to include a measure of the phase of the fringe pattern, and this phase ϕ combined with V as defined above gives the complex visibility V of the fringe system.

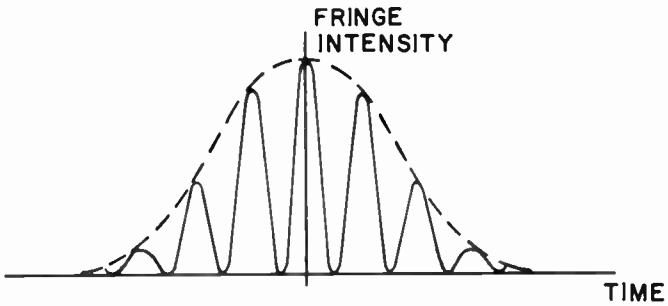
$$V = V e^{j\phi} \quad (17)$$

The determination of fringe visibility and phase for a simple two-element total power interferometer is explained by reference to Fig. 30. The interferometer is shown diagrammatically in 30a, and is assumed to consist of two identical antennas on an east-west baseline connected by equal length cables to a receiving and recording point R. We will imagine the system directed south at zero declination (towards the celestial equator) and consider the response of the system as a radio source on the equator crosses the meridian. Diagram 30b shows the fringes from such a source which is small in angular size compared to the angular size of the antenna lobes. These fringes are enclosed within the envelope determined by the antenna pattern of one of the two antennas. If we suppose there to be perfect equality in the phase paths from the antennas to the receiver, and if the antennas are each pointing directly south, then the central fringe maximum is at the maximum of the envelope pattern and occurs at the sidereal time of transit of the source across the meridian. We measure the phase of the fringe pattern by observing the sidereal time at which the maximum of this central fringe occurs and take $\phi = 0$ for the fringes in 30b. Diagram 30c shows the fringes from a symmetrical extended source whose center has the same position in the sky as the point source of 30b. The visibility is less and the phase is still zero since the transit time is still the same. Diagram 30d shows the fringes from an extended source which has an unsymmetrical brightness distribution measured along the celestial equator. The visibility is less than unity and the phase ϕ is no longer zero. To measure ϕ the displacement ΔT in seconds of time of the central fringe from the envelope maximum is measured and then $\phi = \frac{2\pi\Delta T}{T}$ where T is the period in seconds of the fringe system.

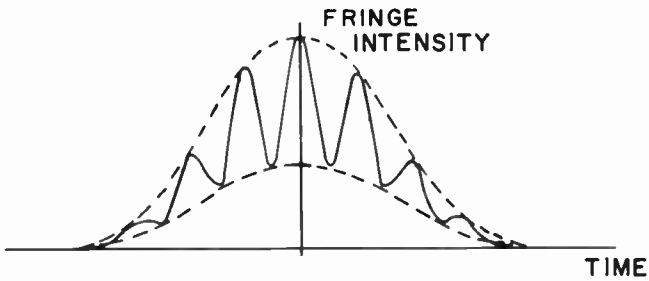
In applying the method of visibility measurements to the determinations of angular size and brightness distribution across the radio source, much may be achieved by the experimentally simpler expedient of observing only



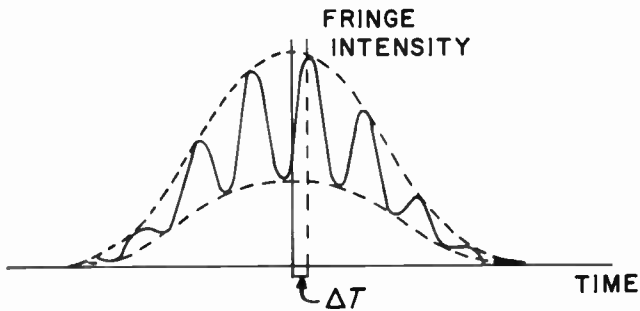
a



b



c



d

FIG. 30. The use of the two-element interferometer to measure the intensity distribution across a source.

FIG. 30a. The simple interferometer.

FIG. 30b. Fringes obtained with a point radio source.

FIG. 30c. Fringes obtained with a symmetrical extended radio source.

FIG. 30d. Fringes obtained with an unsymmetrical extended radio source.

the magnitude V of the complex visibility function rather than attempt to measure both V and ϕ . The results of measurements of V alone cannot lead to unambiguous measures of brightness distribution since (as is well known in the optical case) more than one brightness distribution can be derived from an observed visibility curve unless the brightness distribution is symmetrical. However, for angular diameter measurements this is not of prime importance. In some of the instruments we shall consider both V and ϕ have been measured, while some have measured only V .

2. Two-Element Interferometer Measurements of Position, Angular Size and Brightness Distribution of Sources

From the earliest use of two-element interferometers their value in measuring the positions and sizes of sources has been realized. The positions of a number of radio sources were found by Bolton (1948) using a cliff-edge interferometer. The accurate position of the Cas A radio source found by Smith (1951) led to the identification of this strong radio source with a very faint optical object. Interferometers were used to measure brightness distribution across the solar disk (Stanier, 1950; O'Brien, 1953) and to make measurements of the angular size of sources (Brown *et al.*, 1952; Mills, 1952; Smith, 1952). A great deal of work has followed and we will select for description the instruments and techniques used at the Nançay radio astronomy observatory, the California Institute of Technology, and the Nuffield radio astronomy laboratories at Jodrell Bank.

a. The Twin-Aerial Interferometer at Nançay. This instrument (Blum *et al.*, 1963) consists of two 7.5-m parabolic antennas which can be moved both east-west and north-south along a railroad track. Spacings of 1480 m (7000λ) and 380 m (1000λ) can be used at a wavelength of $\lambda = 21$ cm. The system has good phase stability (10° of phase in several hours), it uses a multiplier to combine the two 5 Mc/s wide signals at the 30 Mc/s intermediate frequency. Although the antenna collecting area is small, a system for integrating the fringe patterns is used in which the integration may take place over as long as an hour. Thus the system has been used to measure sources which give an antenna temperature as low as 0.01°K . The results of measurements on forty sources are given by Lequeux (1962) in the form of scalar visibility curves and the derived brightness distributions across the sources.

b. The California Institute of Technology Interferometer. This instrument consists of two 90-ft diameter polar mounted parabolic antennas which can be moved on both an east-west and a north-south railroad track each 1600 ft long. The principles of the instrument are described by Read (1961). It has been used in a wide variety of measurements of the positions, polarizations and brightness distribution of radio sources. The papers by Moffett and Maltby (1962, I, II and III) describe the brightness distribution results. Amplitudes, and in some cases the phases of the complex visibility functions, were measured for 127 sources (east-west baseline) and 165 sources (north-south baseline) with 99 sources common to the two sets. Antenna spacings

of 200, 400, 800 and 1600 ft were used on both baselines at a frequency of 958 Mc/s ($\lambda = 31.3$ cm) and observations on both baselines were made both at transit and at angles away from transit.

The receiving equipment (Read, 1961) was a simple superheterodyne with a good low noise performance, a separate mixer and preamplifier being used at each antenna focus. An interesting feature was the use in the interferometer of both the signal and image bands of the receiver, each 5 Mc/s wide and 20 Mc/s apart in central frequency. This technique has considerable advantages in making it easier to improve the phase stability of the system, in that the only critical paths over which phase stability must be either maintained or monitored are those the signal and the local oscillator follow to reach the first mixers. The phase stability of the paths of the intermediate frequency signals from the mixers to the point at which the signals are combined are not critical. The IF signals were multiplied rather than added.

The system was carefully calibrated both for gain changes and for phase changes. Sources of measured angular diameter small enough that the fringe visibility would be independent of antenna spacing, and strong sources whose fringes could be easily measured and whose amplitude should be always the same at the same spacings were used to give the gain calibration. Phase calibration was made by using as reference sources those which the amplitude results showed were only partially resolved at the longest spacings, and observations of these sources allowed for a check to be maintained of the phase changes in the instrument. The results obtained with this interferometer demonstrate the value of such instruments when carefully used and also are of much interest in considering the possibilities of large antenna systems based on interferometer techniques.

c. Two-element Interferometers at Jodrell Bank. From the various interferometric work carried out at Jodrell Bank that of measuring the angular sizes of sources has introduced some new and interesting techniques. One of these is the use of a correlation technique (Jennison and Das Gupta, 1956) in a two-element interferometer whereby it is not necessary to preserve the relative phases of the signals from the two antennas before they are combined. A second interesting technique is the use of very long baselines for angular size measurements.

(i) *The post-detector interferometer.* The theory of the use of the correlation coefficient of the two detected outputs from the two elements of an interferometer and the relation between this coefficient and the visibility of the fringes from a conventional interferometer is given by Brown and Twiss (1954). The theory is difficult even when applied to radio wavelengths; the corresponding optical case also has been discussed at great length. A somewhat simpler treatment of the instrument is given by Jennison (1961). Figure 31 shows the block diagram of such a correlation interferometer. The signals from the two antennas are amplified and each is then independently detected by a square-law detector. The low frequency outputs from these detectors, defined by a low pass or audio frequency filter, are then multiplied together, as well as being separately recorded. A delay is introduced to ensure that both

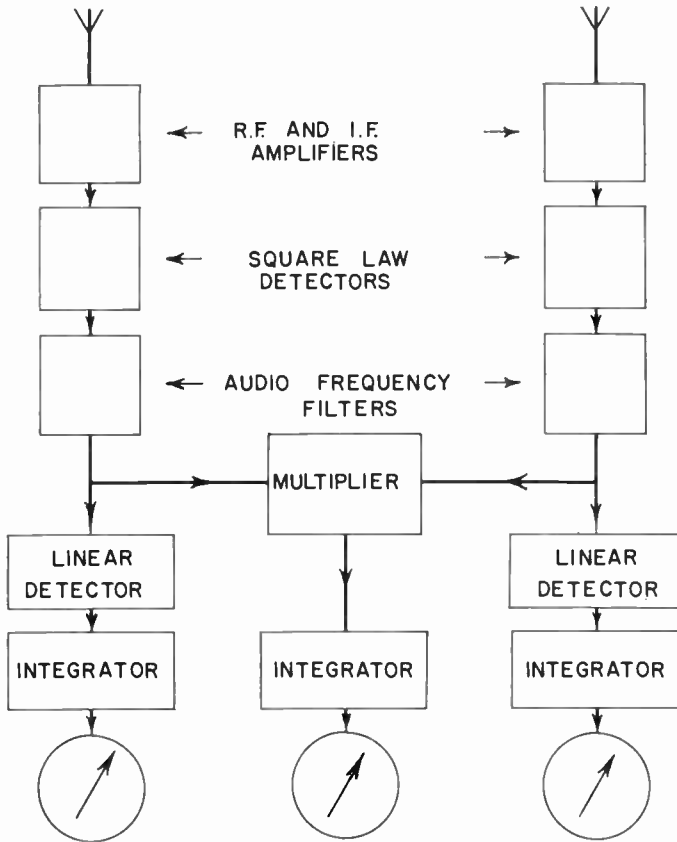


FIG. 31. The post-detector interferometer.

audio signals arrive together at the correlator. The output of the correlator is a measure of the cross correlation coefficient (ρ^2) of the two signals. As the spacing of the antennas is changed, ρ^2 varies as the scalar visibility V of a fringe system varies, and from the variation of ρ^2 the angular size and shape of the source may be found. Just as in the fringe interferometer when no measurements of fringe phase are made, observations of ρ^2 can only be interpreted as symmetrical source distributions, so that the method cannot be used for making true source distribution maps. Also the technique is restricted to sources of intensity sufficient to give a good signal-to-noise ratio. The method is nevertheless of considerable interest since it may be used under conditions where it is difficult in practice to maintain the phase relationship between the signals from two separated antennas sufficiently well to produce interference fringes.

(ii) *Long baseline interferometry.* Two-element interferometry has been extended in baseline to lengths of 61 100 wavelengths at Jodrell Bank (Allen

et al., 1962a). One antenna of the pair was the 250-ft steerable dish, the other was a set of three cylindrical paraboloid antennas each 30 ft long and 25 ft wide placed at varying distances from Jodrell Bank. The observations have been made at 158.6 Mc/s ($\lambda = 1.89$ m) and spacings up to 115 km have been used. The main novelty in the techniques employed has been in the ways in which the phases of the signals from the two antennas have been controlled so that fringe patterns can be recorded at these great spacings. It is not possible, of course, to attempt to observe the phase of the fringes themselves, and it is necessary to calibrate the system for the visibility of fringes by using sources of very small angular diameter such as 3C48 which appeared to be unresolved (Rowson, 1963) even at the greatest antenna separation. These measurements at $61\,100 \lambda$ correspond to an angular separation between interferometer lobes of only $3.4''$ of arc.

The interferometer was operated as follows. Coherent local oscillator power was supplied from the main station at Jodrell Bank to each antenna. This power was derived from a carrier at 175 Mc/s sent by radio to the distant station, and the antenna signal from that station was returned to the home station over a radio link at a low intermediate frequency. A time delay was supplied by either a quartz or mercury delay line, or at shorter spacings by delay cable, so that the signals from the two antennas could be recombined with approximately no time difference between them. At such great spacings the fringe system changes rapidly with time, so that a continuous phase rotation was applied to slow down the fringes to a convenient value. The equipment has been described by Elgaroy *et al.* (1962). Two aspects of the technique, the local oscillator link and the method for slowing down the fringes, were more complex than the above simple description would suggest, and they are described in detail in the paper. The signal was sent over the long path from the remote antenna to the home station by impressing it as a frequency modulation on a microwave radio link. On the longest path, a microwave repeater was used in this link. Tests were conducted of the phase stability of the system over the $32\,000 \lambda$ baseline and it was established that although phase variations can occur in the transmission path of the radio link these are not rapid enough to cause difficulty in the observations. These tests of phase stability were made in fact around a loop of $64\,000 \lambda$. The experimental observations of the phase changes of fringes from radio astronomical sources suggested that ionospheric irregularities were the cause of a major part of the changes leading to unstable fringe movement. The results obtained with this instrument (Allen *et al.*, 1962a) give observations made at four baselines of 384 sources, and the significance of the measurements is discussed by Allen *et al.* (1962b).

D. UNFILLED APERTURES OF HIGH RESOLUTION

It was realized from observations made with interferometers that, particularly at meter wavelengths, resolution of antennas could be increased without requiring a similar increase in collecting area. The first of this type of antenna was proposed by Mills (Mills and Little, 1953) in the form of a

symmetrical cross of two long and narrow antennas in the north–south and east–west directions. Such an antenna system can give an angular response similar to that of a filled-aperture pencil-beam antenna of dimensions approximately the size of the cross, although its collecting area is far less than that of the filled aperture. A second type of unfilled-aperture antenna is the line or cross of separate antennas, with considerable open space between them, first used for radio astronomy by Christiansen and Warburton (1953), and by Tanaka and Kakinuma (1953). Many instruments of similar design have been built at various observatories.

Both these techniques are by now quite familiar, and so we will give here only a brief treatment of the theory and practical use of these antennas.

1. *The Mills Cross*

The first large cross antenna was built (Mills *et al.*, 1958) at the Fleurs Station of the Australian Radiophysics Laboratory to operate on a frequency of 85.5 Mc/s ($\lambda = 3.5$ m). The instrument in principle consists of a cross formed by two arrays of dipoles, each 1500 ft long, one arm being north–south and the other east–west. One such array alone would give a fan beam response about 50° by 0.6° between the half-power points, and by combining the outputs of the two arrays correctly the whole antenna can be made to have a pencil beam response corresponding in size and position in the sky to the overlap of the two fan beams. This pencil beam may be moved in the sky by adjusting the relative phases of signals collected from the individual dipoles of either array, although for most of the work of the antenna it may be used as a transit instrument; in which case the phases of the north–south array only need be adjusted to move the beam to the required declination.

The theory of the array is given in detail in the above paper. It is somewhat complicated by the need to allow for the fact that with two such close arrays the antenna diagrams are not entirely independent but that each array somewhat modifies the pattern of the other. If this complication is neglected it is a simple matter to show that, in the simplest case where the arrays and feeder lengths are equal and when the signals from the two arrays are combined in a phase-switched system with a square-law detector, the response pattern is the product of the voltage responses of each antenna. Thus the array is a pencil beam instrument. Since the pattern of each array is broad in one plane, the total response of the system may contain sidelobes of troublesome magnitude. These may be reduced by a suitable taper of the current distribution along each array, and in the Mills 3.5-m array a quite severe current taper in the form of a truncated Gaussian curve is used, with the current in the end elements one-tenth of that at the center. The sidelobes are then 20 db below the main beam response except the first sidelobe which is 17 db down.

The original Mills cross has been used for a variety of radio astronomical work (for a brief summary see Mills, 1963) and the value of the technique may best be judged by the list in Table X below of cross antennas which have been built since the original cross, or are now in construction.

TABLE X. *A List of Some Mills Cross Type Antennas*

Location	Size	Frequency	Reference	Remarks
Australia, CSIRO	1500 ft	85.5 Mc/s	Mills <i>et al.</i> (1958)	
Australia, CSIRO	3625 ft N-S 3400 ft E-W	19.7 Mc/s	Shain (1958)	
USSR, Serpukov	1 km 3280 ft	Up to 200 Mc/s	Kalachov (1963)	To be completed 1963
Benelux	1.5 km 4900 ft	Up to 1420 Mc/s	Christiansen <i>et al.</i> (1963)	Being designed
Italy	3600 ft N-S 3900 ft E-W	408 Mc/s	Braccesi and Ceccarelli (1962)	Under construction
Australia, Sydney University	1 mile	408 Mc/s and 111.5 Mc/s	Mills <i>et al.</i> (1963)	Under construction

2. Multi-Element Interferometers

Under this general title fall a number of antenna systems, all containing more individual receiving elements than the two-element interferometer. Antennas built for specific functions, such as the Cambridge four-element interferometer (Ryle and Hewish, 1955) used mainly for surveys of radio sources, and the National Research Council of Canada 600-ft compound interferometer (Covington, 1960) used for solar observations, represent examples of multi-element instruments. The type of instrument which consists of a line or cross of individual elements, usually parabolic dishes, has been developed by many workers.

The theory of an array of equally spaced elements in a line is closely parallel to the theory of the optical diffraction grating. The antenna in its simplest form has all its elements connected by equal feeder lengths to a common receiver. The resulting pattern shows an interference maximum whenever the path difference of rays entering adjacent elements is a whole number of wavelengths, and the entire pattern is modified by the pattern of a single antenna element (Fig. 32). Since the purpose of these arrays is to achieve high resolution with a limited number of elements, the element spacing is always a large number of wavelengths so that the resulting pattern from a linear array may contain several main lobes. When two line arrays are used in the form of a cross, the instrument then may be used as a Mills cross and the resulting pattern has a central pencil beam with other pencil beams formed where the products of the separate fan beams are large. Thus, even in the pencil beam use, the antenna gives several beams in the sky. For the main applications of the instrument, which have been the study of the distribution of radio sources on the sun's disk, it can be designed so

that only one beam falls on the disk and the rest fall on the comparatively very cold sky. Thus no appreciable errors occur in observations of the sun, but there may be several limitations to the use of such instruments for the study of the fainter radio sources.

One of the techniques required in using these instruments is the maintenance of the correct phase in the signals collected from the elements and delivered to the receiver, and the means of adjusting this phase in the north-south arm of the cross if the instrument is to be used to track or scan sources

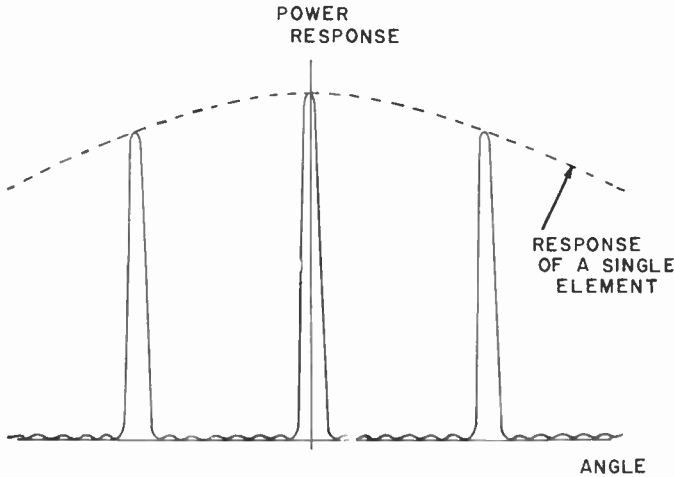


FIG. 32. The antenna pattern of an eight-element interferometer.

at different declinations in the sky. Among methods of changing phase, at 10 cm wavelength Bracewell and Swarup (1961) use a dielectric strip inserted into the waveguide, Christiansen and Mathewson (1958) at 21 cm move the junction points on the feeder system, while at 1.77 m the Nançay system (Blum *et al.*, 1963) makes use of an adjustment by cables at the IF in such a way that the instrument provides records simultaneously at fifteen slightly different declinations. An interesting method of measuring the phasing in such an array was used by the Stanford group (Swarup and Yang, 1961) which directly measures the fractional part of the phase path from a common point in the receiving system to each of the antenna feeds independently. Using this technique the phase can be measured and adjusted.

There are now several large multi-element interferometers of the Christiansen type in use. Some of these are summarized in Table XI below with references to fuller descriptions of the instruments.

It is possible to combine other elements with a linear array of dishes to give specific response characteristics to the whole array. The array of Covington (1960) and the use of the east-west arm of the Sydney 21 cm cross with a 60-ft dish (Labrum *et al.*, 1963) are examples of the performances which can be achieved with such techniques.

TABLE XI. *Multi-Element Interferometers of the Christiansen Type*

Location	Length of array in wavelengths	Wavelength	Number of elements	Reference
Sydney, Australia	1800	21 cm	32 + 32 19-ft dishes	Christiansen and Mathewson (1958) Christiansen and Mullaly (1963)
Nancay, France	875 E-W 435 N-S	177 m	35 5-m dishes for E-W arm; 8 10-m dishes for N-S arm	Blum <i>et al.</i> (1958) Blum <i>et al.</i> (1963)
Stanford, U.S.A.	1255	9.1 cm	16 + 16 3-m dishes	Bracewell and Swarup (1961)
Toyokawa, Japan	1290	3.2 cm	16 1.2-m dishes	Hatanaka (1963)

E. THE TECHNIQUE OF APERTURE SYNTHESIS

1. *General Principles of Synthesis*

The principles of the technique which is now known as aperture synthesis have been appreciated for some considerable time, but it remained for the Cambridge group of radio astronomers under Ryle to show both in theory and in practice how these principles could be applied. The theory is given in Ryle and Hewish (1960) and also, together with the results of the first test of the system in mapping a part of the sky, by Blythe (1957a, b).

a. The Synthesis of a Filled Aperture. We will first consider aperture synthesis as a method of achieving the performance of a filled aperture instrument. It is always assumed that the radio source or area of sky which is to be observed remains unchanged throughout the observations. Such a source might be mapped quite quickly with a pencil beam instrument; the scale of detail available in such a map would be limited by the beamwidth of the telescope, while the ability to detect the source at all would depend both on the collecting area of the telescope and on the excellence of the radiometer system. The operation of an aperture synthesis system equivalent to the use of a filled aperture antenna can be seen by considering a receiving aperture in the form of a plane square (Fig. 33). Radio waves entering the aperture induce a current distribution over the aperture, and if the aperture were to be used as a pencil beam instrument the currents in all elements of the aperture would be sent over equal phase path lengths to a receiver, and there a vector sum, taking account of the amplitude and phase of each

current, would be made. If the aperture were a parabolic dish, this vector addition would take place through the summation of the electric fields at the focus; for a broadside array of dipoles the currents from each dipole would be arranged to add at the receiver.

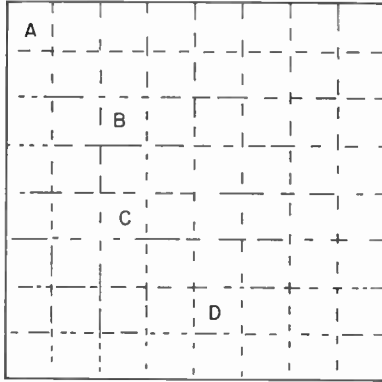


FIG. 33. The principles of aperture synthesis.

However, if the current distribution over the aperture were sampled by a single probe placed at every elementary point on the aperture, and the amplitude and phase of the current induced in the probe were measured (the phase being measured with reference to the phase at some fixed point, the aperture center for example), then the resulting measurements could be summed as vectors in a subsequent calculation to give the same total measured signal as was given by the simultaneous summation of all signals from the aperture. It is, of course, obvious that the incident waves on the aperture are assumed not to be changing with time if this equivalence is to hold. It follows that, if this sampling and summing process were carried out for every one of the positions that a point source at infinity would occupy as it moved in the sky over the aperture, the resulting plot of received power would be identical to the antenna pattern of the filled aperture, and we would have synthesized the pencil beam instrument exactly.

On the other hand, the sampling and summing process could be modified to synthesize pencil beams of different characteristics. Before summing the vector currents measured in the sampling process, these could be changed in amplitude or phase, or both, before computing the sum. A progressive phase shift across the aperture might be introduced. It is obvious that this would simulate a pencil beam instrument with its main beam steered away from the normal to the aperture. The amplitude of the contributions from the positions sampled near the edges of the aperture might be reduced in a regular way, and thus the pattern of a pencil beam instrument with a tapered feed would be synthesized. In practical aperture synthesis both these devices are employed.

Before leaving this idealized description of synthesis, the effect of random

noise on the measurements may be considered. In each sample measurement, the signal to be measured will be obscured by a random noise power, due for example to noise generated in the receiver. When the signals are summed this noise also will be summed. It is, however, uncorrelated in amplitude and phase in the various records so that the total noise in the summed signal will be the sum of the noise powers in each observation. The signal from each sample will be added vectorially so that the signal power in the resultant sum will be proportional to Sn^2 , where n is the number of samples and S is the signal power in any sample. The resultant signal to noise power will be proportional to $\frac{Sn^2}{nP} = Sn/P$ where P is the noise power in a single sample.

Thus the signal to noise power in the sum of n samples is n times that in each sample.

In practice synthesis is not done by this sampling technique, because an easier way of arriving at an equivalent result is not to attempt to measure the phase of the current in each element with respect to a single reference element, but to combine pairs of elements as a phase-switched interferometer. Ryle and Hewish (1960) show this in the following way. Let a plane wave fall on an aperture such as that in Fig. 33. The current induced in the aperture may be written $\sum I_n e^{j\phi_n}$ where I_n and ϕ_n are the current and its phase angle at the n th element. The received power from the whole aperture will be proportional to

$$\sum I_n e^{j\phi_n} \sum I_n e^{-j\phi_n} = \sum I_n^2 + \sum I_m I_n e^{j(\phi_m - \phi_n)} \quad (18)$$

The first term for elements of all the same size is simply n times the power received in a single element. The second terms are of the form which are measured by a phase-switched interferometer using the m and n elements connected first through equal cables to the receiver to measure the term of the type $I_m I_n \cos(\phi_m - \phi_n)$ and then with the antennas connected in phase quadrature to the receiver to get $I_m I_n \sin(\phi_m - \phi_n)$. If these measurements are made for all the possible combinations of positions of the two antennas the filled aperture is synthesized.

Further simplification is still possible. Many of the pairs of positions of the two antennas such as AB, CD in Fig. 33 have the same spacing and the same orientation, i.e. they are identical in so far as the results of making the measurements are concerned. Thus, it should only be necessary to measure each of such pairs once only, and if the equivalent of the filled aperture is required from the synthesis the results of one such measurement should be weighted in the final synthesis by the number of times that particular spacing and orientation occurs. This simplification does, however, alter the signal to noise ratio in the final sum since now, in a weighted contribution to the summing process, correlated noise is introduced, whereas had independent observations been made the noise would have been random. This effect is in practice not serious.

b. An Equivalent Statement of the Synthesis Principle. It is easy to see from a different point of view how it is possible to resolve the detail in an area of sky by aperture synthesis observations. We have already stated in

Section III, C, 1, when describing the two-element interferometer, that an observation with such an instrument of the complex fringe visibility V is equivalent to a measure of one Fourier component of the two-dimensional brightness distribution in the sky. The type of synthesis observations we have been describing clearly give measures of V for a wide range of antenna spacings at all orientations, and therefore provide a discrete set of measurements of the Fourier transform of the brightness distribution in the sky. From this discrete set of measurements the brightness distribution can be recovered. The theory of this statement of synthesis is given by Hewish (1963) and is, of course, physically identical with the earlier description of the principle of synthesis.

2. The Advantages of Synthesis

The most general advantage of aperture synthesis is that it allows a choice, which can be of the greatest importance in antennas of the highest resolving power, of the balance between the resolution and the collecting area of the antenna. This choice can of course be made, for example, in interferometers and crosses, but not with filled aperture antennas.

Particularly at meter wavelengths it would be most expensive to build antennas to give resolving powers of a minute of arc or better except by the use of unfilled aperture such as the Mills cross. Although the collecting area of the filled aperture is not necessary at such wavelengths, since flux densities are fairly high, the aperture of a thin cross may be too low for surveys of the weaker sources. Synthesis is well suited for such work since high resolution and quite large collecting area are obtained at the expense perhaps of more time needed to make observations, although for some types of observation the increase in observing time may not be significant. The advantages of having control at the computing stage of the distribution of the aperture illumination and of the phase are necessary to the use of synthesis but carry with them added advantages.

There are naturally difficulties to be weighed against the gains of synthetic techniques. The individual observations which finally are combined to give the result of a map of an area of sky may take several weeks of observation. The stability of the phase of the system, depending as it does on the constancy of the electrical length of cables, phase shifts in amplifiers or possible phase variations due to transmission through the atmosphere or ionosphere, must be maintained. Also the gain stability must be good. These requirements necessitate great care in the design and construction of the system, together with a reliable system of calibration. The latter can be obtained from observations of strong sources in the sky, and both the observations of the Cambridge group at frequencies up to 178 Mc/s and of the California Institute of Technology (Section III, C, 2b) at 958 Mc/s demonstrate that the problems can be overcome. The assumption that the sky under observation is unchanging with time slightly limits the type of observation program, and care has to be taken to avoid difficulties due to the apparent motion of the sun across the sky. It seems, however, that since the needs of radio

astronomy within the next decade include the desire to study quite weak sources with antennas of resolving power measured in a few seconds of arc, the techniques of aperture synthesis must be used very considerably.

2. Applications of Synthesis

The method has been used by the Cambridge group at 38 Mc/s (Blythe, 1957b) and at 178 Mc/s; while an instrument to work at 408 Mc/s and 1420 Mc/s is under construction (Ryle, 1962). The work at 958 Mc/s at California Institute of Technology already described is also a practical application of synthetic techniques. The 38 Mc/s experiment at Cambridge synthesized a square aperture with a pencil beam of 0.8° wide for a sky survey. At 178 Mc/s a synthetic interferometer to study the positions and intensities of small faint sources is being used for a further sky survey, results of which are appearing (Scott *et al.*, 1961). This paper also describes the computation needed to reduce the results. An experiment at 178 Mc/s to demonstrate the use of the rotation of the earth to permit two antennas to occupy various orientations has been performed and has given a map of the sky near the North Pole (Ryle and Neville, 1962). The basic principles of this experiment are being used in the new Cambridge instrument (Ryle, 1962), which will have three 60-ft fully steerable dishes, two fixed and one movable on an east-west baseline.

REFERENCES: SECTION I

- Adgie, R. L. (1959). An attempt to detect the 327 Mc/s line of galactic deuterium. "Paris Symposium on Radio Astronomy", p. 352, Stanford University Press, Stanford.
- Adler, R. (1958). Parametric amplification of the fast electron wave. *Proc. Inst. Radio Engrs, N.Y.* **46**, 1300.
- Adler, R., Hrbek, G., and Wade, G. (1959). The quadrupole amplifier, A low-noise parametric device. *Proc. Inst. Radio Engrs, N.Y.* **47**, 1713.
- Adler, R., Hrbek, G., and Wade, G. (1960). Comments on "Some possible causes of noise in Adler tubes". *Proc. Inst. Radio Engrs, N.Y.* **48**, 256.
- Altenhoff, W., Mezger, P. G., Strassl, H., Wendker, H., and Westerhout, G. (1960). Messprogramme bei der Wellenlänge 11 cm am 25 m-Radioteleskop Stockert. *Veröff. Sternw. Bonn*, No. 59.
- Apushkinskii, G. P. (1960). A wide band UHF radiometer using a superheterodyne. Translated in *Radio Eng. Electron.* **5**, 224.
- Armstrong, L. D. (1962). Tunnel diodes for low noise microwave amplification. *Microwave J.* **5**, 99.
- Ashkin, A. (1961). A low-noise microwave quadrupole amplifier. *Proc. Inst. Radio Engrs, N.Y.* **49**, 1016.
- Blackwell, L. A., and Kotzabue, K. L. (1961). "Semiconductor Diode Parametric Amplifiers" Prentice Hall, New York.
- Bloembergen, N. (1956). Proposal for a new type of solid-state maser. *Phys. Rev.* **104**, 324.
- Blum, E. J. (1959). Sensibilité des radiotélescopes et récepteurs à corrélation. *Ann. Astrophys.* **22**, 140.

- Burke, B. F., Ecklund, E. T., Firor, J. W., Tatel, H. E., and Tuve, M. A. (1959). Atomic hydrogen survey near the galactic plane. "Paris Symposium on Radio Astronomy", p. 374, Stanford University Press, Stanford.
- Calvin, R. S. (1961). A study of radio astronomy receivers. *Sci. Rep. Radio-science Lab. Stanford Electronics Laboratories* No. 18, Stanford University, Stanford.
- Casey, D. W., and Kuiper, J. W. (1961). A 2-4 kMc sweep-frequency receiver. *Trans. Inst. Radio Engrs, N. Y. on Antennas and Propagation, AP-9*, 36.
- Cooper, B. F. C. (1961). Use of a Y-type circulator switch with a 21-cm maser radiometer. *Rev. sci. Instrum.* **32**, 202.
- Cooper, B. F. C. (1963). Receivers in radio astronomy. *Proc. Instn Radio Engrs Aust.* **24**, 113.
- deGrasse, R. W., Schulz-DuBois, E. O., and Scovil, H. E. D. (1959). The three-level solid state traveling-wave maser. *Bell Syst. tech. J.* **38**, 305.
- deGrasse, R. W., Kostelnick, J. J., and Scovil, H. E. D. (1961). The dual channel 2390 Mc travelling wave maser. *Bell. Syst. tech. J.* **40**, 1117.
- Dicke, R. H. (1946). The measurement of thermal radiation at microwave frequencies. *Rev. sci. Instrum.* **17**, 268.
- Drake, F. D. (1962). 10 cm observations of Venus in 1961. *Publications of the Nat. Radio Astron. Obs.* **1**, No. 11.
- Drake, F. D., and Ewen, H. I. (1958). A broad-band microwave source comparison radiometer for advanced research in radio astronomy. *Proc. Inst. Radio Engrs, N. Y.* **46**, 53.
- Esaki, L. (1958). New phenomenon in narrow germanium *p-n* junctions. *Phys. Rev.* **109**, 603.
- Gardner, F. F., and Milne, D. K. (1963). A 1400 Mc/s continuum radiometer. *Proc. Instn Radio Engrs Aust.* **24**, 127.
- Giordmaine, J. A., Alsop, L. E., Mayer, C. H., and Townes, C. H. (1959). A maser amplifier for radio astronomy at X-band. *Proc. Inst. Radio Engrs, N. Y.* **47**, 1062.
- Goldstein, S. J. (1955). A comparison of two radiometer circuits. *Proc. Inst. Radio Engrs, N. Y.* **43**, 1663.
- Goodman, J., and Lebenbaum, M. (1958). A dynamic spectrum analyser for solar studies. *Proc. Inst. Radio Engrs, N. Y.* **46**, 132.
- Greene, J. C. (1961). Noisemanship: The art of measuring noise figures nearly independent of device performance. *Proc. Inst. Radio Engrs, N. Y.* **49**, 1223.
- Haneman, F. G., and Bridgeman, T. H. (1959). Self calibrating radiometer for measuring noise temperatures from 0° to 750°K. *Trans. Inst. Radio Engrs, N. Y. on Antennas and Propagation, AP-7*, 285.
- Harris, D. E., and Roberts, J. A. (1960). Radio source measurements at 960 Mc/s. *Publ. astr. Soc. Pacif.* **72**, 237.
- Haus, H. A. (1963). Description of the noise performance of amplifiers and receiving systems, I.R.E. Sub-Committee 7.9 on Noise. *Proc. Inst. Radio Engrs, N. Y.* **51**, 436.
- Heffner, H., and Wade, G. (1958). Gain, bandwidth, and noise characteristics of the variable-parameter amplifier. *J. appl. Phys.* **29**, 1321.
- Heinlein, W., and Mezger, P. G. (1962). Theorie des parmetrischen Reflexionsverstärkers. *Frequenz* **16**, Nos. 9, 10, and 11, 347, 391, and 442.
- Höglund, B., and Radhakrishnan, V. (1959). A radiometer for the hydrogen line. *Chalmers tek. Högsk. Handl.* No. 223.
- Hughes, V. A. (1956). Absolute calibration of a standard temperature noise source for use with S-band radiometers. *Proc. Instn elect. Engrs*, **103**, 669.

- Jelley, J. V. (1963). The potentialities and present status of masers and parametric amplifiers in radio astronomy. *Proc. Instn electrical and electronics Engrs* **51**, 30.
- Jelley, J. V., and Cooper, B. F. C. (1961). An operational ruby maser for observations at 21 cms with a 60-foot radio telescope. *Rev. sci. Instrum.* **32**, 166.
- Kleffner, D., Goldenberg, H. M., and Ramsey, N. F. (1962). Properties of the hydrogen maser. *Appl. Optics* **1**, 55.
- Little, A. G. (1961). A wide band single diode parametric amplifier using filter techniques. *Proc. Inst. Radio Engrs, N.Y.* **49**, 821.
- Louisell, W. H. (1960). "Coupled Mode and Parametric Electronics", John Wiley, New York.
- Maxwell, A., Swarup, G., and Thompson, A. R. (1958). The radio spectrum of solar activity. *Proc. Inst. Radio Engrs, N.Y.* **46**, 142.
- McGee, R. X., and Murray, J. D. (1963). A multi-channel hydrogen line (21 cm) receiver. *Proc. Instn Radio Engrs Aust.* **24**, 191.
- McNeill, J. D. (1961). "The calibration of argon discharge tubes for use as secondary sources of radio-frequency noise in radio astronomy", Thesis, University of Toronto, Canada.
- Mezger, P. G. (1962). Ein Verfahren zur Messung kleiner Rauschtemperaturen von Empfängern und Antennen. *Frequenz* **16**, 375.
- Mezger, P. G. (1963). A two stage parametric amplifier for the spectroscopy of the 21-cm line of interstellar hydrogen. *Proc. Inst. Radio Engrs, N.Y.* **51**, 356.
- Müller, C. A. (1956). A receiver for the radio waves from interstellar hydrogen. *Philips tech. Rev.* **17**, Nos. 11 and 12, 305 and 351.
- Orhaug, T., and Waltman, W. (1962). A switched load radiometer. *Publication Nat. Radio Astron. Obs.* **1**, 179.
- Roberts, M. S. (1963). Hydrogen in galaxies. *Sci. Amer.* **208**, 94.
- Robinson, B. J. (1961). Theory of variable-capacitance parametric amplifiers. *Proc. Instn elect. Engrs. Monograph* No. 480E, 109C, 198.
- Robinson, B. J. (1963). Development of parametric amplifiers for radio astronomy. *Proc. Instn Radio Engrs Aust.* **24**, 119.
- Robinson, B. J., and de Jager, J. T. (1962). Optimum performance of parametric diodes at S-band. *Proc. Instn elect. Engrs* **109B**, 267.
- Robinson, B. J., Seeger, C. L., van Damme, K. J., and de Jager, J. T. (1960). On stabilizing the gain of varactor amplifiers. *Proc. Inst. Radio Engrs, N.Y.* **48**, 1648.
- Ryle, M. (1952). A new radio interferometer and its application to the observation of weak radio stars. *Proc. roy. Soc. A* **211**, 351.
- Ryle, M., and Vonberg, D. D. (1948). An investigation of radio frequency radiation from the sun. *Proc. roy. Soc. A* **193**, 98.
- Seeger, C. L., Stumpers, F. L., and van Hurck, N. (1959-60). A 75-cm receiver for radio astronomy and some observational results. *Philips tech. Rev.* **21**, 317.
- Selove, W. (1954). A D-C comparison radiometer. *Rev. sci. Instrum.* **25**, 120.
- Sheridan, K. V. (1963). Techniques for the investigation of solar radio bursts at meter wavelengths. *Proc. Instn Radio Engrs Aust.* **24**, 174.
- Singer, J. R. (1959). "Masers", John Wiley & Sons, New York.
- Stelzried, C. T. (1961). A liquid helium-cooled coaxial termination. *Proc. Inst. Radio Engrs, N.Y.* **49**, 1224.
- Strum, P. D. (1958). Considerations in high sensitivity microwave radiometry. *Proc. Inst. Radio Engrs, N.Y.* **46**, 43.
- Thomson, J. H., Taylor, G. M., Ponsonby, J. E. B., and Roger, R. S. (1961). A new determination of the solar parallax by the means of radar echoes from Venus. *Nature, Lond.* **190**, 519.

- Troup, G. (1959). "Masers", Methuen & Co., London.
- Tucker, D. G. (1955). Signal/noise performance of multiplier (or correlation) and addition (or integration) types of detector. *Instn Elect. Engrs Monograph* No. 120R, London, England.
- Tucker, D. G. (1957). A comparison of two radiometer circuits. *Proc. Inst. Radio Engrs, N.Y.* **45**, 365.
- Uenohara, M. (1960). Noise consideration of the variable capacitance parametric amplifier. *Proc. Inst. Radio Engrs, N.Y.* **48**, 169.
- Uenohara, M., and Seedel, H. (1961). 961 Mc lower-sideband upconverter for satellite-tracking radar. *Bell Syst. tech. J.* **40**, 1183.
- Valley, G. E., and Wallman, H. (1948). "Vacuum Tube Amplifiers" (Mass. Inst. Tech. Rad. Lab. Series 18), McGraw-Hill, New York.
- van der Hulst, H. C., Muller, C. A., and Oort, J. H. (1954). The spiral structure of the outer part of the galactic system derived from the hydrogen emission at 21 cm wavelength. *B. A. N.* **12**, 117.
- van de Ziel, A. (1948). On the mixing properties of non-linear condensers. *J. appl. Phys.* **19**, 999.
- Wade, G., Ano, K., and Watkins, D. A. (1954). Noise in transverse field travelling-wave tubes. *J. appl. Phys.*, **25**, 1514.
- Weinreb, S. (1961). Digital radiometer. *Proc. Inst. Radio Engrs, N.Y.* **49**, 1099.
- Weinreb, S. (1962). A new upper limit to the galactic deuterium to hydrogen ratio. *Nature, Lond.* **195**, 367.
- Wielebinski, R., Shakeshaft, J. R., and Pauliny-Toth, I. I. K. (1962). A search for the linearly polarized component of the galactic radio emission at 408 Mc/s. *Observatory* **82**, 158.
- Wild, J. P., and McCready, L. L. (1950). Observations of the spectrum of high-intensity solar radiation at meter wavelengths. *Aust. J. Sci. Res.* **A3**, 387.

REFERENCES: SECTION II

- Altenhoff, W., Mezger, P. G., Strassl, H., Wendker, H., and Westerhout, G. (1960). Messprogramme bei der Wellenlänge 11 cm am 25 m-Radioteleskop Stockert. *Veröff Sternw. Bonn* No. 59.
- Bolton, J. G. (1963). The Australian 210-foot reflector and its research program. *Proc. Instn Radio Engrs Aust.* **24**, 106.
- Bowen, E. G., and Minnett, H. C. (1963). The Australian 210-foot radio telescope. *Proc. Instn Radio Engrs Aust.* **24**, 98.
- Cohen, M. H. (1958a). Radio astronomy polarization measurements. *Proc. Inst. Radio Engrs, N.Y.* **46**, 172.
- Cohen, M. H. (1958b). The Cornell radio polarimeter. *Proc. Inst. Radio Engrs, N.Y.* **46**, 183.
- Cooper, B. F. C., and Price, R. M. (1962). Faraday rotation effects associated with the radio source Centaurus A. *Nature, Lond.* **195**, 1084.
- Drake, F. D. (1960). The position-determination program of the National Radio Astronomy Observatory. *Publ. astr. Soc. Pacif.* **72**, 494.
- Findlay, J. W. (1963). The 300-foot radio telescope at Green Bank. *Sky & Telesc.* **25**, 68.
- Husband, H. C. (1958). The Jodrell Bank radio telescope. *Min. Proc. Instn civ. Engrs* **9**, 65; **10**, 410.
- Jasik, H. (1961). "Antenna Engineering Handbook", McGraw-Hill, New York.
- Kerr, F. J. (1962). 210-foot radio telescope's first results. *Sky & Telesc.* **24**, 254.
- Lovell, A. C. B. (1957). The Jodrell Bank radio telescope. *Nature, Lond.* **180**, 60.

- Mayer, C. H., McCullough, T. P., and Sloanaker, R. M. (1957). Evidence for polarized radio radiation from the Crab Nebula. *Astrophys. J.* **126**, 468.
- Minnett, H. C. (1962). The Australian 210-foot radio telescope. *Sky & Telesc.* **24**, 184.
- Morris, D., and Radhakrishnan, V. (1963). Tests for linear polarization in the 1390 Mc/s radiation from six intense radio sources. *Astrophys. J.*, **137**, 147.
- Pauliny-Toth, I. I. K., Shakeshaft, I. R., and Wielebinski, R. (1962). The use of a paraboloidal reflector of small focal ratio as a low-noise antenna system. *Proc. Inst. Radio Engrs, N.Y.* **50**, 2483.
- Potter, P. D. (1962). Unique feed system improves space antennas. *Electronics* **35**, 36.
- Robieux, J. (1956). Influence of the manufacturing accuracy of an antenna on its performance. *Ann. Radioelect.* **11**, 29.
- Ruze, J. (1952). The effect of aperture errors on the antenna radiation pattern. *Suppl. Nuovo Cimento* **9**, 364.
- Schuster, D., Stelzried, C. T., and Levy, G. S. (1962). The determination of noise temperatures of large paraboloid antennas. *Trans. Inst. Radio Engrs, N.Y.* on Antennas and Propagation *AP-10*, 286.
- Silver, Samuel (1949). "Microwave Antenna Theory and Design", McGraw-Hill, New York.
- Spencer, R. C. (1949). A least squares analysis of the effect of phase errors on antenna gain. *Rep. Air Force Cambridge Res. Center* No. 5025, Bedford, Mass.
- Wallis, Barnes (1955). Improvement in telescope mountings. Vickers Armstrong (Aircraft) Ltd., *British Patent Application* No. 29248/55.
- Westerhout, G., Seeger, C. L., Broun, W. N., and Timbergen, J. (1962). Polarization of the galactic 75-cm radiation. *Bull. Astr. Insts Netherlds* **16**, 187.

REFERENCES: SECTION III

- Allen, L. R., Anderson, B., Conway, R. G., Palmer, H. P., Reddish, V. C., and Rowson, B. (1962a). Observations of 384 radio sources at a frequency of 158 Mc/s with a long baseline interferometer. *Mon. Not. R. astr. Soc.* **124**, 477.
- Allen, L. R., Brown, R. H., and Palmer, H. P. (1962b). An analysis of the angular sizes of radio sources. *Mon. Not. R. astr. Soc.* **125**, 57.
- Ashmead, J., and Pippard, A. B. (1946). The use of spherical reflectors as microwave scanning aerials. *J. elect. Engrs* **93**, Part IIIa, 627.
- Blum, E. J., Denisse, J. F., and Steinberg, J. L. (1958). Radio astronomy at the Meudon Observatory. *Proc. Inst. Radio Engrs, N.Y.* **46**, 39.
- Blum, E. J., Boisshot, A., and Lequeux, J. (1963). Radio astronomy in France. *Proc. Instn Radio Engrs Aust.* **24**, 208.
- Blythe, J. H. (1957a). A new type of pencil beam aerial for radio astronomy. *Mon. Not. R. astr. Soc.* **117**, 644.
- Blythe, J. H. (1957b). Results of a survey of galactic radiation at 38 Mc/s. *Mon. Not. R. astr. Soc.* **117**, 652.
- Bolton, J. G. (1948). Discrete sources of galactic radio frequency noise. *Nature, Lond.* **162**, 141.
- Braccesi, A., and Ceccarelli, M. (1962). The Italian cross radiotelescope. *Nuovo Cim.* **23**, 208.
- Bracewell, R. N. (1958). Radio interferometry of discrete sources. *Proc. Inst. Radio Engrs, N.Y.* **46**, 97.

- Bracewell, R. N., and Swarup, G. (1961). The Stanford microwave spectroheliograph antenna, a microsteradian pencil beam interferometer. *Trans. Inst. Radio Engrs, N.Y. on Antennas and Propagation, AP-9*, 22.
- Brown, R. H., and Twiss, R. Q. (1954). A new type of interferometer for use in radio astronomy. *Phil. Mag.* **45**, 663.
- Brown, R. H., Jennison, R. C., and Das Gupta, M. K. (1952). Apparent angular sizes of discrete radio sources. *Nature, Lond.* **170**, 1061.
- Christiansen, W. N., and Mathewson, D. S. (1958). Scanning the sun with a highly directional array. *Proc. Inst. Radio Engrs, N.Y.* **46**, 127.
- Christiansen, W. N., and Mullaly, R. F. (1963). Solar observations at a wavelength of 20 cm with a crossed grating interferometer. *Proc. Instn Radio Engrs Aust.* **24**, 165.
- Christiansen, W. N., and Warburton, J. A. (1953). A new highly directional aerial system. *Aust. J. Phys.* **6**, 190.
- Christiansen, W. N., Erickson, W. C., and Hogbom, J. A. (1963). The Benelux Cross Antenna Project. *Proc. Instn Radio Engrs Aust.* **24**, 219.
- Covington, A. E. (1960). A compound interferometer. *J. R. astr. Soc. Can.* **54**, No. 1, 17; No. 2, 58.
- Dyson, J. D. (1959). The unidirectional equiangular spiral antenna. *Trans. Inst. Radio Engrs, N.Y. on Antennas and Propagation, AP-7*, 329.
- Elgaroy, O., Morris, D., and Rowson, B. (1962). A radio interferometer for use with very long baselines. *Mon. Not. R. astr. Soc.* **124**, 395.
- Gordon, W. E., and LaLonde, L. M. (1961). The design and capabilities of an ionospheric radar probe. *Trans. Inst. Radio Engrs, N.Y. on Antennas and Propagation, AP-9*, 17.
- Hatanaka, T. (1963). Radio astronomy in Japan. *Proc. Instn Radio Engrs Aust.* **24**, 243.
- Head, A. K. (1957). A new form for a giant radio telescope. *Nature, Lond.* **179**, 692.
- Hewish, A. (1963). The realization of giant radio telescopes by synthesis techniques. *Proc. Instn Radio Engrs Aust.* **24**, 225.
- Jennison, R. C. (1961). "Fourier Transforms and Convolutions for the Experimentalist", p. 102, Pergamon Press, Oxford.
- Jennison, R. C., and Das Gupta, M. K. (1956). Measurement of the angular diameter of two intense radio sources, I and II. *Phil. Mag. Series 8*, 55.
- Kalachov, P. D. (1963). Some radio telescopes in the U.S.S.R. *Proc. Instn Radio Engrs Aust.* **24**, 237.
- Kay, A. F. (1961). Design of line feed for world's largest aperture antenna. *Electronics* **1**, 46.
- Kraus, J. D. (1955). Radio telescopes. *Sci. Amer.* **192**, 36.
- Kraus, J. D. (1963). The large radio telescope at Ohio State University. *Sky & Telesc.* **26**, 12.
- Kraus, J. D., Nash, R. T., and Ko, H. C. (1961). Some characteristics of the Ohio State University 360-foot radio telescope. *Trans. Inst. Radio Engrs, N.Y. on Antennas and Propagation, AP-9*, 4.
- Labrum, N. R., Harting, E., Krishnan, T., and Paylin, W. J. (1963). A compound interferometer with a 1.5 minute of arc fan beam. *Proc. Instn Radio Engrs Aust.* **24**, 148.
- Lequeux, J. (1962). High resolution interferometric measurements of the diameter and structure of the principle radio sources at 1420 Mc/s; (in French). *Ann. Astrophys.* **25**, 221.
- Love, A. W. (1962). Spherical reflecting antennas with corrected line sources. *Trans. Instn Radio Engrs, N.Y. on Antennas and Propagation, AP-10*, 529.

- McCready, L. L., Pawsey, J. L., and Payne, Scott R. (1947). Solar radiation at radio frequencies and its relation to sunspots. *Proc. roy. Soc., A*, **190**, 357.
- Mills, B. Y. (1952). Observations at Sydney. *Nature, Lond.* **170**, 1063.
- Mills, B. Y. (1963). Cross-type radio telescopes. *Proc. Instn Radio Engrs Aust.* **24**, 132.
- Mills, B. Y., and Little, A. G. (1953). A high-resolution aerial system of a new type. *Aust. J. Phys.* **6**, 272.
- Mills, B. Y., Little, A. G., Sheridan, K. V., and Slee, O. B. (1958). A high resolution telescope for use at 3.5 M. *Proc. Inst. Radio Engrs, N.Y.* **46**, 67.
- Mills, B. Y., Aitchison, R. E., Little, A. G., and McAdam, W. B. (1963). The Sydney University cross-type radio telescope. *Proc. Instn Radio Engrs Aust.* **24**, 156.
- Moffett, A. T., and Maltby, P. (1962). Brightness distribution in discrete radio sources, I, II, and III. *Astrophys. J. Suppl.* No. 67, 7, 93.
- O'Brien, P. A. (1953). The distribution of radiation across the solar disk at meter wave-lengths. *Mon. Not. R. astr. Soc.* **113**, 597.
- Read, R. B. (1961). Two-element interferometer for accurate position determinations at 960 Mc/s. *Trans. Inst. Radio Engrs, N.Y. on Antennas and Propagation, AP-9*, 31.
- Rowson, B. (1963). High resolution observations with a tracking radio interferometer. *Mon. Not. R. astr. Soc.* **125**, 177.
- Ryle, M. (1952). A new radio interferometer and its application to the observation of weak radio stars. *Proc. roy. Soc. A* **211**, 351.
- Ryle, M. (1962). The new Cambridge radio telescope. *Nature, Lond.* **194**, 517.
- Ryle, M., and Hewish, A. (1955). The Cambridge radio telescope. *Mon. Not. R. astr. Soc.* **67**, 97.
- Ryle, M., and Hewish, A. (1960). The synthesis of large radio telescopes. *Mon. Not. R. astr. Soc.* **120**, 220.
- Ryle, M., and Neville, A. C. (1962). A radio survey of the North Pole region with a 4.5 minute of arc pencil-beam system." *Mon. Not. R. astr. Soc.,* **125**, 39.
- Schell, A. C. (1963). The diffraction theory of large-aperture spherical reflector antennas. *Trans. Instn electrical and electronic Engrs, N.Y. on Antennas and Propagation. AP-11*, 428.
- Scott, P. F., Ryle, M., and Hewish, A. (1961). First results of radio star observations using the method of aperture synthesis. *Mon. Not. R. astr. Soc.* **122**, 95.
- Shain, C. A. (1958). The Sydney 19.7 Mc radio telescope. *Proc. Inst. Radio Engrs, N.Y.* **46**, 85.
- Smith, F. G. (1951). An accurate determination of positions of four radio stars. *Nature, Lond.* **168**, 555.
- Smith, F. G. (1952). Observations at Cambridge. *Nature, Lond.* **170**, 1065.
- Spencer, R. C., Sletten, C. J., and Walsh, J. E. (1949). Correction of spherical aberration by a phased line source *Proc Nat. Electron. Conf.* **5**, 320.
- Stanier, H. M. (1950). Distribution of radiation from the undisturbed sun at a wavelength of 60 cm. *Nature, Lond.* **165**, 354.
- Swarup, G., and Yang, K. S. (1961). Phase adjustments of large antennas. *Trans. Inst. Radio Engrs, N.Y. on Antennas and Propagation, AP-9*, 75.
- Swenson, G. W., and Lo, Y. T. (1961). The University of Illinois radio telescope. *Trans. Inst. Radio Engrs, N.Y. on Antennas and Propagation, AP-9*, 9.
- Tanaka, H., and Kakinuma, T. (1953). Equipment under construction for locating sources of solar noise at 4000 Mc/s. *Proc. Res. Inst. Atmospherics* **1**, 89.

REFERENCES: GENERAL

- Bracewell, R. N. (1962). Radio astronomy techniques. *Handb. der Phys.* **54**, 42. Springer, Berlin.
- Pawsey, J. L., and Bracewell, R. N. (1955). "Radio Astronomy", Oxford University Press, London.
- Shklovsky, I. S. (1960). "Cosmic Radio Waves", translated by Rodman and Varsavsky, Harvard Press, Cambridge, Mass.
- Steinberg, J. L., and Lequeux, J. (1963). "Radioastronomy", translated by R. N. Bracewell, McGraw-Hill, New York.

RADIO NOISE FROM THUNDERSTORMS

F. HORNER

D.S.I.R. Radio Research Station, Slough, England

I.	Terrestrial Noise: Origins and Importance	122
II.	Sources of Noise and Nature of Lightning Discharges	124
	A. Thunderstorms and Types of Discharge	124
	B. Investigations of Lightning by Radar	127
	C. Quantitative Models of the Discharge	128
III.	Field Changes and Atmospherics Near the Source	130
IV.	Spectrum Near the Source	133
	A. Methods of Deriving Spectra	134
	B. Experimental Spectrum Data	137
	C. The Spectrum derived from the Discharge Model	139
	D. Radiated Energy	140
V.	Amplitude Variability of Atmospherics	142
VI.	Numbers and Distributions of Lightning Discharges	143
VII.	Propagation of Atmospherics	147
	A. Theoretical Studies	147
	B. Experimental Data at Low Frequencies	149
	C. Propagation at Higher Frequencies	153
	D. Summary of Propagation Results Most Relevant to Noise	153
VIII.	Characteristics and Measurement of Atmospheric Noise	154
	A. Methods of Specifying and Measuring Noise Power	156
	B. Average Envelope Voltage	160
	C. Average Logarithm of the Voltage	161
	D. Amplitude Probability Distribution	161
	E. Envelope Crossing Rate	169
	F. Quasi-Peak Amplitude	171
	G. Slideback Peak Amplitude	172
	H. Time Functions	172
IX.	Direct Measurement of Interference	174
X.	World Distribution of Noise Intensity	175
	A. Presentation of Data	176
	B. Noise on Directional Aerials	180
XI.	Noise Interference to Radio Services	181
XII.	Locating Sources of Atmospherics	183
	A. Direction Finding Techniques	183
	B. Single Station Techniques	187
	C. Time-Delay Technique	189
XIII.	Whistling Atmospherics	189
	A. Correlation of Whistlers with Storms and Visible Discharges	192
	B. Whistlers and the Originating Lightning Discharge	192
	C. Propagation of Whistlers below the Ionosphere	193
XIV.	Conclusion	194
	References	194

I. TERRESTRIAL NOISE: ORIGINS AND IMPORTANCE

Attempts to receive radio signals of low intensity suffer interference from unwanted signals and from various forms of noise. The noise is either generated in the receiving equipment, or is external, arising in sources on the earth (e.g. thunderstorms, machinery) or extraterrestrial (e.g. the galaxy and the sun). Some of these sources emit noise of thermal or fluctuation type; shot and thermal noise in receivers and galactic noise are in this category. The properties of the noise can then be expressed in rigorous statistical terms and are well known. Noise from thunderstorms and many man-made sources, on the other hand, have more complicated structure, not so readily amenable to description or to analytical treatment.

This chapter summarizes the considerable advances which have been made in the last few years in the understanding, and particularly the measurement of atmospheric noise. This noise arises from natural sources on the earth, and although snowstorms, dust-storms and volcanoes have been at times mentioned as significant noise sources, lightning discharges in thunderstorms account for nearly all the atmospheric noise encountered as interference in communications up to about 30 Mc/s, neglecting local effects such as precipitation on the aerial or on its immediate surroundings, and corona discharge near the aerial. Lightning discharges and their electrical effects, therefore, are the main topics discussed. The energy which they radiate is spread over a wide range of the radio spectrum, with the greatest energy per unit bandwidth at very low frequencies. The spectrum is modified when the noise is propagated over the earth, and the receiver, with its limited frequency range, selects a portion of the energy which then constitutes the interference.

Interest in atmospheric noise has fluctuated considerably over the years according to its influence on practical communications. It was of great importance when radio communication was at low frequencies, and less so when high frequencies came into use, with their relative freedom from interference from atmospherics. Even at these frequencies, however, atmospherics are a serious source of interference at low latitudes, especially with modern receivers of high sensitivity, but the increasing usage of the radio spectrum is leading to a situation in which other transmissions are often the main limitation to reception. Recently there has been a resurgence of interest in noise at low frequencies, partly because of their potential value for navigation and standard frequency transmissions, and partly because atmospherics provide a useful source of energy for propagation studies at frequencies lower than those of any operational transmissions.

Research in atmospherics has been in progress for a very long time, and the developments of the last few years have been based on pioneer work over a much longer period. Since it is not practicable to make all the relevant references to the early work, it should be mentioned here that the research carried out before 1940 by teams led by Schonland in South Africa, Appleton and Watson-Watt in the United Kingdom, Bureau in France, Lugeon in Switzerland, Austin in the United States, Norinder in Sweden and others in

many countries laid the foundation of the later work described here. In many instances the recent investigations have been refinements and extensions of past research, made possible by the improved technical facilities now available. Much of the early work was reviewed by Thomas and Burgess in 1947.

Atmospheric noise depends on so many factors, and is so variable in its influence on radio services, that many investigations over the years have tended to concentrate on obtaining data in a form directly applicable to a specific and limited problem. Notable features of the work of the last few years have been the emphasis on obtaining information of more general applicability, the use of standardized methods of measurement, and the expression of the quantitative results in precise and unambiguous terms.

In a field in which the interests of various specialists—meteorologists, radio engineers and power engineers—overlap, there is some lack of uniformity in terminology. It is therefore desirable to describe briefly the meanings which are attached here to some of the main terms. The electrical breakdown phenomenon giving rise to noise is called the lightning discharge. The lightning flash is regarded as the visible manifestation of the discharge. However, the term lightning flash counter has come into general use for a device which is in fact a counter of discharges, or rather of the atmospherics radiated by them. A discharge usually continues, somewhat intermittently, for a few tenths of a second. An individual component of a discharge is referred to as a stroke, for example a stroke to the ground. The whole discharge may consist of several such strokes, with many other small sparks resulting from minor breakdown processes. A discharge with several ground strokes is called a multiple discharge.

It is difficult to restrict the term atmospheric to a unique and precisely defined phenomenon because of the variety in past usage of the term. Here it is limited to the electromagnetic field change resulting from a single discharge, and when parameters such as the energy or duration are discussed, the whole discharge is considered, possibly including several strokes to ground and any minor, connected partial discharges. The term has often been used, however, for the field change resulting from part of a discharge, e.g. one stroke to ground, and this usage will also be retained where it will not lead to confusion or ambiguity. In either case the atmospheric may include components extending over a wide range of frequencies, or it may be what is observed in a narrow-band receiver. There has sometimes been a tendency to restrict the term to the field change at a distance, but this limitation seems rather arbitrary. The term atmospheric noise will be used for the succession of atmospherics resulting from many lightning discharges.

The relevant characteristics of lightning discharges as noise generators are described in early sections of this chapter, followed by a summary of some recent work on the propagation of atmospherics. The remaining sections are concerned mainly with noise measurements and typical results. Finally, there are notes on some aspects of whistling atmospherics.

II. SOURCES OF NOISE AND NATURE OF LIGHTNING DISCHARGES

Many studies have been made of the meteorological situations which give rise to the storms in which atmospheric discharges originate. An analysis of the meteorological aspects of thunderstorms is not within the scope of this review, but special mention should be made of the recent extensive and detailed work by Kimpara and his co-workers in Japan. Locations of many sources were plotted, using direction finders, and were found to coincide with areas of considerable meteorological disturbance, caused, for example, by the interaction of fronts. Maps showing the main centres of activity in the Far East were given for different times of year (Kimpara, 1955).

A full description of the physical processes in a thunderstorm, including the outstanding question of the mechanism of electrical charge separation, would not be appropriate here, but some knowledge of the types of discharge which occur helps towards an understanding of the radiated noise. The properties of discharges which are especially relevant to noise generation are outlined in the following notes.

A. THUNDERSTORMS AND TYPES OF DISCHARGE

Thunderstorms contain a number of cells, which exist for about half an hour and pass through various phases of development. Two main types of discharge are generated within them, those which strike the ground and those which do not. The latter are referred to as cloud discharges, but some, which extend from a cloud into clear air, are sometimes called air discharges to distinguish them from the type which are entirely within the cloud. In temperate regions discharges normally occur at a rate of one or two a minute in each cell (Brook and Kitagawa, 1960a), but in tropical storms in which there are more cloud discharges the rate may be much higher and more variable (Takagi *et al.*, 1959). There is evidence that the types of discharge occurring change with the state of development of the storm (Ishikawa and Takagi, 1953; Brook and Kitagawa, 1960a).

The most commonly-occurring thunderstorms are often divided broadly into heat types and frontal types. The first type is caused by local heating, mainly on land masses during summer afternoons, and thunderstorm cells occur somewhat sporadically. The second type is usually associated with the unstable air of a cold front and may occur over land or sea, and in any season; the storms tend to extend for a long distance along the line of the front. Apart from these differences in geographical and temporal incidence, one or two differences in the nature of the discharges have been reported, and are mentioned later, but they are not yet sufficiently well established to be an important consideration in assessing the noise. The large and intense storms which produce tornadoes must evidently be considered as a third category, with markedly different characteristics from those of normal storms.

The basic model of the charge distribution in an ordinary thunderstorm consists of a negative charge near the cloud base at a height of the order of 3 km in temperate regions, a positive charge above at perhaps 6 km, and a

small induced positive charge below the cloud (Pierce, 1955a). The earth under the cloud also has an induced positive charge. For lower latitudes a height of 6 km for the negative charge has been quoted (Tamura, 1958; Kitagawa and Brook, 1960). Recent accounts suggest that a more complicated model is generally appropriate, possibly with several concentrations of negative charge near the base or additional positively charged regions (Tamura, 1958).

Early research on lightning was concerned largely with visible flashes, either from the cloud to ground or from the cloud into clear air. It was known that there were other discharges confined to the cloud, but as these were obscured from view they were more difficult to study. Pierce (1955b, 1956a) has estimated that in a temperate region about 40 per cent of discharges reach the ground while the proportion in tropical areas is only about 10 per cent. The temperate figure has been confirmed by Brook and Kitagawa (1960a), although they found that the ratio varied with the state of development of the storm, but a proportion of about 20 per cent for the sub-tropics has been quoted by Prentice (1960).

The sequence of events in a discharge to ground has been investigated extensively, using the scanning camera invented by Boys to distinguish successive strokes along the same channel, and measuring, often at the same time, the electric field changes in the vicinity. A long series of investigations has been carried out by Schonland and his associates in South Africa (Schonland, 1956). In a typical ground discharge in that country, for example, a leader stroke proceeds downwards from the cloud in a series of steps (a stepped-leader). If this reaches the ground a heavy-current return stroke occurs up the ionized channel thus formed, and the negative charge in the cloud is at least partially neutralized by the positive charge from the ground. If the neutralization is incomplete the process may be repeated, once or more often, a typical separation between return strokes being 50 msec. The leader preceding subsequent return strokes is usually continuous since the channel is already ionized, but if an interval exceeds 100 msec the ionization nearly disappears and the leader may then travel in a large number of short steps (a dart-stepped leader) (Schonland, 1956). Subsequent strokes often follow substantially the same path as the first but may branch from it. There are published reports of multiple discharges with large numbers of return strokes. Malan (1956a) considers that in some instances minor partial discharges along branches of the main channel have been mistaken for separate main strokes, but nevertheless there are occasional examples with more than 20 return strokes (Workman *et al.*, 1960). Most multiple discharges contain not more than five return strokes (Norinder, 1947; Kamada, 1953; Malan, 1956a). Pierce (1955b) and Kamada (1953), in support of earlier observations by Schonland (1938), have found a tendency for multiple discharges to be more prevalent in frontal than in heat storms. An example is quoted by Pierce, when in frontal storms in England 45 per cent of discharges had three or more strokes, compared with 22–38 per cent in heat storms. In the intervals between return strokes there are so-called junction (J) streamers which extend towards concentrations of charge in other parts

of the cloud, and thus initiate further ground strokes from these. J streamers extend generally upwards, in directions determined by the spatial distributions of the charges, but may be nearly horizontal (Brook and Vonnegut, 1960). They exhibit brief enhancements of current (K changes) when they meet minor accumulations of charge (Kitagawa and Kobayashi, 1958).

The horizontal extent of a discharge may be comparable with or much greater than its vertical extent, and the duration of a long horizontal discharge is usually correspondingly long. Horizontal or inclined discharges in the cloud can be seen frequently from the ground and have been photographed (Malan, 1956b; Norinder and Knudsen, 1958). A single peal of thunder is commonly observed to last 20 sec or more, and it seems probable that this results partly from the difference in horizontal range between the nearest and most distant parts of the discharge, but Kimpara (1953) reported seeing long cloud discharges without thunder. Malan (1961) has also reported discharges of very great length (up to 50 km) and Jones (1958) has seen them up to at least 25 km long. Horner (1960a) has on one occasion seen them extending overhead, in clear air, and linked with ground strokes 20 km away; some of these had unusual and extensive branching upwards, and total durations of several seconds. There is also a report of a radar echo from a discharge more than 100 km long (Ligda, 1956), but such lengths are rare and seem more likely to occur in an extended storm associated with a front than in the more sporadic and isolated heat storms.

The type of ground discharge described by the workers in South Africa is not necessarily universal. For example, Pierce (1955a) has stated that the usual type of leader in England is continuous rather than stepped even before the first stroke, and other types of stroke may occur, such as one from a positive charge concentration to the ground (Malan, 1961).

The stepped-leader/return-stroke process occupies a small part of the total duration in most discharges, perhaps 30 msec in several hundred msec (Norinder, 1947). Malan (1955) has recorded luminosity within the cloud both before and after the main visible flashes and Wormell (1939) and Pierce (1955b) have shown that the electrostatic field changes are often of long duration and more or less continuous. Clarence and Malan (1957) have made a study of the preliminary processes in ground discharges, which may last up to 500 msec and be either continuous or intermittent. The process can sometimes be broken down into three stages. In the first there are preliminary discharges between the negative charge and the positive space charge below; an intermediate stage then follows in which some neutralization takes place. Finally, there is the true leader stage which may or may not be stepped (see Section III and Fig. 2). Takeuti *et al.* (1960) have suggested that in some long preliminary discharges there is a different discharge mechanism preceding the sequence described by Clarence and Malan and related to the subsequent number of return strokes, but it is not clear whether different mechanisms are in fact involved.

It now seems that in studying the noise-generating properties of lightning discharges over a wide frequency range, they may be considered as more-or-less continuous phenomena, usually lasting for a time from one-tenth to a

few tenths of a second, and taking place mainly within the cloud. The visible flashes to ground are additional features of some discharges, occupying a relatively short time but nevertheless having an important influence on the total radiated energy, and particularly on the noise at low frequencies. The nature of the differences between cloud and ground discharges as noise generators is becoming clearer as a result of recent work. There is evidence that those parts of the discharges within the cloud have some similarities and radiate similar high frequency noise, but Ishikawa and Kimpara (1958) have said that cloud discharges are more complex, and Kitagawa and Brook (1960) have drawn attention to recognizable differences in fine structure, particularly in the early stages. Larger differences occur at very low frequencies at which the presence or absence of a return stroke is important (Malan, 1958). Although cloud discharges are thought not to include return strokes of the same form as those in ground discharges (Schonland *et al.*, 1938), they may radiate low-frequency energy comparable with, though usually smaller than that from return strokes (Ishikawa and Takagi, 1954; Tantry *et al.*, 1957), and in known ground discharges there are often significant low-frequency components other than those resulting from the return strokes themselves (Horner and Clarke, 1958). Tepley (1959) found it possible to explain the polarities of ELF field changes on the basis of an origin in cloud discharges.

Evidence on the nature of noise sources in snowstorms is meagre. Norinder (1949) and Kimpara (1955) have reported that the waveforms of atmospherics from snowstorms are significantly different from those from thunderstorms and Norinder stated that the causative discharges cannot be seen or heard. However, the differences in the amplitudes of the radiated atmospherics do not appear to be large and for practical purposes, until definite differences in the source spectra can be established, it is reasonable to regard snowstorms as a further sporadic source of noise of intensity comparable with ordinary thunderstorms.

B. INVESTIGATIONS OF LIGHTNING BY RADAR

It is well known that strong radar reflections can be received from precipitation in thunderstorms and that they can be used to locate the storms and to follow their movements. Transitory reflections can also be received from the lightning discharges (Hewitt, 1962) and are presumed to be from the ionization produced by the discharge. The intense heating will also lead to changes in refractive index which will have reflecting properties, but Brown (1951) has stated that this effect is many orders of magnitude too small to be detected.

Lightning echoes have been observed at 3000 Mc/s (Ligda, 1950; Marshall, 1953; Miles, 1953; Jones, 1954; Atlas, 1958) and at 10 000 Mc/s (Ligda, 1950; Brown, 1951). Brown calculated that they could be accounted for by the presence of 5×10^{13} electrons per centimetre length of the channel. Hewitt (1957) used a lower frequency (600 Mc/s) to minimize the reflections from precipitation and he attributed the lightning echoes he observed to junction streamers and, less frequently, to air discharges. Successive echoes

were found to occur from higher regions of the cloud in support of the theory by which junction streamers develop generally in an upwards direction. Echoes seen by Atlas extended above the precipitation and he considered that they were reflections from a stepped-leader type of discharge. The models postulated by Atlas and by Hewitt to account for the reflections were quite different. Hewitt assumed a thin streamer of high electron density while Atlas assumed a much thicker discharge of low electron density. Long discharges with a substantially horizontal orientation were detected by Ligda (1956) using radar at 10 000 Mc/s.

These experiments also showed that noise from discharges could be received at frequencies up to 10 000 Mc/s, bursts of the order of 1 msec in duration being received just before the radar echoes. Hewitt (1957) and Ligda (1956) reported that individual pulses within the bursts had durations of the order of 1 μ sec. Atlas (1958) reported longer pulses (27 μ sec on the average), but it has been suggested that dynamic range limitations in the equipment might have led to these larger values.

Radar methods are potentially capable of yielding much more information about the structure and development of lightning discharges, but the technique is difficult, owing to the requirement that the radar beam be pointing towards the lightning discharge at the moment it occurs.

C. QUANTITATIVE MODELS OF THE DISCHARGE

Currents in return strokes have been measured directly, and photographs with Boys cameras provide information on their speed of growth. Reasonably satisfactory models of the return stroke therefore exist, and derived estimates of radiated noise at low frequencies are in good agreement with measured values (Horner, 1958). The instantaneous current in the return stroke is usually expressed in the form

$$i = i_0 [\exp(-\alpha t) - \exp(-\beta t)] \quad (1)$$

with the channel extending upwards from the ground with a speed

$$v = v_0 \exp(-\gamma t) \quad (2)$$

Various values have been given for i_0 and the coefficients α and β in (1). Two sets of figures which are frequently quoted are those due to Bruce and Golde (1941), $i_0 = 28\,000$ A, $\alpha = 4.4 \times 10^4 \text{ sec}^{-1}$, $\beta = 4.6 \times 10^5 \text{ sec}^{-1}$ and those derived by Morrison (1953) from records of Norinder (1951), $i_0 = 30\,000$, $\alpha = 7 \times 10^3$, $\beta = 4 \times 10^4$. These both give peak currents of about 20 000 A and maximum energy at a frequency of a few kc/s, but the Morrison values represent a longer pulse with more energy at ELF. Pierce (1960a) has suggested that the differences may be more apparent than real, since Bruce and Golde quote currents measured at the bottom of the discharge channel while Norinder's records were derived from the field changes, and result from the integrated effect of the whole channel. He also suggested that the Bruce-Golde values may apply to the first stroke of a multiple discharge but that a value of $\beta = 7 \times 10^5$ may be more appropriate for subsequent strokes. Experimental results by Kimpara (1953) show lower

frequency components in later strokes than in the first, but records obtained by Norinder *et al.* (1958) did not exhibit a consistent effect, apart from a tendency for the first return stroke to give the largest field change.

Bruce and Golde have given $v_0 = 8 \times 10^7$ m/sec and $\gamma = 3 \times 10^4$ sec⁻¹ for the velocity formula (2), and here again Schonland (1956) has suggested that subsequent strokes may be different from the first, and have a velocity tending to be constant (i.e. $\gamma = 0$). These changes affect mainly the energy at frequencies below the maximum in the frequency spectrum at about 10 kc/s. Barlow *et al.* (1954) and Hepburn (1957a) consider that a third exponential term, with a slow rate of decay, should be added to the formula of Bruce and Golde, to account for energy at frequencies below 1 kc/s, and there is little doubt that continuing currents following the return stroke, whatever their precise form, account for some radiated energy in this frequency range. Hill (1957) has derived an expression for the spectrum of the energy radiated from a return stroke, by consideration of the probable movements of charge. Although in a form different from the exponential functions given above, the spectrum, after normalization to give the maximum energy at 11 kc/s, is rather similar.

Some of the parameters of the leader are also known reasonably well; for example, the steps in a stepped-leader are typically 20 to 50 m long, last for 1 μ sec and are separated in time by about 50 μ sec. The currents involved are of the order of hundreds of amperes. The model of the stepped-leader is incomplete, however, since the rate at which the current decreases at the end of a step has not been specified and this is of great importance in determining the high-frequency radiation. No satisfactory quantitative model exists for the current variations in a major stroke of a discharge within the cloud.

Noise radiated from a discharge is closely linked to the physical lengths of the channels, the magnitudes of the currents and the rates at which they change. Return strokes, which are long and contain large currents, changing slowly, radiate maximum energy in the VLF range, with a peak somewhat below 10 kc/s, but may have continuing currents with energy in the ELF range. (ELF is here used generally for frequencies below 3 kc/s.) Changes in charge distributions which are relatively slow when considered as a bulk phenomenon, although resulting from a large number of small, rapid discharges, also have ELF components of energy. For example, a change occupying a time of 100 msec would be expected to emit significant noise energy at 10 c/s. Tepley (1959) has found that nearly all atmospherics have a measurable ELF component and about 30 per cent of those he observed had ELF, but no VLF component. Leaders, by comparison with return strokes, have smaller but more rapidly varying currents and radiate energy at higher frequencies, predominantly 20–30 kc/s according to Kimpara (1955). The chief source of the noise at still higher frequencies appears to be relatively short sparks, mainly in the cloud, which initiate the larger discharges and which have small but rapidly changing currents. Distant storms give rise to appreciable field changes at frequencies down to a few c/s; at lower frequencies, movements of local concentrations of charge may be the predominant source (Aarons, 1956; Large and Wormell, 1958).

All the preceding discussion has related to the phenomena in ordinary thunderstorms. Those which cause tornadoes in some parts of the world appear to have different characteristics. The clouds reach great heights and lightning discharges occur at a very fast rate (of the order of 10 per sec), largely in the upper part of the cloud. The spectra of the radiated atmospherics have also been said to be unusual with very little energy at VLF (Jones, 1951, 1958; Vonnegut and Moore, 1958), but it is not definitely established that they are in fact different from normal cloud discharges except possibly for their rate of occurrence.

III. FIELD CHANGES AND ATMOSPHERICS NEAR THE SOURCE

When the changes in the vertical component of electric field are recorded in a wide bandwidth at a point near a discharge, the major features are long, slow changes, with relatively rapid changes superimposed, the rapid changes being particularly prominent in ground discharges, as shown in Fig. 1

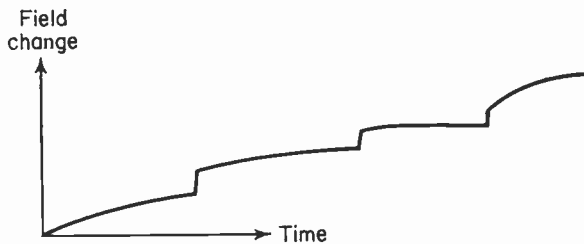


FIG. 1. Main field changes near a ground discharge.

(Pierce, 1955b). The signs of the changes depend on the nature and distance of the discharge, and while they are of interest in studies of the source, they have little relevance to the properties of radio-frequency noise. The whole process usually lasts for a few tenths of a second.

Slow changes in electrostatic field are the result of breakdown processes, leaders and junction streamers which change the distributions of charge in a gradual way when regarded as a bulk phenomenon. The relatively rapid field changes near ground discharges are attributed to return strokes or to the enhancements of current which occur when a weak discharge encounters a minor charge concentration. It was once thought that field changes near cloud discharges were entirely slow (Schonland *et al.*, 1938; Pierce, 1955a), but it is now clear that there are discharges in the cloud which produce rapid changes of field similar to, though generally of smaller magnitude than those from return strokes (Ishikawa and Kimpara, 1958; Kitagawa and Brook, 1960; Pierce, 1962). A typical ground discharge may produce a slow field change due to the breakdown and leader processes, a rapid change due to a return stroke, a slow change due to a junction streamer, a rapid change due to a second return stroke, and a final slow change. The number of return strokes, however, varies between wide limits. Slow changes represent noise with frequencies of the order of cycles per second, but they are to a

large extent the result of many small partial discharges, and closer examination reveals that they have, superimposed upon them, very rapid changes. A typical sequence preceding the first return stroke has been described by Clarence and Malan (1957), and is shown in Fig. 2. The effect of increasing the distance is to emphasize the importance of the rapid changes in the

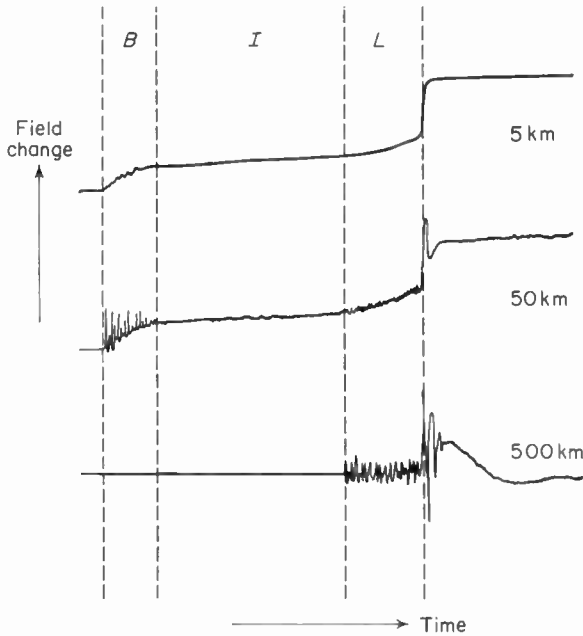


FIG. 2. Sequence of preliminary discharges at various distances. *B*, breakdown phase; *I*, intermediate phase; *L*, leader phase. Total duration up to $\frac{1}{2}$ sec. (Reproduced with permission from Clarence and Malan.)

leader stage. It is surprising that the rapid changes in the breakdown and intermediate stages disappear at the longest distance, but it has been assumed that they do not contain such high-frequency components as does the leader stage. Müller-Hillebrand (1961) has shown that pulses in the preliminary discharges can be much shorter than $1 \mu\text{sec}$. and can therefore represent noise extending to the high frequency range. Thus noise at the highest and the lowest frequencies is associated with the so-called slow changes, while noise in the intermediate range (VLF and LF) arises in the so-called rapid changes. It is evident that use of the terms slow and rapid are liable to lead to confusion.

The characteristics of narrow-band atmospheric at different frequencies are illustrated in Fig. 3,† which shows an atmospheric from a near ground discharge. The following interpretation is placed on these records:

- (a) The atmospheric contained two return strokes, which radiated the two main pulses on 6 kc/s and 10 kc/s, separated by 75 msec. The

† The figure does not show true relative amplitudes at different frequencies.

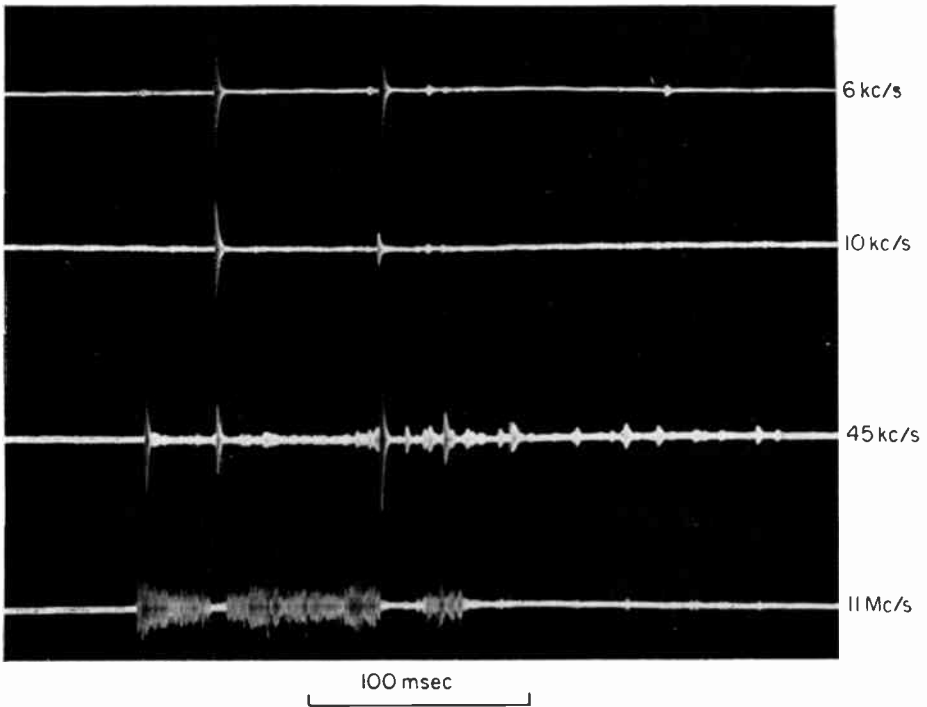


FIG. 3. Atmospherics from a near discharge.
(Reproduced with permission from Horner and Bradley, 1964.)

relative amplitudes from the two strokes on these two frequencies were markedly different. The shapes of the pulses were determined by the bandwidth of the receiver; use of a wider bandwidth would have resulted in narrower pulses.

- (b) At 45 kc/s the return stroke pulses are again prominent, but other parts of the discharge have emitted several pulses comparable with those from the return strokes, including one large pulse only 4 msec after the start of the discharge. There was little corresponding energy at 6 or 10 kc/s.
- (c) Noise at 11 Mc/s consists of bursts characteristic of the breakdown and leader processes. There is a burst 35 msec long preceding the first return stroke and one 70 msec long between the strokes. Some high frequency noise is radiated in the final stages of the discharge. With the occurrence of each return stroke the high frequency noise is suppressed, for 8 msec in the first case and 20 msec in the second.
- (d) The total duration must be deduced by an inspection of all records and is about 300 msec. A false impression of the duration might be obtained from the VLF records unless high gain were used.

The atmospheric in Fig. 3 was recorded in England (Horner and Bradley,

1964) and similar characteristics have been observed in South Africa (Malan, 1958) and in Sweden (Norinder, 1947). Malan also showed that although cloud discharges produced atmospherics with much smaller pulses than those from ground discharges at frequencies of a few kc/s, the differences were small at frequencies above 100 kc/s except that the breaks in high frequency noise following a return stroke did not exist in atmospherics from cloud discharges.

Durations of atmospherics recorded in England, mainly from ground discharges, are mainly in the range 200–400 msec (Horner, 1961). Brook and Kitagawa (1960a) quote a median value of 500 msec for storms in New Mexico, and suggest that shorter durations quoted earlier by Bruce and Golde (1941) were in error owing to low sensitivity. However, these were also at higher latitudes, and there appears to be a real increase in duration as the equator is approached. It has been observed in England that atmospherics with durations much longer than average tend to have smaller amplitudes at VLF, possibly suggesting that they are from cloud discharges (Horner and Clarke, 1958), and cloud discharges in Japan have been found to have a most common duration of 350–550 msec (Ishikawa and Kimpara, 1958; Takagi *et al.*, 1959).

An atmospheric at any frequency consists of three components, the electrostatic, induction and radiation components, whose magnitudes vary inversely as the distance to the power three, two and one respectively at distances large compared with the discharge length. The electrostatic component is predominant at distances less than a sixth of a wavelength and the radiation component predominates at greater distances. Near fields are often referred to as electrostatic fields since most of the energy from a discharge is then at wavelengths which greatly exceed the distance from the source, but they do in fact contain radiation components of the higher frequencies, which may not be recorded either because they are too small or because the recorder does not respond to a sufficiently wide band of frequencies. As the distance from the source increases, the low frequency components are attenuated more rapidly than those of higher frequencies (see Fig. 2). Ultimately a distance may be reached such that the radiation component is predominant at all frequencies of interest. Most discussions on radio noise relate to frequencies greater than 5 kc/s and since the distance from the source is then usually much larger than $\lambda/6$ (10 km), it is the radiation field which is important. The atmospheric in Fig. 3, recorded at 9 km, shows mainly the radiation component. However, interest is now being extended to frequencies of the order of 1 c/s and below, and in this range the electrostatic component is significant at all terrestrial distances. Nearly all the following discussion relates to the radiation field alone.

IV. SPECTRUM NEAR THE SOURCE

Several difficulties are encountered when an attempt is made to assemble information on the frequency spectrum of a single atmospheric. In the first place many observations of the field changes are not absolute. Secondly, the distance of the source is often not known, which introduces uncertainties

not only in the absolute amplitudes but also in the extent to which the results represent the radiation field alone. Thirdly, many observations are confined to a small range of frequencies, and fourthly, the spectrum quoted is sometimes that of only part of the atmospheric, say the return stroke and possibly an associated leader, and sometimes that of the whole atmospheric with perhaps several return strokes. However, attempts have been made in recent investigations to remove these limitations.

A. METHODS OF DERIVING SPECTRA

Spectra have been measured by two methods. In the first the field variations are recorded in a receiver with a wide frequency response, and Fourier analysis is applied to the resulting waveforms to determine the spectra. Use of this technique has been confined to low frequencies, since interference from radio transmitting stations at higher frequencies makes wide-band recording difficult. In the second method the fields are measured with a number of narrow-band receivers and the spectrum plotted directly, the curve being assumed to be smooth between the frequencies of observation. This method has been used over a wide frequency range since the use of narrow filters enables interference to be avoided.

The wide-band waveform of an atmospheric can be represented by a function showing how the instantaneous value $e(t)$ of a field component, or a voltage derived from it, varies with time t . The modulus $S(f)$ of the spectral component of $e(t)$ is then derived by use of the Fourier integral theorem from which

$$[S(f)]^2 = \left[\int_0^T e(t) \cos(2\pi ft) \right]^2 + \left[\int_0^T e(t) \sin(2\pi ft) \right]^2 \quad (3)$$

the integrals being taken over the duration T of the atmospheric. This process is now normally carried out by the use of digital electronic computers, the greatest labour being in transforming the data representing the waveform into a form suitable for computation.

When a narrow band of frequencies is selected, the waveform becomes effectively an oscillation at the centre frequency of the passband, with amplitude modulation superimposed. It is convenient to ignore the oscillation and to discuss the noise in terms of the envelope voltage, remembering that the mean square value is then twice the mean square value of the radio-frequency voltage. The form of the envelope is dependent on the characteristics of the selective circuits, and these must be known in some detail if the spectrum is to be deduced.

At low frequencies and with the bandwidths normally used, an atmospheric may be regarded as a short pulse (or a series of short pulses). When a pulse has passed through the tuned circuits, the output pulse is longer and has a smooth envelope whose peak value is sometimes taken as a measure of the energy at the chosen frequency. It must be borne in mind, however, that the relationship between peak amplitude and energy depends in a complicated way on the number and selectivity of the individual tuned circuits. The overall selectivity may be expressed in terms of the power

bandwidth B , defined by the equation

$$B = \frac{1}{G_0} \int_0^\infty G df \tag{4}$$

where G is the power gain at any frequency f and G_0 is the gain at the centre frequency, f_0 .

Suppose there are n tuned circuits of equal selectivity defined by the damping coefficient a , equal to f_0/Q where Q is the magnification of each stage (assumed large). The overall bandwidth is then

$$B = \frac{(2n-2)!}{2^{2n-1} [(n-1)!]^2} a \tag{5}$$

or if n is large, by use of Stirling's formula (Weatherburn, 1957)

$$B = \frac{a}{2\sqrt{\pi(n-1)}} \tag{6}$$

If the peak amplitude of the envelope of the output pulse is e_p , when a short input pulse is applied, the waveform of this envelope is given by

$$e = e_p \left(\frac{\varepsilon at}{n-1} \right)^{n-1} \varepsilon^{-at} \tag{7}$$

where ε is the base of natural logarithms.

Now by the Fourier integral energy theorem,

$$\int_0^\infty [S(f)]^2 df = \frac{1}{2} \int_{-\infty}^\infty e^2 \sin^2(2\pi ft) dt \tag{8}$$

If $S(f)$ is assumed to be constant over the narrow band of frequencies B accepted by the receiver, the integral taken over this bandwidth becomes

$$[S(f)]^2 B = \frac{1}{2} \int_{-\infty}^\infty e^2 \sin^2(2\pi ft) dt \tag{9}$$

or since e is a slowly varying function compared with the radio frequency period

$$[S(f)]^2 = \frac{1}{4B} \int_{-\infty}^\infty e^2 dt \tag{10}$$

The integral, in relation to the peak amplitude, depends on the number of tuned stages, n , according to the equation

$$I = \int_{-\infty}^\infty e^2 dt = \frac{e_p^2}{2a} (2n-2)! \left(\frac{\varepsilon}{2n-2} \right)^{2n-2} \tag{11}$$

or in terms of the bandwidth B

$$I = \frac{1}{B} \left[\frac{e_p(2n-2)!}{2^n(n-1)!} \frac{\epsilon^{n-1}}{(2n-2)^{n-1}} \right]^2 \quad (12)$$

The relationship between this integral and n is shown in Table I. For $n > 2$, the integral is nearly independent of n if the amplitude and overall bandwidth are fixed.

TABLE I. *Dependence of I on n*

n	$\frac{IB}{e_p^2}$
1	0.250
2	0.461
3	0.479
4	0.485
5	0.487

From this table and equation (10), for amplifiers with two or more tuned circuits in cascade, and to an accuracy normally sufficient for calculations on atmospherics

$$S(f) = \frac{e_p}{2\sqrt{2}B} \quad (13)$$

Another case of interest is the ideal rectangular bandpass filter. Suppose, for example, that the filter has uniform amplitude response within the bandwidth B and zero outside it, and has a phase transfer proportional to frequency (Kf). The envelope of the output pulse resulting from an applied impulse function then has a form

$$e = e_p \frac{\sin [2\pi B(t-K)]}{t-K} \quad (14)$$

and the Fourier component is

$$S(f) = \frac{e_p}{2B} \quad (15)$$

Although ideal rectangular filters cannot be achieved in practice, Fourier analysis of wideband waveforms may be carried out in a manner which simulates such a filter.

Equation (13) or (15) can be used to determine the spectral component from the amplitude of the pulse provided that the incident atmospheric is known to be very short. This representation is most appropriate in the VLF range where the return strokes provide isolated pulses of short duration compared with the reciprocal of the bandwidth. If there are several pulses

in the atmospheric the energies may be added to find the spectral component. At higher frequencies the noise becomes more continuous, and successive pulses tend to overlap. In this more general case the spectral component can be determined from equation (10) if the integral can be evaluated for the whole atmospheric.

The formulae presented above can be used whether the integrals are measured or calculated from a knowledge of the currents in the discharges. The spectrum of the atmospheric from a return stroke, for example, can be determined from the current variations (Sao, 1955; Horner, 1958). Aiya (1955) has also used the technique in an analysis of the noise to be expected from the stepped-leader. The integrals can be measured by recording the amplitude probability distributions, by methods described in Section VIII, D, and performing a numerical integration.

B. EXPERIMENTAL SPECTRUM DATA

The way in which peak amplitudes vary with the frequency is shown in Fig. 4, derived from measurements in temperate latitudes (Horner and Bradley, 1964). As mentioned earlier, the spectral component cannot be

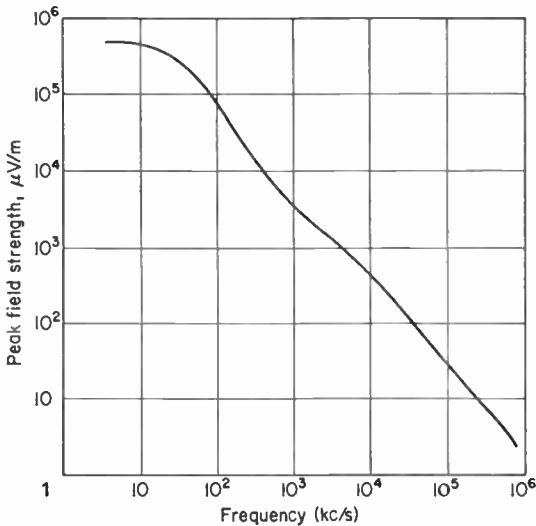


FIG. 4. Peak field strengths of atmospheric.
Distance 10 km. Bandwidth 250 c/s.
(Reproduced with permission from Horner and Bradley, 1964.)

obtained directly from the amplitude alone, but is related to the integral $I = \int e^2 dt$ defined in equation (11). This in turn can be related empirically to the amplitude e_p for an average atmospheric, and Table II shows typical values of I/e_p^2 for a receiver with two or more tuned circuits.

TABLE II. Ratio $\frac{\int e^2 dt}{e_p^2}$ in 250 c/s bandwidth

f	Mean ratio	Range
6 kc/s	0.008	0.002-0.03
10 kc/s	0.005	0.002-0.02
50 kc/s	0.005	0.002-0.008
500 kc/s	0.015	0.003-0.04
10 Mc/s	0.02	0.005-0.05
100 Mc/s	0.02	insufficient data

An atmospheric resulting from a single very short impulse would have a value 0.0018 for this ratio, while a burst of fluctuation noise of duration 200 msec would have a value of about 0.02, depending on how the peak value was defined.

Measurements of the spectrum which have been made by various workers, using both wideband and narrowband techniques, have been combined in Fig. 5. A recent review (Horner, 1962a) contains a similar plot, but since that review was prepared further information published by Watt (1960) shows that errors had been made in the interpretation of the Watt and Maxwell data, and these have been corrected in Fig. 5. The spectral component is seen to have a maximum at about 5 kc/s and to follow an inverse frequency law over a wide range of higher frequencies.

Some explanation of the plotted values from Schafer and Goodall and from Atlas is required, as they are derived from measurements of peak noise, and various assumptions were made in deriving spectral components. Schafer and Goodall (1939) observed near storms and their results show that at 10 km distance the peak value of the noise was 1.2 mV/m in a bandwidth of 1.5 Mc/s at 150 Mc/s. This peak value was measured on a cathode ray tube and if the atmospheric is assumed to be similar to a burst of fluctuation noise, the r.m.s. value of the noise envelope can be assumed to be about one-third the observed peak value, or 0.4 mV/m. If the noise bursts were 200 msec long, a value found to be typical in other work, then the mean square envelope voltage can be calculated and, using equation (10), $S(f)$ can be derived. Noise bursts recorded by Atlas (1958) at 2800 Mc/s had a typical peak value of 6×10^{-4} V/m in a bandwidth of 600 kc/s when normalized to a distance of 10 km. In this case the noise bursts were said to be only up to 1 msec long, and using this duration, a similar calculation to that given above leads to the plotted result. The short duration is, however, difficult to reconcile with observations at lower frequencies, and it is possible that the spectral component should be an order of magnitude larger.

The values of $S(f)$ plotted represent only the radiation component of the vertically polarized field, and they have been normalized to a distance of 10 km. At this distance and at frequencies below 5 kc/s the actual field would

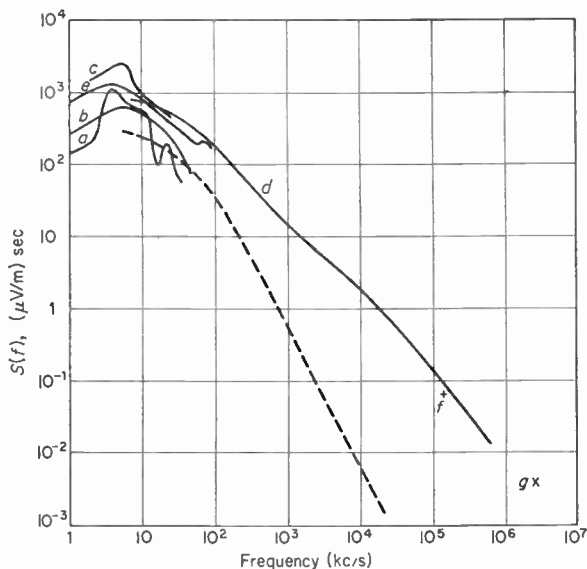


FIG. 5. Frequency spectra of atmospherics.

- a. Watt and Maxwell (1957a) †
- b. Taylor and Jean (1959) †
- c. Edwards (1956) ††
- d. Horner and Bradley (1964)
- e. Taylor (1963) †
- f. Schafer and Goodall (1939)
- g. Atlas (1959)
- Bruce-Golde model †
- † Return stroke only
- †† Return stroke plus precursor

(Reproduced with permission from Horner and Bradley, 1964.)

be mainly the electrostatic component, so the curve shown is somewhat artificial, and derived from estimates of the radiation fields at greater distances, using an inverse distance law of propagation. The general shape of the spectral curve has been confirmed by Takagi and Takeuti (1963), but the absolute values cannot be readily related because quasi-peak detectors were used and the precise distances of the discharges were not given.

All quoted measurements appear to have been made on ordinary storms. There is evidence that big storms in which tornadoes occur have very large numbers of discharges at high altitudes and have unusually strong energy components in the region of 150 kc/s (Jones, 1951). However, no spectrum measurements are known to have been made.

C. THE SPECTRUM DERIVED FROM THE DISCHARGE MODEL

It is well established that the measured spectra at very low frequencies are consistent with a return-stroke model of the form described in Section II, C,

although there is still discussion about the best values to adopt for the coefficients, particularly at frequencies well below 10 kc/s. The derivation of the spectrum from the current variations is straightforward (Horner, 1958) and the spectrum of the Bruce-Golde model is shown in Fig. 5. The alternative model based on the waveforms of Norinder (1951) has longer duration and more energy at frequencies below 10 kc/s. Above 50 kc/s the return stroke model does not provide a satisfactory explanation of the measured atmospherics and it is evident that either the model is incomplete, or other forms of discharge become more important, or both. In the example of Fig. 3, the return stroke pulses have certainly ceased to predominate at 45 kc/s.

There have been very few attempts to postulate a precise model and derive a spectrum for discharges other than the return stroke. Hill's (1957) treatment of low frequency noise includes a discussion of the leader but neglects the rapid current variations which cause energy to be radiated at the higher frequencies. Aiya (1958) has carried out an analysis of the stepped leader as a source of high frequency noise, taking as a model a sequence of four such leaders, each lasting for 1 msec, the overall sequence having a duration of 200 msec. The parameters deduced were related to a particular method of noise measurement which he had developed (Aiya, 1954) (see Section VIII) and cannot easily be compared with the spectra shown in Fig. 5. Furthermore, the current variations assumed were deduced by extrapolation from measurements at much lower frequencies and are subject to considerable uncertainty. The results of spectral analysis of waveforms by Watt and Maxwell (1957a) suggest that the stepped-leader, immediately preceding the return stroke, radiates energy at frequencies of the order of 30 kc/s, but there is evidence that the model of the stepped-leader described by Schonland (1956) is not the main source of energy in the high frequency range, where there are bursts of noise of much longer duration. The noise may, however, originate in discharges of the stepped-leader type, taking place in the cloud and therefore usually unseen. Alternatively, it may result from smaller, but more rapidly varying discharges for which there is no accepted quantitative model.

D. RADIATED ENERGY

Since the received energy spectrum is known in absolute terms it is possible, with certain assumptions, to estimate the total radiated energy at different frequencies and also various related power functions. Consider first what happens at very low frequencies and particularly the radiation from the return stroke when this is assumed to be effectively a grounded vertical aerial. If the earth is a good conductor the field will be distributed approximately according to a cosine law with the angle of elevation from the source. If e is the instantaneous envelope field strength in V/m measured on a short vertical grounded aerial at distance d , the instantaneous power flux is $e^2/240\pi$ W, and by integration over the hemisphere the total instantaneous power is found to be $e^2d^2/180$ W. The maximum value is $e_p^2d^2/180$, and the total energy is

$$\frac{d^2}{180} \int_0^T e^2 dt = \frac{Bd^2}{45} [S(f)]^2 \text{ Joules (from equation 10)}$$

where T is the duration of the atmospheric. The mean power over the interval T is this expression divided by T . At much higher frequencies the return stroke is no longer the main source of noise and it seems more reasonable to consider the discharge as being at least at the height of the cloud base (of the order of 2 km) and to be randomly orientated. On the average, the radiated energy will then be isotropic and the instantaneous power becomes $e^2 d^2 / 120 \text{ W}$, the maximum power $e_p^2 d^2 / 120$, and the total energy

$$\frac{Bd^2}{30} [S(f)]^2 \text{ Joules}$$

It can be seen that at least three power parameters are of interest, the peak power, the mean power over the duration of the atmospheric, and the mean power from atmospheric occurring at a specified rate, for example, those in a given storm area. The peak power will be proportional to the square of the bandwidth, if this is not large, while the other parameters will be proportional to the bandwidth.

Typical values for various amplitude, power and energy parameters are listed in Table III, for a few selected frequencies. The peak amplitudes and spectral components are for a vertical grounded receiving aerial and represent the radiation field component normalized to a distance of 10 km. The peak amplitudes and power parameters are for a bandwidth of 1 kc/s obtained with two or more similar tuned circuits in cascade. The radiating discharge has been assumed to be vertical and near the ground for frequencies up to 50 kc/s, and elevated and isotropic at higher frequencies.

TABLE III. *Parameters of Typical Atmospherics and Discharges*

Frequency	Peak amplitude in 1 kc/s at 10 km e_p (mV/m)	Peak radiated power in 1 kc/s	$S(f)$ at 10 km [$\mu\text{V/m}$ sec]	Radiated energy in 1 kc/s (J)	Mean power over 200 msec in 1 kc/s
5 kc/s	1200	500 kW	900	1800	9 kW
10 kc/s	1600	1400 kW	800	1400	7 kW
50 kc/s	300	50 kW	200	90	450 W
1 Mc/s	8	30 W	10	3×10^{-1}	1.5 W
10 Mc/s	2	2 W	2	1.3×10^{-2}	60 mW
100 Mc/s	0.1	3 mW	0.1	3×10^{-5}	160 μW

In deriving the mean power during the atmospheric, listed in the final column, the duration has been assumed to be a nominal 200 msec. The figures should therefore be taken as indicating only the order of magnitude.

The total power from a number of atmospherics is the number per second times the indicating energy.

There are, in the literature, few specific estimates of the energy radiated per unit bandwidth in different parts of the spectrum, as deduced from the characteristics of the discharge. Computations of the amplitudes and frequency spectra of very low frequency pulses from return strokes have, however, been made on several occasions and, with certain assumptions, can readily be expressed in terms of radiated peak power and energy. The energy per atmospheric will be greater since it will contain more than one return stroke on the average. Aiya (1955) from his model of the stepped-leader, deduced that the power in the high frequency range is $45/f^2$ W, in a bandwidth of 6 kc/s, where the frequency f is in Mc/s. There is no explicit statement about which the various power parameters this represents, but from a discussion in a later paper (Aiya, 1959) it seems probable that it was intended to be the mean power over the duration of one atmospheric. If so, the values can be compared with those in the final column of Table III. Converting to a bandwidth of 1 kc/s Aiya's power formula would be very nearly $8/f^2$. At 10 Mc/s, for example, the power would be 80 mW, which is of the same order of magnitude as the figure in the table.

V. AMPLITUDE VARIABILITY OF ATMOSPHERICS

Atmospherics have an established reputation for variability, both in form and amplitude, and it is desirable to express these variations in statistical terms. The differences in the sources are those related to the currents, their rates of change, and the lengths and orientations of the discharge channels. To study source effects, amplitude observations must be normalized to the same distance, but even so there are uncertainties in propagation and in the estimated distances, which may appear to indicate differences in the radiating properties of the source. Nevertheless, reasonable agreement has been found between the results of different workers. When the amplitude parameters are expressed in logarithmic units, e.g. decibels, their statistical distribution is usually nearly normal. For example, if the peak amplitudes e_p (in decibels) are considered, the probability of a value falling in the range x to $x+dx$ is

$$\frac{1}{\sigma\sqrt{2\pi}} \exp \left[-\frac{(x-e_{pm})^2}{2\sigma^2} \right] dx$$

Where e_{pm} is the median value, and σ the standard deviation of e_p . Thus the probability of a value e_p being exceeded is

$$Q(e_p) = \frac{1}{\sigma\sqrt{2\pi}} \int_{e_p}^{\infty} \exp \left[-\frac{(x-e_{pm})^2}{2\sigma^2} \right] dx \quad (16)$$

The standard deviation is a convenient measure of the variability of the selected parameter (Horner, 1958; Satyam, 1962).

Perhaps the most marked amplitude differences would be expected between return strokes and other types of discharge. The peak currents in return

strokes quoted by Bruce and Golde (1941) have a log-normal distribution with a standard deviation of about 8 db (Horner, 1958). It is found that atmospheric, whether measured in a wide or a narrow bandwidth, have standard deviations of 10 db or less, at frequencies above 5 kc/s. It seems from this reasoning that the inclusion of cloud discharges does not extend the amplitude range by a large factor, and that they therefore radiate atmospheric with amplitudes comparable with those from return strokes. This is inconsistent with the statement of Malan that the amplitudes differ by a factor of ten at 10 kc/s, on the average.

There is evidence that the intensity of a return stroke, and of the radiated atmospheric, depends on whether the stroke is to land or to sea, and on whether it is to high or low ground. For example, Robertson *et al.* (1942) have said that the peak currents in ground strokes decrease with increasing height of the terrain, from a median value of 26 kA at sea level to 5 kA at 12 000 ft. Such differences are believed to have a bearing on the prevalence of whistling atmospheric (see Section XIII).

Experiments designed to measure the variability of the radiated energy in atmospheric have two main difficulties. The first is to know the distance of each discharge and to normalize to a constant distance; the second is to be sure that the full range of amplitudes has been recorded, since all recording apparatus has a threshold of sensitivity. The following data for England have been obtained from near storms, and it is believed that atmospheric from even the weakest discharges are included (Horner, 1961; Horner and Bradley, 1964). Peak amplitudes of atmospheric from a single storm have been found to be distributed log-normally with a standard deviation of about 6 db at 6 kc/s, decreasing somewhat to below 5 db at 10 Mc/s. Such a change with frequency would be expected, as atmospheric from cloud and ground discharges are more similar at high frequencies. Mean amplitudes in different storms had a standard deviation of about 4 db at 6 kc/s decreasing to below 3 db at 10 Mc/s. Taking into account both variations in a storm and variations from one storm to another, the overall standard deviations were about 8 db at 6 kc/s and 6 db at 10 Mc/s. The value at 6 kc/s is similar to the standard deviations of return stroke currents; a larger value would have been expected from the inclusion of cloud discharges. Standard deviations of about 4 db at high frequencies have been recorded in India (Satyam, 1962).

The values quoted are for amplitudes of atmospheric recorded in narrow-band receivers. Variations in the total energy of narrow-band atmospheric have also been found to be similar to those of amplitudes, despite the fact that a wide variety of waveforms can occur. These waveforms are complex and difficult to describe quantitatively in simple terms, but some indication of the type is given by the ratio of the energy to the square of the peak voltage given in Table II.

VI. NUMBERS AND DISTRIBUTIONS OF LIGHTNING DISCHARGES

In 1925, Brooks made a study of reports of thunderstorms, and estimated that on the average some 2000 thunderstorms are in progress at any one

time and that at least 100 lightning discharges occur every second. These figures have generally been accepted, and although there has been little work aimed specifically at checking them, such data as have become available indicate that the order of magnitude is correct. In temperate latitudes thunderstorms consist of a number of cells (Byers and Braham, 1953), each of which lasts for a time of the order of half an hour and in which discharges occur at a rate of one or two per minute. About 40 per cent are ground discharges. In equatorial regions the frequency of discharges is reputed to be somewhat higher, but a smaller proportion, perhaps 10 to 20 per cent, reach the ground (Pierce, 1956a; Prentice, 1960). The world distribution of thunderstorms has been assessed in terms of the number of days in each month that thunder is heard at any one location. Data from a large number of stations have been collected and tabulated by the World Meteorological Organization (WMO, 1953), but they are of limited use for noise work because there is no information about intensity, duration, or diurnal variation of the storms.

Some progress towards a more useful measure of thunderstorms as noise generators has been made by the development of lightning flash counters which aim to record the discharges within a defined radius from the instrument (Schonland and Gane, 1947; Ito *et al.*, 1955; Pierce, 1956a; Lugeon and Rieker, 1957; Sullivan and Wells, 1957; Horner, 1960b). They usually consist of wideband, low-frequency receivers which respond to atmospherics having amplitudes greater than some defined threshold level. Unfortunately, owing to the variation in the amplitudes of atmospherics from any one distance, the ideal objective of recording all the discharges within the specified radius and none outside cannot be realized, and use of counters has been criticized on this account. Brook and Kitagawa (1960b) have even suggested that counters operating on electromagnetic fields are fundamentally incapable of providing useful information on lightning discharge distributions and prefer methods designed to record the visual flashes. Nevertheless, for radio noise investigations the conventional types of counter have their merits and by a suitable statistical treatment of the results an assessment of the density of discharge over the area surrounding the counter can be made. This is the quantity of interest in radio noise work. It should not be inferred that the results are necessarily as useful for meteorological purposes which are not so closely related to the radiated atmospherics. The effective range of a counter has been defined as the range within which the number of discharges occurring, over a long enough time for the local geographical distribution to be statistically uniform, is equal to the number counted (Horner, 1960b). Using this concept, the density of the discharges can be inferred even though there is not complete correspondence between those flashes which are within the effective range and those which are counted. Comparisons between counter records and observations by visual and aural techniques may be used to establish the effective range.

Two designs of counter have been subjected to considerable investigation. One, a development of the design of Sullivan and Wells (1957), is intended to count all discharges and has been recommended by the International

Radio Consultative Committee (CCIR) for providing information applicable to radio noise investigations. It has a frequency response of about 1 to 50 kc/s, and when set to trigger on a step-function voltage equivalent to a field change of 3 V/m, it has been found to have an effective range of 30 km in England (Horner, 1960b). Müller-Hillebrand (1963) in Sweden has reported some inconsistency in the results of his attempts to estimate the effective range, depending on whether near or distant storms were used, but his figures deduced from near storms agree reasonably well with the experience in England. The other design of counter, in which an attempt is made to count only ground discharges, by using lower frequencies, is based on the work of Pierce (1956a) and has been adopted by power engineers (Müller-Hillebrand, 1959, 1961). In practice the counters do not differ as much as was intended in their ability to select particular types of discharge. One reason is that although cloud discharges radiate less low frequency energy than do ground discharges, on the average, there is considerable spread in the amplitudes and spectra from both types, and no well-defined demarcation between them. Malan (1962) has described a new design of counter, intended to count only ground strokes. It is based on the finding that cloud and ground discharges radiate atmospherics with different relative amplitudes on 5 kc/s and 100 kc/s. Insufficient tests have been carried out in thunderstorms to determine whether the objectives are achieved.

Counters provide a record of thunderstorm activity related to noise generation, including diurnal variations. They do not necessarily provide a record of thunderstorm days, strictly comparable with aural observations. Nevertheless, in view of the wealth of existing data on thunderstorm days appropriate relationships have been sought. In England it has been found that the number of thunderstorm days per month is approximately the same as the number of days on which the count, with a CCIR counter of standard 3 V/m sensitivity exceeds 30 in at least 1 h of the day. This is physically reasonable because a single thunderstorm cell lasts for $\frac{1}{2}$ -1 h and produces about one discharge per minute, say about forty discharges on the average. Long-duration discharges may trigger the counter, which has a response time of about $\frac{1}{4}$ sec, twice, or occasionally three times, so the count is rather more than the actual number of discharges. On the other hand, if the storm is just within audible range, the minimum requirement for a thunderstorm day, only about 60 per cent of the discharges will be counted, the smaller ones being missed, and the net result is likely to be about 30 counts. There will be occasions when thunder is heard but only a few discharges are produced, and conversely an active storm outside audible range may result in a count of more than 30, but this appears to be the correct minimum requirement for an average occasion.

This relationship may be expected to apply when the thunderstorm cells are so scattered that when one is within audible range others are sufficiently distant not to affect the count. Under the stormy conditions of the equatorial regions the cells may at times be so dense that a counter is often affected by more than one cell. In addition, the rate at which discharges occur tends to be higher in equatorial storms. For these reasons an average thunderstorm

day will correspond to a higher minimum count, and a count of 30 per hour may often occur without storms within audible range. It has been found that days with at least one hourly count greater than 100 are about equal in number to thunderstorm days. Thus the relationship between thunderstorm days and counts is dependent on the density of storms. The average number of counts per hour on the equatorial land masses during periods of maximum activity (season and time of day) is about 150 with the CCIR counter. Since the effective range is 30 km, the number within a radius of 1000 km would be 50 per sec if the activity were uniform over this area. On this basis one large tropical thunderstorm area during its diurnal period of maximum activity would contribute about half the 100 discharges per sec estimated by Brooks (1925) for the whole world.

Another source of information is the incidence of lightning strikes to power lines. From a review of data, Golde (1961) concluded that a typical number of lightning strokes to ground per square kilometre per thunderstorm day is substantially the same over much of the world, with a value of about 0.16. There have been some views expressed that a lower figure might be more correct for temperate regions, based partly on general experience in observing thunderstorms. Davis (1962) first deduced a value of 0.05 from strikes to power lines in England, but later amended this to a value in close agreement with that of Golde (Davis, 1963). In any case the figure of 0.16 seems reasonable for the tropical thunderstorm areas. It is of interest to determine whether lightning flash counter data agree with this result. Suppose the figure of 150 is accepted for the average count per hour on a CCIR counter during times of maximum thunderstorm activity in the tropics, and suppose also that this represents the total number of discharges of all types within the effective range of 30 km. The ratio of cloud to ground discharges has been quoted as 9 : 1 (Pierce, 1956a) and as $4\frac{1}{2}$: 1 (Prentice, 1960). Taking a value of 6 : 1 the number of ground discharges h becomes $0.01/\text{km}^2$. Now lightning flash counter data show that on an average thunderstorm day in the tropics the stormy period lasts about 4 h, while a range of 4–6 h has been quoted by Aiya and Phadke (1955). Assuming a duration of 5 h the number of ground discharges per thunderstorm day is $0.05/\text{km}^2$. The number of strikes to power lines will be related to the number of strokes down different channels, which is likely to be somewhat greater than the number of discharges, so the final figure of stroke channels derived from counter data is perhaps half that quoted by Golde. Lower figures of 0.03–0.05 have been quoted by Müller-Hillebrand (1959) derived from flash counters in Sweden, where the duration of stormy periods is likely to be less than in the tropics. No great accuracy can be claimed for the figures deduced by either method, but the fact that they are of the same order and not inconsistent with the estimates of Brooks is reassuring. Knowledge of the frequency of occurrence of lightning discharges cannot, however, be considered satisfactory until the incidence of different types is known as a function of geographical location, and much additional work is required. In the meantime it seems reasonable to assume an average hourly figure of about 0.1 discharges/ km^2 during active periods in the tropics, including all types.

It is in the stormy equatorial regions and at the most stormy times of the day and year that the number of discharges per unit area over a short interval of time (say a few hours) is most useful as a parameter in noise studies, since conditions can approach some degree of statistical stability. At other times, at higher latitudes or over the oceans the number is variable between very wide limits. In temperate regions many months may be almost free from thunderstorms, but occasionally in summer the density may approach that in the tropics, for perhaps a few hours, but only over a much smaller area.

If a more complete knowledge existed of the densities of lightning discharges in different parts of the world, it could be coupled with a knowledge of the energy radiated by an average discharge, to give the world distribution of radiated power. Hitherto this distribution has been assumed to follow the distributions of thunderstorm days, for want of a better index. Lightning flash counters, though they have some functional shortcomings, and are more expensive than ears, provide an index of thunderstorm activity closely related to the radio noise and are automatic in operation. Unfortunately counter records are available for only a few locations, and the problem of obtaining accurate figures for the densities of discharges in different parts of the world and at different times require much more extensive investigation.

VII. PROPAGATION OF ATMOSPHERICS

Since atmospheric noise occurs at all frequencies of the radio spectrum, including the range below that currently used for communication, the propagation of this noise is a very wide subject. Here it is possible to mention only some of the principal features. The discussion is mainly on the low-frequency end of the spectrum, where interference from noise is most serious and where the study of atmospherics has provided much of the experimental propagation data. Only the vertically polarized field is considered.

A. THEORETICAL STUDIES OF PROPAGATION AT LOW FREQUENCIES

At frequencies of the order of 10 kc/s and at distances large compared with the length of the discharge channel, but not very large, the field strength of the ground wave, propagated over water or well-conducting earth, is inversely proportional to the distance from the source. This relationship is modified at distances greater than a few hundred kilometres, depending on ground conductivity, but since waves propagated via the ionosphere become important at shorter distances, particularly at night, the range over which the ground wave predominates is small, typically up to about 200 km at night and 500 km by day at 10 kc/s. When ionospheric waves must be taken into account, the theory is complicated by the fact that the wavelength is not short compared with the lengths of the paths through the ionosphere. Considerable attention has been paid to the problems which then arise and the phenomena have been explained in terms of waveguide modes of propagation in the space between the earth and the ionosphere. This work has been summarized by Wait (1962a, 1962b), by Al'pert (1960) and by Borodina *et al.* (1960), who have listed extensive bibliographies of the subject.

Propagation depends on the height of reflection in the ionosphere and on the electrical properties of the ionosphere and of the ground. The waveguide mode analysis was first based on the assumption that the ionosphere and the surface of the earth were smooth, sharp boundaries and that the magnetic field could be neglected. A selection of curves typical of those derived by Wait (1957a) is reproduced in Fig. 6, where the spectra at various distances

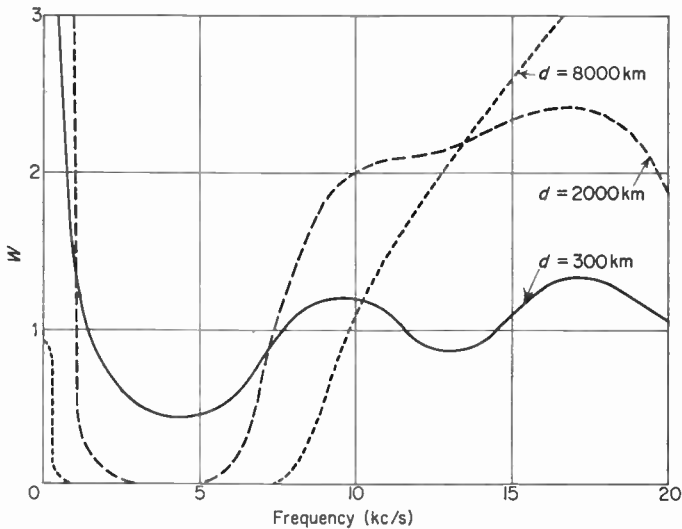


FIG. 6. Calculated VLF propagation curves.

$$\text{Field strength} = WE_0, \text{ where } E_0 \text{ (mV/m)} = \frac{300\sqrt{\text{radiated power (kW)}}}{\text{distance (km)}}$$

from a short vertical aerial radiating white noise are shown. The parameter W is the multiplying factor to be applied to the field $E = 300\sqrt{P}/d$ mV/m, appropriate to ground wave propagation over a perfectly-conducting flat earth. P is the radiated power in kilowatts and d the distance in kilometres. Notable features of the curves are the poor long-distance propagation in the region of 2 to 4 kc/s and the relatively good propagation above 10 kc/s. The latter characteristic, coupled with the high source energy at 10 kc/s, accounts for the tendency for wideband atmospherics to become long quasi-sinusoids with approximately this frequency at large distances from the source. Good propagation below 1 kc/s leads to the phenomenon known as the slow tail, which is a slow change composed of frequencies of the order of 500 c/s, arriving somewhat later than the main part of the atmospheric (Pierce, 1960b).

At any one frequency it is usual to express the propagation in terms of an attenuation coefficient α , defined by the following equation for the variation

of field strength e with the distance d :

$$e = \frac{A}{\left(\sin \frac{d}{R}\right)^{\frac{1}{2}}} \exp\left(-\frac{\alpha d}{8680}\right) \quad (17)$$

where R , the radius of the earth, and d are in km, A is a constant and α is in db/Mm † (Wait, 1957b; Taylor, 1960a). Values of α have been derived, in later work, using more realistic models of the physical conditions. The earth's magnetic field was taken into account (Barber and Crombie, 1959; Crombie, 1960) and a difference in the propagation of VLF waves in easterly and westerly directions was predicted, the easterly direction involving smaller attenuation. The theory of Wait and Spies (1960) indicates that the magnetic field is likely to change the attenuation coefficients by about ± 30 per cent for propagation along the equator. In further extensions to the theory, more general models of the ionosphere were adopted, in which a single sharp ionospheric boundary was not assumed (Al'pert, 1956; Schmoys, 1956). Typical models, for example, had layers with different properties, or an electron density increasing exponentially with height. An explanation of certain experimental results at ELF was advanced by postulating a variation in the reflection height with frequency (Pierce, 1960b).

The mathematical treatments have yielded information on phase spectra as well as amplitude spectra and are therefore suitable for the analysis of the effects of propagation on transients such as atmospheric. Several papers have dealt specifically with this problem. The best-known effect is the progressive time separation of the slow tail from the main part of the atmospheric, frequencies of about 500 c/s travelling more slowly than those near 10 kc/s, and the intermediate frequencies being absorbed as shown in Fig. 6 (Hales, 1948; Hepburn, 1957; Wait, 1960a). According to Wait, the time separation t_s between the oscillatory part of an atmospheric and the maximum of the slow tail is given by $(t_s)^{\frac{1}{2}} = C + Dd$, where d is the distance and C and D are constants. The changes in shape of various idealized source pulses during ground wave propagation have also been studied, including the model represented by the parameters of the return stroke given in Section II, C (Wait, 1956, 1957c, 1958b). The general effect of propagation is to extend the pulse durations.

Attenuations predicted by the mode theory (values of α in equation (17)) for various assumed properties of the ground and ionosphere can vary between 0.2 and 10 db/Mm at 50 c/s and between 2 and 15 db/Mm at 1 kc/s depending on the assumed electron density and collision frequency in the ionosphere (Wait, 1960b). Maximum attenuation occurs at about 3 kc/s and thereafter decreases again, as can be seen from Fig. 6.

B. EXPERIMENTAL DATA AT LOW FREQUENCIES

In view of the marked dependence of propagation on ionospheric properties and the inadequate knowledge of these, there is an evident need for experi-

† 1 Mm = 1000 km.

mental data on VLF and ELF propagation. Verification of the mode theory at frequencies below 16 kc/s has relied largely on observations of atmospherics. A reasonable amount of information is available at VLF, the atmospherics work being supported by observations on transmissions in the rather higher frequency range 16–20 kc/s. A few experiments have been carried out at ELF. A selection of experimental results is shown in Fig. 7, in the form of attenuation coefficients. Daytime data of Chapman and Macario (1956) show attenuations of 1.5 db/Mm at 100 c/s, rising to 20 db/Mm at 1 kc/s, a broad peak in the region of 2 kc/s, and falling to 3 db/Mm at 10 kc/s. At night the peak is only about 8 db/Mm. Holzer (1958) quoted 1 db/Mm at 100 c/s,

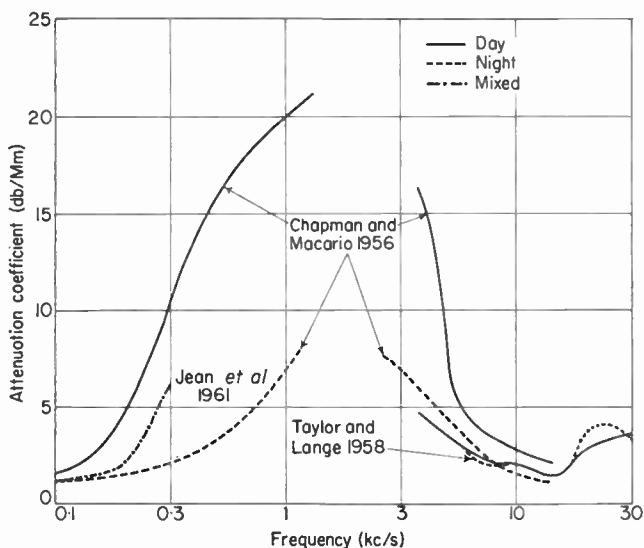


FIG. 7. Experimental attenuation data.

apparently with little diurnal variation. Taylor and Lange (1958), by studying the spectra of the same atmospheric recorded at widely spaced stations, have continued the attenuation curve to show a minimum of 1.5 db/Mm at 13 kc/s by night and day, and then an increase to about 3 db/Mm at 30 kc/s. These values at the higher frequencies are considerably lower than the early data of Eckersley (1932), but are in agreement with values derived by Wait (1958c) from a new analysis of old measurements of long-wave transmissions. Hepburn (1960), from a study of smooth-type atmospherics deduced a low attenuation at 4 kc/s in contrast with the other workers and with mode theory. Jean *et al.* (1961) analysed waveforms at spaced stations for the ELF range and for mixed light and dark paths deduced values lying between the night and day curves of Chapman and Macario. Propagation at frequencies below 500 c/s was said, by Liebermann (1956) to be good both by day and by night, resulting in only slightly higher noise at night, but Aarons

(1956) showed diurnal variations of the order of 20 db in noise at 100 c/s, apparently related to propagation, with maximum noise at night.

The observations at spaced stations have also been used to derive the phase characteristics at VLF. Phase velocities at frequencies below 20 kc/s were found to exceed the free-space velocity by a small amount, increasing at the lower frequencies in a manner consistent with the mode theory (Jean *et al.*, 1960).

Hepburn and Pierce (1953) deduced that an empirical formula of the form $C + Dd$ could be used to represent either the time delay of the slow tail or its quasi-period, and were supported by further work by Hepburn (1957b), but Wait (1960a) re-examined their data and concluded that they supported his theoretical finding that the square root of the time delay was of the above form.

Different propagation characteristics for atmospherics received from different directions were recorded by Caton and Pierce (1952), and source effects, nature of the path (land or sea), and the earth's magnetic field were advanced as possible reasons. Chapman (1957) considered that the nature of the path was an important factor. Later the work of Taylor (1960a) showed marked differences between east-west and west-east propagation and supported the theories dealing with the effect of the earth's magnetic field. His experimental curves of attenuation are shown in Fig. 8.†

Although most experimental results available for comparison with theory have been gathered by observing single atmospherics (or more frequently components of atmospherics from single ground strokes), integrated noise from many sources has sometimes been used. Spectrograms of noise from distant sources have confirmed the absorption band at 2–4 kc/s, with attenuations of 5 db (night) and 10 db (day) per Mm at 4 kc/s compared with 2 db and 3 db respectively at 10 kc/s. Values of about 5 db/Mm occurred at 70 kc/s by night and 7 db/Mm by day (Obayashi, 1960; Obayashi *et al.*, 1959). Gardner (1950), by measuring noise in narrow-band receivers, showed that the daytime attenuation, by comparison with that at night, was small in the region of 10–20 kc/s and increased considerably at both lower and higher frequencies. Lauter and Schmelovsky (1958) have used the regular changes of noise at 27 kc/s, particularly near sunrise, coupled with waveguide mode theory to study solar effects in the ionospheric *D*-region. Lugeon (1939), Kimpara and Kimura (1958) and Rieker (1960) have also studied the ionospheric effects at sunrise and sunset, at 27 kc/s, and have related these effects to the locations of the sources.

Among the propagation measurements which have been made using VLF transmissions are those of Heritage, Weisbrod and Bickel at 16.6 kc/s. They were presented at a symposium in 1957 and have been compared with the mode theory by Wait (1958a). One of the comparisons is shown in Fig. 9. The general features predicted by the mode theory are confirmed, at least for an oversea path, and the general trend conforms approximately to an

† The curves were derived by Fourier analysis of waveforms of atmospherics. Taylor has recently pointed out that the values at frequencies below 6 kc/s are unreliable because they can be seriously affected by small errors in establishing the datum from which the voltage fluctuations were measured.

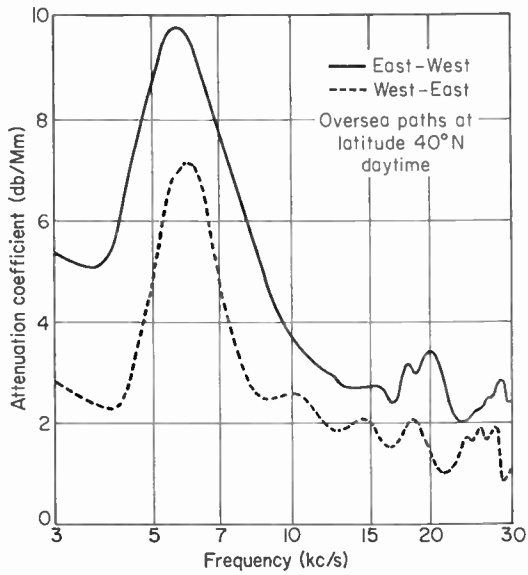


FIG. 8. Measured dependence of attenuation on direction of propagation.
(Reproduced with permission from Taylor, 1960a.)

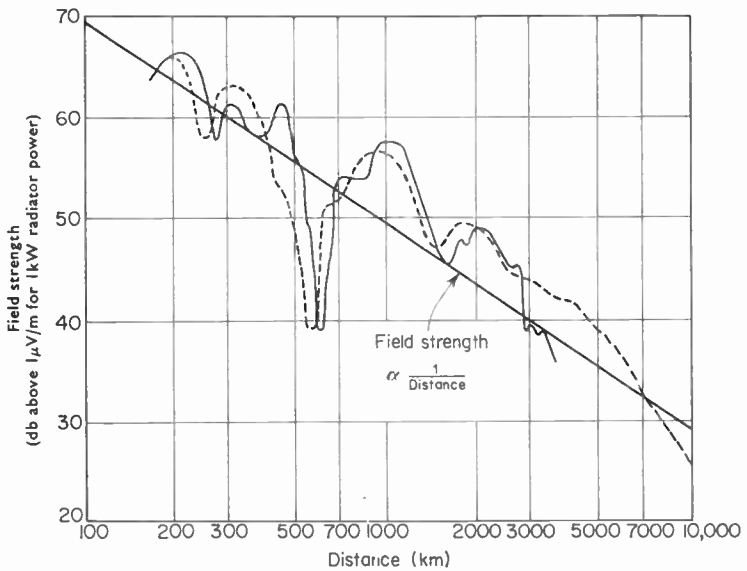


FIG. 9. Variation of field strength with distance at 16.6 kc/s.
Daytime, over sea.

—— measured
----- calculated from mode theory

(Reproduced with permission from Wait, 1958a.)

inverse distance law over a considerable range. This is a useful approximation when dealing with a diffuse source of atmospherics whose location may be changing and not accurately known.

Mode theory is especially valuable at frequencies below 10 kc/s. At higher frequencies, and particularly at short ranges, the treatment of propagation by ray theory becomes increasingly valid and often more convenient (Wait and Murphy, 1957). In his early treatment of the propagation of an atmospheric Budden (1951) showed how a series of modes could be combined to give discrete echoes corresponding to the various numbers of reflections between the earth and the ionosphere. These reflections, treated by ray theory, have been the subject of many investigations and have yielded valuable information about the effective height of reflection in the *D*-region (Rivault, 1945, 1950; Caton and Pierce, 1952; Horner and Clarke, 1955; Al'pert and Borodina, 1956; Skeib, 1957). The simplest theory assumes reflection at constant height and either 0 or 180 degrees phase change on reflection. The theory for the more realistic changes has been worked out by Wait and Murphy (1956). The range of application of geometrical optical theory can be extended by corrections at distances where the singly reflected wave becomes nearly tangential to the earth's surface (Wait, 1960c).

C. PROPAGATION AT HIGHER FREQUENCIES

Propagation at frequencies below 20 kc/s has been discussed here in some detail because much of the practical information has been derived from investigations using atmospherics, and because it is in this part of the spectrum that there have been the most notable advances in recent years. Propagation at higher frequencies has long been more fully understood from experiments using transmissions, and data are widely available. The most significant factors relevant to noise are the high absorption in the low and medium frequency ranges in daytime and the ionospheric cut-off in the high frequency range. There have been some interesting recent experiments at high frequencies providing a better understanding of the modes of propagation which are most effective over long distances (Kift, 1960). These and any further work leading to improvements in the accuracy of calculation of signal field strengths will also have applications in the assessment of noise distributions.

D. SUMMARY OF PROPAGATION RESULTS MOST RELEVANT TO NOISE

Sources of noise are geographically diffuse and variable and the energy is spread over a wide frequency range, so many of the detailed propagation phenomena which are of interest with single frequency transmissions are of little consequence in a study of the world distribution of noise. The important factor is the way in which the field strength decreases generally with increase in distance. It has been seen that energy at frequencies below 1 kc/s is propagated with low attenuation and at distances where the radiation component of field predominates, the field strength varies as $d^{-\frac{1}{2}}$. Noise may therefore be received from very distant storms, and at some locations all world sources may contribute significantly to the noise level (Holzer and

Deal, 1956). At frequencies of about 10 c/s (and at harmonics of this) according to theoretical analysis originally carried out at the end of the last century and later developed by Schumann (1952), the whole of the space between the earth and the ionosphere becomes a form of resonant cavity and enhanced noise may be expected. König (1959) and Balsler and Wagner (1960) have reported the detection of such a resonance at about 8 or 9 c/s.

The absorption band at 2–4 kc/s results in low noise levels, in the absence of local sources, but from 6 kc/s to about 20 kc/s the sources are powerful radiators and propagation is good, so long distance sources again become effective. The radiation field strength varies as d^{-1} at short ranges, where the ground wave predominates. At greater distance the variation is described by an equation of the form shown in (17) and values have been quoted for the attenuation rates. Wait (1962c) has shown that for moderate distances (up to 2000 km) over sea or ground of good conductivity the general trend of field strength with distance is rather more rapid than a d^{-2} law and the overall effect is that an inverse distance law is a reasonably good approximation for distances up to a few thousand kilometres. Beyond this range, owing to the combined effects of earth curvature and attenuation the field decreases more rapidly. However, the main equatorial thunderstorms can evidently be significant sources of VLF noise received in temperate regions and even at higher latitudes, especially at night, and the variations of noise over the world are not large. In equatorial regions especially, noise in this frequency range is more likely to be received from the west than from the east, owing to the non-reciprocal effects of the earth's magnetic field.

At frequencies above 20 kc/s, propagation follows the pattern which is known from the accumulated experience in operating communications circuits. Low and medium frequencies are propagated well at night but suffer considerable absorption by day, and this absorption leads to large diurnal changes in the noise received from distant sources. In fact at frequencies in the region of 1 Mc/s, noise from distant storms is too low to be measurable by day, except on sites unusually free from man-made noise and by using receivers with especially low internal noise. At low frequencies, additional attenuation of noise may occur at high latitudes if the path extends over ice, which has low conductivity (Watt *et al.*, 1959).

Absorption decreases again as the frequency is raised through the high frequency range, and significant noise may again be received from long distances at frequencies up to the maximum that can be propagated via the ionosphere. The varying ionospheric conditions during a solar cycle would be expected to affect the propagation of high frequency noise and particularly the cut-off frequency. In practice no marked solar cycle influences on noise levels have been observed during the intensive programme of the last few years. This point is discussed further in Section X.

VIII. CHARACTERISTICS AND MEASUREMENT OF ATMOSPHERIC NOISE

It is convenient to reserve the term atmospheric noise for the total noise from many sources as distinct from single atmospheric. Furthermore, the term has been used mainly for noise in narrow-band receivers, and it is this

aspect which is discussed here. Atmospheric noise exhibits some of the characteristics of the individual atmospheric of which it is composed; for example, at low frequencies it retains its impulsive character, as contrasted with the more continuous noise at high frequencies. Methods of measuring and describing noise must therefore be suitable for all these various types.

The complexity of atmospheric noise and of the mechanism by which it interferes with radio services has led frequently to the adoption of direct measurement of interference as a means of obtaining operational data on required signal strengths. A network of stations was in use for many years, based on a method in which a locally produced morse signal was applied to a receiver in parallel with the noise from an aerial, and adjusted in intensity until the signal was just intelligible (Thomas, 1950; Yabsley, 1950; Horner, 1953a; Harwood and Harden, 1960). The adoption of such techniques, though providing useful data for limited purposes, has led to considerable difficulty in the comparison between different sets of data, and in recent years there has been a trend towards the measurement of parameters of the noise field which can be specified precisely and in a way which is largely independent of the properties of any particular recording apparatus.

The parameter now widely adopted for describing the general intensity of the noise is the mean power, averaged over some specified period of the order of a few minutes to an hour (Crichlow, 1957; URSI, 1962). This parameter may be used to describe the variations of the noise over longer periods such as a day or a year. The average field strength has also been used extensively because it can be more easily measured than can the noise power (Sullivan *et al.*, 1952; Harwood, 1958), and a quasi-peak value is often favoured because it shows some correlation with the interference to a sound-broadcasting service. All parameters other than the noise power, however, suffer from the disadvantage that they vary with the bandwidth in a manner dependent on the type of noise, while the noise power is always, for practical purposes, proportional to bandwidth.

Within the period of a few minutes over which the mean value of the noise power is often taken, there are short-term changes, and these have been referred to as the structure of the noise. These amplitude fluctuations may be described partially by using the amplitude probability distribution (APD) which, in its cumulative form, shows the fraction of the time for which the noise exceeds a series of amplitudes; it is usually the envelope waveform which is so described rather than the instantaneous field. The APD is not a complete description since, for example, it does not differentiate between a large number of short pulses and a small number of long ones. Various other parameters have been used to describe the structure. At low frequencies, where the noise consists largely of discrete pulses, a distribution of the amplitudes of these pulses is useful, but even this does not show whether the pulses occur at random or in groups. At high frequencies where the noise resembles bursts of more-or-less continuous noise, the lengths of the bursts and of the intervals between them have been studied.

Whatever parameter is adopted, the apparatus must be designed with considerable care, bearing in mind the impulsive nature of the noise. Some

of the general principles of design have been discussed by Dinger and Paine (1947) in relation to the quasi-peak method of measurement. The apparatus must be calibrated for gain and bandwidth, and the aerial characteristics must be known. Calibration is usually effected by means of a signal generator, and the amplitude is then expressed in terms of an equivalent CW signal, but alternatively a noise generator can be used. In France, equipment has been calibrated by applying a short pulse, by discharging a condenser from a known voltage and through a known resistance. This technique was used only at low frequencies and was based on the philosophy that the calibration is achieved with a pulse similar to the short pulse from an atmospheric; the calibrating signal and the atmospheric are then influenced to a similar extent by changes in bandwidth and this need not be specified. The noise is measured as an equivalent value of $\int e(t)dt$ of the calibration impulse or more commonly by the equivalent changes of magnetic flux of the incident field (Carbenay, 1956).

In the following discussion of amplitudes it is convenient to refer to voltages rather than to field strengths, the voltage being that at some point in the receiver following the selective circuits. This voltage is assumed to be proportional to the equivalent field strength from which it is derived unless otherwise stated.

Noise measurements can be facilitated by the use of magnetic tape recording, since this enables noise to be recorded in one place and examined in another, where there may be more comprehensive apparatus. Other advantages are that the noise sample can be preserved indefinitely, that it can be replayed repeatedly while its characteristics are studied, and that it can be used to observe directly its effects on a radio system. Tape-recording was used first at frequencies below 10 kc/s, which could be recorded directly at tape speeds commonly available (Chapman and Macario, 1956), and then extended to higher frequencies by frequency-changing methods (Horner and Clarke, 1958). Clarke (1960a) has shown that the characteristics of the noise can be accurately preserved.

A. METHODS OF SPECIFYING AND MEASURING NOISE POWER

Several parameters of noise are directly related to the mean noise power. The one most commonly used for describing the intensity of atmospheric noise is the effective noise factor F_a of an equivalent loss-free aerial, related to some arbitrary temperature. The available power from the aerial is $F_a k T_0 B$, where k is Boltzmann's constant (1.38×10^{-23} J/°K), T_0 is the reference temperature, usually taken as 290°K, and B is the power bandwidth in c/s as defined in Section IV. Alternatively, an effective aerial temperature T_{eff} can be quoted, equal to $F_a T_0$; this parameter is widely used in radio astronomy, but not for atmospheric noise. Both noise factor and effective temperature are independent of bandwidth if this is small compared with the centre frequency. A further method of specifying noise power is by the flux density of the field, and this is often useful when considering the power from a distant, localized source. The power flux for one component E (r.m.s. value in $\mu\text{V/m}$) of polarization of a field is $E^2/120\pi \mu\text{W/m}^2$. The

equivalent loss-free aerial which has been selected for reference in recent presentations of noise data is a vertical monopole, short compared with the wavelength, over a highly conducting earth. This is in effect a way of specifying a particular polar diagram and the component of field to which the aerial responds, the two characteristics which determine the noise factor in a given ambient field. Aerials used for communications, particularly at high frequencies, normally have some directivity at least in the horizontal plane, but in general surveys of the distribution of noise it has been considered undesirable to introduce the additional complications of directional aerials. The effects of directivity can be considered as a separate problem which is discussed in a later section. The noise factor is usually expressed in decibels F_a relative to kT_0B . For a short vertical aerial, F_a is related to the field strength E (in db above $1 \mu\text{V/m}$) by

$$F_a = E + 155.5 - 20 \log_{10} f - 10 \log_{10} B \quad (18)$$

where the frequency f is in kc/s and B is in c/s.

A typical noise-measuring installation consists of an aerial system of known characteristics (usually a vertical monopole over a ground mat), a receiver with a known bandwidth, means for measuring one or more selected parameters of the receiver output, and a calibration system (URSI, 1962). For noise power measurements, the receiver output, usually at an intermediate frequency, is first squared, and the squared voltage is averaged over some specified time interval. Equipment for this purpose, designed at the Central Radio Propagation Laboratory, U.S.A., embodies these features and will be described in some detail as an example. Only the noise power measurements are described here; the recording of other parameters which can also be done with the same equipment will be discussed in later sections.

The CRPL equipment is designed to record noise power automatically on eight frequencies in the range 13 kc/s to 20 Mc/s (Crichlow, 1957; URSI, 1962). The frequencies are sampled two at a time for 15 min, a complete cycle thus occupying an hour. A small bandwidth (200 c/s) is used to take advantage of narrow clear channels between station transmissions. A block diagram showing the essential features of one channel, but omitting the control circuits for changing frequency and for making the action automatic, is shown in Fig. 10. The aerial is a vertical monopole over a network of radial wires. Calibration signals can be applied to the aerial terminals from a noise generator, through a dummy aerial (one for each frequency), or a CW signal can be coupled capacitively to the aerial from an auxiliary stub aerial. The CW oscillator and noise generator can be compared, as shown by the broken line connection, and the combined facility enables the recorder to be calibrated either including or excluding the aerial. Frequent checks are made to ensure that the two calibrations are correctly related. The basic principle of the recorder is that the input to the voltage squaring and detecting circuits is maintained substantially constant, so that these can be designed to give optimum performance. A stepped-attenuator is interposed between the RF unit and the squaring circuit, and is controlled by the smoothed output from the second detector to give a constant mean power to

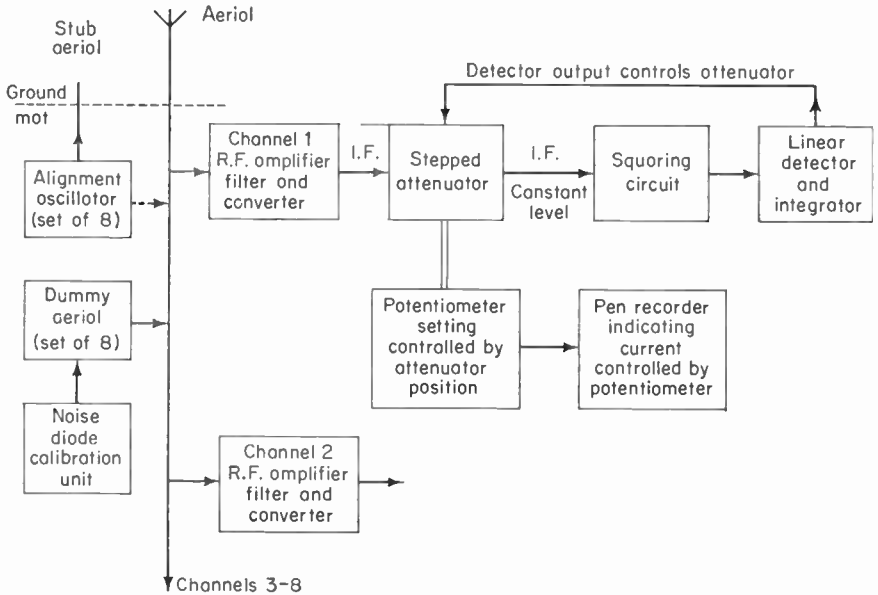


FIG. 10. Schematic diagram of CRPL noise recorder.

this section. The output of the IF section is squared and the mean squared voltage applied to the detector is thus proportional to the mean power. If this varies by more than 1 db, the attenuator is caused to change by 2 db in a direction tending to restore its output to the correct level. The attenuator position is thus a measure of the noise power, and by means of a potentiometer the position is recorded on a pen chart, on a scale which is linear in decibels.

The attenuator has a range of 100 db. The output voltage of the squaring circuit is proportional to the square of the input voltage within 1 db for an input range of 1000 (60 db). The detector, however, is not linear over the corresponding output voltage range of 10^6 , and so is the limiting factor. By careful design it has been made linear over a range of 10^4 in voltage (80 db) and mean noise powers are correctly recorded if the instantaneous input power does not fluctuate outside the limits -10 to 30 db relative to the mean value. This performance is adequate for all conditions except possibly for low frequency observations during local storms (see Section VIII, D, and Clarke, 1962). The squaring circuit is a two-valve amplifier with the control grids excited in phase opposition and the anodes connected together. The transfer characteristic has an approximately parabolic shape. At the output, taken between the anodes and the earth, the component with twice the frequency of the input signal has an amplitude proportional to the square of the input voltage, and this component is selected by means of filters. The use of a push-pull circuit facilitates the filtering, since the output at the fundamental frequency is intrinsically low. The detector unit incor-

porates a peak detector and a power amplifier capable of linear amplification at high voltages. Feedback from the diode-cathode circuit to the amplifier stage is used to improve the linearity at low voltages, and the transfer characteristic is linear within 1 db between input limits of 0.1 to 1000 V. The special features which make the equipment suitable for automatic noise measurements are the gain and frequency stability, the high selectivity of the tuned circuits, the ability to operate in the desired manner with noise having a wide range of mean power levels and having instantaneous values fluctuating between wide limits, and the comprehensive calibration facilities.

Another approach to the measurement of noise power is to use a thermojunction which delivers an output voltage proportional to the input power. Although this method is simple in principle there are difficulties in preserving stability, as thermojunctions are sensitive to ambient temperature changes and the environment must be carefully controlled. As with the parabolic amplifier technique, the thermojunction is best used as a component in a feed-back circuit which enables it to be operated with a constant input (Carbenay, 1959).

A third method of deducing power is from the amplitude probability distribution (APD) discussed in a later section (Horner and Harwood, 1956). The APD, in its cumulative form, shows the fraction of the time $Q(e)$ (occupation time) for which the noise envelope exceeds a series of voltages e , and the mean square envelope voltage is $2\int eQ(e)de$ which can be determined from the APD by numerical integration. This method, though somewhat slow, has the advantage that occupation time can be determined at any voltage by methods which are independent of whether there is amplitude limitation at voltages much higher than e . In other words, small amplitude ranges can be studied independently in equipment having small dynamic range, provided that the circuits are so designed that the reception of high amplitude pulses does not produce transient changes in the gain.

Comparisons have been made in Singapore and Ibadan (Nigeria) between values of noise power recorded with CRPL equipment, and using the above APD technique, as developed at the Radio Research Station, England. At low and medium frequencies there was close agreement between the two results, the CRPL values being on the average about 1 db higher. At high frequencies, however, the discrepancy was greater, the average CRPL value being about 4 db higher at 10 Mc/s. The reason for the differences have not been discovered, but the CRPL values are known to be affected, on occasion by interference from transmitters. Uncertainties in the aerial characteristics of one or both equipments may also contribute to the differences. In the absence of a satisfactory explanation of the discrepancies, it appears that the accuracy of the measurements by either method may be assumed to be better than 1 db at low frequencies but no better than 2-3 db at high frequencies.

Studies have been made of the relationship between noise power and other parameters. As a result it is possible to derive approximate values of noise power from other types of data and, although the relationships are time dependent, in a way which is partly systematic and partly random, the

derivation of values in this way is worthwhile when there is no direct measurement of the power itself. Some of the relationships are quoted in the appropriate sections.

B. AVERAGE ENVELOPE VOLTAGE

Measurements of average envelope voltage are somewhat easier than those of noise power and have been made over a much longer period. The equipment required is broadly the same as for noise power but without the squaring circuit. The CRPL equipment incorporates an average voltage unit in which a linear detector is connected directly to the output of the IF amplifier. Since this output is maintained at a constant power level by means of the feedback loop, the unit effectively records the ratio of the average to the r.m.s. voltage. However, the dynamic range requirements of an average-voltage recorder are not so stringent as those for noise power, and satisfactory measurements have been made simply by recording the output of the detector of a receiver of conventional design (Sullivan *et al.*, 1952; Kamada and Nakajima, 1954; Horner and Harwood, 1956; Clarke, 1960b). The average voltage can also be derived by numerical integration of an APD since it is equal to $\int Q(e)de$.

With impulsive noise the power or r.m.s. voltage is largely determined by the noise peaks, while the average voltage depends more on the lower-amplitude but more continuous background. The ratio of the two parameters is therefore a useful indication of the type of noise. Typical median values for temperate latitudes are given in Table IV (Clarke, 1962).

TABLE IV. *Typical Ratios of r.m.s. to Average Envelope Voltage (Power bandwidth 370 c/s)*

Frequency	Ratio (db)
24 kc/s	10
135 kc/s	5-8
11 Mc/s	4
20 Mc/s	2

The range shown for 135 kc/s covers seasonal variations, which are small at other frequencies. There are systematic diurnal variations of about ± 2 db at the two low frequencies, with occasional very high values which presumably relate to local storm conditions.

A large number of measurements of average noise voltage have been made in South Africa by the National Institute for Telecommunications Research. The NITR recorder operated at 100 kc/s and had an effective bandwidth of 6 kc/s. A linear detector was used and an AGC voltage was taken as a measure of the noise (Hogg, 1950, 1955). Records from this instrument were used in an investigation of the behaviour, in noise, of various radio

aids to navigation. Recent unpublished comparisons between data recorded simultaneously by the NITR and CRPL instruments indicate that the NITR values at 100 kc/s may be converted to F_a values by adding 90 db.

C. AVERAGE LOGARITHM OF THE VOLTAGE

The average of the envelope voltage when this voltage is expressed in logarithmic units (e.g. decibels) is another parameter which has been measured. The CRPL equipment described in Section VIII, A, sometimes has associated facilities for measuring this quantity by incorporating a logarithmic amplifier. As with the average voltage, the mean logarithmic voltage is then measured as a deviation from the logarithm of the r.m.s. voltage by performing the measurement on the stabilized output from the IF amplifier. These measurements were introduced into the CRPL programme to provide additional information on the noise structure, as discussed in the next section. Some measurements in Canada at LF and VLF have also been based on the logarithmic parameter (McKerrow, 1957).

D. AMPLITUDE PROBABILITY DISTRIBUTION (APD)

The interference caused by noise is not solely a function of the noise power since the interference from highly impulsive noise may be quite different from that of more continuous noise of the same mean power, depending on the type of service. A description of the noise sufficiently complete to enable the interference to all types of service to be assessed would involve many parameters, but a knowledge of the amplitude probability distribution (APD) satisfies some requirements. This approach was adopted by Hoff and Johnson (1952) following suggestions made many years earlier and has now been used by many investigators (Horner and Harwood, 1956; Lichter, 1956; Yuhara *et al.*, 1956; Watt and Maxwell, 1957b; Harwood, 1958; Nakai, 1958, 1959, 1960; Lichter and Terina, 1960; Clarke, 1960b, 1962; Nakai and Suzuki, 1961). As stated earlier, it is usually the APD of the envelope voltage e , which is quoted. The form of the APD depends on the bandwidth, except for fluctuation noise, which has a Rayleigh probability distribution, given by

$$Q(e) = \exp(-e^2/e_{ms}^2) \quad (19)$$

where e_{ms} is the mean square value of e .

Typical APD curves of noise for a bandwidth of 300 c/s are shown in Fig. 11, plotted on "Rayleigh paper" on which the coordinate system is such that fluctuation noise is represented by a straight line, shown broken, having a particular slope. Atmospheric noise has a distribution resembling that of fluctuation noise at low amplitudes, but the distributions diverge at the higher voltage levels to an extent which increases with the impulsiveness of the noise. The contrast between impulsive noise at low frequencies and more continuous noise at high frequencies is evident. Reducing the bandwidth has the effect of broadening the peaks and reducing their amplitude and as they become more and more superimposed on each other the noise becomes more similar to fluctuation noise. This is shown in Fig. 12, taken

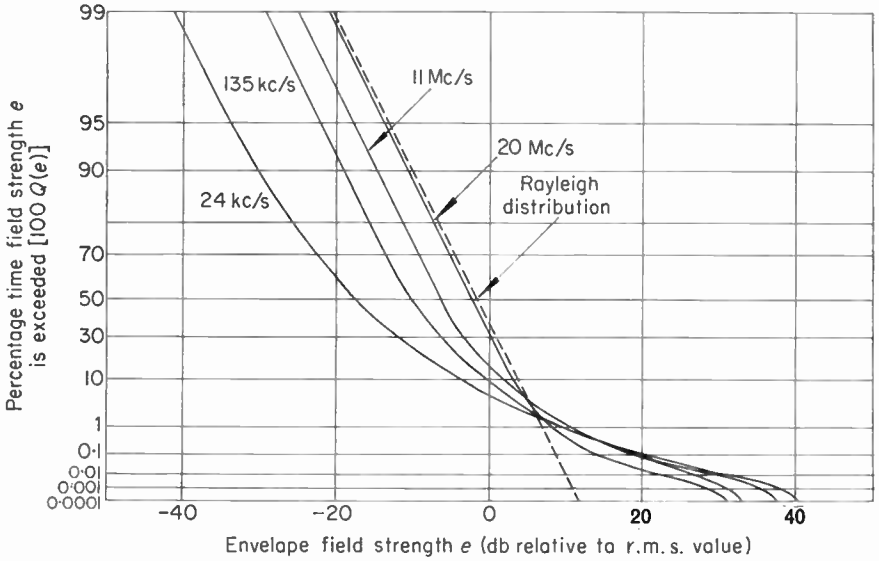


FIG. 11. Typical amplitude probability distributions. (Rayleigh coordinates.)
(Reproduced with permission from Clarke, 1962.)

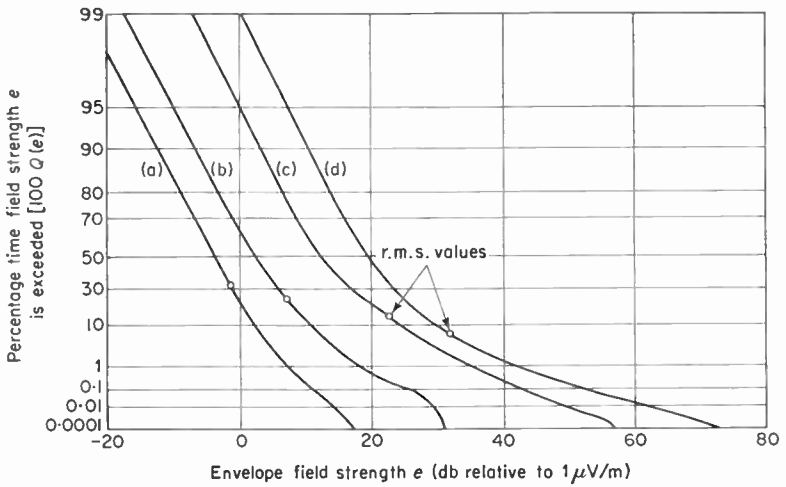


FIG. 12. Variation of APD with bandwidth at a frequency of 22 kc/s.
(Rayleigh coordinates.)

Bandwidths, c/s.

- (a) 0.64
- (b) 6
- (c) 170
- (d) 1100

(Reproduced with permission from Watt and Maxwell, 1957b.)

from Watt and Maxwell (1957b). The r.m.s. value for each curve is marked. From both Fig. 11 and Fig. 12 it is seen that there can be significant fluctuations exceeding the r.m.s. value by 30 db or more even in a bandwidth of only 300 c/s. At times, therefore, a detector which limits at 30 db above the r.m.s. level, as in the CRPL recorder, can have small negative errors, as mentioned previously. This is unlikely to happen, however, except at low frequencies. Any one point on an APD can be regarded as representing another single parameter, the occupation time. Some measurements have been confined to the occupation time at some stated threshold.

The general shape of the APD changes markedly with frequency as shown in Fig. 11. The r.m.s. values at different frequencies, for one particular bandwidth, correspond approximately with the occupation times shown in Table V (Clarke, 1962).

TABLE V. *Occupation Times Corresponding with r.m.s. Level (Bandwidth 370 c/s)*

Frequency	Occupation time
24 kc/s	5%
135 kc/s	9%
11 Mc/s	15%
20 Mc/s	30%

These data are for England but similar values have been found in other parts of the world. The value for fluctuation noise is 36.8 per cent.

The APD has been measured by several related but different methods. The first method, adopted at the University of Florida, was to select a section of the waveform, between two closely-spaced amplitude levels, as shown shaded in Fig. 13a, the lower limit being set by a threshold and the upper one by amplitude limitation (Hoff and Johnson, 1952). The result is a series of pulses of constant and known amplitude and with a combined length over any period equal to the time of occupation. If these pulses are passed through an averaging circuit with any desired time-constant, a continuous record of the time of occupation is obtained. Equipment based on this principle and designed at the University of Florida recorded the time of occupation automatically at four threshold levels, and it was shown that for the low frequencies considered a reasonable approximation to the whole APD could be obtained by suitable choice of these levels and smooth interpolation between them. This general technique has also been used in Japan (Nakai, 1958) and the U.S.S.R. (Lichter, 1956).

A slightly different approach was adopted by Horner and Harwood (1956) in England. Part of the envelope waveform shown shaded in figure was selected by introducing a threshold, and the average value of the part above the threshold was taken. The cumulative APD was derived by numerical

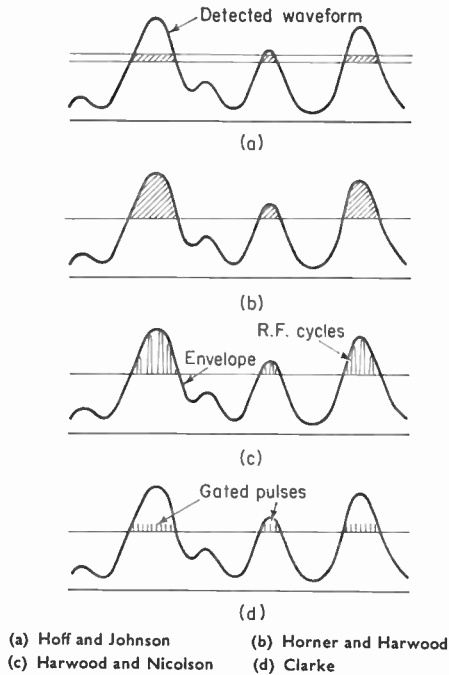


FIG. 13. Techniques for APD recording.

differentiation of the curve relating the average value to the threshold, since

$$Q(e) = \frac{dA_e}{de} \quad (20)$$

where A_e is the average of the voltage measured above the threshold e taken as the zero. This technique was used to obtain the APD automatically by varying the threshold in steps and recording the average voltage above each threshold on a pen recorder. Later an alternative method was used (Harwood and Nicolson, 1958), also at low frequencies. The portion of the undetected waveform above a threshold was selected and the resulting r.f. pulses counted for a fixed interval (Fig. 13c). The ratio of the count to the product of the interval times the frequency was the occupation time. To delineate the whole curve, the threshold was maintained constant and the noise amplified to a greater or lesser extent. The method had the advantage that the measurement of occupation time at any threshold was unaffected by any distortion of the waveform at higher levels due to amplitude limitation. A further modification was introduced at high frequencies, by Clarke (1960c), who detected the waveform and used the parts above the threshold to gate a series of pulses (10 000/sec) from an oscillator, which were then counted (Fig. 13d). A programme based on this technique was undertaken during the International Geophysical Year (Clarke, 1962).

To avoid the necessity for specifying the APD either by a curve or by listing the occupation times for a series of amplitudes, many attempts have been made to fit a mathematical formula to the curves and so to describe these by a small number of parameters (preferably not more than three). Sullivan and his co-workers in the University of Florida found that the distribution at low frequencies was approximately log-normal and could thus be expressed as

$$Q(e) = \frac{1}{\sigma_e \sqrt{2\pi}} \int_e^{\infty} \frac{1}{x} \exp \left[-\frac{(\ln x - \ln e_m)^2}{2\sigma_e^2} \right] dx \tag{21}$$

This distribution is defined by only two parameters, e_m , the median value of e , and σ_e , the standard deviation of $\ln e$. The average value of e is then $e_m \exp(\frac{1}{2}\sigma_e^2)$ and the r.m.s. value $e_m \exp(\sigma_e^2)$.

Theoretical justification for a log-normal distribution is lacking, although it has been shown that it could result from the product of a large number of independent variables (Foldes, 1960). The formula becomes less appropriate as the frequency is raised and the noise becomes more similar to fluctuation noise which has a Rayleigh-distributed envelope. Representations suitable for all frequencies have been sought by combining a Rayleigh distribution at low amplitudes with non-Rayleigh distributions representing the discrete pulses at high amplitudes. In Japan, plots have been made in coordinates in which a log-normal distribution is a straight line; the high amplitude part of the distribution is then linear and the lower amplitude part lies on a known curve representing a Rayleigh distribution (Yuhara *et al.*, 1956). An example is shown in Fig. 14 and it can be seen that three parameters are involved, which for instance could be the value of $Q(e)$ for a specified high value of e , the slope of the log-normal part of the plot, and the value of e at which the change to a Rayleigh distribution takes place. Other work in Japan has also shown that the distributions can be interpreted as fluctuation noise with the addition of peaks with a log-normal amplitude distribution (Nakai, 1960).

Horner and Harwood (1956) showed that at low frequencies the function $Q(e)/[1 - Q(e)]$ gave nearly a straight line when plotted against e , both in logarithmic units, from which Harwood (1958) deduced an approximate relationship

$$Q(e) = [1 + (2e/e_{av})^q]^{-1} \tag{22}$$

depending on two parameters, the average value e_{av} and an index q . An example is shown in Fig. 15. In Japan a better fit was obtained at 50 kc/s by replacing the factor 2 by 2.7 (Nakai, 1959), while Lichter and Terina (1960) in the U.S.S.R. found a satisfactory fit by using the form

$$Q(e) = [1 + (e/e_m)^q]^{-1} \tag{23}$$

which has the correct median value e_m .

A drawback in the use of these formulae is that the expression for the mean square value of e (corresponding with noise power) becomes infinite

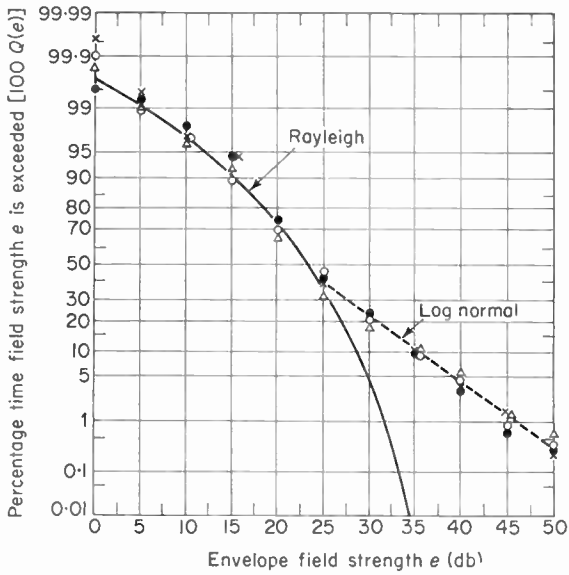


FIG. 14. Amplitude probability distribution at 3.5 Mc/s.
(Log-normal coordinates.)
Bandwidth, 1600 c/s.

(Reproduced with permission from Yuhara *et al.* 1956.)

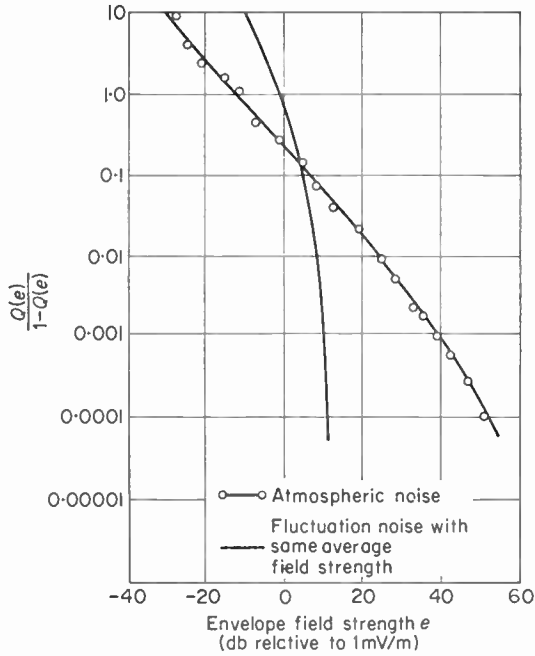


FIG. 15. Amplitude probability distribution at 10 kc/s.
(Logarithmic coordinates.)
Bandwidth, 300 c/s.

(Reproduced with permission from Horner and Harwood, 1956.)

if $q < 2$, which it usually is at low frequencies. In order to keep the power finite, therefore, an upper limit to the distribution must be specified, which introduces a third parameter.

Clarke (1960) has proposed for high frequencies an empirical formula, for a bandwidth of 400 c/s

$$Q(e) = \exp(-y^2) \tag{24}$$

where
$$\frac{e}{e_{r.m.s.}} = y + \left(\frac{e_{r.m.s.}}{e_{av}} - 1.13 \right) y^{3.5} \tag{25}$$

This specifies a Rayleigh distribution of y , which is equal to $\frac{e}{e_{r.m.s.}}$ if it is small or if the noise is of fluctuation type for which the expression in brackets in (25) is zero. For large values of y (or e) the plot (on Rayleigh paper) is a straight line at a slope defined by the index 3.5, which was found empirically to give the best fit with experimental results at 11 Mc/s. If this index were constant universally, the distribution could be represented by two variable parameters, but since the index will vary with frequency and bandwidth, three parameters are required for more general application.

Fulton (1961) has used four parameters to define the distribution. This procedure again starts with a Rayleigh distribution of a parameter y , as in equation (24), but y is related to e by the equation

$$e = a_1 y + a_2 y^{4(b+1)} + a_3 y^b \tag{26}$$

Lichter (1956) proposed a formula

$$Q(e) = (1 - c) \exp(-ae^2) + c \exp(-be^2) \tag{27}$$

The use of a mathematical formula to represent the distribution is justified only if it is simple, defined by very few parameters, satisfactory over a wide frequency range and if well-known quantities such as e_{av} and $e_{r.m.s.}$ are either used at the parameters or can be easily derived. It is also desirable that it should have some logical physical basis. None of the proposals so far entirely meets these requirements and a graphical means of presentation is perhaps still the most satisfactory. Crichlow *et al.* (1960a) showed that if three parameters, the r.m.s., average, and mean logarithmic voltages are known, a close approximation to the distribution curve can be constructed by a graphical process. The assumptions made are that, when plotted on Rayleigh paper, the APD may be represented by two straight lines, at high and low amplitudes, joined by an arc of a circle in the intermediate range. A series of idealized curves based on the three parameters has been published (Crichlow *et al.*, 1960b). It was later stated that for a given mean noise power the average and mean logarithmic voltages are closely correlated, even when the bandwidth is changed over wide limits (Spaulding *et al.*, 1962). This enables the APD to be constructed from only two basic parameters, the r.m.s. and average voltages being the most convenient. Families of idealized curves were drawn to which, it is claimed, any practical curve can be fitted

from a knowledge of V_d , the ratio of r.m.s. to average voltages (in db). Figure 16 shows a selection from their curves. It can be verified that these curves are in reasonable agreement with the figures given in Tables IV and V. For example, if the curves on Fig. 16 are identified by the occupation times corresponding to the r.m.s. level, from Table V, the derived values of V_d are, for the four frequencies, 10, 6, $3\frac{1}{2}$ and $1\frac{1}{2}$ db respectively, which are

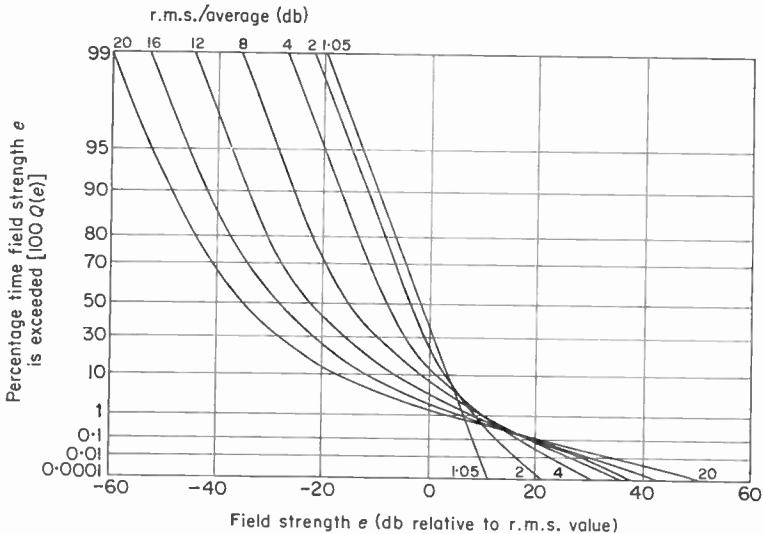


FIG. 16. Idealized APD curves. (Rayleigh coordinates.)
(Redrawn with permission from Spaulding *et al.*, 1962.)

similar to those in Table IV. The curves are slightly unrealistic, however, in that experimental distributions are often limited rather more abruptly at the high voltage end, as can be seen from Fig. 11, and the probabilities of very high voltages are therefore somewhat less than indicated by the idealized curves of Fig. 16.

It has been stated that the shape of the APD is dependent on the bandwidth, a decrease in bandwidth tending to make the noise more similar to fluctuation noise. It is possible to modify an APD to take account of bandwidth changes. Harwood (1958) and Fulton (1961) both discussed the modifications to the high amplitude, low probability part of the curve on the assumption that the noise was in the form of discrete pulses, with a shape determined only by the bandwidth. Spaulding *et al.* (1962) have discussed the implications of bandwidth changes on the whole curve. If it is assumed that the APD always fits one of the family shown in Fig. 16, the problem is one of determining how the value of V_d changes with the bandwidth. The relationship is complex, but can be represented by the family of curves shown in Fig. 17. These show corresponding values V_{dw} and V_{dn} for wider and narrower bandwidths B_w and B_n respectively, as a function of B_w/B_n .

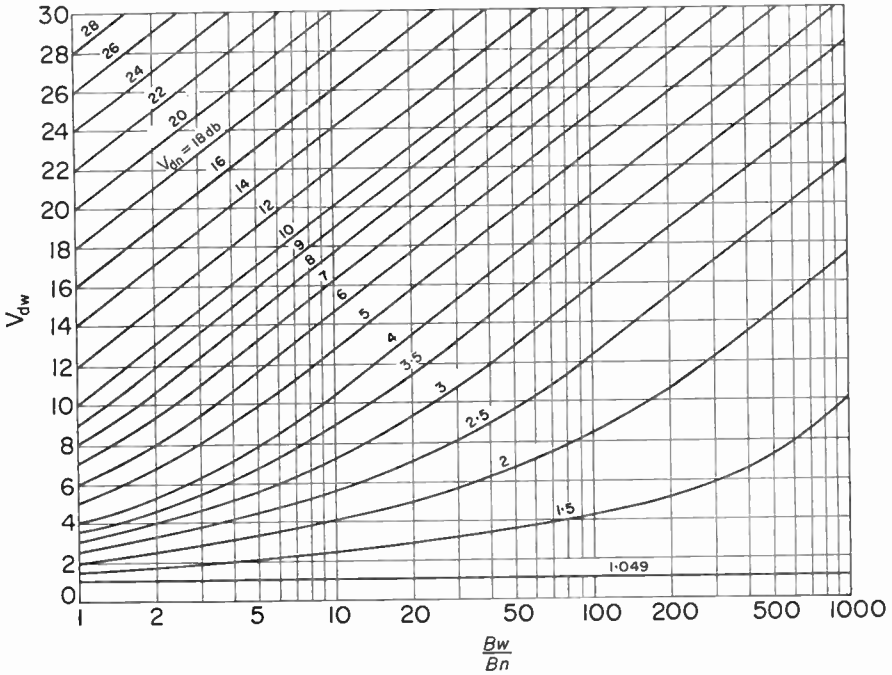


FIG. 17. Dependence of r.m.s./average ratio on bandwidth. (Reproduced with permission from Spaulding *et al.*, 1962.)

The idealized curves of Fig. 16 and the technique for bandwidth conversion result in approximations to the APD which are convenient because they can be specified with very few parameters. Insufficient comparisons with experimental results have yet been made to indicate what errors may be involved in the use of the idealized presentation, but in view of the variations which occur in the structure of noise, even at one location and frequency and at a given time of day the method will be justified if the voltage corresponding to any given occupation time can be related to the r.m.s. voltage with an error of no more than one or two decibels.

E. ENVELOPE CROSSING RATE

One of the characteristics of noise which has long been of interest is the rate at which atmospherics occur. In the early days, figures were often quoted without reference to their amplitudes, and this is done even in some recent work in which the rates have been used only as a general indication of changes in noise intensity (Chiplonkar *et al.*, 1958). In more quantitative experiments the number exceeding a given peak amplitude e_p has been related to e_p . It has been shown that the distribution at low frequencies at least, approximates to a power law of the form

$$N = C e_p^{-z} \tag{28}$$

with C and z constant for any small sample of noise (Horner, 1954). This formula is most meaningful at low frequencies where the noise is impulsive, although it is not always made clear in reports whether the number refers to atmospheric discharges, or to separate pulses of which several may be contained in one atmospheric. For whole atmospheric discharges a value of z of 1.3 has been quoted for narrow bandwidths at 10 kc/s, recorded in England (Horner, 1954), while later records of individual pulses showed that z varied with time of day and with season but was usually in the range 1.1 to 1.4 (Harwood, 1958). When dealing with atmospheric noise in general, the separate atmospheric discharges cannot be distinguished and it is the pulse rate which is significant rather than the number of atmospheric discharges. The relationship

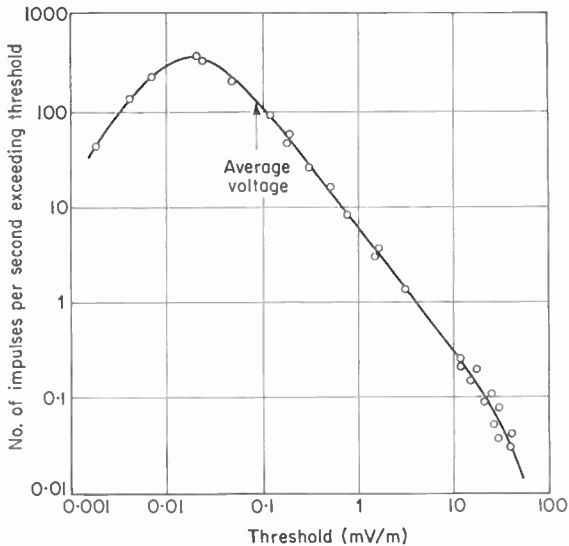


FIG. 18. Crossing-rate data for 10 kc/s, bandwidth 300 c/s. (Reproduced with permission from Harwood, 1958.)

shown is valid only for the stronger and more discrete atmospheric discharges. The smaller and more numerous pulses tend to overlap and the concept of the number of atmospheric discharges, or even of pulses, ceases to be useful. However, a parameter known as the envelope crossing rate may be used; this is the number of occasions, in unit time, on which the envelope crosses a specified threshold in a positive-going direction. A typical crossing-rate curve for low frequencies is shown in Fig. 18, which illustrates the power law distribution at high amplitudes and also shows that the rate passes through a maximum, which is approximately equal to the bandwidth. The crossing rate must necessarily be zero at zero amplitude if the noise is continuous. At the highest amplitudes the distribution falls somewhat below the extrapolated power law curve.

Harwood (1958) has shown that at very low frequencies (10–30 kc/s) the slope of the crossing rate curve can be related to that of the APD and he has

investigated the effects of changing the bandwidth. He also demonstrated the empirical relationship that for a bandwidth of 300 c/s a threshold equal to seven times the average voltage was exceeded by 10 pulses/sec. Since he also showed that the r.m.s./average ratio of the envelope was about six, this implies that the r.m.s. voltage was exceeded by about 10 pulses/sec or that the constant C in equation (28) was $10 e_{r.m.s.}^2$. Thus the crossing rate can be expressed in terms of the r.m.s. voltage or noise power, but the relationship would be different at other frequencies or bandwidths. At high frequencies the crossing rate can still be measured, but is less useful because the noise is a random superposition of very many pulses. If at a given threshold e there are N crossings/sec and from the APD the probability of e being exceeded is $Q(e)$, the average duration of a pulse at this threshold is $Q(e)/N$ sec. The actual durations will, however, vary widely (see Section VIII, H).

F. QUASI-PEAK AMPLITUDE

A parameter which is widely used, particularly by those who study man-made noise, is the quasi-peak voltage. This is a quantity obtained when the noise is passed through a detector circuit with short charge and long discharge time constants, often about 10 msec and 500 msec respectively (Dinger and Paine, 1947). Readings weighted in this way are regarded as a good indication of the nuisance value of the noise in sound broadcasting services (Thomas and Burgess, 1947). Because the quasi-peak value is not solely an amplitude function of the noise waveform, but depends also on the time sequence of the fluctuations, it is difficult to relate it to the parameters already discussed. For example, it cannot be derived from the APD, as can the average or r.m.s. value of the noise. It is perhaps most closely related to the envelope crossing rate, since it may be expected to correspond approximately with the peak amplitudes of pulses which occur at intervals of the order of the discharge time constant, for example, 2/sec with the usual time constant of 500 msec. At low frequencies this rate occurs at a threshold about 10 db above the r.m.s. value when the bandwidth is 300 c/s.

A method of noise measurement which has been developed by Aiya (1954) is based on the quasi-peak reading with the time constants quoted above. In this method the recorded parameter is the average of the ten largest impulses per minute. The equipment is calibrated in a way which includes the effect of the audio stages, using a signal modulated 30 per cent by a 400 c/s tone. It is evident that no unique relationship between this quasi-peak reading and the mean noise power can exist, but Aiya (1959) has stated that the r.m.s. field during a single atmospheric is equal to 0.37 times his parameter over the range 2.5 to 20 Mc/s. This relationship is based on the assumption that the atmospheric is a burst of fluctuation or thermal-type noise. The observed ten atmospherics in a minute, if each of duration 200 msec, would give a long-term r.m.s. noise field of about 0.07 times the Aiya parameter, if all smaller atmospherics were neglected. Simultaneous measurements of both parameters would be desirable to check this relationship.

G. SLIDEBACK PEAK AMPLITUDE

Another form of peak amplitude which may be measured is that obtained by reducing the gain of a receiver until the largest pulse in the output, in a specified time, just fails to exceed some arbitrary threshold. This value will normally be greater than the quasi-peak value discussed above. The parameter has been found useful in investigations of man-made noise, which tends to be periodic and some commercial noise meters are designed to measure it. However, its usefulness for atmospheric noise is severely limited because the reading is obviously dependent on the length of time over which the measurement is made. For usual times of observation the slideback peak values are likely to correspond approximately to the field strengths exceeded by 1 impulse in 100 sec, in crossing rate curves similar to Fig. 18.

H. TIME FUNCTIONS

The parameters discussed so far refer almost solely to amplitudes, although at low frequencies the crossing rate gives the number of pulses and, in conjunction with the APD, their average duration and the average duration of the intervals between them. More information than this may be required, for example whether the pulses at low frequencies occur at random with time (a Poisson distribution if the rate of occurrence is small) or arrive in groups. The statistical distributions of the pulse lengths and intervals are therefore useful additional data. At high frequencies the noise is in bursts; the lengths of these bursts and of the intervals between them is of practical significance, and can be described statistically.

Few studies of the statistical time distributions have been made. Watt and Maxwell (1957b) have measured the distribution of time intervals between pulses in a bandwidth of 1170 c/s at 22 kc/s, with the results shown in Fig. 19. Distributions are shown for three threshold levels. It can be seen that at the highest threshold, 1 mV/m, nearly all the intervals exceeded 10 msec, while this interval rarely occurred at the 10 μ V/m level. A typical r.m.s. value at this frequency would be about 100 μ V/m. The upper curve shows a tendency for the separations of the largest pulses (> 1 mV/m) to be more frequently in the range 10–40 msec than would be so with a random distribution, perhaps resulting from the occurrence of multiple discharges with this order of separation between strokes. Nakai and Suzuki (1961) have recorded the distributions of both pulse durations and intervals between them, at 50 kc/s. Unfortunately, the threshold levels for which the time distributions have been published have not been related to the mean noise power at the time, and it is difficult to differentiate between changes in the noise structure and changes in the absolute level.

Clarke (1960c) has obtained the data shown in Fig. 20 for the duration of noise bursts in a bandwidth of 300 c/s at 11 Mc/s, again at three threshold levels. The definition of a burst is to some extent arbitrary and, in this work the duration was taken as the longest time for which the noise envelope was almost continuously above the given threshold level, an allowance of up to 5 per cent in the time being made for the small breaks in noise which occur

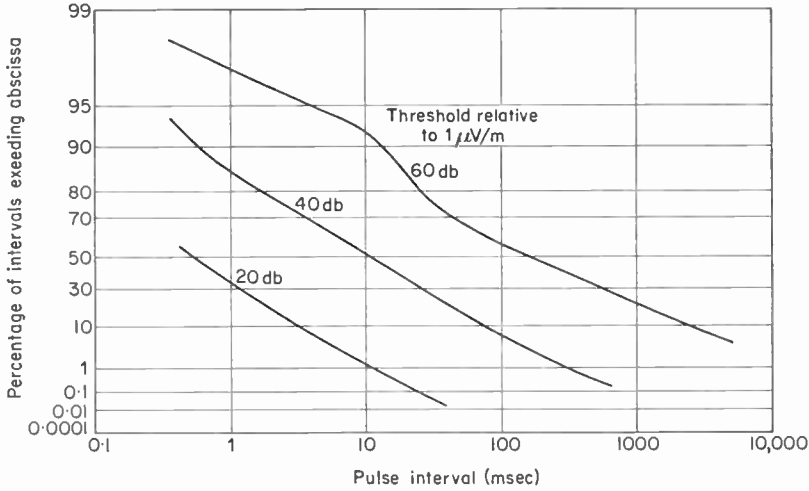


FIG. 19. Statistical distribution of intervals between pulses at 22 kc/s. Bandwidth, 1170 c/s. (Reproduced with permission from Watt and Maxwell, 1957b.)

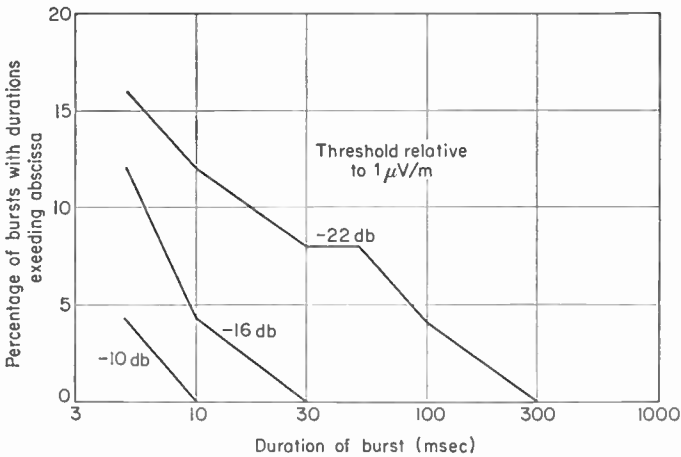


FIG. 20. Statistical distribution of durations of high-frequency atmospherics. (Reproduced with permission from Clarke, 1960c.)

in many atmospherics. At the time when the data in Fig. 20 were obtained, the r.m.s. noise would have been about -10 db and it is seen that bursts at this level were very short. Durations of noise bursts and of intervals have also been measured in India (Lakshminarayan, 1962), and both time functions were found to be distributed according to a log-normal law. Mean values and standard deviations of durations were similar to corresponding published data on lightning discharges.

IX. DIRECT MEASUREMENT OF INTERFERENCE

When one or more of the objective parameters discussed so far has been measured, there remains the problem of deciding how they are related to interference. This is the subject of a later section, from which it will be evident that the relationships are not simple. If a quick answer is required to an interference problem with a specific type of existing service, therefore, it is often expedient to measure the interference directly. This procedure has the additional advantage that the characteristics of the receiver, and where appropriate the observer, are taken into account under operational conditions in which the signal and noise are being received together. Furthermore, if the relationship between the readings and some more objective parameter is known, interference measurements may be a convenient, though not highly accurate, method of obtaining objective data at a number of operational stations.

One method of interference measurement was used by Austin (1927) and later, on a wider scale, by Thomas (1950), using standardized equipment at a number of stations. In the later measurements the noise was picked up on a vertical rod aerial and applied to a receiver in parallel with a simulated slow-speed morse signal from a local generator. The operator adjusted the strength of this signal until he judged by ear that the morse was 95 per cent intelligible, and recorded the output of the generator. Tests were carried out with a number of observers, both skilled and unskilled, and it was estimated that the final results were accurate to about 3 db. The technique has been used at about twenty stations, first at high frequencies and later, at fewer stations, at medium and low frequencies. In the presentation of the high frequency records for the first few years, it was stated that the signal power required for the specified intelligibility was one-quarter of the noise power, when the measurements were made in a bandwidth of 10 kc/s (Horner, 1953a). The aerial noise factor F_a can then be derived from the value of the required signal by the equation

$$F_a = S_1 - 20 \log_{10} f + 122 \quad (29)$$

where S_1 is the r.m.s. required signal in a 10 kc/s bandwidth (db $> 1 \mu\text{V/m}$) and the frequency f is in kc/s. From a series of comparisons in Australia, Yabsley, in an unpublished report, has quoted a relationship which makes F_a less than the above value by 2 db which is within the experimental error of the technique. For low frequencies (20–500 kc/s) Harwood and Harden (1960) stated that with a bandwidth of 300 c/s, the r.m.s. value of the required signal is 6 db above the average value of the noise *envelope*. The conversion to F_a therefore depends on the ratio of r.m.s. to average value of the envelope V_d (in db), which varies with frequency. The conversion formula is

$$F_a = S_2 + V_d - 20 \log f + 122 \quad (30)$$

where S_2 is measured in a 300 c/s bandwidth. Sample values of V_d are given in Table IV (Section VIII, B).

It is difficult to generalize equations (29) and (30) to apply to any frequency

and bandwidth. A change of frequency alters the character of the noise, and therefore the required signal to noise ratio in a given bandwidth. An increase in the bandwidth does not necessarily increase the noise power and the required signal power in the same ratio because some of the noise components introduced in a wide bandwidth are at frequencies to which the ear is relatively unresponsive. The formulae are therefore applicable only to circumstances similar to those in which they were obtained.

This comparison type of measurement has not been wholly confined to slow-speed morse modulation. Silleni (1953) compared two channels from a local keyed teletype generator, one in which the signal was mixed with the noise and one which was noise-free. The number of errors could then be recorded as a function of the signal strength, and used as a measure of the noise. Measurements with simulated radiotelegraphy channels have also been made in France (Carbenay, 1952) and in Japan.

X. WORLD DISTRIBUTION OF NOISE INTENSITY

For the general planning of radio services there is a need to know the distribution of noise over the whole world. Even when a single parameter has been selected to represent the intensity, and a standardized omnidirectional aerial has been adopted, there remain systematic changes with frequency, with time of day and with the season of the year. In presenting noise data for practical use these changes must be shown, and some indication is needed of the extent of random and unpredictable variations.

The main features of the geographical distribution of noise are controlled by the regular occurrence of tropical thunderstorms and by propagation characteristics. At frequencies near 10 kc/s, propagation is efficient over long distances and noise tends to spread itself uniformly over a large part of the world. At medium frequencies, and particularly by day, noise is more localized in the neighbourhood of the storms and diurnal changes and variations from day to day at the same time tend to be large, depending on whether there are nearby storms or not. At high frequencies long-distance propagation is again possible and the geographical and temporal variations are smaller than at medium frequencies. The general pattern is illustrated by the curves in Fig. 21. Propagational factors lead to higher noise levels at night except at 20 Mc/s where daytime propagation may be better. The severe absorption at medium and some high frequencies is evident, but there is a tendency for the noise to be enhanced in the afternoon period because the thunderstorms are then nearest to the receiving location.

Attempts to depict the world-wide distribution of noise have so far been confined to frequencies above 10 kc/s, which are those used for radio services. The form of presentation described here is that adopted in publications of the International Radio Consultative Committee (CCIR) since 1957. The parameter used is the noise power averaged over an hour expressed as the effective noise factor F_a of a short vertical aerial, and emphasis has been placed in Section VIII on methods of measuring or deducing this parameter. Variations of F_a in periods from a few minutes to an hour are

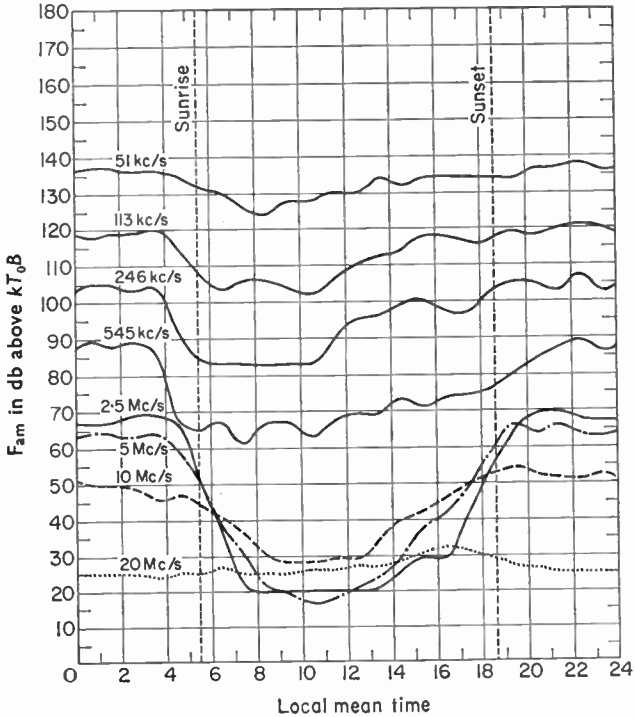


FIG. 21. Diurnal variations of atmospheric noise.
(Reproduced with permission from URSI, 1962.)

small, except possibly at twilight or during local storms, and variations in periods much less than a few minutes may be regarded as the noise structure and discussed as a separate topic. In summarizing the available information on the distribution and variation of F_a it must be decided which changes are to be treated as systematic and which as random and unpredictable. The geographical distribution must be shown, and it is usual to show systematic diurnal and seasonal variations. Any changes with the sunspot cycle would also be partly systematic, but no significant effect has yet been detected in recent noise surveys (see below).

A. PRESENTATION OF DATA

The hourly values of F_a are grouped according to time blocks, each block consisting of the same 4-h period of the day for the successive days of a season. Thus for one time block there are about 360 values of F_a forming a statistical group, within which the values are assumed to vary in a random manner. They are represented by the median value F_{am} and by the upper and lower decile values. The ratios of the upper decile to median value (D_u) and median to lower decile value (D_l) are in general not equal, as the dis-

tribution of the individual values (in decibels) is not symmetrical about the median value. Very high values are more probable than very low values, owing to the background of noise from widespread sources.

We have thus arrived at a parameter F_{am} for each of twenty-four time blocks, and its geographical distribution could be plotted for any frequency. The plot is usually in terms of local time at the receiving location. To plot twenty-four charts for each of a large number of frequencies would, however, still be excessively cumbersome, and further simplification is obtained by assuming that the variation with frequency is the same for a range of conditions. A chart can then be drawn for a single frequency, and 1 Mc/s has been chosen as being near the centre of the range of main interest. In the first presentation of data by the CCIR (1957), the frequency law was assumed to depend only on the general noise level (as defined by the intensity at the reference frequency) and on whether the receiving location was in daylight or in darkness. Subsequently sufficient data have become available to differentiate between frequency laws appropriate to each time block.

Even with the greatly increased recording programme of recent years the number of stations is quite inadequate, without other information, to enable contours of equal noise intensity to be drawn for all the world. Use has therefore been made of data on the distribution of thunderstorms (WMO, 1953), coupled with a knowledge of propagation, in deciding how the contours should be drawn, the numbering of the contours then being determined by the noise measurements. An example of the type of chart produced is shown in Fig. 22. It is plotted in local time and for the same season in each hemisphere, so does not represent the distribution at a given instant. Three main equatorial noise areas are shown, and these reach their noisiest phases in succession, during the late afternoon, local time.

The noise at any other frequency can be deduced by reference to a set of curves of the form shown in Fig. 23, which is for the same time block as Fig. 22. The range of values is smaller at both low and high frequencies than in the middle range for the reasons given above. If only terrestrial noise were significant, any sunspot cycle effect would be expected to be greatest at high frequencies since the optimum frequency for ionospheric propagation from distant sources will vary. The curves shown have been derived from data obtained near sunspot maximum, but examination of results for a longer period suggest that the solar cycle variation of the total received noise is not large. There are two reasons for this. With distributed sources such as thunderstorms, changes in ionospheric conditions will often result in noise being received from a different area, but may not change its intensity. Secondly, if the critical frequency of the ionosphere becomes so low in relation to the frequency of observation that long distance propagation of noise is no longer possible, galactic noise will be received. On Fig. 23 the values of galactic noise which would be expected in the absence of the ionosphere are shown. These are similar to the values of atmospheric noise in the high frequency range in middle latitudes, so changes of ionospheric conditions tend to change the source of noise from atmospheric to galactic, or vice versa, without a marked change in its intensity. The apparent absence

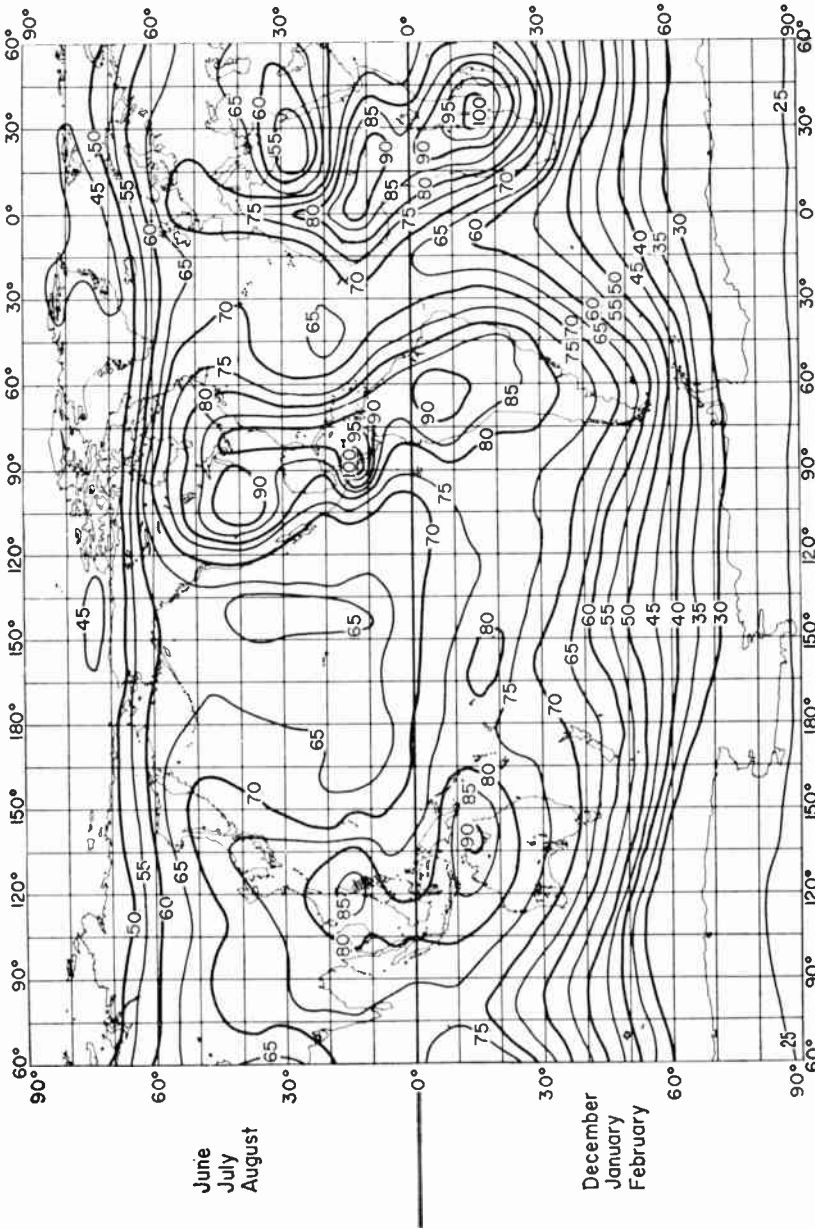


Fig. 22. World distribution of noise intensity, Fam, at 1 Mc/s. Night (2000-2400 LMT) Summer. (Reproduced with permission of the National Bureau of Standards, Boulder, U.S.A.)

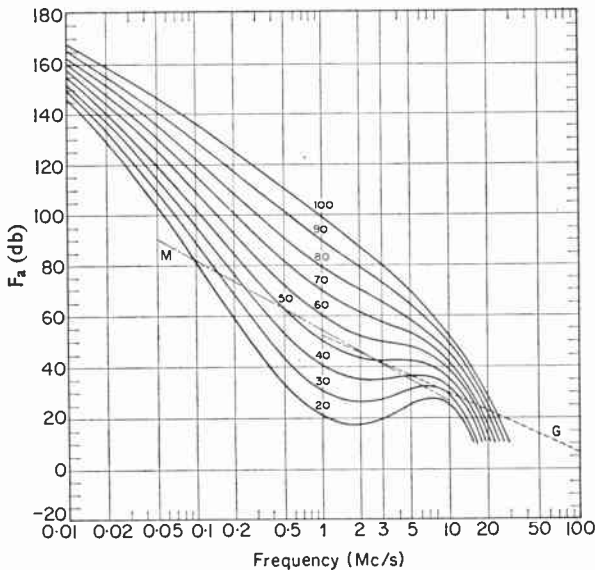


FIG. 23. Variation of F_a with frequency.

G Galactic noise.

M Man-made noise on typical good receiving site.

(Reproduced with permission of the National Bureau of Standards, Boulder, U.S.A.)

of a solar cycle influence is in contrast with the tentative conclusions of Austin (1927) from low frequency observations.

Some information is becoming available for extending the noise curves down in frequency to about 10 c/s, below which different phenomena are important. There is a general tendency for the curves to continue to rise more steeply than the $-20 \log f$ term in equation (18), but the absorption band at 2-4 kc/s has a marked effect on the shapes of the curves (Maxwell and Stone, 1963). There have been a few measurements below 1 kc/s where propagation is reasonably good. Results of Willis (1948) and of Large and Wormell (1958) show agreement at 100 c/s with an F_a value of about 205 db, probably obtained in the daytime, but Willis shows a larger increase as the frequency is further reduced. Maxwell and Stone's values for 100 c/s were also about 205 db by both day and night except in summer when they were a few decibels higher. On the other hand, Aarons' (1956) night-time value at 100 c/s was only about 180 db, with much smaller values by day. All these measurements were in temperate regions. There is clearly a need for more measurements in this frequency range.

Also shown on Fig. 23 is a curve indicating the approximate values of man-made noise which may be expected on a typical, good receiving site. At medium frequencies in particular, man-made noise from power lines, electrical equipment, etc., will often be more significant than atmospheric noise, especially by day.

Problems of radio interference require a knowledge of the unpredictable variations of noise in addition to its long-term median value. An indication of the variations in the hourly values within a time block may be given by quoting the upper and lower decile values. The ratio of the upper decile value to the median is greatest in the medium frequency range, where typical values are 18 db by day and 10 db by night. Values at very low and at high frequencies are about 5 db at all times. The ratio of median to lower decile values tends to be rather less than the ratio of the upper decile to the median.

The data on the world distribution of noise will require continual revision as more information is gathered, and it is becoming common practice for the results of new measurements to be compared with the predictions. Recent comparisons have been made by McKerrow (1957, 1960), Aiya (1959), Harwood and Harden (1960), Lichter and Terina (1960), Herman (1961) and Clarke (1962). Comprehensive revisions of the noise data published by CCIR are in preparation and include, in addition to the geographical and systematic temporal variations, additional statistical information on the variability of the noise and on its structure.

B. NOISE ON DIRECTIONAL AERIALS

Presentation of world distributions of noise have been based on measurements with omnidirectional aerials because the introduction of still more variables, defining the aerial directivity, would be a serious complication. However, long-distance communication at high frequencies is normally accomplished by using large aerials with narrow beams, and some noise measurements have been made with aerials of this type. On general grounds the noise factor of a directional aerial would be expected to be more variable than that of an omnidirectional aerial, since it is dependent on the occurrence of storms in the direction of the main beam. The average noise factor will be reduced by the directivity if the beam is not pointing towards a stormy area, or if the aerial pattern in the vertical plane is such as to differentiate against the noise.

In a series of measurements at about 10 Mc/s in the southern part of Australia it was found that the diurnal variations of noise were controlled mainly by the variations in propagation conditions from day to night, but the pattern of variations was modified by directivity. For example, aerials beamed in an easterly direction showed an increase from the daytime to the night-time value 2 or 3 hours before the corresponding change on westerly beams. In general, the average noise factors for several aerials over long periods tended to be a few decibels lower on directional aerials, and it was concluded that the main noise was incident at elevation angles somewhat higher than the main beam; on some occasions higher than would have been expected in the prevailing ionospheric conditions. On the other hand, experiments in Singapore have shown that the noise power available from a highly directional rhombic aerial is somewhat higher than from a vertical monopole, by perhaps 6 db on the average, suggesting that the improvement in signal-to-noise ratio will be less than that expected from the signal gain

alone. Further work is required to enable more precise allowances for directivity to be made, and to be related to distributions of thunderstorms.

XI. NOISE INTERFERENCE TO RADIO SERVICES

One of the main problems in designing a radio system is the evaluation of the signal strength, at the receiver, required to provide a desired quality of service in the presence of noise or other interference. The solution is usually split into two parts. In the first the required signal-to-noise ratio is determined when the signal is steady and the noise is statistically constant. In the second, allowance is made for the fading of the signal and for the fluctuations in the noise over periods of a few minutes or more.

Although the assessment of the interfering properties of the atmospheric noise should take account of both its absolute intensity and its structure, the required signal has often been related to a single noise parameter, usually the r.m.s. voltage, the average voltage, or a quasi-peak voltage as recorded in a meter with specific weighting circuits. There is no general consensus of opinion as to what single parameter is the most satisfactory index of interference for a wide range of radio services, but the r.m.s. voltage is one of the most useful and has the advantage of being directly related to the noise power, which is the basis of recent presentations of noise data.

Some indication of the signal-to-noise power ratio required for slow-speed morse communication was given in the discussion on the direct measurement of interference. Signal-to-noise ratios for many other services have been derived either from specific tests or from long experience, and are in common use in radio planning.

A notable contribution has been made in South Africa to the problem of assessing the behaviour of various low-frequency radio aids to navigation in the presence of atmospheric noise. The required signal strengths for specified observational accuracies were determined, while the noise was measured simultaneously using the NITR recorder described in Section VIII, B. As the noise was measured at a frequency of 100 kc/s while the interference measurements were not necessarily at this frequency, or in the same bandwidth, the experiments did not yield signal-to-noise ratios in the usual sense. It was assumed that there was good correlation between the noise as measured and the noise causing the interference, and the performance was then stated in terms of the general ambient noise level measured at 100 kc/s in the standard way. However, the noise measurements can be converted to noise power, approximately, as suggested in Section VIII, B and allowance can also be made for changes in frequency and bandwidth, so actual required signal-to-noise ratios at the operating frequency can be deduced. In a series of reports on the tests in South Africa, data have been given for low-frequency Loran, an automatic radio compass and the Decca and Consol navigation systems.

Many theoretical studies have been made of the influence of thermal-type noise on radio services, since this problem is often readily amenable to mathematical treatment. Less attention has been given to the theoretical

analysis of interference from the more complex atmospheric noise, but now that the noise structure is better understood it can be taken into account in a more systematic way. For example, it is evident, when the amplitude probability distribution is considered, that the high instantaneous amplitudes which are present for a small fraction of the time are capable of degrading a service for a correspondingly small fraction of the time. Where the deterioration takes the form of a measurable increase in errors, as in a radio teletype service, it seems reasonable that there should be some correspondence between the APD and the curve showing the percentage of errors as a function of signal strength. This aspect of the problem has been studied at the University of Florida, where it was found that the noise fluctuations at low frequencies could be represented by a log-normal distribution, and the plot of percentage errors against signal strength, plotted in log-normal coordinates, also gave a straight line. Relationships were given between the parameters defining the noise distributions and the performance data.

Watt *et al.* (1958) have compared, experimentally, the performance of aural morse and frequency shift teletype systems in the presence of thermal or atmospheric noise. The required carrier signals were related to the noise in a 1 kc/s bandwidth. With aural morse at 12 words/min, in typical VLF noise, a good operator made 10 per cent errors with a carrier-to-noise power ratio of -11.5 db and 1 per cent errors with a ratio of -2 db. These figures are consistent with those derived independently for relating noise power to direct measurements of interference to a morse service, which at 20 kc/s can be interpreted as a requirement of -9 db in a 1 kc/s bandwidth for 5 per cent errors (see Section IX). Required signal-to-noise ratios were also derived for the teletype system, as a function of frequency deviation, information rate, type of noise and grade of service. It was shown that the plot of error rate against signal strength tended to follow a curve similar to the amplitude probability distribution of the noise, for instance the increase of signal required to reduce the errors from 10 per cent to 1 per cent was greater the larger the dynamic range of the noise. The same authors give an example of the way in which the required signal for different grades of service can be calculated from the amplitude probability distribution. The method is based on the statement of Montgomery (1954) that with a frequency shift teletype system a binary digit will be correctly identified if the noise is less than the carrier over the duration of the digit, while if the noise is greater than the carrier, there is a 50 per cent probability that the digit will be correctly identified, by chance. The probability of a binary error is therefore half the probability that the noise envelope exceeds the carrier envelope, and this enables a curve of binary errors against signal strength to be plotted from the noise APD as in Fig. 24. A statistical analysis of the coding of the information then enables the probability of character errors to be derived from that of the binary errors. The example discussed is a five-unit start-stop teletype system for which the percentage of character errors is shown to be seventeen times the percentage of binary errors if these are infrequent and uncorrelated. The character errors calculated in this way are plotted in Fig. 24, and show good agreement with the results of measurements.

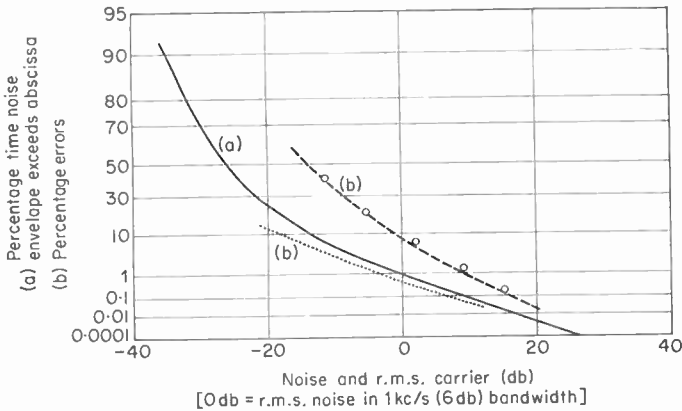


FIG. 24. Comparison of calculated and measured errors at VLF.
Bandwidth, 120 c/s.

— Noise APD
 Per cent binary errors } Deduced from APD
 - - - - Per cent character errors }
 o Measured character errors

(Reproduced with permission from Watt *et al.*, 1958)

The signal-to-noise ratios discussed above are for steady-state conditions. When both the signal and the noise are varying in intensity, additional allowances must be made to ensure a satisfactory service. This requires a knowledge of the noise variations in times comparable with the fading periods of the signal. Although there have been many studies of the diurnal variations of noise and of its structure, less attention has been paid to variations over periods of a few minutes, and further work on this topic is desirable.

XII. LOCATING SOURCES OF ATMOSPHERICS

The introduction of methods of locating the sources of atmospheric noise was originally prompted by a desire to know the nature of the physical processes involved in noise generation. When the sources were positively identified as, in the main, thunderstorms, it was recognized that the location facilities, based on direction finding, were potentially of great value to meteorology since thunderstorms could be located at distances of many thousands of kilometres, and much of the subsequent development has been for this purpose. The number of observing stations equipped with direction finders for routine use is now about 100. The techniques in common use do not differ basically from those originally used, but their potentialities and limitations are better understood. In addition, radar is now used for locating storms at relatively short range.

A. DIRECTION FINDING TECHNIQUES

Sources of atmospheric noise have been located by direction finding from two or more observing points, by measuring direction and range from a single

point, and by measuring differences of time of arrival at three or more points. The purely direction finding method is almost universally used for routine work, the equipment being either the cathode ray direction finder (CRDF) or the narrow sector recorder. The first is capable of recording all atmospheric within a range set by the sensitivity, while the second uses a sampling technique particularly well adapted for obtaining chart records automatically.

In the cathode ray direction finder, introduced 40 years ago by Watson-Watt, the atmospheric are picked up on two vertical loop aerials orientated in north-south and east-west planes, amplified in identical amplifiers, and applied to the orthogonal plates of a cathode ray tube. The arrival of an atmospheric results, ideally, in a straight line trace along a diameter of the tube, at an angle corresponding to the azimuth from which the atmospheric was received. In its simplest form there is a 180° ambiguity in the bearing, but this can be resolved by adding a vertical aerial, and using the output, suitably phased, to suppress the appropriate half of the diametral trace. Frequencies of about 10 kc/s are usual but 175 kc/s has been used in India (Chiplonkar *et al.*, 1958) and up to 1.5 Mc/s in the United States for special purposes (Jones, 1951; Stergis and Doyle, 1958). The following discussion of errors will relate only to the work at very low frequencies.

Apart from general improvements in convenience of operation, developments in equipment have been largely concerned with the matching and stability of the amplifiers, and with obtaining accurate bearing indications at amplitudes several times those giving full-scale deflection on the display tube (Iwai *et al.*, 1953; Clarke and Harrison, 1955). In these respects, modern instruments are sufficiently good for most practical purposes.

In practice the traces are often not straight lines, but ellipses or more complicated configurations, and correspondingly the indicated bearings may be in error. These departures from ideal performance are caused partly by the reception of waves which are not vertically polarized, and partly by shortcomings of the sites on which the instruments are installed. Much research work has been done on the explanation and reduction of the errors.

Dealing first with errors on waves of mixed polarization (polarization errors), reference may be made to an earlier discussion on the propagation of atmospheric, in which it was seen that energy is in general received both by ground wave and also by a number of reflections between the earth and the ionosphere. The VLF ground wave is essentially vertically polarized and in the absence of ionospheric waves, correct bearings may be expected. The ionospheric waves, however, have horizontally polarized components which, on a loop direction finder, cause errors or elliptical traces or both, depending on the relative phase angles of the vertically and horizontally polarized components of the field. More complicated traces result from continual changes in the relative amplitudes and phase angles within the duration of the atmospheric. Ionospheric waves are stronger at night than by day, and large errors are essentially a night-time phenomenon (Horner, 1957a). Particularly large errors up to 40° or more can occur at a distance of about 300 km, where the ground and ionospheric waves are approximately equal. Figure 25 shows a direction-finding display photographed on

moving film so that later parts of the trace are displaced to the right, enabling the sequence of events to be followed. The early parts of the trace indicate an azimuth of 20° (or 200°), but with the arrival of high-angle ionospheric waves the trace became elliptical and rotated in a clockwise direction, the final portions indicating bearings with errors of about 90° . A visual bearing

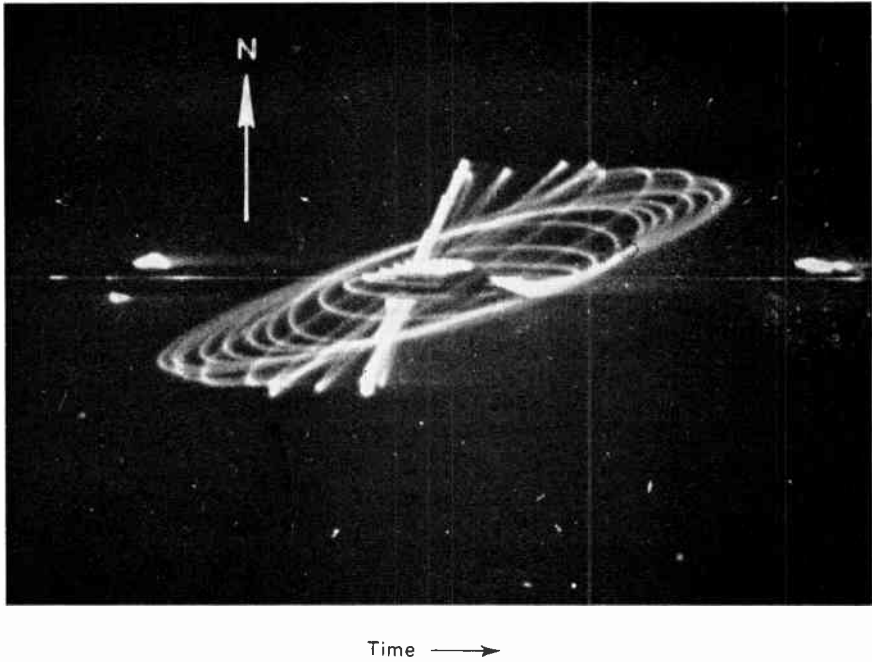


FIG. 25. Direction finding trace showing polarization errors.
(Reproduced with permission of the Controller of H.M. Stationery Office.)

taken on the maximum amplitude of the trace would have been in error by 50° . Such large errors are not common, and the complicated nature of the trace gives a warning that the bearing may not be reliable. Errors of bearings taken on station transmissions are dependent on the direction of the path (possibly in relation to the magnetic field) so a corresponding effect presumably occurs with atmospherics (Horner, 1957a, 1957b).

Various methods of avoiding or reducing these errors have been investigated. Attempts to develop a spaced vertical aerial (Adcock) system, which might be intrinsically more free from polarization error, have not been a marked success, at low frequencies, partly owing to difficulties in preserving an adequate balance between the channels, but some useful results have been obtained at medium frequencies (Stergis and Doyle, 1958). Another method is suggested by the fact that the initial part of an atmospheric such as that shown in Fig. 25 results from the ground wave only and should

indicate the correct bearing. The maximum amplitude on which the bearing is normally taken occurs considerably later (with a narrow-band instrument) when the ionospheric waves have caused some distortion. If a wideband instrument is used with a more rapid response the maximum ground wave amplitude occurs earlier, as observed at the output of the receiver, and is easier to distinguish from the ionospheric waves. This method has been exploited by Taylor and Jean (1959) in research applications using an instrument with a frequency range 1–100 kc/s. It has not been adapted for more general routine observations, possibly because the traces require photographic recording and skilled interpretation, and because in many parts of the world wideband receivers are susceptible to serious interference from transmitters.

The narrow sector recorder is an instrument in which the outputs of a loop, with a figure of eight reception pattern, and a loop and vertical rod combination, with a cardioid pattern, are superimposed differentially so that an atmospheric is received only over a narrow sector, where the second output exceeds the first. When an atmospheric is received from the appropriate sector, a pen records a mark on a chart. The whole aerial system rotates at a uniform rate and the chart is fixed to a drum, rotating in synchronism. The pen moves slowly in a direction parallel to the drum axis, so the chart when detached from the drum shows the directions of the principal storms as a function of the time of day, plotted in cartesian coordinates. This system was developed by Lutkin (1938), and Lugeon (1939) by whom it has been exploited extensively. Because the loops of the aerial system respond to horizontally polarized waves, the narrow sector recorder is susceptible to polarization errors similar to those of the CRDF, although the form of the record is such that they are less obvious. The effect is that the storms appear to be more widespread than they really are. Another disadvantage of this system, when compared with the CRDF is that when several storms exist at the same time, the intersections of bearing lines from only two stations do not provide unique fixes, since the atmospherics from the same discharge are not identified, and may not even be received at both stations. However, Lugeon and Rieker (1958) have shown that each instrument has its merits and disadvantages, and that a combination of both can be used effectively.

Errors due to imperfections of sites have been investigated mainly with the CRDF, although similar effects may be expected with narrow sector recorders. One of the important conclusions is that serious errors can be caused by ground irregularities which were previously thought to be unimportant because of their small size relative to the wavelength. Errors of about 10 degrees have been found when waves passed obliquely over sites which had slopes of 1 in 10 (Horner, 1954). The effects have not been fully explained quantitatively, but it is evident that if the direction finder itself is on a slope, and there is an ionospheric wave incident at a steep angle, the image of the source in the sloping ground will not in general be at the same azimuth as the real source. The bearing will then be in error by an amount depending on the relative amplitudes and phases of the direct and ground

reflected waves. It has also been shown that the arrangement of any power or other cables in the neighbourhood of the direction finding aerials needs more care than had been considered necessary, and that they can in some circumstances cause greater errors when buried than when exposed. This happens because a metal-sheathed, buried cable in good contact with the ground has a low characteristic impedance and is therefore inherently capable of carrying high currents in relation to the strength of an impressed electromagnetic field. The magnetic fields of these currents then induce unwanted voltages in the loops (Horner, 1953b).

Another form of error is due to interference between successive atmospherics. With narrow-band amplifiers the pulse at the output is long (usually several milliseconds), and the bearing of an atmospheric will be affected if it arrives before the effects of the previous one on the tuned circuits have completely disappeared. The likely errors can be calculated if the rate of occurrence and amplitude distribution of the atmospherics are known (Horner, 1954; Otsu and Shiga, 1955).

B. SINGLE STATION TECHNIQUES

The errors which occur with purely direction finding methods, and the inconvenience of operating two or more well-separated stations, preferably in continuous communication, have led many workers to consider other possible means of location. The most convenient, operationally, would involve measurements of bearing and distance from a single station. The use of radar is a valuable method of locating storm centres, but is unfortunately limited to line-of-sight distances, say 100 km. Furthermore, it is not always certain that the precipitation causing radar reflections is coincident with, or even associated with lightning discharges. Some other possible single-station techniques based on bearings and distance measurements have been reviewed by Pierce (1956b). The errors inherent in the bearing determination would of course remain, unless new and more accurate methods were developed, but with present direction finding techniques the bearing of a distant storm from a reference point near the centre of a network can in general be measured with adequate accuracy; the more serious positional errors are introduced in the determination of distance by the use of intersecting bearing lines.

The amplitude of an atmospheric cannot be used as an accurate indication of the distance of the source, because of the variations in radiated energy from one discharge to another. The average amplitude from a large number of discharges from the storm is a better index, but still not accurate, and has obvious drawbacks when more than one storm exists in the same direction. A more promising approach is to study the spectra of the atmospherics, which change with distance. It has been shown that the ratios of amplitudes on different frequencies in the VLF range can be related to the distance travelled (Bowe, 1951), the relatively high absorption at 2-4 kc/s being of particular interest, and Sao and Jindo (1961) have suggested that a study of the phase spectrum, rather than the amplitude spectrum, may lead to a more

accurate distance estimate. Another example of the use of this technique is the study of the delay and quasi-period of the slow tail component present in some atmospherics. In Section VII the dependence of these quantities on distance was discussed and empirical relationships given.

The use of the high-frequency spectrum has also been suggested as a means of distance measurement. If the highest frequency at which atmospherics from a given storm are received by ionospheric propagation can be determined, the storm is at the skip-distance for that frequency, and this is known if the state of the ionosphere is known sufficiently well. Experimental results indicate that this method is feasible (Horner, 1953c), but that the ionospheric information from the existing network of ionospheric sounders is not sufficiently detailed for an accurate estimate of the skip-distance to be made, even if it were rapidly available. The method would be more practicable if it were combined with the backscatter method of ionospheric sounding, by means of which the skip-distance for the frequency and direction of interest could be ascertained from the same station (Clarke and Byrne, 1956). The additional complexity of this arrangement would, however, offset the attractiveness of single station operation.

In an earlier section a method of deducing the distance of a source from the waveform of an atmospheric was mentioned. Energy may be received by ground wave propagation and by various numbers of reflections between the earth and the ionosphere, and measurement of the time delays between the echoes enables both the source distance and the height of the ionosphere to be calculated (Schonland *et al.*, 1940; Laby *et al.*, 1940). Suitable waveforms occur mainly at night, although they may also be received from short distances (less than 1000 km) by day. For the distance to be obtained to a useful accuracy the relative delays of the echoes must be measured to within a few microseconds. This is possible with the best waveforms and the accuracy of the distance measurement at the longer ranges is then better than can normally be achieved with direction finding networks (Caton and Pierce, 1952). If the delay measurements are subject to greater errors and if, in addition, there is uncertainty about whether the first visible pulse has been received by ground wave propagation or by one or more reflections at the ionosphere, large errors can occur (Horner and Clarke, 1955; Nakai, 1956; Skeib, 1957). The difficulty of interpretation, the scarcity of suitable daytime waveforms, and the time taken for photographic recording of the waveforms and for their analysis combine to make the technique unsuitable as a replacement for the method based solely on direction finding, at least for routine use for meteorological purposes (Kessler and Hersperger, 1952).

Some indication of the location of sources can be obtained at times near sunrise and sunset by observing the change in the intensity of the atmospherics as the part of the ionosphere where the energy is being reflected passes from light to dark, or *vice versa*. The position line then obtained, combined with a bearing taken on the storms, enables the location of the reflecting point to be known, and the location of the storms can be deduced. This method is also unsuitable for routine use since it is confined to such short periods of the day.

C. TIME-DELAY TECHNIQUE

The recording of relative times of arrival of atmospherics at several stations is another method which has often been considered and recently demonstrated to be feasible, at least under the particular conditions chosen. A given time delay between corresponding atmospherics at two stations implies that the source lies on a certain hyperbola with the stations as foci. Measurement of two time delays, which can be achieved with three stations, provides two hyperbolae intersecting at the location of the source. Tests of this system were made with three stations in the Eastern United States spaced by about 100 km, locating sources in and near Europe which were fixed by the British direction finding network (Lewis *et al.*, 1960). At such distances (more than 4000 km) a pair of stations behaves almost as a direction finder with a wide baseline, the lines of equal time difference being almost radial but with slight curvature. Polarization errors should be practically non-existent and site errors should be small. Time differences were measured by recording waveforms at the three stations on time bases which were interrelated by timing signals. The features of the waveforms were sufficiently similar to be matched accurately.

The fixes obtained by the British direction finders were regarded as an adequate standard of reference, since the sources were at short ranges, but would not be entirely free from error. The directions measured by the timing network differed from these fixes by an angle of average magnitude about half a degree, which no doubt included a contribution from the errors of the direction finding network. The system therefore worked well over long oversea paths and it appears that two suitably placed networks could be used to obtain accurate fixes. Further tests are desirable to assess the more general potentialities of the system since the experiments described were carried out over daylight paths, and only small errors would then have been expected with conventional direction finders on good sites. Also the long oversea paths would be most favourable to the reception of identical waveforms, suitable for accurate matching, at all three stations. Greater difficulty in matching might be expected with sources at distances more comparable with the station separations, over land or mixed land and sea paths, and at night. Although multiple stations are required for this technique, each network could consist of one control centre and two or three unmanned outstations. In principle, a second network could be remotely controlled from the first. The alternative of using a single network of widely spaced stations would depend on similar waveforms being received over quite different paths. The method in its present form is not sufficiently rapid to replace direction finding for routine use as an aid to weather forecasting.

XIII. WHISTLING ATMOSPHERICS

Whistling atmospherics, or whistlers, are audio-frequency atmospherics which originate in lightning discharges and travel over long dispersive paths, so that the different frequency components are received at different times. They can be detected by using a wide-band radio receiver responding to

audio-frequencies, and a large aerial on a site free from man-made noise. The dispersion gives the atmospheric a musical character, the most usual sound being a whistle of descending pitch. Although whistlers were first heard on telephone systems in the last century, it was not until 1935 that they were explained in terms of dispersive propagation paths (Eckersley, 1935) and only after the Second World War that the nature of these paths was discovered. Storey (1953) showed that radio waves of audio-frequency can penetrate the regular layers of the ionosphere and can then be guided along the lines of the earth's magnetic field. The disturbance from a lightning discharge can thus be propagated along a field line, through the outer regions of the earth's atmosphere, to the magnetic conjugate point in the other hemisphere. There it is partially reflected at the ionospheric layers, but some of the energy passes through the ionosphere and can be heard, by using an audio-frequency receiver, as a so-called short whistler. The reflected energy returns along the field line to the neighbourhood of the lightning discharge and may there be heard as a long whistler. The main characteristics of a whistler are described by its dispersion D , which specifies the time of travel $t(f)$ of a component of frequency f by the relationship

$$t(f) = Df^{-\frac{1}{2}} \quad (31)$$

The dispersion of a long whistler, which has travelled along the field line twice, is double that of the corresponding short whistler, and both the time of travel and the dispersion depend on the length of the field line as well as on the strength of the magnetic field, and hence on the latitude of the lightning discharge and of the place of observation. Energy can be partially reflected several times at the ends of a field line and a series of echoes is then produced (a whistler train) whose times of travel are in the ratios 2 : 4 : 6, etc., for long whistlers and 1 : 3 : 5, etc., for short whistlers. From equation (31) the dispersion also increases with the number of the echo in the same ratios.

Whistlers are usually recorded on magnetic tape and replayed through a spectrograph which produces a record of the frequencies received as a function of time, as shown in Fig. 26, in which the predominant frequency decreases from 16 kc/s to 4 kc/s in $\frac{1}{2}$ sec. These records enable the times of arrival and the dispersions to be measured. The method of recording and display also reveals the presence of atmospherics of whistling type, but with very small dispersions. These are known as tweeks and are the atmospherics described in an earlier section as reflection types, not to be confused with whistlers. The successive echoes received by reflections below the ionosphere constitute a train with a natural frequency which decreases with time as the echo-spacings increase, reaching a final frequency of about 2 kc/s corresponding to echoes reflected between the earth and the lower boundary of the ionosphere at nearly vertical incidence. Some tweeks can be seen in Fig. 26. The similar traces which finish at about 4 kc/s may be harmonics of the tweeks, introduced by instrumental limitations, but it has been suggested that they can arise in the propagation mechanism.

Many forms of whistler are observed (Dinger, 1957), for example, diffuse types in which a band of frequencies rather than a single tone is received at

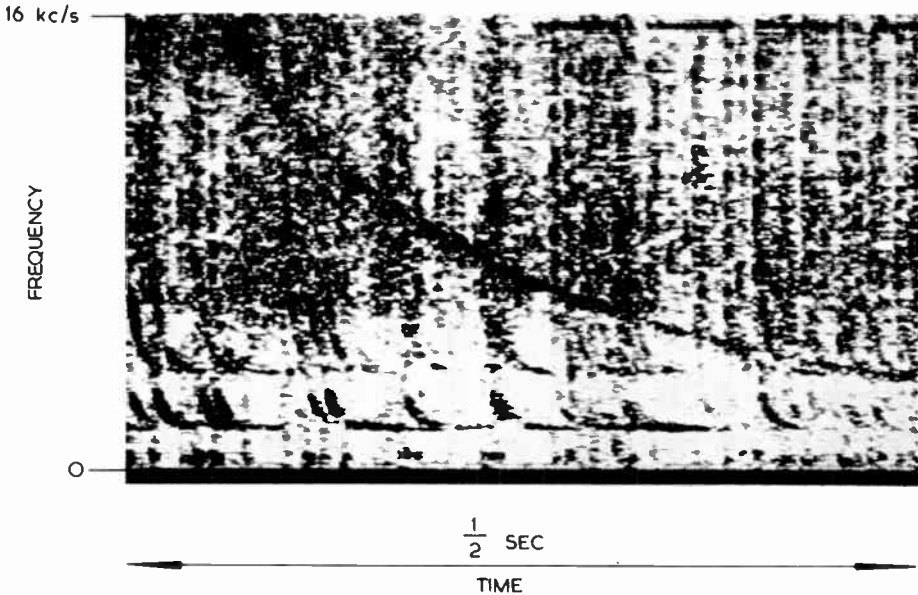


FIG. 26. Spectrogram of a whistler.

(Reproduced with permission of Professor Helliwell of Stanford University, U.S.A.)

any instant, and those in which rising and falling tones are received simultaneously (nose whistlers). These variations are mainly the result of different characteristics of the outer ionosphere, or exosphere, and a great deal of information on these regions has been deduced from the study of whistlers. The theoretical work on the mechanisms of propagation of whistlers and on their relation to the field-aligned inhomogeneities in the exosphere are not within the scope of this chapter, but it is useful to review what is known of the relationships between whistlers and the causative lightning discharges, whose characteristics have already been described. A review of the related ionospheric and exospheric phenomena has been given by Storey (1962).

Whistlers occur most frequently at mid-latitudes; at high latitudes there are few lightning discharges and at low latitudes conditions are unfavourable to the trapping of energy in the magneto-ionic duct. They are more common at night than by day, but apart from this diurnal variation there are times favourable to their reception and other times when none are heard at the same location. The occurrence of lightning discharges either near the observing point or near the conjugate point favours the production of whistlers, but they are not necessarily heard even when there are suitably placed storms. They may be heard for periods up to a few hours and then disappear, even though the storms are still in progress. Special ionospheric conditions are evidently required for the reception of whistlers, but we will be concerned here with the question of whether special characteristics of the storms or lightning discharges are also required.

A. CORRELATION OF WHISTLERS WITH STORMS AND VISIBLE DISCHARGES

Considering the many investigations of whistlers which have been carried out, the number of correlations of whistlers with known storms is not large, and some deliberate attempts to identify whistlers with visible flashes have been notable for their lack of success (Morgan and Dinger, 1956; Dinger, 1960). One difficulty is that local storms produce strong atmospheric noise which tends to mask the much weaker whistlers. However, among recent observations Morgan (1958) has seen one storm in which, for about an hour, each visible flash produced a whistler. Short whistlers observed in France by Rivault and Corcuff (1960) were correlated with storms occurring near the magnetic conjugate point, and Lauter has made similar observations in Germany from storms in Madagascar (Allcock, 1962). Atmospheric whistlers were received in Japan both by the whistler mode and by more conventional ionospheric propagation from the same discharges. Norinder and Knudsen (1959) observed bearings and waveforms of atmospheric whistlers from near lightning discharges and correlated these with whistlers. In their early observations of several storms most lightning discharges were found to give rise to whistlers, and it was noticed particularly that vertical discharges were accompanied by strong whistlers; in their later work it was observed that whistlers could be heard from one thunderstorm while none could be heard from another at a similar distance but in a different direction. It was concluded that special features of the lightning discharge were required, and the proportion of discharges producing whistlers was found to vary during the development of a storm. In experiments in the United States it was noticed that there was a greater tendency for whistlers to originate in storms over the sea than over land, and the direction of the storms from the recording station was also found to be significant, as in the Swedish work (Helliwell *et al.*, 1958). Rivault, on the other hand, observed whistlers from storms over Europe rather than over the Mediterranean Sea (Horner, 1962b). In view of this conflicting evidence it is still uncertain whether storms from which whistlers are heard have special meteorological characteristics.

B. WHISTLERS AND THE ORIGINATING LIGHTNING DISCHARGE

In attempts to discover the features of the individual lightning discharge which give rise to whistlers, three aspects have been considered, the orientation, the intensity and the spectrum.

It was stated above that whistlers had been associated with visible discharges with substantially vertical orientation. On the other hand, it has been suggested that long horizontal discharges, or discharges between the cloud and the ionosphere, might be particularly favourable and Rivault thought that whistlers in France tended to originate in non-vertical discharges (Horner, 1962b). However, in view of the fact that transmissions from a vertical aerial have been received at the conjugate point by the whistler mode (Helliwell and Gehrels, 1958), it seems probable that no special orientation is necessary.

Norinder and Knudson (1959) found that whistlers were associated with lightning discharges producing the largest field changes. Currents in ground strokes have been said to decrease with increasing height of the terrain (Robertson *et al.*, 1942), which might partially explain a tendency for the whistlers to originate over sea. Several investigations have been carried out to determine whether amplitude was the main consideration, or whether the distribution of the energy through the spectrum was important. Whistlers are most easily detected at frequencies of a few kc/s and it might therefore be expected that they would follow lightning discharges with strong components in this range. Whistlers have long been associated with atmospherics of a type known as a "click" (Storey, 1953). Helliwell and his co-workers (1958) observed that whistlers were preceded by atmospherics with a distinctive "thud" sound; these were found to have waveforms which consisted of a few cycles with a period of the order of 5 kc/s and thus had strong components in this region of the spectrum. The type was said to be relatively rare. Norinder and Knudsen (1959) confirmed the nature of the waveforms and suggested that they probably resulted from multiple discharges. Rivault (1957) and Iwai and Otsu (1958) found a tendency for whistlers to be associated with atmospherics with waveforms of the reflection type. From these results it seems likely that whistler-producing discharges are of greater than average intensity and also have a favourable spectrum.

A theory of Hoffmann (1959) refers to the possibility that the lightning discharge itself could produce the field-aligned ionization necessary to guide the energy through the ionosphere. The first of a pair of discharges closely spaced in time, between the cloud and the ionosphere, could create an ionized path, and the energy from the second discharge would then be guided along this path. The required separation of the two discharges was of the order of $\frac{1}{2}$ sec. Experimental evidence, from the statistical analysis of relative times of whistlers and discharge pairs, has been quoted as giving some support to the theory, but is not generally regarded as conclusive.

C. PROPAGATION OF WHISTLERS BELOW THE IONOSPHERE

It has long been known that whistlers can be heard over a considerable area (1000 km or more in radius) around the source or its conjugate point, and one suggested mechanism involves the propagation of the energy below the ionosphere from the point where penetration of the ionospheric layers occurs. On occasion energy can travel several thousand kilometres, and this can account for the reception of whistlers at very high latitudes where no thunderstorms would be expected (Ungstrup, 1959; Allcock, 1960). The spectra of these whistlers are modified by the sub-ionospheric propagation, with a low frequency cut-off in the region of 4–5 kc/s. This long-distance propagation also gives rise to what are known as hybrid whistlers. At a station near the source, for example, the normal long whistler may be received, but a short whistler may be superimposed, resulting from the propagation of energy from the source along a whistler path, and then back to the receiving point along paths below the ionosphere.

XIV. CONCLUSION

Although advances have been made on many aspects of radio noise, during the past few years, there are several important problems which still need to be solved. More accurate information is required on the numbers of cloud discharges and ground discharges in various parts of the world. Knowledge of the spectrum needs to be confirmed down to frequencies of a few c/s and up to several Gc/s. Although the distribution of noise over much of the world is known, there is still a lack of information for polar regions. The influence of noise on radio communication needs to be studied quantitatively for more types of service than have so far received attention, and methods of allowing for aerial directivity require further study.

The development of more convenient methods of locating sources of atmospheric noise, preferably from a single station, would have many applications; several methods appear to warrant further study, either individually or in combination. Finally, investigations of whistlers would benefit from a more thorough knowledge of the distribution of sources and of their special characteristics.

Thus there are seen to be many further opportunities for investigations of both the scientific aspects of atmospheric noise and also the practical problems which are introduced when this noise interferes with radio services. These problems are complicated, and often difficult to define, but the more thorough quantitative knowledge of the noise characteristics which now exists provides a firm basis for their solution.

REFERENCES

- Aarons, J. (1956). Low frequency electromagnetic radiation 10–900 cycles per second. *J. geophys. Res.* **61**, 647–661.
- Aiya, S. V. C. (1954). Measurement of atmospheric noise interference to broadcasting. *J. atmos. terr. Phys.* **5**, 230–242.
- Aiya, S. V. C. (1955). Noise power radiated by tropical thunderstorms. *Proc. Inst. Radio Engrs, N.Y.* **43**, 966–974.
- Aiya, S. V. C. (1958). Atmospheric noise interference to short-wave broadcasting. *Proc. Inst. Radio Engrs, N.Y.* **46**, 580–589.
- Aiya, S. V. C. (1959). Measurement and description of the characteristics of atmospheric radio noise. *J. sci. industr. Res. India* **18B**, 43–47.
- Aiya, S. V. C., and Phadke, K. R. (1955). Atmospheric noise interference to broadcasting in the 3 Mc/s band at Poona. *J. atmos. terr. Phys.* **7**, 254–277.
- Allcock, G. McK. (1960). Propagation of whistlers to polar latitudes. *Nature, Lond.* **188**, 732–733.
- Allcock, G. McK. (1962). IGY whistler results. In “Radio Noise of Terrestrial Origin” (Horner, ed.), pp. 116–133, Elsevier, Amsterdam.
- Al’pert, Ya. L. (1956). Calculation of the field strength of long and very long radio waves above the earth’s surface in practical conditions. *Radiotekhnika i Elektronika* **1**, 281–282.
- Al’pert, Ya. L. (1960). “Radio Wave Propagation and the Ionosphere”, Chapter VII, U.S.S.R. Academy of Sciences Press, Moscow. (English translation published by Consultants Bureau, New York.)

- Al'pert, Ya. L., and Borodina, S. V. (1956). Investigation of the propagation of long and very long radio waves by the analysis of atmospheric waveforms. *Radiotekhnika i Elektronika* 1, 293–308.
- Atlas, D. (1958). Radar lightning echoes and atmospheric in vertical cross-section. In "Recent Advances in Atmospheric Electricity" (Smith, ed.), pp. 441–459, Pergamon Press, Oxford.
- Austin, L. W. (1927). Radio atmospheric disturbances and solar activity. *Proc. Inst. Radio Engrs, N. Y.* 15, 837–842.
- Balsler, M., and Wagner, C. A. (1960). Observations of earth-ionosphere cavity resonances. *Nature, Lond.* 188, 638–641.
- Barber, N. F., and Crombie, D. D. (1959). VLF reflections from the ionosphere in the presence of a transverse magnetic field. *J. atmos. terr. Phys.* 16, 37–45.
- Barlow, J. S., Frey, G. W., and Newman, J. B. (1954). Very low frequency noise power from the lightning discharge. *J. Franklin Inst.* 258, 187–203.
- Borodina, S. V., Kalinin, Yu K., Mikhailova, G. A., and Fligel, D. S. (1960). Survey of the present state of investigation of the propagation of very long electromagnetic waves. *Izv. vyssh. uch. Zav. Radiofizika* 3, 5–32.
- Bowe, P. W. A. (1951). The waveforms of atmospheric and the propagation of very-low-frequency radio waves. *Phil. Mag.* 42, 121–138.
- Brook, M., and Kitagawa, N. (1960a). Some aspects of lightning activity and related meteorological conditions. *J. geophys. Res.* 65, 1203–1210.
- Brook, M., and Kitagawa, N. (1960b). Electric-field changes and the design of lightning-flash counters. *J. geophys. Res.* 65, 1927–1931.
- Brook, M., and Vonnegut, B. (1960). Visual confirmation of the junction process in lightning discharges. *J. geophys. Res.* 65, 1302–1303.
- Brooks, C. E. P. (1925). Distribution of thunderstorms over the globe. *Met. Office Geophys. Memoirs and Prof. Notes*, No. 24.
- Brown, I. C. (1951). A radar echo from lightning. *Nature, Lond.* 167, 438.
- Bruce, C. E. R., and Golde, R. H. (1941). The lightning discharge. *J. Instn elect. Engrs* 88, 487–505.
- Budden, K. G. (1951). The propagation of a radio-atmospheric. *Phil. Mag.* 42, 1–19.
- Byers, H. R., and Braham, R. R. (1953). Thunderstorm structure and dynamics. In "Thunderstorm Electricity" (Byers, ed.), pp. 46–65, University of Chicago Press.
- Carbenay, F. (1952). Correlation between the mean level of atmospheric and the degree of intelligibility of a kilometre-wave radio link. *C. R. Acad. Sci., Paris* 235, 423–425 and 652.
- Carbenay, F. (1956). Recording the mean level of atmospheric at kilometric and myriametric wavelengths. *C. R. Acad. Sci., Paris* 243, 1904–1906.
- Carbenay, F. (1959). Recording the mean square value of atmospheric noise. *C. R. Acad. Sci., Paris* 249, 67–68.
- Caton, P. G. F., and Pierce, E. T. (1952). The waveforms of atmospheric. *Phil. Mag.* 43, 393–407.
- CCIR (1957). Revision of atmospheric noise data. *Report No. 65*. International Telecommunication Union, Geneva.
- Chapman, F. W., and Macario, R. C. V. (1956). Propagation of audio frequency radio waves to great distances. *Nature, Lond.* 177, 930–933.
- Chapman, J. (1957). The waveforms of atmospheric and the propagation of very low frequency radio waves. *J. atmos. terr. Phys.* 11, 223–236.
- Chiplonkar, M. W., Karekar, R. N., Raju, T. A., and Hattiangadi, M. S. (1958). A preliminary report on the nature and origin of atmospheric. *J. sci. industr. Res. India* 17A (Supplement) 3–23.

- Clarence, N. D., and Malan, D. J. (1957). Preliminary discharge processes in lightning flashes to ground. *Quart. J. R. met. Soc.* **83**, 161–172.
- Clarke, C. (1960a). Recording atmospheric radio noise. *Electron. Technol.* **37**, 346–349.
- Clarke, C. (1960b). A study of atmospheric radio noise received in a narrow bandwidth at 11 Mc/s. *Proc. Instn elect. Engrs* **107B**, 311–319.
- Clarke, C. (1960c). Atmospheric noise structure. *Electron. Technol.* **37**, 197–204.
- Clarke, C. (1962). Atmospheric radio noise studies based on amplitude-probability measurements at Slough, England, during the International Geophysical Year. *Proc. Instn elect. Engrs* **109B**, 393–404.
- Clarke, C., and Byrne, B. J. (1956). The location of thunderstorms by a single station high frequency ranging technique. *J. atmos. terr. Phys.* **9**, 210–228.
- Clarke, C., and Harrison, V. A. W. (1955). Low-frequency direction finder: twin channel cathode-ray design. *Wireless Engr* **32**, 109–114.
- Crichlow, W. Q. (1957). Noise investigation at VLF by the National Bureau of Standards. *Proc. Inst. Radio Engrs, N.Y.* **45**, 778–782.
- Crichlow, W. Q., Roubique, C. J., Spaulding, A. D., and Beery, W. M. (1960a). Determination of the amplitude-probability distribution of atmospheric radio noise from statistical moments. *J. Res. nat. Bur. Stand.* **64D**, 49–56.
- Crichlow, W. Q., Spaulding, A. D., Roubique, C. J., and Disney, R. T. (1960b). Amplitude-probability distributions for atmospheric radio noise. *Monogr. Nat. Bur. Stand.* No. 23, U.S. Government Printing Office, Washington, D.C.
- Crombie, D. D. (1960). On the mode theory of VLF propagation in the presence of a transverse magnetic field. *J. Res. nat. Bur. Stand.* **64D**, 265–267.
- Davis, R. (1962). Frequency of lightning flashovers on overhead lines. In “Gas Discharges and the Electricity Supply Industry” (Forrest, Howard and Littler, eds.), pp. 125–138, Butterworths, London.
- Davis, R. (1963). Lightning flashovers on the British grid. *Proc. Instn elect. Engrs* **110**, 969–974.
- Dinger, H. E. (1957). Unusual whistling atmospherics. *Onde élect.* **37**, 526–534.
- Dinger, H. E. (1960). A four-year summary of whistler activity at Washington, D.C. *J. geophys Res.* **65**, 571–575.
- Dinger, H. E., and Paine, H. G. (1947). Factors affecting the accuracy of radio noise meters. *Proc. Inst. Radio Engrs, N.Y.* **35**, 75–81.
- Eckersley, T. L. (1932). Studies in radio transmission. *J. Instn elect. Engrs* **71**, 405–454.
- Eckersley, T. L. (1935). Musical atmospherics. *Nature, Lond.* **135**, 104–105.
- Edwards, A. G. (1956). The effect of atmospherics on tuned circuits. *J. Brit. Instn Radio Engrs* **16**, 31–39.
- Foldes, G. (1960). The lognormal distribution and its applications to atmospheric studies. In “Statistical Methods of Radio Wave Propagation” (Hoffman, ed.), pp. 227–232, Pergamon Press, Oxford.
- Fulton, F. F. (1961). Effect of receiver bandwidth on the amplitude distribution of VLF atmospheric noise. *J. Res. nat. Bur. Stand.* **65D**, 299–304.
- Gardner, F. F. (1950). The use of atmospherics to study the propagation of very long radio waves. *Phil. Mag.* **41**, 1259–1269.
- Golde, R. H. (1961). Theoretical considerations on the protective effect of lightning conductors. *Elektrotech. Z (A)* **82**, 273–277.
- Hales, A. L. (1948). A possible mode of propagation of the “slow” or tail component of atmospherics. *Proc. roy. Soc.* **A193**, 60–71.
- Harwood, J. (1958). Atmospheric radio noise at frequencies between 10 kc/s and 30 kc/s. *Proc. Instn elect. Engrs* **105B**, 293–300.

- Harwood, J., and Harden, B. N. (1960). The measurement of atmospheric radio noise by an aural comparison method in the range 15–500 kc/s. *Proc. Instn elect. Engrs* **107B**, 53–59.
- Harwood, J., and Nicolson, C. (1958). Atmospheric radio noise. *Electronic Radio Engr* **35**, 183–190.
- Helliwell, R. A. and Gehrels, E. (1958). Observations of magnetoionic duct propagation using man-made signals of very low frequency. *Proc. Inst. Radio Engrs, N. Y.* **46**, 785–787.
- Helliwell, R. A., Jean, A. G., and Taylor, W. L. (1958). Some properties of lightning impulses which produce whistlers. *Proc. Inst. Radio Engrs, N. Y.* **46**, 1760–1762.
- Hepburn, F. (1957a). Waveguide interpretation of atmospheric waveforms. *J. atmos. terr. Phys.* **10**, 121–135.
- Hepburn, F. (1957b). Atmospheric waveforms with very low frequency components below 1 kc/s known as slow tails. *J. atmos. terr. Phys.* **10**, 266–287.
- Hepburn, F. (1960). Analysis of smooth-type atmospheric waveforms. *J. atmos. terr. Phys.* **19**, 37–53.
- Hepburn, F., and Pierce, E. T. (1953). Atmospheric with very low-frequency components. *Nature, Lond.* **171**, 837–838.
- Herman, J. (1961). Reliability of atmospheric radio noise predictions. *J. Res. nat. Bur. Stand.* **65D**, 565–574.
- Hewitt, F. J. (1957). Radar echoes from inter-stroke processes in lightning. *Proc. phys. Soc.* **70**, 961–979.
- Hewitt, F. J. (1962). Radar studies of sources of noise in lightning. In “Radio Noise of Terrestrial Origin” (Horner, ed.), pp. 72–84, Elsevier, Amsterdam.
- Hill, E. L. (1957). Electromagnetic radiation from lightning strokes. *J. Franklin Inst.* **263**, 107–119.
- Hoff, R. S. and Johnson, R. C. (1952). A statistical approach to the measurement of atmospheric noise. *Proc. Inst. Radio Engrs, N. Y.* **40**, 185–187.
- Hoffman, W. C. (1959). The current-jet hypothesis of whistler generation. *Planet. Space Sci.* **2**, 72–73.
- Hogg, D. (1950). The measurement of atmospheric radio noise in South Africa in the low frequency band. *Trans. S. Afr. Inst. elect. Engrs* **41**, 209–225.
- Hogg, D. (1955). Low-frequency atmospheric noise levels in Southern and Central Africa. *Trans. S. Afr. Inst. elect. Engrs* **46**, 341–348.
- Holzer, R. E. (1958). World thunderstorm activity and extra low frequency sferics. In “Recent Advances in Atmospheric Electricity” (Smith, ed.), pp. 559–607, Pergamon Press, Oxford.
- Holzer, R. E., and Deal, E. O. (1956). Low audio-frequency electromagnetic signals of natural origin. *Nature, Lond.* **177**, 536–537.
- Horner, F. (1953a). Measurements of atmospheric noise at high frequencies during the years 1945–1951. *Radio Research Special Report No. 26*, H.M.S.O. London, Code No. 47–29–26.
- Horner, F. (1953b). Radio direction finding: influence of buried conductors on bearings. *Wireless Engr* **30**, 187–191.
- Horner, F. (1953c). The reception of atmospheric noise at high frequencies. *J. atmos. terr. Phys.* **4**, 129–140.
- Horner, F. (1954). The accuracy of the location of sources of atmospheric noise by radio direction-finding. *Proc. Instn elect. Engrs* **101**, Part III, 383–390.
- Horner, F. (1957a). Very-low-frequency propagation and direction finding. *Proc. Instn elect. Engrs* **104B**, 73–80.
- Horner, F. (1957b). The relationship between the propagation of very long waves and the direction. *Onde élect.* **37**, 535–538.

- Horner, F. (1958). The relationship between atmospheric radio noise and lightning. *J. atmos. terr. Phys.* **13**, 140–154.
- Horner, F. (1960a). The thunderstorms of 5 September 1958—lightning discharges and atmospherics. *Met. Mag.* **89**, 257–260.
- Horner, F. (1960b). The design and use of instruments for counting local lightning flashes. *Proc. Instn elect. Engrs* **107B**, 321–330.
- Horner, F. (1961). Narrow band atmospherics from two local thunderstorms. *J. atmos. terr. Phys.* **21**, 13–25.
- Horner, F. (1962a). Atmospherics from near lightning discharges. In “Radio Noise of Terrestrial Origin” (Horner, ed.), pp. 85–97, Elsevier, Amsterdam.
- Horner, F. (1962b). Discussion on “IGY Whistler Data”. In “Radio Noise of Terrestrial Origin” (Horner, ed.), pp. 16–17, Elsevier, Amsterdam.
- Horner, F., and Bradley, P. A. (1964). The spectra of atmospherics from near lightning discharges. In course of publication.
- Horner, F., and Clarke, C. (1955). Some waveforms of atmospherics and their use in the location of thunderstorms. *J. atmos. terr. Phys.* **7**, 1–13.
- Horner, F., and Clarke, C. (1958). Radio noise from lightning discharges. *Nature, Lond.* **181**, 688–690.
- Horner, F., and Harwood, J. (1956). An investigation of atmospheric radio noise at very low frequencies. *Proc. Instn elect. Engrs* **103B**, 743–751.
- Ishikawa, H., and Kimpara, A. (1958). Lightning mechanism and atmospheric radiation. In “Recent Advances in Atmospheric Electricity” (Smith, ed.), pp. 583–588, Pergamon Press, Oxford.
- Ishikawa, H., and Takagi, M. (1953). On the atmospherics from a summer cumulonimbus. *Proc. Res. Inst. Atmospherics, Nagoya* **1**, 12–30.
- Ishikawa, H., and Takagi, M. (1954). On the fine structure of atmospherics from near origins. *Proc. Res. Inst. Atmospherics, Nagoya* **2**, 9–25.
- Ito, K., Kato, T., and Iwai, A. (1955). Local lightning flash counter within 20 km. *Proc. Res. Inst. Atmospherics, Nagoya* **3**, 69–74.
- Iwai, A., and Otsu, J. (1958). On the characteristic phenomena for short whistlers observed at Toyokawa in winter. *Proc. Res. Inst. Atmospherics, Nagoya* **5**, 53–63.
- Iwai, A., Ito, K., Tanaka, T., and Ebuchi, T. (1953). Direction finder of atmospherics. *Proc. Res. Inst. Atmospherics, Nagoya* **1**, 54–61.
- Jean, A. G., Taylor, W. L., and Wait, J. R. (1960). VLF phase characteristics deduced from atmospheric wave forms. *J. geophys Res.* **65**, 907–912.
- Jean, A. G., Murphy, A. C., Wait, J. R., and Wasmundt, D. F. (1961). Observed attenuation rate of ELF radio waves. *J. Res. nat. Bur. Stand.* **65D**, 475–479.
- Jones, H. L. (1951). A spheric method of tornado identification and tracking. *Bull. Amer. met. Soc.* **32**, 380.
- Jones, H. L. (1958). The identification of lightning discharges by spheric characteristics. In “Recent Advances in Atmospheric Electricity” (Smith, ed.), pp. 543–556, Pergamon Press, Oxford.
- Jones, R. F. (1954). Radar echoes from lightning. *Quart. J. R. met. Soc.* **80**, 579–582.
- Kamada, T. (1953). Some notes on the record of multiple strokes obtained with the atmospherics direction finder. *Proc. Res. Inst. Atmospherics, Nagoya* **1**, 90–98.
- Kamada, T., and Nakajima, J. (1954). The measurement of the intensity of atmospherics (1). *Proc. Res. Inst. Atmospherics, Nagoya* **2**, 31–39.
- Kessler, W. J., and Hersperger, S. P. (1952). Recent developments in radio location of thunderstorm centres. *Bull. Amer. met. Soc.* **33**, 153–157.

- Kift, F. (1960). The propagation of high-frequency radio waves to long distances. *Proc. Instn elect. Engrs* **107B**, 127–140.
- Kimpara, A. (1953). The waveform of atmospherics in the daytime. *Proc. Res. Inst. Atmospheric, Nagoya* **1**, 1–11.
- Kimpara, A. (1955). Atmospherics in the Far East. *Proc. Res. Inst. Atmospheric, Nagoya* **3**, 1–28.
- Kimpara, A., and Kimura, Y. (1958). On field intensity recording of atmospherics at 27 kc/s in accordance with the recommendation of W.M.O. *Proc. Res. Inst. Atmospheric, Nagoya* **5**, 21–29.
- Kitagawa, N., and Kobayashi, M. (1958). Field-changes and variations in luminosity due to lightning flashes. In “Recent Advances in Atmospheric Electricity” (Smith, ed.), pp. 485–501, Pergamon Press, Oxford.
- Kitagawa, N. and Brook, M. (1960). A comparison of intracloud and cloud-to-ground lightning discharges. *J. geophys. Res.* **65**, 1189–1201.
- König, H. (1959). Atmospherics of very low frequency. *Z. angew. Phys.* **11**, 264–274.
- Laby, T. H., McNeill, J. J., Nicholls, F. G., and Nickson, A. F. B. (1940). Waveform, energy and reflexion by the ionosphere of atmospherics. *Proc. roy. Soc.* **174**, 145–163.
- Lakshminarayan, K. N. (1962). Short term time characteristics of impulsive atmospheric noise. *J. Sci. Ind. Res. India* **21D**, 228–232.
- Large, M. I., and Wormell, T. W. (1958). Fluctuations in the vertical electric field in the frequency range from 1 c/s to 500 c/s. In “Recent Advances in Atmospheric Electricity” (Smith, ed.), pp. 603–607, Pergamon Press, Oxford.
- Lauter, E. A., and Schmelovsky, K. H. (1958). On the interpretation of the sunrise effect in the very long wave range. *Beitr. Geophys.* **67**, 218–231.
- Lewis, E. A., Harvey, R. B., and Rasmussen, J. E. (1960). Hyperbolic direction finding with sferics of transatlantic origin. *J. geophys. Res.*, **65**, 1879–1905.
- Lichter, Ya. I. (1956). Some statistical properties of atmospherics. *Radiotekhnika i Elektronika* **1**, 1295–1302.
- Lichter, Ya. I., and Terina, G. J. (1960). Some results of the investigations of the intensity of atmospheric radio noise in Moscow. In “Some Ionospheric Results Obtained during the IGY” (Beynon, ed.), pp. 376–382. Elsevier, Amsterdam.
- Liebermann, L. (1956). Extremely low-frequency electromagnetic waves. *J. appl. Phys.* **27**, 1473–1483.
- Ligda, M. G. H. (1950). Lightning detection by radar. *Bull. Amer. met. Soc.* **31**, 279–283.
- Ligda, M. G. H. (1956). The radar observation of lightning. *J. atmos. terr. Phys.* **9**, 329–346.
- Lugeon, J. (1939). The radiogoniograph of the Swiss Central Meteorological Station and its use for weather forecasting. *Ann. Sta. cent. Suisse de Meteorologie, Zurich*, No. 10.
- Lugeon, J., and Rieker, J. (1957). The Swiss storm counter. *Ann. schweiz. met. Zent Anst.* No. 9.
- Lugeon, J., and Rieker, J. (1958). Comparison between the narrow-sector recorder and the cathode ray direction finder. *Verh. schweiz. naturf. Ges.* 106–107.
- Lutkin, F. E. (1938). Directional recording of radio atmospherics. *J. Instn elect. Engrs* **82**, 289–302.
- Malan, D. J. (1955). Luminous discharges in storm clouds. *Ann. Geophys.* **11**, 427–434.

- Malan, D. J. (1956a). The relation between the number of strokes, stroke interval and the total durations of lightning discharges. *Geofis. pur. appl.* **34**, 224–230.
- Malan, D. J. (1956b). Visible electrical discharges inside thunderclouds. *Geofis. pur. appl.* **34**, 221–223.
- Malan, D. J. (1958). Radiation from lightning discharges and its relation to the discharge process. In “Recent Advances in Atmospheric Electricity” (Smith, ed.), pp. 557–563. Pergamon Press, Oxford.
- Malan, D. J. (1959). Lightning. *Endeavour* **18**, 61–69.
- Malan, D. J. (1961). Unusual types of lightning discharges. *Ann. Geophys.* **17**, 388–394.
- Malan, D. J. (1962). Lightning counter for flashes to ground. In “Gas Discharges and the Electricity Supply Industry” (Forrest, Howard and Littler, eds.), pp. 112–116. Butterworths, London.
- Marshall, J. S. (1953). Frontal precipitation and lightning observed by radar. *Canad. J. Phys.* **31**, 194–203.
- Martin, L. H. (1958). Whistlers in the Antarctic. *Nature, Lond.* **181**, 1796–1797.
- Martin, L. H. (1960). Observations of whistlers and chorus at the South Pole. *Nature, Lond.* **187**, 1018–1019.
- Maxwell, E. L., and Stone, D. L. (1963). Natural noise fields from 1 c/s to 100 kc. *Trans. Inst. electrical and electronics Engrs AP-11*, 339–343.
- McKerrow, C. A. (1957). Some recent measurement of atmospheric noise in Canada. *Proc. Inst. Radio Engrs, N.Y.* **45**, 782–786.
- McKerrow, C. A. (1960). Some measurements of atmospheric noise levels at low and very low frequencies in Canada. *J. geophys. Res.* **65**, 1911–1926.
- Miles, V. G. (1953). Radar echoes associated with lightning. *J. atmos. terr. Phys.* **3**, 258–262.
- Montgomery, G. F. (1954). A comparison of amplitude and angle modulation for narrow-band communication of binary-coded messages in fluctuation noise. *Proc. Inst. Radio Engrs, N.Y.* **42**, 447–454.
- Morgan, M. G. (1958). Correlation of whistlers and lightning flashes by direct aural and visual observation. *Nature, Lond.* **182**, 332–333.
- Morgan, M. G., and Dinger, H. E. (1956). Observations of whistling atmospheric at geomagnetically conjugate points. *Nature, Lond.* **177**, 29–30.
- Morrison, R. B. (1953). The variation with distance in the range 0–100 km of atmospheric waveforms. *Phil. Mag.* **44**, 980–986.
- Müller-Hillebrand, D. (1959). Lightning counter and results obtained in Sweden during the thunderstorm period 1958. *J. Sci. tech. Res., Stockholm* **30**, 217–233.
- Müller-Hillebrand, D. (1961). The physics of the lightning discharge. *Elektrotech. Z. (A)* **82**, 232–249.
- Müller-Hillebrand, D. (1963). Lightning counters: I. The change in electric field due to lightning strokes, with reference to its effect on lightning counters. *Ark. Geophys.* **4**, 247–269. II. The effect of changes of electric field on counter circuits. *Ibid.* **271**–291.
- Nakai, T. (1956). The distance of the source and the height of reflection deduced from the waveforms of ionospheric reflection type. *Proc. Res. Inst. Atmospherics, Nagoya* **4**, 20–28.
- Nakai, T. (1958). Atmospheric noise study by measurement of the amplitude probability distribution. *Proc. Res. Inst. Atmospherics, Nagoya* **5**, 30–49.
- Nakai, T. (1959). A study of atmospheric noise at 50 kc. *Proc. Res. Inst. Atmospherics, Nagoya* **6**, 22–37.
- Nakai, T. (1960). The study of the amplitude probability distributions of atmospheric radio noise. *Proc. Res. Inst. Atmospherics, Nagoya* **7**, 12–27.

- Nakai, T., and Suzuki, Y. (1961). Study of various parameters of atmospheric radio noise at 50 kc/s. *Proc. Res. Inst. Atmospherics, Nagoya* 8, 23–37.
- Norinder, H. (1947). Some aspects and recent results of electromagnetic effects of thunderstorms. *J. Franklin Inst.* 244, 109–130 and 167–207.
- Norinder, H. (1949). On the measurement and nature of atmospherics produced by electric discharges in snow squalls and from other sources. *Tellus* 1, 1–13.
- Norinder, H. (1951). The electrical field variations radiated from lightning discharges. *Proc. Second Meeting of the Joint Commission on Radio Meteorology, URSI Brussels*, 17–37.
- Norinder, H., and Knudsen, E. (1958). Analysis of daylight photographs of lightning paths. In “Recent Advances in Atmospheric Electricity” (Smith, ed.), pp. 503–524. Pergamon Press, Oxford.
- Norinder, H., and Knudsen, E. (1959). The relation between lightning discharges and whistlers. *Planet. Space Sci.* 1, 173–183.
- Norinder, H., Knudsen, E., and Vollmer, B. (1958). Multiple strokes in lightning channels. In “Recent Advances in Atmospheric Electricity” (Smith, ed.), pp. 525–542. Pergamon Press, Oxford.
- Obayashi, T. (1960). Measured frequency spectra of very-low-frequency atmospherics. *J. Res. nat. Bur. Stand.* 64D, 41–48.
- Obayashi, T., Fujii, S., and Kidokoro, T. (1959). An experimental proof of the mode theory of VLF ionospheric propagation. *J. Geomagn. Geoelect., Kyoto* 10, 47–55.
- Otsu, J., and Shiga, T. (1955). Calculation of interference error on a crossed-loop type CRDF. *Proc. Res. Inst. Atmospherics, Nagoya* 3, 63–68.
- Pierce, E. T. (1955a). The development of lightning discharges. *Quart. J. R. met. Soc.* 81, 229–240.
- Pierce, E. T. (1955b). Electrostatic field-changes due to lightning discharges. *Quart. J. R. met. Soc.* 81, 211–228.
- Pierce, E. T. (1956a). The influence of individual variations in the field changes due to lightning discharges upon the design and performance of lightning flash counters. *Arch. Met., Wien* 9, 78–86.
- Pierce, E. T. (1956b). Some techniques for locating thunderstorms from a single observing station. In “Vistas in Astronomy” (Beer, ed.), Vol. 2, pp. 850–855. Pergamon Press, Oxford.
- Pierce, E. T. (1960a). Atmospherics from lightning flashes with multiple strokes. *J. geophys Res.* 65, 1867–1871.
- Pierce, E. T. (1960b). The propagation of radio waves of frequency less than 1 kc. *Proc. Inst. Radio Engrs, N.Y.* 48, 329–331.
- Pierce, E. T. (1960c). Some ELF phenomena. *J. Res. nat. Bur. Stand.* 64D, 383–386.
- Pierce, E. T. (1962). Sources of atmospheric noise in lightning. In “Radio Noise of Terrestrial Origin” (Horner, ed.), pp. 55–71. Elsevier, Amsterdam.
- Prentice, S. A. (1960). Thunderstorms in the Brisbane area. *J. Instn elect. Engrs Australia* 32, 33–45.
- Rieker, J. (1960). Sunrise in the ionosphere and its influence on the propagation of long waves. *Geofis. pur. appl.* 46, 241–328.
- Rivault, R. (1945). The fine structure of atmospherics; contribution to the study of the ionosphere. *C. R. Acad. Sci., Paris* 221, 540–542.
- Rivault, R. (1950). The fine structure of atmospherics; ionospheric and meteorological applications of Type 4. *C. R. Acad. Sci., Paris* 230, 1846–1847.
- Rivault, R. (1957). Characteristics of whistlers observed in the course of a year. *Onde élect.* 37, 539–540.

- Rivault, R., and Corcuff, Y. (1960). Research on the magnetic conjugate point to Poitiers; night-time variations in dispersion of whistlers. *Ann. Geophys.* **16**, 550–554.
- Robertson, L. M., Lewis, W. W., and Forest, C. M. (1942). Lightning investigation at high altitudes in Colorado. *Elect. Engng, N.Y.* **61**, 201–208.
- Sao, K. (1955). Frequency spectrum of the daytime waveform of atmospherics radiated from the return streamer of a lightning flash. *Proc. Res. Inst. Atmospherics, Nagoya* **3**, 43–45.
- Sao, K., and Jindo, H. (1961). Researches in the frequency analysis of waveforms of atmospherics III. *Proc. Res. Inst. Atmospherics, Nagoya* **8**, 19–21.
- Satyam, M. (1962). Short term amplitude probability distribution of impulsive atmospheric radio noise. *J. Sci. Ind. Res. India* **21D**, 221–227.
- Schafer, J. P., and Goodall, W. M. (1939). Peak field strengths of atmospherics due to local thunderstorms at 150 megacycles. *Proc. Inst. Radio Engrs, N.Y.* **27**, 202–207.
- Schmoys, J. (1956). Long-range propagation of low-frequency radio waves between the earth and the ionosphere. *Proc. Inst. Radio Engrs, N.Y.* **44**, 163–170.
- Schonland, B. F. J. (1938). Progressive lightning IV. The discharge mechanism. *Proc. roy. Soc.* **A164**, 132–150.
- Schonland, B. F. J. (1956). The lightning discharge. In “Handbuch der Physik” (Flügge, ed.), Vol. 22, pp. 576–628. Springer Verlag, Berlin.
- Schonland, B. F. J., and Gane, P. G. (1947). A lightning warning device. *Trans S. Afr. Inst. elect. Engrs* **38**, 119–122.
- Schonland, B. F. J., Hodges, D. B., and Collins, H. (1938). Progressive lightning V. A comparison of photographic and electrical studies of the discharge process. *Proc. roy. Soc.* **A166**, 56–75.
- Schonland, B. F. J., Elder, J. S., Hodges, D. B., Phillips, W. E., and Van Wyk, J. W. (1940). The waveform of atmospherics at night. *Proc. roy. Soc.* **A176**, 180–202.
- Schumann, W. O. (1952). Nonradiative natural oscillations of a conducting sphere surrounded by a layer of air and an ionospheric sheath. *Z. Naturf.* **7a**, 149–154.
- Silleni, S. (1953). Measurement of the intelligibility of radiotelegraph signals. *Ann. Geofis.* **6**, 137–153.
- Skeib, G. (1957). On the accuracy of the determination of height of reflection and distances of atmospheric disturbances from their waveforms. *Z. Met.* **11**, 129–135.
- Spaulding, A. D., Roubique, C. J., and Crichlow, W. Q. (1962). Conversion of the amplitude-probability distribution function for atmospheric radio noise from one bandwidth to another. *J. Res. nat. Bur. Stand.* **66D**, 713–720.
- Stergis, C. G., and Doyle, J. W. (1958). Location of near lightning discharges. In “Recent Advances in Atmospheric Electricity” (Smith, ed.), pp. 589–596. Pergamon Press, Oxford.
- Storey, L. R. O. (1953). An investigation of whistling atmospherics. *Phil. Trans.* **246A**, 113–141.
- Storey, L. R. O. (1962). Whistler theory. In “Radio Noise of Terrestrial Origin” (Horner, ed.), pp. 134–160. Elsevier, Amsterdam.
- Sullivan, A. W., and Wells, J. D. (1957). A lightning stroke counter. *Bull. Amer. met. Soc.* **38**, 291–294.
- Sullivan, A. W., van Valkenburg, H. M., and Barney, J. M. (1952). Low frequency atmospheric radio noise in Florida. *Trans. Amer. geophys. Un.* **33**, 650.
- Takagi, M., and Takeuti, T. (1963). Atmospherics radiation from lightning discharges. *Proc. Res. Inst. Atmospherics, Nagoya* **10**, 1–11.

- Takagi, M., Ishikawa, H., and Takeuti, T. (1959). On the structures of flashes and atmospherics accompanied by cloud discharges. *Proc. Res. Inst. Atmospheric, Nagoya* 6, 1-16.
- Takeuti, T., Ishikawa, H., and Takagi, M. (1960). On the cloud discharge preceding the first ground stroke. *Proc. Res. Inst. Atmospheric, Nagoya* 7, 1-6.
- Tamura, Y. (1958). Investigations on the electrical structure of thunderstorms. In "Recent Advances in Atmospheric Electricity" (Smith, ed.), pp. 269-276. Pergamon Press, Oxford.
- Tantry, B. A. P., Srivastava, R. S., and Khastgir, S. R. (1957). Waveform studies of electric field changes during cloud-to-cloud lightning discharges. *Proc. nat. Inst. Sci. India* 23A, 499-503.
- Taylor, W. L. (1960a). VLF attenuation for east-west and west-east daytime propagation using atmospherics. *J. geophys Res.* 65, 1933-1938.
- Taylor, W. L. (1960b). Daytime attenuation rates in the very low frequency band using atmospherics. *J. Res. nat. Bur. Stand.* 64D, 349-355.
- Taylor, W. L. (1963). Radiation-field characteristics of lightning discharges in the band 1 kc/s to 100 kc/s. *J. Res. nat. Bur. Stand.* 67D, 539-550.
- Taylor, W. L., and Jean, A. G. (1959). Very-low-frequency radiation spectra of lightning discharges. *J. Res. nat. Bur. Stand.* 63D, 199-204.
- Taylor, W. L., and Lange, L. J. (1958). Some characteristics of VLF propagation using atmospheric waveforms. In "Recent Advances in Atmospheric Electricity" (Smith, ed.), pp. 609-617. Pergamon Press, Oxford.
- Tepley, L. R. (1959). A comparison of sferics as observed in the very low frequency and extremely low frequency bands. *J. geophys Res.* 64, 2315-2329.
- Thomas, H. A. (1950). A subjective method of measuring radio noise. *Proc. Instn elect. Engrs* 97, Part III, 329-334.
- Thomas, H. A., and Burgess, R. E. (1947). Survey of existing information and data on radio noise over the frequency range 1-30 Mc/s. *Radio Research Special Report No. 15*, H.M.S.O. London, Code No. 47-29-15.
- Ungstrup, E. (1959). Observations of whistlers and very low frequency phenomena at Godhavn, Greenland. *Nature, Lond.* 184, 806-807.
- URSI (1962). The measurement of characteristics of terrestrial radio noise. *Special Report No. 7*, Elsevier, Amsterdam.
- Vonnegut, B., and Moore, C. B. (1958). Giant electric storms. In "Recent Advances in Atmospheric Electricity" (Smith, ed.), pp. 399-411. Pergamon Press, Oxford.
- Wait, J. R. (1956). On the waveform of a radio atmospheric at short ranges. *Proc. Inst. Radio Engrs, N. Y.* 44, 1052.
- Wait, J. R. (1957a). The attenuation versus frequency characteristics of VLF radio waves. *Proc. Inst. Radio Engrs, N. Y.* 45, 768-771.
- Wait, J. R. (1957b). The mode theory of VLF ionospheric propagation for finite ground conductivity. *Proc. Inst. Radio Engrs, N. Y.* 45, 760-767.
- Wait, J. R. (1957c). A note on the propagation of the transient ground wave. *Canad. J. Phys.* 35, 1146-1151.
- Wait, J. R. (1958a). Transmission loss curves for propagation at very low radio frequencies. *Trans. Instn Radio Engrs (PGCS) CS-6*, 58-61.
- Wait, J. R. (1958b). Propagation of very-low-frequency pulses to great distances. *J. Res. nat. Bur. Stand.* 61, 187-203.
- Wait, J. R. (1958c). A study of VLF field strength data, both old and new. *Geofis. pur. appl.* 41, 73-85.
- Wait, J. R. (1960a). On the theory of the slow-tail portion of atmospheric waveforms. *J. geophys. Res.* 65, 1939-1946.

- Wait, J. R. (1960b). Mode theory and the propagation of ELF radio waves. *J. Res. nat. Bur. Stand.* **64D**, 387–404.
- Wait, J. R. (1960c). Diffractive corrections to the geometrical optics of low frequency propagation. In “Electromagnetic Wave Propagation” (M. Désirant and J. L. Michiels, eds.), pp. 87–101. Academic Press, London.
- Wait, J. R. (1962a). Survey and bibliography of recent research in the propagation of VLF radio waves. In “Radio Noise of Terrestrial Origin” (Horner, ed.), pp 176–202. Elsevier, Amsterdam.
- Wait, J. R. (1962b). “Electromagnetic Waves in Stratified Media”, Pergamon Press, Oxford.
- Wait, J. R. (1962c). Average decay laws for VLF fields. *Proc. Inst. Radio Engrs, N. Y.* **50**, 53–56.
- Wait, J. R., and Murphy, A. (1956). Multiple reflections between the earth and the ionosphere in VLF propagation. *Geofis. pur. appl.* **35**, 61–72.
- Wait, J. R., and Murphy, A. (1957). The geometrical optics of VLF sky wave propagation. *Proc. Inst. Radio Engrs, N. Y.* **45**, 754–760.
- Wait, J. R., and Spies, K. (1960). Influence of earth curvature and the terrestrial magnetic field on VLF propagation. *J. geophys. Res.* **65**, 2325–2331.
- Watt, A. D. (1960). ELF electric fields from thunderstorms. *J. Res. nat. Bur. Stand.* **64D**, 425–433.
- Watt, A. D., and Maxwell, E. L. (1957a). Characteristics of atmospheric noise from 1 to 100 kc. *Proc. Inst. Radio Engrs, N. Y.* **45**, 788–794.
- Watt, A. D., and Maxwell, E. L. (1957b). Measured statistical characteristics of atmospheric radio noise. *Proc. Inst. Radio Engrs, N. Y.* **45**, 55–62.
- Watt, A. D., Coon, R. M., Maxwell, E. L., and Plush, R. W. (1958). Performance of some radio systems in the presence of thermal and atmospheric noise. *Proc. Inst. Radio Engrs, N. Y.* **46**, 1914–1923.
- Watt, A. D., Maxwell, E. L., and Whelan, E. H. (1959). Low frequency propagation paths in arctic areas. *J. Res. nat. Bur. Stand.* **63D**, 99–112.
- Weatherburn, C. E. (1957). “A First Course in Mathematical Statistics”, p. 64. Cambridge University Press, London.
- Willis, H. F. (1948). Audio frequency magnetic fluctuations. *Nature, Lond.* **161**, 887–888.
- WMO (1953). World distribution of thunderstorm days. *Report WMO/OMM No. 21*. World Meteorological Organisation, Geneva.
- Workman, E. G., Brook, M., and Kitagawa, N. (1960). Lightning and charge storage. *J. geophys. Res.* **65**, 1513–1517.
- Wormell, T. W. (1939). The effects of thunderstorms and lightning discharges on the earth’s electric field. *Phil. Trans.* **A238**, 249–303.
- Yabsley, D. E. (1950). Atmospheric noise levels at radio frequencies near Darwin. *Aust. J. sci. Res. Series A3*, 409–416.
- Yuhara, H., Ishida, T., and Hagashimura, M. (1956). Measurement of the amplitude probability distribution of atmospheric noise. *J. Radio Labs. Tokyo* **3**, 101–108.

AUTHOR INDEX

*Numbers in italics refer to the pages on which references are listed
at the end of each article*

A

Aarons, J., 129, 151, 179, *194*
Adgie, R. L., 67, *112*
Adler, R., 50, 52, *112*
Aitchison, R. E., 106, *118*
Aiya, S. V. C., 137, 140, 142, 146, 171,
180, *194*
Allcock, G. McK., 192, 193, *194*
Allen, C. W., 11, 16, 24, 35
Allen, L. R., 103, 104, *116*
Al'pert, Ya. L., 147, 149, 153, *194, 195*
Alsop, L. E., 53, *113*
Altenhoff, W., 70, 76, *112, 115*
Anderson, B., 104, *116*
Ano, K., 50, *115*
Appleton, E. V., 7, 8, 31, 32, 35
Apushkinskii, G. P., 49, *112*
Armstrong, L. D., 56, *112*
Ashkin, A., 52, *112*
Ashmead, J., 94, *116*
Atlas, D., 127, 128, 138, 139, *195*
Austin, L. W., 174, 179, *195*

B

Balsler, M., 154, *195*
Barber, N. F., 149, *195*
Barlow, J. S., 129, *195*
Barney, J. M., 155, 160, *202*
Bazzard, G. H., 8, 9, 10, 11, 13, 14, 15,
16, 17, 21, 22, 23, 24, 29, 30, 35, 36
Beery, W. M., 167, *196*
Beynon, W. J. G., 8, 15, 35
Blackwell, L. A., 49, *112*
Bloembergen, N., 53, *112*
Blum, E. J., 69, 96, 101, 107, 108, *112,*
116
Blythe, J. H., 108, 112, *116*
Boischot, A., 96, 101, 107, 108, *116*
Bolton, J. G., 87, 101, *115, 116*
Borodina, S. V., 147, 153, *195*
Bowe, P. W. A., 187, *195*
Bowen, E. G., 76, 86, *115*

Braccesi, A., 106, *116*
Bracewell, R. N., 37, 38, 39, 41, 98, 99,
107, 108, *116, 119*
Bradley, P. A., 132, 137, 139, 143, *198*
Braham, R. R., 144, *195*
Bridgeman, T. H., 59, *113*
Brook, M., 124, 125, 126, 127, 130, 133,
144, *195, 199, 204*
Brooks, C. E. P., 146, *195*
Broun, W. N., 80, *116*
Brown, G. M., 8, 15, 35
Brown, I. C., 127, *195*
Brown, R. H., 101, 102, 104, *116, 117*
Bruce, C. E. R., 128, 133, 143, *195*
Budden, K. G., 153, *195*
Burgess, R. E. 123, 171, *203*
Burkard, O., 19, 35
Burke, B. F., 67, *113*
Byers, H. R., 144, *195*
Byrne, B. J., 188, *196*

C

Calvin, R. S., 63, *113*
Carbenay, F., 156, 159, 175, *195*
Casey, D. W., 71, *113*
Caton, P. G. F., 151, 153, 188, *195*
Ceccarelli, M., 106, *116*
Chapman, F. W., 150, 156, *195*
Chapman, J., 151, *195*
Chapman, S., 4, 8, 35
Chiplonkar, M. W., 169, 184, *195*
Christiansen, W. N., 105, 106, 107, 108,
117
Clarence, N. D., 126, 131, *196*
Clarke, C., 127, 133, 153, 156, 158, 160,
161, 162, 163, 167, 172, 173, 180, 184,
188, *196, 198*
Cohen, M. H., 80, *115*
Collins, H., 127, *202*
Conway, R. G., 104, *116*
Coon, R. M., 182, 183, *204*
Cooper, B. F. C., 48, 53, 54, 80, *113,*
114, 115

Corcuff, Y., 192, 202
 Covington, A. E., 8, 36, 106, 107, 117
 Crichlow, W. Q., 155, 157, 167, 168, 169,
 196, 202
 Crombie, D. D., 149, 195, 196

D

Das Gupta, M. K., 101, 102, 117
 Davis, R., 146, 196
 Deal, E. O., 154, 197
 De Grasse, R. W., 54, 55, 113
 De Jager, J. T., 51, 52, 114
 Denisse, J. F., 8, 35, 108, 116
 Dicke, R. H., 44, 57, 113
 Dinger, H. E., 156, 171, 190, 192, 196,
 200
 Disney, R. T., 167, 196
 Doyle, J. W., 184, 185, 202
 Drake, F. D., 49, 59, 84, 113, 115
 Dyson, J. D., 94, 117

E

Ebuchi, T., 184, 198
 Eckersley, T. L., 150, 190, 196
 Ecklund, E. T., 67, 113
 Edwards, A. G., 139, 196
 Elder, J. S., 188, 202
 Elgaroy, O., 104, 117
 Erickson, W. C., 106, 117
 Esaki, L., 55, 113
 Ewen, H. I., 49, 59, 113
 Eyfrig, R., 8, 10, 11, 25, 36

F

Findlay, J. W., 88, 115
 Firor, J. W., 67, 113
 Fligel, D. S., 195
 Foldes, G., 165, 196
 Forest, C. M., 143, 193, 202
 Frey, G. W., 129, 195
 Fujii, S., 151, 201
 Fulton, F. F., 167, 168, 196

G

Gallet, R., 25, 36
 Gane, P. G., 144, 202
 Gardner, F. F., 51, 113, 151, 196
 Gehrels, E., 192, 197

Giordmaine, J. A., 53, 113
 Golde, R. H., 128, 133, 143, 146, 195, 196
 Goldenberg, H. M., 53, 114
 Goldstein, S. J., 69, 113
 Goodall, W. M., 18, 19, 36, 138, 139, 202
 Goodman, J., 71, 113
 Gordon, W. E., 95, 117
 Greene, J. C., 48, 113

H

Hagashimura, M., 161, 165, 166, 204
 Hales, A. L., 149, 196
 Haneman, F. G., 59, 113
 Harden, B. N., 155, 174, 180, 197
 Harnischmacher, E., 11, 36
 Harris, D. E., 48, 113
 Harrison, V. A. W., 184, 196
 Harting, E., 107, 117
 Harvey, R. B., 189, 199
 Harwood, J., 155, 159, 160, 161, 163,
 165, 166, 168, 170, 174, 180, 196, 197,
 198
 Hatanaka, T., 108, 117
 Hattiangadi, M. S., 169, 195
 Haus, H. A., 40, 47, 113
 Head, A. K., 94, 117
 Heffner, H., 50, 113
 Heinlein, W., 50, 113
 Helliwell, R. A., 192, 193, 197
 Hepburn, F., 129, 149, 150, 151, 197
 Herman, J., 180, 197
 Hersperger, S. P., 188, 198
 Hewish, A., 106, 108, 110, 111, 112, 117,
 118
 Hewitt, F. J., 127, 128, 197
 Hill, E. L., 129, 140, 197
 Hodges, P. B., 127, 188, 202
 Hoff, R. S., 161, 163, 197
 Hoffman, W. C., 193, 197
 Highbom, J. A., 106, 117
 Hogg, D., 160, 197
 Hogland, B., 67, 113
 Holzer, R. E., 150, 153, 197
 Horner, F., 126, 127, 128, 132, 133, 137,
 138, 139, 140, 142, 143, 144, 145, 153,
 155, 156, 159, 160, 161, 163, 165, 166,
 169, 170, 174, 184, 185, 186, 187, 188,
 192, 197, 198
 Hrbek, G., 50, 52, 112
 Hughes, V. A., 70, 113
 Husband, H. C., 87, 115

I

Ishida, T., 161, 165, 166, 204
 Ishikawa, H., 124, 126, 127, 130, 133,
 198, 203
 Ito, K., 144, 184, 198
 Iwai, A., 144, 184, 193, 198

J

Jasik, H., 76, 77, 115
 Jean, A. G., 139, 150, 151, 186, 192, 193,
 197, 198, 203
 Jelley, J. V., 50, 53, 55, 114
 Jennison, R. C., 101, 102, 117
 Jindo, H., 187, 202
 Johnson, R. C., 161, 163, 197
 Jones, H. L., 126, 130, 139, 184, 198
 Jones, R. F., 127, 198

K

Kakinuma, T., 105, 118
 Kalachov, P. D., 98, 106, 117
 Kalinin, Yu. K., 147, 195
 Kamada, T., 125, 160, 198
 Karekar, R. N., 169, 195
 Kato, T., 144, 198
 Kay, A. F., 96, 117
 Kerblai, T. S., 30, 36
 Kerr, F. J., 87, 115
 Kessler, W. J., 188, 198
 Khastgir, S. R., 203
 Kidokoro, T., 151, 201
 Kift, F., 153, 199
 Kimpapa, A., 124, 126, 127, 128, 129,
 130, 133, 151, 198, 199
 Kimura, Y., 151, 199
 Kitagawa, N., 124, 125, 126, 127, 130,
 133, 144, 195, 199, 204
 Kleffner, D., 53, 114
 Knudsen, E., 126, 129, 192, 193, 201
 Ko, H. C., 96, 117
 Kobayashi, M., 126, 199
 König, H., 154, 199
 Kostelnick, J. J., 55, 113
 Kotzabue, K. L., 49, 112
 Kovalevskaya, E. M., 30, 36
 Kraus, J. D., 96, 117
 Krishnan, T., 107, 117
 Kuiper, J. W., 71, 113
 Kundu, M. R., 8, 35

L

Labrum, N. R., 107, 117
 Laby, T. H., 188, 199
 Lakshminarayan, K. N., 173, 199
 La Londe, L. M., 95, 117
 Lange, L. J., 150, 203
 Large, M. I., 129, 179, 199
 Lauter, E. A., 151, 199
 Lebenbaum, M., 71, 113
 Lequeux, J., 96, 101, 107, 108, 116, 117,
 119
 Levy, G. S., 79, 116
 Lewis, E. A., 189, 199
 Lewis, W. W., 143, 193, 202
 Lichter, Ya. I., 161, 163, 165, 167, 180,
 199
 Liebermann, L., 151, 199
 Ligda, M. G. H., 126, 127, 128, 199
 Little, A. G., 51, 104, 105, 106, 114, 118
 Lo, Y. T., 93, 118
 Louisell, W. H., 49, 114
 Love, A. W., 94, 95, 117
 Lovell, A. C. B., 87, 115
 Lugeon, J., 144, 151, 186, 199
 Lutkin, F. E., 186, 199
 Lyon, A. J., 8, 35

M

McAdam, W. B., 106, 118
 Macario, R. C. V., 150, 156, 195
 McCready, L. L., 71, 98, 115, 118
 McCullough, T. P., 80, 116
 McGee, R. X., 67, 114
 McKerrow, C. A., 161, 180, 200
 McNeill, J. D., 70, 114
 McNeill, J. J., 188, 199
 Malan, D. J., 125, 126, 127, 131, 133,
 145, 196, 199, 200
 Maltby, P., 101, 118
 Marshall, J. S., 127, 200
 Martin, L. H., 200
 Mathewson, D. S., 107, 108, 117
 Maxwell, A., 71, 114
 Maxwell, E. L., 139, 140, 154, 161, 162,
 163, 172, 173, 179, 182, 183, 200, 204
 Mayer, C. H., 53, 80, 113, 116
 Medd, W. J., 8, 36
 Mezger, P. G., 50, 51, 70, 76, 112, 113,
 114, 115

Mikhailova, G. A., 147, 195
 Miles, V. G., 127, 200
 Mills, B. Y., 101, 104, 105, 106, 118
 Milne, D. K., 51, 113
 Minnett, H. C., 76, 87, 115, 116
 Minnis, C. M., 4, 8, 9, 10, 11, 13, 14, 16,
 17, 20, 21, 22, 23, 24, 29, 30, 36
 Moffett, A. T., 101, 118
 Montgomery, G. F., 182, 200
 Moore, C. B., 130, 203
 Morgan, M. G., 192, 200
 Morris, D., 80, 104, 116, 117
 Morrison, R. B., 128, 200
 Mullaly, R. F., 108, 117
 Müller, C. A., 43, 64, 114, 115
 Müller-Hillebrand, D., 131, 145, 146,
 200
 Murphy, A. C., 150, 153, 198, 204
 Murray, J. D., 67, 114

N

Naismith, R., 7, 35
 Nakai, T., 161, 163, 165, 172, 188, 200,
 201
 Nakajima, J., 160, 198
 Nash, R. T., 96, 117
 Neville, A. C., 112, 118
 Newman, J. B., 129, 195
 Nicholls, F. G., 188, 199
 Nickson, A. F. B., 188, 199
 Nicolson, C., 197
 Norinder, H., 125, 126, 127, 128, 129,
 133, 140, 192, 193, 201

O

Obayashi, T., 151, 201
 O'Brien, P. A., 101, 118
 Oort, J. H., 43, 115
 Orhavg, T., 59, 60, 114
 Otsu, J., 187, 193, 198, 201

P

Paine, H. G., 156, 171, 196
 Palmer, H. P., 104, 116
 Pauliny-Toth, I. I. K., 73, 79, 115, 116
 Pawsey, J. L., 38, 41, 98, 118, 119
 Paylin, W. J., 107, 117
 Payne, Scott R., 98, 118

Phadke, K. R., 146, 194
 Phillips, M. L., 19, 36
 Phillips, W. E., 188, 202
 Pierce, E. T., 125, 126, 128, 130, 144,
 145, 146, 148, 149, 151, 153, 187, 188,
 195, 197, 201
 Piggott, W. R., 31, 32, 35, 36
 Pippard, A. B., 94, 116
 Plush, R. W., 182, 203
 Ponsonby, J. E. B., 114
 Potter, P. D., 73, 79, 116
 Prentice, S. A., 125, 144, 146, 201
 Price, R. M., 80, 115

R

Radhakrishnan, V., 67, 80, 113, 116
 Raju, T. A., 169, 195
 Ramsey, N. F., 53, 114
 Rasmussen, J. E., 189, 199
 Rawer, K., 14, 15, 25, 36
 Read, R. B., 101, 102, 118
 Reddish, V. C., 104, 116
 Rieker, J., 144, 151, 186, 199, 201
 Rivault R., 153, 192, 193, 201, 202
 Roberts, J. A., 48, 113
 Roberts, M. S., 54, 114
 Robertson, L. M., 143, 193, 202
 Robieux, J., 76, 116
 Robinson, B. J., 49, 50, 51, 52, 114
 Roger, R. S., 114
 Roubique, C. J., 167, 168, 169, 196, 202
 Rowson, B., 104, 116, 117, 118
 Ruze, J., 76, 116
 Ryle, M., 59, 67, 98, 106, 108, 110, 112,
 114, 118

S

Sao, K., 137, 187, 202
 Satyam, M., 142, 143, 202
 Schafer, J. P., 138, 139, 202
 Schell, A. C., 94, 118
 Schmelovsky, K. H., 151, 199
 Schmoys, J., 149, 202
 Schonland, B. F. J., 125, 127, 129, 130,
 140, 144, 188, 202
 Schulz-Dubois, E. O., 54, 113
 Schumann, W. O., 154, 202
 Schuster, D., 79, 116
 Scott, P. F., 112, 118
 Scovil, H. E. D., 54, 55, 113

- Seedel, H., 51, 115
 Seeger, C. L., 52, 57, 60, 80, 114, 116
 Selove, W., 63, 114
 Shain, C. A., 106, 118
 Shakeshaft, J. R., 73, 79, 115, 116
 Sheridan, K. V., 71, 105, 106, 114, 118
 Shiga, T., 187, 201
 Shimazaki, T., 11, 36
 Shklovsky, I. S., 38, 119
 Silleni, S., 175, 202
 Silver, S., 74, 75, 116
 Singer, J. R., 53, 114
 Skeib, G. 153, 188, 202
 Slee, O. B., 105, 106, 118
 Sletten, C. J., 94, 118
 Sloanaker, R. M., 80, 116
 Smith, F. G., 101, 118
 Spaulding, A. D., 167, 168, 169, 196, 202
 Spencer, R. C., 76, 94, 116, 118
 Spies, K., 149, 204
 Srivastava, R. S., 203
 Stanier, H. M., 101, 118
 Steinberg, J. L., 108, 116, 119
 Stelzreid, C. T., 70, 79, 114, 116
 Stergis, C. G., 184, 185, 202
 Stone, D. L., 179, 200
 Storey, L. R. O., 190, 191, 193, 202
 Strassl, H., 70, 76, 112, 115
 Strum, P. D., 63, 114
 Stumpers, F. L., 57, 60, 114
 Sullivan, A. W., 144, 155, 160, 202
 Suzuki, Y., 161, 172, 201
 Swarup, G., 71, 107, 108, 114, 117, 118
 Swenson, G. W., 93, 118
- T
- Takagi, M., 124, 126, 127, 133, 139, 198, 202, 203
 Takeuti, T., 124, 126, 133, 139, 202, 203
 Tamura, Y., 125, 203
 Tanaka, H., 105, 118
 Tanaka, T., 184, 198
 Tantry, B. A. P., 127, 203
 Tatel, H. E., 67, 113
 Taylor, G. M., 114
 Taylor, W. L., 139, 149, 150, 151, 152, 186, 192, 193, 197, 198, 203
- Tepley, L. R., 127, 129, 203
 Terina, G. J., 161, 165, 180, 199
 Thomas, H. A., 123, 155, 171, 174, 203
 Thompson, A. R., 71, 114
 Thompson, J. H., 114
 Timbergen, J., 80, 116
 Townes, C. H., 53, 113
 Troup, G., 53, 115
 Tucker, D. G., 69, 115
 Turnbull, A. G., 8, 35
 Tuve, M. A., 67, 113
 Twiss, R. Q., 102, 117
- U
- Uenohara, M., 50, 51, 115
 Ungstrup, E., 193, 203
- V
- Valley, G. E., 49, 115
 Van Damme, K. J., 52, 114
 Van der Hulst, H. C., 43, 115
 Van de Ziel, A., 50, 115
 Van Hurck, N., 57, 60, 114
 Van Valkenburg, H. M., 155, 160, 202
 Van Wyk, J. W., 188, 202
 Vollmer, B., 129, 201
 Vonberg, D. D., 59, 114
 Vonnegut, B., 126, 130, 195, 203
- W
- Wade, G., 50, 52, 112, 113, 115
 Wagner, C. A., 154, 195
 Wait, J. R., 147, 148, 149, 150, 151, 152, 153, 154, 198, 203, 204
 Wallis, Barnes, 88, 116
 Wallman, H., 49, 115
 Walsh, J. E., 94, 118
 Waltman, W., 59, 60, 114
 Warburton, J. A., 105, 117
 Wasmundt, D. F., 150, 198
 Watkins, D. A., 50, 115
 Watt, A. D., 138, 139, 140, 154, 161, 162, 163, 172, 173, 182, 183, 204
 Weatherburn, C. E., 135, 204
 Weinreb, S., 71, 115

- Wells, J. D., 144, 202
Wendker, H., 70, 76, 112, 115
Westerhout, G., 70, 76, 80, 112, 115,
116
Whelan, E. H., 154, 203
Wielebinski, R., 73, 79, 115, 116
Wild, J. P., 71, 115
Willis, H. F., 179, 204
Workman, E. G., 125, 204
Wormell, T. W., 126, 129, 179, 199, 204

Y

- Yabsley, D. E., 155, 204
Yang, K. S., 107, 118
Yuhara, H., 161, 165, 166, 204

SUBJECT INDEX

A

- Adler tube, 50, 52
- Aerial temperature, 41, 44, 156
measurement of, 79
sky background noise contribution, 45–46
- Aerials,
Cassegrain-type, 73 foll., 79
cylindrical parabolic, 93–94
directional,
noise measurements by, 180–181
noise factor, 156 foll., 174 foll., 180
parabolic reflector, 72–92
characteristics of, 80–92
performance of, 74–80
for radio astronomy, 72–112, 115–119
(*see also* Radio telescopes)
spherical reflector, 94–96
tilted plate, 96–98
- Amplifiers for radiometers, 46–56
maser, 53–55
parametric, 49–52
fast-cyclotron-wave (Adler tube), 50, 52
variable capacitance, 50–52
tunnel-diode, 55–56
- Amplitude Probability Distribution (APD) of noise, 155, 159 foll., 170 foll., 182–183
idealized curves, 167–169
- Antenna, *see* Aerial
- Aperture synthesis, 108–112
- Atmosphere,
electron production rate in, 4–5
- Atmospheric noise,
average envelope voltage, 160–161
average logarithmic voltage, 161
characteristics of, 154–173
data presentation, 176–180
envelope crossing rate, 169–171
field-strength variation with distance, 154
flux density of field, 156
interference by, 181–183
magnetic tape recording of, 156
- Atmospheric noise,
mean power, 155–160
measurement of, 154–173
using APD technique, 159 foll.
automatic recorders for, 157 foll.
by directional aerials, 180–181
using thermojunction, 159
quasi-peak amplitude, 156, 171
slideback peak amplitude, 172
statistical time distribution, 172–173
terminology, 123
world distribution, 175–181
- Atmospherics,
amplitude variability of, 142–143
from cloud and ground discharges, 127
near source, 130–142
propagation of, 147–154
at high frequencies, 153
at low frequencies, 147–153
slow tail, 148–149, 151, 188
from snowstorms, 127
source location, 183–189
by cathode-ray direction finder, 184–186
by narrow-sector recorder, 186–187
by single-station techniques, 187–188
by time-delay technique, 189
spectra of, 133–142
derived from discharge model, 139–140
typical parameters, 141
whistling, *see* Whistlers

B

Boys camera, 125, 128

C

CCIR (International Radio Consultative Committee)
index recommendations, 29–30

CCIR (International Radio Consultative Committee)
 lightning flash counter, 144 foll.
 noise data, 175, 177, 180
 reports on solar activity indices, 4
 Chapman-layer model, 4, 8, 16, 18
 Communication systems,
 atmospheric noise interference, 181–183
 signal/noise ratio requirements, 182–183
 CRPL (Central Radio Propagation Laboratory)
 noise recording equipment, 157 foll.
 Crystal mixers for radiometers, 46–49

D

Dicke switch, 55, 57 foll.
 Direction-finding techniques for locating
 atmospherics, 183–187, 189
 D layer,
 absorption index, 31–32
 ionization, 31

E

Earth-ionosphere cavity,
 resonance in, 154
 waveguide modes in, 148 foll.
 E and F_2 layers,
 noon critical frequency variation, 17
 E layer,
 anomaly at middle latitudes, 8, 10
 character figures, 5–16
 critical frequency,
 association with solar flares, 11
 day-to-day changes, 15–16
 effect of geomagnetic currents, 8
 variation with latitude, 11
 daily character figure, 11–14
 autocorrelation function, 15
 comparison with green line index,
 14–15
 comparison with solar noise flux,
 13 foll.
 ionospheric indices, 4–16
 critical frequency ratio, 16
 monthly character figure, 7–11
 correlation with solar noise, 10
 relations between daily indices, 14–16

F

F_1 layer character figures, 7
 F_2 layer,
 disturbance index, 31
 ionospheric indices,
 applications of, 23
 based on data from several stations,
 20–23
 based on primary index, 18–20
 correlation with critical frequency,
 23, 29–30
 critical frequency ratio, 24
 depending on ionospheric data, 23–25
 relation to sunspot number, 20 foll.
 variability index, 22
 24-h mean critical frequency, 25

G

Gain-modulator technique, 59

H

Haystack aerial, 73, 74
 Hydrogen line,
 radiometer observations of, 46, 63
 foll., 71–72

I

Indices,
 ionospheric, 1–36
 of solar activity,
 primary, 2–3, 18 foll., 33 foll.
 secondary, 3–4
 Interference,
 direct measurement of, 155, 174–175
 to radio services, 181–183
 Interferometers, *see* Radio telescopes
 International Geophysical Year (IGY),
 11, 23, 31, 164
 Ionosphere (*see also* D, E and F layers)
 D region,
 reflection height, 153
 solar effects on, 151
 models of, 149
 Ionospheric disturbance forecasts, 27
 Ionospheric indices, 1–36
 based on D layer absorption, 31–32
 based on E layer data, 4–16

- Ionospheric indices,
 - based on F_2 layer, 17–25, 31
 - based on particle streams, 30–31
- Ionospheric predictions,
 - based on solar activity indices, 25–30
 - choice of index for, 27–29
 - classification of, 27
 - merits of indices for, 29–30
- Ionospheric sunspot number, 19–20
- Ionospheric variations,
 - classification of, 26–27

L

- Lightning,
 - flash counters, 123, 144 foll.
 - strikes to power lines, 146
- Lightning discharges, 123 foll.
 - energy radiated by, 128–130, 140–142
 - field changes near, 130–133
 - noise generation by, 124–130
 - numbers and distributions of, 143–147
 - quantitative models of, 128–130
 - radar echoes from, 126, 127–128
 - sequence of events in, 125 foll.
 - spectrum of atmospheric near, 133–142
 - types of, 124–127
 - whistler-producing, 192–193

M

- Masers, 53–55

N

- Navigational aids,
 - interference by atmospherics, 181
- NITR (National Institute for Telecommunication Research)
 - noise recorder, 160–161, 181
- Noise, *see* Atmospheric noise; Radio noise
- Noise factor,
 - of aerial, 156 foll., 174 foll., 180
 - of receiver, 40
- Noise temperature,
 - of Adler tube systems, 52
 - of crystal mixer radiometers, 48
 - of maser systems, 54–55
 - of radiometer, 39–40
 - of tunnel-diode system, 56
 - of variable-capacitance amplifiers, 51

O

- Occupation time, 159, 163 foll.

P

- Polar blackout index, 31
- Propagation, ionospheric,
 - affecting noise distribution, 153–154
 - ELF and VLF experimental data, 149–153
 - mode theory, 148 foll.
 - ray theory, 153
 - VLF theoretical results, 148

R

- Radar,
 - investigation of lightning, 127–128
 - location of atmospherics, 183, 187
- Radio astronomy,
 - aerials and receivers for, 37–119
 - aperture synthesis technique, 108–112
 - signal characteristics, 40–41
- Radio noise,
 - atmospheric, *see* Atmospheric noise
 - galactic, 177, 179
 - man-made, 179
 - solar, 2, 8 foll., 13, 18, 22, 28 foll.
 - terrestrial, origins of, 122–123
 - from thunderstorms, 121–204
- Radio sources,
 - interferometer measurements of, 101 foll.
 - measured spectra, 41–43
 - polarization measurement of, 80, 91
- Radio telescopes,
 - aperture synthesis, 108 foll.
 - Arecibo, 1000-ft, 95–96
 - Australia, 210-ft, 76, 77, 86–88
 - Bonn, 25-m, 76
 - calibration of, 83 foll.
 - California Institute of Technology, 101–102
 - Cambridge, 108 foll.
 - coordinate conversion system for, 87–88
 - effects of aperture blocking, 75
 - effects of surface irregularities, 75–76
 - feed systems for, 72 foll., 85, 93 foll.
 - “haystack”, 73, 74
 - interferometers,
 - long-baseline, 103–104

- Radio telescopes,
interferometers,
 multi-element, 106–108
 phase-switched, 67–69
 post-detector, 102–103
 two-element, 67–69, 98–104
Jodrell Bank, 73, 87, 102–104
Mills Cross, 105–106
Nançay, 96, 101
National Radio Astronomy Observa-
 tory, 85-ft, 55, 56, 77 foll., 81–85
 300-ft, 56, 76 foll., 88–92
Ohio State University, 97–98
parabolic dish, 72–92
 radiation pattern, 76–79
 surface measurements on, 82–84,
 89–90
polarization performance, 80
Pulkovo, 98
unfilled aperture types, 104–108
University of Illinois, 93–94
- Radiometers, 37–72, 112–115, 119
 using Adler tube, 52
 autocorrelation-type, 71–72
 calibration of, 70–71
 correlation-type, 67 foll.
 with crystal mixer front-end, 46–49
 d.c. comparison-type, 63
 desirable characteristics of, 44
 Dicke-type, 57–63
 frequency-switched, 64–67
 for hydrogen line observations, 46, 63
 foll., 71–72
 low-noise types, 45–56
 main parameters of, 38–40
 using masers, 53–55
 multichannel, 66–67
 using parametric amplifiers, 49–
 52
 phase-switched, 67–69
 for solar observations, 71
 stabilization of, 54, 56–69
 swept-frequency-type, 64–67
 switched-load-type, 57–63
 total-power, 57, 60 foll.
 using travelling-wave tubes, 49
 using tunnel diodes, 55–56
- Receivers,
 noise temperature of, 39–40
 for radio astronomy, 37–72, 112–115,
 119
- S
- Solar activity,
 relation to *E* layer index, 14–15
Solar activity indices,
 CCIR reports on, 4
 used for ionospheric predictions, 25–
 30
 primary, 2–3, 18 foll., 33 foll.
 relative merits of, 29–30
 secondary, 3–4
 URSI report on, 4
Solar corona,
 green-line index, 14–15
Solar flares,
 association with critical frequency,
 11
Solar radio noise,
 comparison with ionospheric indices,
 8–9, 13 foll., 22
 correlation with character figure, 10
 used for ionospheric predictions, 28
 foll.
 polarization measurement of, 80
 radiometer observations of, 71
Spectrograph, 190
Sun,
 calcium character figure, 19
 changes in visible features, 2–3
Sunspot cycle,
 effect on radio noise, 176, 177
Sunspot number,
 comparison with ionospheric indices,
 13 foll., 20 foll., 32–35
 used for ionospheric predictions,
 27–28
- T
- Thunderstorm days, 145 foll.
Thunderstorms,
 discharge rate in, 143 foll.
 meteorological maps, 124
 producing tornadoes, 124, 130, 139
 radio noise from, 121–204
 tropical, 124, 146, 175
 types of, 124
 world distribution of, 144 foll., 181
Travelling-wave tubes in radiometers,
 49
Tunnel diode in radiometer, 55–56
Tweeks, 190

U

URSI (Union Radio-Scientifique Internationale)
report on solar activity indices, 4

W

Whistlers, 143, 189–193

Whistlers,

correlation with storms, 192
features of originating discharges,
192–193
propagation below ionosphere, 193
WMO (World Meteorological Organization)
thunderstorm data, 144, 177

